Physiological, genetic and molecular analysis of two *Arabidopsis* mutants with defects in normal development

Von der Fakultät für Mathematik, Informatik und Naturwissenschaften der Rheinisch Westfälischen Technischen Hochschule Aachen zur Erlangung des akademischen Grades eines Doktors der Naturwissenschaften genehmigte Dissertation

vorgelegt von

Master of science
Rana Pooraiiouby
Aus Tabriz, Iran

Berichter: Universitätsprofessor Dr. A. J. Slusarenko
Privatdozent Dr. N.L. Schlaich

Tag der mündlichen Prüfung: 31.10.2008
Diese Dissertation ist auf den Internetseiten der Hochschulbibliothek online verfügbar

Institute for Biology III (Plant Physiology)

RHEINISCH WESTFÄLISCHE TECHNISCHE HOCHSCHULE AACHEN

PhD Thesis

Physiological, genetic and molecular analysis of two *Arabidopsis* mutants with defects in normal development

Presented by

Master of Science

Rana PoorAiiouby

Scientific Supervision

University Professor Dr. A. Slusarenko

Dr. Nikolas Schlaich

Aachen, October 2008

Zusammenfassung

Im Gegensatz zu tierischen Zellen, haben Pflanzenzellen eine feste Zellwand und können sich deswegen nicht bewegen. So sind sie nach der Zellteilung fest eingebettet in ihrer relativen Position zu den Nachbarnzellen. Daher ist die Orientierung der Zellteilungsebene kritisch für eine normale Pflanzenorganmorphogenese. Kortikale Mikrotubuli (MT) spielen eine wichtige Rolle in diesem Vorgang indem sie die Präprophasebande (PPB). Nach der Mitose bildet sich eine neue Zellwand während der Zellteilung in der Ebene zwischen den zwei Tochterzellen. Der Phragmoplast, eine weitere Struktur, die MT beinhaltet, bildet eine Ebene zwischen den zwei Tochterzellkernen aus und an ihm wird die neue Zellwand abgelagert.MT kommt bei der Festlegung des Pflanzenwuchshabitus eine weitere Rolle zu, da MT wichtig für die parallele Ausrichtung von Zellulosemikrofibrillen in der Zellwand sind. So bestimmen die MT-Muster das Muster der Zellulosemikrofibrillen auf der Außenseite der Plasmamembran. Die Ausrichtung der Zellulosemikrofibrillen hat wiederum Auswirkungen auf die Flexibilität der Zellwand und kontrolliert die Richtung des Zellexpansionswachstums. Pflanzenzellen werden durch pektische Polysaccharide, die Polygalakturonsäure enthalten, miteinander verbunden und Pektin ist ein Bestandteil der Matrix, die die Zellulosemikrofibrillen umgibt.Somit kommt MT und pektischen Polysacchariden eine aktive und wichtige Rolle bei der Ausprägung der Zell- und Organmorphologie zu.

Während der Selektion von transgenen *Arabidopsis* Linien fielen zwei Mutanten auf, die interessante Phänotypen aufwiesen und wurden ausgewählt für weitere Untersuchungen. In der einen Mutante war ein Gen defekt, das für ein Enzym kodiert, das im Metabolismus von pektischen Polysacchariden beteiligt ist ("*pgase*"). Die andere Mutante ("*bushy-ff*") hatte T-DNA Insertionen in zwei Genen: eine in einem Gen, das bekanntermaßen Auswirkungen auf die MT Organisation hat und die andere in einem Gen mit unbekannter Funktion.

In meiner Doktorarbeit charakterisierte ich diese beiden Mutanten. Im Spezifischen ging ich die folgenden Fragen an:

Was sind die morphologischen und anatomischen Defekte in der "*pgase*" Mutante?

Mit Licht- und Rasterelektronenmikroskopie konnte ich zeigen, dass die Pflanze im Durchmesser und der Höhe reduziert war und dass die Blätter etwas uneben waren. Bei den Geweben waren die auffallendsten Defekte, dass die Zahl der Trichome um ca. 30% verringert war und auch die Anzahl der Schließzellen der Spaltöffnungen im Vergleich zu dem Wildtyp verringert war.

Was war die molekulare Ursache dieser Mutante?

Thermal asymmetric interlaced (=TAIL) PCR zeigte eine T-DNA Insertion in einem Mitglied der Familie der Polygalakturonasen von *Arabidopsis*, At3g07970. Semi-quantitative RT-PCR zeigte eine ungefähr um Faktor 3 verringerte Expression von At3g07970 in der "*pgase*" Mutante im Vergleich zum Wildtyp. Komplementation der Phänotypen der "*pgase*" Mutante durch Überexpresssion des "*PGase*" Gens

und Untersuchungen an einer weiteren T-DNA Insertionsmutante im At3g07970 Gen, die morphologische Phänotypen aufwies, die sich nicht von denen der ursprünglichen „*pgase*“ Mutante unterschieden, zeigten, dass diese Mutation verantwortlich für die beobachteten Phänotypen war.

Zellwände sind wichtige Barrieren für biotische und abiotische Stressoren. Da die Mutation in einem “*PGase*” Gen wahrscheinlich zu Veränderungen in der Zellwand führt untersuchte ich die Antwort der “*pgase*” Mutante auf biotischen und abiotischen Stress. Dafür wurde die Mutante einer Infektion mit *Hyaloperonospora arabidopsidis*, Kälte, Hitze und Trockenstress ausgesetzt. Wir fanden dass diese Mutante erhöht anfällig gegenüber der Infektion mit *H. arabidopsidis*, Kälte und Hitze Stress war.

Folgende Fragen wurden an der “*bushy-ff*” Mutante untersucht:

Was sind die morphologishen und anatomischen Defekte in der “*bushy-ff*” Mutante?

Mit dem Licht- und Rasterelektronenmikroskop fanden wir, dass alle Organe einschließlich der Wurzeln, Blätter und Blüten abnormal in dieser Mutante waren. Die “*bushy-ff*” Pflanzen waren in allen Dimensionen stark komprimiert. Auf der Gewebe- und Zellebene wurden verschiedene Defekte beobachtet, z. B. waren die Wurzelzellen der “*bushy-ff*” Pflanzen um ~30 % kleiner als die von Col-0 Wurzelzellen, die Zahl der Trichome war ungefähr halbiert, die Verzweigung der Trichome war verändert und die Differenzierung des Mesophylls in Schwamm- und Palisadenmesenchym war fehlerhaft.

Was war die molekulare Ursache dieser Mutante?

Thermal asymmetric interlaced (=TAIL) PCR zeigte zwei unabhängige T-DNA Insertionen, eine im Promoter eines bis dato uncharakterisierten *F-box* Gens (At1g77000) und eine weitere im Promoter des bereits als kortikale MT organisierenden bekannten *FASS* Gens (At5g18580). Molekulare Analysen wiesen auf eine im Vergleich zum Wildtyp um 50% reduzierte Expression der *FASS* and *F-box* Gene hin.

In Linien, in denen entweder *F-box* oder *FASS* konstitutiv im “*bushy-ff*” Mutanten Hintergrund exprimiert wurden, wurde beobachtet, dass in beiden Fällen die beobachteten “*bushy-ff*” Phänotypen komplementiert wurden. Dies legt nahe, dass die Mutationen in beiden Genen gleichzeitig vorhanden sein muss, um die “*bushy-ff*” Mutanten Phänotypen hervorzurufen. Genetische Experimente, die Kreuzungen von “*bushy-ff*” mit Wildtyp sowie Kreuzungen zwischen Einzelgen-Mutanten in *f-box* und *fass* Mutanten beinhalteten, bestätigten, dass beide Mutationen auftreten mussten und ausreichend waren für den “*bushy-ff*” Phänotyp.

Das Gewebe-spezifische Expressionsmuster von *F-box* and *FASS* zeigte, dass beide Gene auf ungefähr gleichem Niveau in allen getesteten Geweben exprimiert wurden beruht die genetische Interaktion zwischen dem *F-box* und dem *FASS* Gen auf einer physikalischen Interaktion?

Mittels dem Hefe-Zwei-Hybrid Systems konnten wir zeigen, dass F-box und FASS Proteine miteinander interagierten.

Wo in der Pflanzenzelle findet sich das F-box Protein?

Transgene Linien, die konstitutiv eine Fusion aus F-box und Grün-Fluoreszierendem Protein (GFP) im "*bushy-ff*" Mutanten Hintergrund exprimierten (35S::*F-box*-GFP), zeigten eine intrazelluläre Verteilung von F-box Protein, die sehr ähnlich zu der Verteilung eines MT-assoziierten Proteins war (GFP-TUA6).

Zusammengefasst legen unsere Daten nahe, dass FASS kortikale MT organisieren könnte mittels der Interaktion mit dem F-box Protein.

SUMMARY

Unlike animal cells, plant cells have a rigid wall and hence cannot migrate. Rather, they are permanently fixed in their relative position to neighbouring cells after cell division. Therefore, for normal plant organ morphogenesis the orientation of the cell division plane is critical. Cortical microtubules (MTs) play an important role in this process by forming a structure called the preprophase band (PPB). After mitosis, a new cell wall is formed during cytokinesis in the plane between the two daughter cells. The phragmoplast, another structure containing MTs, forms in the plane between the two daughter nuclei and lays down the new cell wall.

A further role for MTs in determining plant stature stems from the fact that MTs are important for the parallel deposition of cellulose fibres in the cell wall. Thus, the patterns formed by the MTs direct the patterning of cellulose microfibrils on the outer side of the plasma membrane. Cellulose microfibril orientation has consequences on cell wall flexibility and controls the direction of cell expansion-growth. Plant cells are cemented together by pectic polysaccharides containing polygalacturonic acid, and pectin is a component of the matrix surrounding the cellulose microfibrils.

Thus, MTs and pectic polysaccharides play an active and important role in establishing cell and organ morphology.

In the process of selecting *Arabidopsis* transgenic lines two mutants were noticed with interesting phenotypes and these were selected for further study. In one mutant a gene coding for an enzyme involved in pectic polysaccharide metabolism was affected ("*pgase*") and the other mutant ("*bushy-ff*") had T-DNA insertions in two genes: one in a gene known to affect MT organization and the other in a gene of unknown function.

During my thesis I characterized those mutants. Specifically I addressed the following aspects:

What are the morphological and anatomical defects in the "*pgase*" mutant?

Using light and scanning electron microscopy, it was shown that the total size of the plant in diameter and height was reduced and the leaves were somewhat twisted. At the tissue level the most obvious defects were the ~30% decreased number of the trichomes and reduced number of the epidermal guard cells in comparison to wild-type plants.

What was the molecular basis of this mutant?

Thermal asymmetric interlaced (=TAIL) PCR showed a T-DNA insertion in the *Arabidopsis* polygalacturonase (PGase) family member, At3g07970. Semi-quantitative RT-PCR showed a ~3-fold lower expression of At3g07970 in the "*pgase*" mutant compared to the wild-type. Complementation of the "*pgase*" mutant phenotypes by over expression of the *PGase* At3g07970 gene, and analysis of an independent T-DNA insertion in At3g07970 that displayed an indistinguishable morphological phenotype to the original mutant, showed that this mutation was responsible for the observed phenotypes.

Cell walls are important barriers for biotic and abiotic stresses. Since a mutation in a *PGase* At3g07970 gene likely results in altered cell walls, the responses of the "*pgase*" mutant to biotic and abiotic stresses were studied. To this end, this mutant was exposed to infection with *Hyaloperonospora arabidopsidis*, cold, heat and drought stress. We found that this mutant was hyper-susceptible to infection with *H. arabidopsidis*, cold and heat stress.

SUMMARY

For the "*bushy-ff*" mutant the following aspects were addressed:

What are the morphological and anatomical defects in the "*bushy-ff*" mutant?

Using light and scanning electron microscopy, we found all of the organs including roots, leaves and flowers were abnormal in this mutant. The "*bushy-ff*" plants were strongly compressed in all dimensions. At the tissue and cellular level, several defects were observed, e.g. the size of the root cells of "*bushy-ff*" was ~30 % smaller than Col-0 root cells, the total number of the trichomes was half of that in wild-type plants, branching of the trichomes was altered and differentiation of mesophyll cells into palisade and spongy cells in the"*bushy-ff*" mutant was aberrant.

What was the molecular basis of this mutant?

Thermal asymmetric interlaced (=TAIL) PCR showed that two independent T-DNA insertions, one in the promoter of a so far uncharacterized *F-box* At1g77000 gene and another in the promoter of the previously characterized, cortical microtubule organizing *FASS* At5g18580 gene occurred in this mutant. Further molecular analysis indicated about 50% lowered expression of the *FASS* and *F-box* At1g77000 gene as compared to wild-type.

By generating lines constitutively expressing either *F-box* At1g77000 or *FASS* in the "*bushy-ff*" mutant background, it was observed that the "*bushy-ff*" phenotype could be complemented in both cases. This suggested that concomitant mutations in both genes were required for the "*bushy-ff*" mutant phenotype. Genetic experiments involving crosses between "*bushy-ff*" and wild-type as well as crossing single *f-box* At1g77000 to single *fass* mutants further confirmed that both mutations occurring in the "*bushy-ff*" mutant were both necessary and responsible for the "*bushy-ff*" phenotype.

The expression pattern and organ specificity analysis of the *F-box* At1g77000 and *FASS* showed that both genes were expressed at similar levels relative to each other in all organs tested.

Does the genetic interaction between the *F-box* At1g77000 and *FASS* genes reflect a physical interaction?

Using yeast two hybrid analysis we could in fact show that the F-box At1g77000 and FASS proteins can also interact physically with each other.

Where is the F-box At1g77000 protein localized inside the plant cell?

Transgenic lines constitutively expressing a fusion protein of *F-box* At1g77000 with green fluorescent protein (35S::*F-box* At1g77000-GFP) in the "*bushy-ff*" mutant background were generated and showed an intracellular distribution of F-box At1g77000 that was similar to that of a microtubule associated protein (GFP-TUA6).

In summary our data suggest that *FASS* might organize cortical microtubules through its interaction with an F-box At1g77000 protein.

Table of content

1 INTRODUCTION

Plants show extensive and complex variations in stature and form. 'Stature' refers to overall size; height, tallness, and size are common synonyms. 'Form' is a much more vague term, and has diverse connotations that depend on context. Roget's Thesaurus (2007) has six senses as a noun and four senses as a verb. As a noun with the sense of 'shape', common synonyms include anatomy, appearance, architecture, design, model, and structure. Both stature and form show plasticity, which is itself widely known to vary among genotypes and species (Busov et al., 2008).

Although plant architecture is to some extent influenced by environmental factors such as light, temperature, humidity, nutrition, and plant density but plant architecture is determined mainly by the plant's genetic program (Wang and Li, 2008). There Final plant size and form are determined by the cell number and cell size resulting from post embryonic cell division, expansion, and differentiation (Mizukami, 2001; Weiss et al., 2005). Early studies, which were later substantiated by detailed molecular experiments, suggested that there is an intrinsic mechanism for coordination of cell division and expansion to produce a developmentally predefined 'normal' species size and form. The genes that encode plant hormones and their signaling, transcription and other regulatory factors, cell cycle regulators and finally cytoskeleton organizers clearly play a major role in regulation of these mechanisms.

I will focus on the advances in understanding the genetic basis of both size and form of plants and plant organs, with an emphasis on genes that can be used as tools for control of plant architecture.

So far five classes of genes useful for control of plant size and form (architecture) have been identified:

- Those affecting hormone metabolism and signaling
- Transcription and other regulatory factors
- The genes involved in control of the cell cycle
- Cytoskeleton organizing genes
- The genes involved in the cell wall components and related enzymes biosynthesis and function (Busov et al., 2008).

In this section I mostly focused on strong modifiers of stature and form that may be useful for directed modification of plant architecture, rather than the detailed mechanisms of gene action.

1.1 Plant hormones

Plant hormones are major regulators of growth and development, and have dramatic effects on stature, form, and physiology. Early experiments with exogenous application of various hormones pointed to roles in regulation of elongation, growth, timing of flowering, apical dominance,

lateral/adventitious root formation, and vascular differentiation (Davies, 1995). Some of these applications have been commercialized and provided important improvements in crop propagation and management (Woodward and Bartel, 2005). More recently, genetic dissection has allowed new insights into the molecular mechanism of hormone biosynthesis and signal transduction pathways, and has provided new options for crop improvement (Sakamoto, 2006). I review the effect of auxin, gibberellins, brassinosteriods and cytokinins (CKs). I ignore the roles of ethylene. It can also modulate plant growth responses, but because its effects are frequently less specific, it is more prone to have undesirable pleiotropic effects, limiting its value for manipulation of plant stature and form.

1.1.1 Auxin

Auxins are a class of plant growth substance which plays an essential role in coordination of many growth and behavioral processes in the plant life cycle. They were the first of the major plant hormones to be discovered and are a major coordinating signal in plant development. Auxins coordinate development at all levels in plants, from the cellular level to organs and ultimately the whole plant. (Taiz and Zeiger, 1998). The multiplicity of auxin responses reflects the central role that this hormone plays in coordinating growth and developmental effects in plants, and thus it is not surprising that genes involved in auxin biosynthesis and signal transduction can be strong modifiers of plant size and form (Busov et al., 2008).

In the molecular levels, auxins directly stimulate or inhibit the expression of specific genes. Auxin induces transcription by targeting for degradation members of the Aux/IAA family of transcriptional repressor proteins, the degradation of the Aux/IAAs leads to the derepression of auxin response factors ARF-mediated transcription. Aux/IAAs are targeted for degradation by ubiquitination, catalysed by an SCF-type ubiquitin-protein ligase (Taiz and Zeiger, 1998).

Arabidopsis has 29 *Aux/IAA* genes. Isolated mutations in this gene family are predominantly gain-of-function lesions in the conserved domain II that is present in all gene family members. Several size and form characteristics were found to be modified in the mutant plants. *Aux*/*IAA* genes have a strong effect on apical dominance in inflorescence stems (Leyser et al., 1998; Rogg et al., 2001). Lateral root branching is also affected in several mutants (Tian and Reed, 1999; Fukaki et al., 2002; Tian et al., 2002). Loss-of-function mutations in *Aux*/*IAA* genes seem to condition very subtle phenotypes likely because of redundancy and/or a feedback mechanism. However, antisense suppression of *IAA*9 in tomato (*Lycopersicon esculentum*) produced numerous growth and form alterations (Wang et al., 2005). Wild-type compound leaves were transformed into simple leaves (Figure 1-1), stem/hypocotyl elongation was enhanced, and apical dominance was reduced.

Auxin response factors (ARFs) are transcription factors that bind to the cis-elements (AuxRE) found in promoters of early auxin response genes (Ulmasov et al., 1997). Three identified *Arabidopsis* null ARF2 alleles produce plants that display longer, thicker inflorescence stems, larger, darker green leaves, and larger seeds (Figure 1-2) compared with wild-type plants (Okushima Y, 2005). Although many of the ARF single loss-of-function mutants do not show growth and developmental defects,

Figure 1-1 Tomato (*Lycopersicon esculentum*) phenotypes produced by down-regulation of the gene encoding an AUX/IAA transcription factor *IAA9*.
The wild type is shown on the left, an antisense (AS) mutant in the middle, and a monogenic spontaneous entire putative *iaa9* mutant on the right (AC, Ailsa Craig; reproduced with (Wang et al., 2005); Bar, 100 mm.

presumably because of functional redundancy among the 23 members some of the double mutations have a significant effect on stature and form (Okushima et al., 2005).

On the cellular level, auxin is essential for cell growth, affecting both cell division and cellular expansion. Depending on the specific tissue, auxin may promote axial elongation (as in shoots), lateral expansion (as in root swelling), or isodiametric expansion (as in fruit growth). In some cases (coleoptile growth) auxin-promoted cellular expansion occurs in the absence of cell division. In other cases, auxin-promoted cell division and cell expansion may be closely sequenced within the same tissue (root initiation, fruit growth). In a living plant it appears that auxins and other plant hormones nearly always interact to determine patterns of plant development (Taiz and Zeiger, 1998).

According to the acid growth hypothesis for auxin action, auxins may directly stimulate the early phases of cell elongation by causing responsive cells to actively transport hydrogen ions out of the

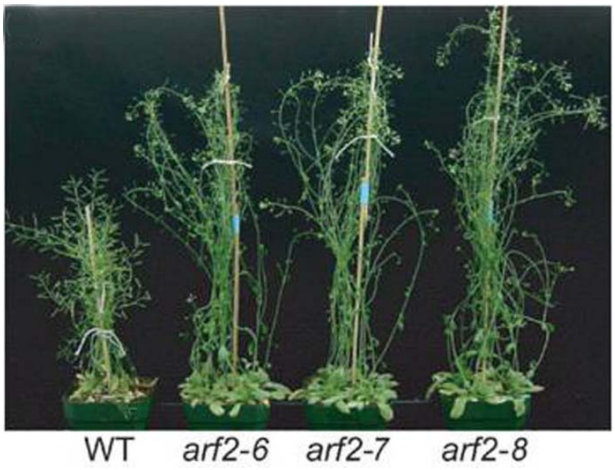

Figure 1-2 Morphological phenotypes of the ARF2 T-DNA insertion mutants.
Eight-week-old WT, *arf2-6*, *arf2-7* and *arf2-8* plants. Each pot contains four plants. Pictures taken from (Okushima Y, 2005).

cell, thus lowering the pH around cells. This acidification of the cell wall region activates wall-loosening proteins known as expansins, which allow slippage of cellulose microfibrils in the cell wall, making the cell wall less rigid. When the cell wall is loosened by the action of auxins, this now-less-rigid wall is expanded by cell turgor pressure, which presses against the cell wall (Taiz and Zeiger, 1998).

That was shown *Arabidopsis* H+-PPase AVP1 in addition to maintaining vacuolar pH, controls auxin transport and consequently auxin-dependent development. AVP1 overexpression results in increased cell division at the onset of organ formation, hyperplasia, and increased auxin transport (Figure 1-3). In contrast, avp1-1 null mutants have severely disrupted root and shoot development and reduced auxin transport (Grebe, 2005; Li et al., 2005).

Auxin transport and it's role in axillary meristem initiation: axillary meristems are major determinants of plant architecture. The initiation of an AM at a certain position involves changes in cell proliferation and growth, accompanied by drastic and concerted modifications in gene expression profiles and hormonal actions (Shimizu-Sato and Mori, 2001; Ward and Leyser, 2004).

Auxin has a broad effect on plant development, particularly on AM initiation and development. Various AMs for leaves, branches, and flowers are derived from the peripheral zone of the vegetative or reproductive shoot apical meristems (SAMs). Auxin has been proposed as an essential regulator in the keeping of balance of SAM activities that determine the position and timing of a primodium (Wang and Li, 2008).

Based on a series of studies on auxin transport and distribution, auxin is mainly transported along the shoot-root axis from cell to cell in a polar manner, namely polar auxin transport (PAT), which requires both influx and efflux carriers (Sieberer and Leyser, 2006). In *Arabidopsis*, auxin carriers, especially the efflux carriers, have been identified and well characterized; eight members of the PIN protein family have been demonstrated to facilitate auxin efflux (Petrasek et al., 2006). *PIN1*, the most well-

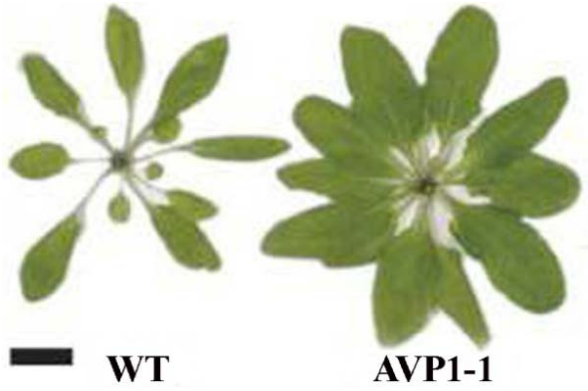

Figure 1-3 *Arabidopsis vacuolar pyrophosphatase1* (*AVP1*) overexpression phenotypes.
With the wild type (WT) shown on the left and AVP1-overexpressing lines on the right, figure reproduced from (Li et al., 2005), Bar represent 1cm.

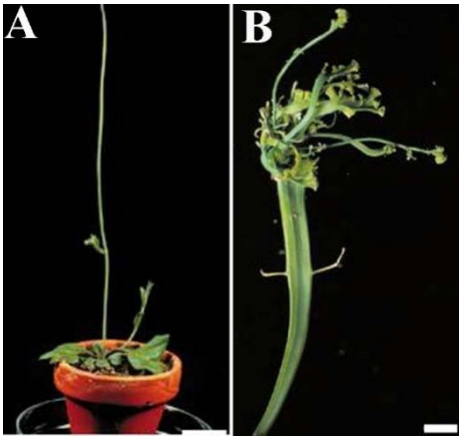

Figure 1-4 Phenotype of the transposon insertional mutant *Atpin1::En134*.
A, The most obvious phenotypic aspect of the homozygous mutant represents the naked, pinforming inforescence with no or just a few defective flowers. B, Drastically fasciated inflorescence of an aged mutant. Bars represent 25 mm in A and 10 mm in B.Pictures taken from (Galweiler et al., 1998).

characterized auxin efflux carrier, mediates auxin distribution and thus triggers AM initiation (Benkova et al., 2003).

In addition, the loss-of-function *pin1* mutant is unable to form lateral organs (Figure 1-4), but the defect can be reversed by exogenous application of auxin (Okada et al., 1991; Reinhardt et al., 2000). These data suggest an auxin patterning model where the initiation of lateral organ primordia is induced by a local auxin maximum accumulated in the periferl zone of the SAM and the subsequent primodium initiates at the site most distant to the preexisting primordium because the established primordia act as a sink to deplete auxin accumulation within surrounding cells (Reinhardt et al., 2000; Benkova et al., 2003; Reinhardt et al., 2003; Fleming, 2005).

In many plant species, axillary buds become dormant owing to the inhibiting effects of the primary shoot apex on the outgrowth of AMs, a phenomenon known as apical dominance. That was shown that auxin in cooperating with cytokinin has an indirect effect on outgrowth of AMs (Cline, 1991; Palni et al., 1993; Bangerth, 1994; Nordstrom et al., 2004). Also, MAX-dependent branching signals have been proposed to function within a network auxin and cytokinins (Bainbridge et al., 2005; Bennett et al., 2006; Gabor and Howard, 2006).

1.1.2 Gibberellin-the “Green Revolution” hormon

Gibberellin was first recognized in 1926 by a japanese scientist, studying bakanae, the "foolish seedling" disease in rice. It was first isolated in 1935 by Teijiro Yabuta, from fungal strains (Gibberella fujikuroi) provided by Kurosawa. Yabuta called the isolate gibberellin. Gibberellins (GAs) are a complex family of tetracyclic diterpenoid growth regulators that play a critical role in many plant growth and developmental processes especially in stem elongation, germination, dormancy, flowering, sex expression, enzyme induction and leaf and fruit senescence (Hooley, 1994; Davies, 1995; Swain et al., 2001).The results of several last studies showed that mutants with a deficiency in

GA concentrations or response are dwarf or semi-dwarf in stature, while elevated GA concentrations or increased signaling result in taller plants (Busov et al., 2008).

Gibberellin and control of the plant height: Gibberellin-related mutants in several species such as *Arabidopsis* and rice exhibit typical phenotypes of dark green leaves and dwarfism attributable to reduced stem elongation (Koornneef and van der Veen, 1980; Talon et al., 1990b; Sun and Kamiya, 1994; Peng and Harberd, 1997; Sakamoto et al., 2004). Based on recent progress in the analysis of dwarf mutants and the molecular characterization of their corresponding genes, both signaling and biosynthesis of GAs have been shown to participate in regulating plant height.

The semidominant *gai* mutation of *Arabidopsis* (Figure 1-5) affects GA perception and its subsequent signal transduction (Koornneef and van der Veen, 1980; Talon et al., 1990a; Wilson et al., 1992; Peng and Harberd, 1993; Wilson and Somerville, 1995).

GAI is a negative GA-response regulator in *Arabidopsis* (Peng et al., 1997) , and its orthologs in wheat (*Rht*) (Gale et al., 1975) and maize (D8) (Figure 1-5), (Harberd and Freeling, 1989; Winkler and Freeling, 1994) are the “Green Revolution” genes that have greatly enhanced grain yields since the 1960s. SLR1, the ortholog of GAI in rice, was also identified by characterizing a rice mutant showing a slender phenotype (Tanaka et al., 2001). These plant height regulating genes share a conserved DELLA domain that is important for GA detection in the GA signaling pathway (Peng et al., 1999) .

GAs are synthesized in three successive steps localized in separate intracellular compartments, with the first stage in chloroplasts, the second in the endoplasmic reticulum, and the third in the cytoplasm (Hedden and Phillips, 2000a). The flux of bioactive GAs is controlled by the enzymes in the third compartment, such as GA20-oxidase (GA20ox), GA3-oxidase (GA3ox), and GA2-oxidase (GA2ox) (Hedden and Phillips, 2000b).

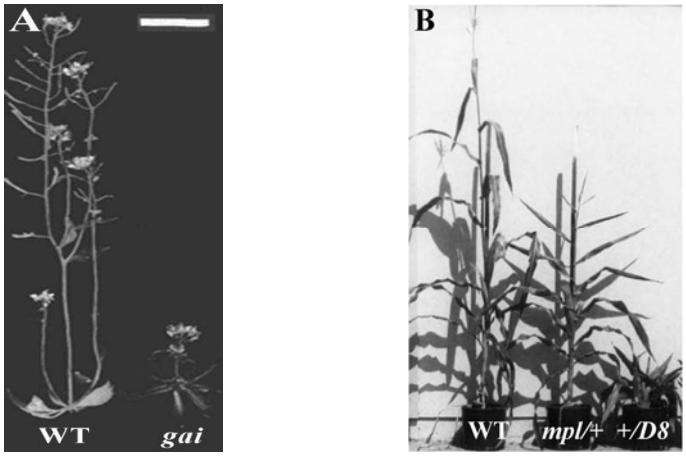

Figure 1-5 Phenotype of *Arabidopsis ga*i mutant (A) and maize heterozygous *D8* mutatnt (B) in compare to wild type plants. A; Flowering *gai* line and wild-type Col-0. Bar: 5cm.Picture taken from (Peng et al., 1997) B; Flowering D8 mutant, *mpl* and wild type.Pictures from (Harberd and Freeling, 1989).

Figure 1-6 Ectopic expression of *OsGA2ox1* in transgenic rice plants.
Typical phenotype of transgenic rice plants carrying the *Act::OsGA2ox1* gene approximately 120 d after germination. Left, wild-type (cv Nipponbare); center and right, Act::OsGA2ox1 transformants. In contrast to wild-type plants, flowering of transformants was impeded. Bar= 10 cm. Pictures taken from (Sakamoto et al., 2001).

GA20ox and GA3ox are biosynthetic enzymes that catalyze the last two steps in the biosynthetic pathway.

Loss-of function mutations in the GA20ox and GA3ox genes or overexpression of the GA2ox genes has a dwarfing effect and has been observed in numerous plant species, including *Arabidopsis* (Sun and Kamiya, 1994; Helliwell et al., 1998; Yamaguchi et al., 1998), rice (Figure 1-6) (Sakamoto et al., 2001), potato (*Solanum tuberosum*) (Carrera et al., 2000), and poplar (*Populus tremula*) (Hedden and Phillips, 2000a; Busov et al., 2003).

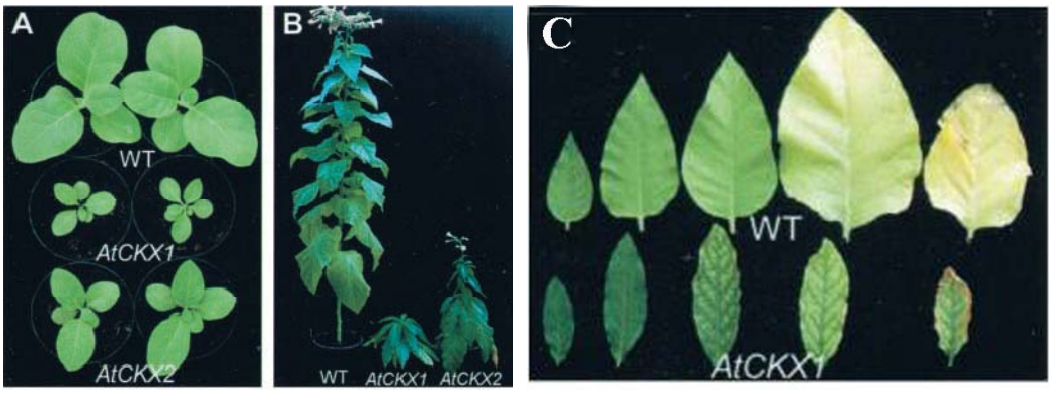

Figure 1-7 Shoot phenotype of *AtCKX1*-expressing tobacco plants.
A, Top view of 6-week-old plants. B, tobacco plants at the flowering stage. C, comparison of leaf size and senescence. Leaves were from nodes number 4, 9, 12, 16, and 20 from the top (from left to right). Figures taken from (Werner et al., 2001).

Figure 1-8 Stature of normal-type and semidwarf rice plants at ripening.
Normal-type (Sasanishiki,a japonica cultivar) and semidwarf-type *sd1*.Picture taken from (Monna et al., 2002).

The semidwarf "Green Revolution" rice *sd1* (Figure 1-8) which results from a deficiency in the GA 20-oxidase gene (Os20ox2) (Sakamoto et al., 2001; Monna et al., 2002; Sasaki et al., 2002; Spielmeyer et al., 2002). Consistent with the loss-of-function of Os20ox2 in *sd1* plants, they show an elevated GA53 content and a reduced amount of GA20 and GA1 (Spielmeyer et al., 2002).

1.1.3 Cytokinins (CKS) and their role in Shoot Apical Meristem Maintenance

Cytokinins are compounds with a structure resembling adenine. Kinetin was the first cytokinin discovered and so named because of the compounds ability to promote cytokinesis (cell division) (Wang and Li, 2008). They regulate cell division, cell growth, differentiation, and are the best known hormones involved in maintaining meristem activity (Riou-Khamlichi et al., 1999). It is reported that the constitutive expression of CycD3 in transgenic *Arabidopsis* plants induces and maintains cell division when the plants are deprived of exogenous cytokinins (Riou-Khamlichi et al., 1999); the overexpression of CKX genes decreases the endogenous cytokinin content in tobacco plants, producing stunted shoots with smaller apical meristems (Figure 1-7) accompanied by a prolonged plastochrone and leaf cell production, (Werner et al., 2001). The direct evidence that cytokinins are involved in maintaining SAM activity comes from the experiments that revealed the relationship between cytokinins and the homeobox gene *SHOOTMERISTEMLESS* (*STM*). Earlier observations that the shoot meristems overproducing cytokinins showed a similar phenotype to that of the transgenic plants overexpressing KNAT1 or KN1 suggested that cytokinins and homeobox genes may be involved in regulating SAM function in the same pathway and that cytokinins may act upstream of KNAT1 and STM (Rupp et al., 1999) .

Cytokinin also controls the SAM size by participating in the CLV-WUS loop. WUS can directly repress the transcription of ARR5, ARR6, ARR7, and ARR15, negative regulators in the cytokinin signaling pathway (Hwang and Sheen, 2001) . These findings suggest that ARR genes might negatively influence

Figure 1-9 Phenotypes of type-A *ARR* mutant plants.
Wild type and an adult 35S::*ARR7* plant. Duplicated rosettes. Arrowheads indicate irregular side-shoot positions. Figure reassembled from (Leibfried et al., 2005).

meristem size and that their repression by WUS might be necessary for the proper function of meristems (Leibfried et al., 2005) . Consistent with this hypothesis is the observation that overexpression of an active form of ARR7 produces an aborting SAM in *Arabidopsis* (Figure 1-9), (Leibfried et al., 2005) . Conversely, a loss-of function mutation in a maize ARR homolog has an enlarged SAM (Giulini et al., 2004)

1.1.4 Brassinosteroids

Brassinosteroids (BRs) are a class of more than 40 sterol derivatives in plants that have profound effects on plant size and architecture (Busov et al., 2008). BRs are required for normal plant growth, reproduction and development. Plants that are deficient either in the biosynthesis or perception of these hormones are typically dark green dwarfs with epinastic leaves, have reduced or no fertility, and exhibit delayed development (Bishop and Koncz, 2002). For most BR-deficient mutants, a wild-type phenotype can be partially or fully restored with the addition of exogenous BRs. Conversely, BR synthesis mutations can be phenocopied in dicots by applying brassinazole (Asami et al., 2000) or brz2001 (Sekimata et al., 2001) , specific BRs biosynthesis inhibitors.

1.1.4.1 BRs biosynthetic mutants

BRs biosynthetic mutants such as *constitutive photomorphogenesis* and *dwarfism* (*cpd*) and *de-etiolated 2* (*det2*) from *Arabidopsis thaliana* were identified based on their altered skotomorphogenesis (Chory et al., 1991; Szekeres et al., 1996). Wild-type seeds germinated in darkness produce etiolated seedlings with long hypocotyls and a closed apical hook. In contrast, *det2* and *cpd* dark-grown seedlings have the appearance of seedlings grown in the light with *det2* and *cpd* seedlings exhibit expression of light-regulated genes (Chory et al., 1991; Szekeres et al., 1996) . *CPD* and *DET2* genes encode a cytochrome P450 monooxygenase (Szekeres et al., 1996) and a steroid 5 α -reductase (Li et al., 1997), respectively, similar to the enzymes utilized in animal steroid biosynthesis.

Since the pathway to functional BRs is quite long, a number of mutants have been found all showing a dwarfed phenotype.

1.1.4.2 BRs perception mutants

Wild-type *Arabidopsis* root growth is inhibited by the presence of micromolar quantities of brassinolide. The *bri1* mutant was identified based on the phenotype of root growth in the presence of the BRs, indicating a lack of BR perception or BR signal transduction (Clouse et al., 1996; Jianming and Chory, 1997). Like *cpd* or *det2* seedlings, the *bri1* mutants also showed a de-etiolated phenotype when grown in the dark, and light-grown plants are dark green dwarves with reduced male fertility.

BR-insensitive 2 (*bin2*)/*dwf12* was another isolated BRs signaling mutant that displayed a dwarf phenotype, accompanied by curved leaves and an impaired cell elongation (Li et al., 2001).

The *BIN2* gene encodes a homolog of animal glycogen synthase kinase-3 (GSK-3) or Shaggy kinase involved in various developmental processes. *bin2* was allelic to two previously isolated genes: *Arabidopsis Shaggy-like kinase eta* (*ASK*) and *Ultracurvata 1* (*UCU1*), (Li and Nam, 2002).

Unlike the biosynthetic mutants, *bri1* and *bin2*/*dwf12* mutants cannot be rescued by exogenous application of BRs. Gain-of-function mutations in *BIN2* (Li et al., 2001) or over-expression of *BIN2* (Li and Nam, 2002) resulted in semi-dwarfed plants with a *bri1*-like phenotype, indicating that *BIN2* acts as a negative regulator of BRs signaling.

The *BR Enhanced Expression* 1, 2 and 3 (*BEE*) genes which encode putative basic helix-loop-helix transcription factors are induced by brassinolide (BL) and affect growth responses in the hypocotyl and floral organs. A mutant phenotype is just observed in triple knockouts (*bee1 bee2 bee3*), which have a weak *bri1* phenotype. Therefore, BEE1, BEE2 and BEE3 appear to be positive regulators of the BL response, and they may share some functional redundancy (Friedrichsen et al., 2002).

A potential BRI1 kinase substrate was recently identified (Nam and Li, 2004). The transthyretin-like (TTL) protein shares some sequence similarity with the thyroid hormone binding protein found in animals *in vitro*, the BRI1 kinase domain phosphorylated TTL. Over-expression of the *TTL* produced plants with a phenotype similar to weak *bri1* mutants, indicating that TTL functions as a negative regulator of BRs. This was supported by analysis of T-DNA knockouts of TTL. Loss-of-function *ttl* mutants were more sensitive to BL in root growth bioassays and showed increased plant growth in comparison to wild-type plants (Nam and Li, 2004).

1.2 Transcription factors and other regulatory genes

1.2.1 The *AINTEGUMENTA* (*ANT*) and ARGOS pathway

One of the main controllers of plant organ size is *AINTEGUMENTA* (*ANT*). It was originally discovered as a mutant affecting flower development (Elliott et al., 1996; Klucher et al., 1996). Strong *ant* mutants have ovules that fail to form integuments or a female gametophyte. Flower development is

also altered, with a random reduction of organs in the outer three whorls. In addition, organs present in the outer three floral whorls often have abnormal morphology. Ovules from a weak *ant* mutant contained both inner and outer integuments but generally failed to produce a functional female gametophyte (Elliott et al., 1996). *ANT* overexpression dramatically increased both leaf and floral size in *Arabidopsis* (Krizek, 1999; Mizukami and Fischer, 2000). The increase in flower size in *35S::ANT* expressing plants was manifested in both the Columbia (Col-0) and Landsberg *erecta* (L-*er*) ecotypes but the leaf size promoting effect was not described in the L-*er* ecotype. *ANT* encodes an *APETALA2* (*AP2*)-domain transcription factor that negatively regulates expression of the floral organ specifying transcription factor *AGAMOUS*. There are seven *ANT*-like (*AIL*) genes in *Arabidopsis*, some of which have similar growth and size promoting effects (Nole-Wilson et al., 2005). The size increase is associated with increased cell proliferation rather than cell size, suggesting that the gene prolongs the meristematic capacity of cells during organ growth and differentiation. Recently, ANT was found to be part of an auxin-regulated signaling cascade. A central gene in this cascade, called *ARGOS* (auxin-regulated gene controlling organ size) has a similar growth-promoting effect as *ANT* when overexpressed in transgenic plants (Figure 1-10). Transgenic plants expressing sense or antisense *ARGOS* cDNA display enlarged or reduced aerial organs, respectively. Ectopic expression of *ARGOS* prolongs the expression of *ANT*. *ARGOS* appears to be upstream of *ANT* in the signaling cascade, as loss of *ANT* function blocks the growth-promoting effect of *ARGOS* (Busov et al., 2008).

1.2.2 TCP transcription factors

The TCP-domain proteins are plant-specific transcription factors that regulate shape and form characteristics of plants (Cubas et al., 1999).They were named after the three founding members of the family – *TEOSINTE BRANCHED1* (*TB1*) from maize, *CYCLOIDEA* (*CYC*) from *Antirrhinum*, and *PROLIFERATION CELL FACTOR1* (*PCF1*) from rice (Li et al., 2005).

In *Arabidopsis* the family consists of 24 members that play important roles in branching, floral symmetry, and leaf curvature by synchronization of cell division and growth, likely by binding to promoters and transcriptionally regulating genes involved in the cell cycle and ribosomal machinery (Li et al., 2005). The importance of this gene family in the evolution of modern crop plants is exemplified by the *TB1* gene from maize. Its mutant form made a major contribution to development

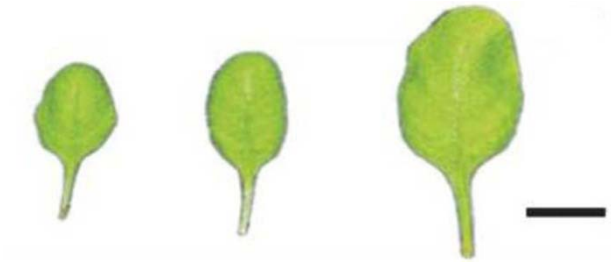

Figure 1-10 Arabidopsis *ARGOS* (auxin-regulated gene controlling organ size) mutant phenotypes.
Antisense knockdown (left), vector control (middle), and 35S overexpression (right) mutants are shown. Bar, 5 mm. Figure taken from (Hu et al., 2003).

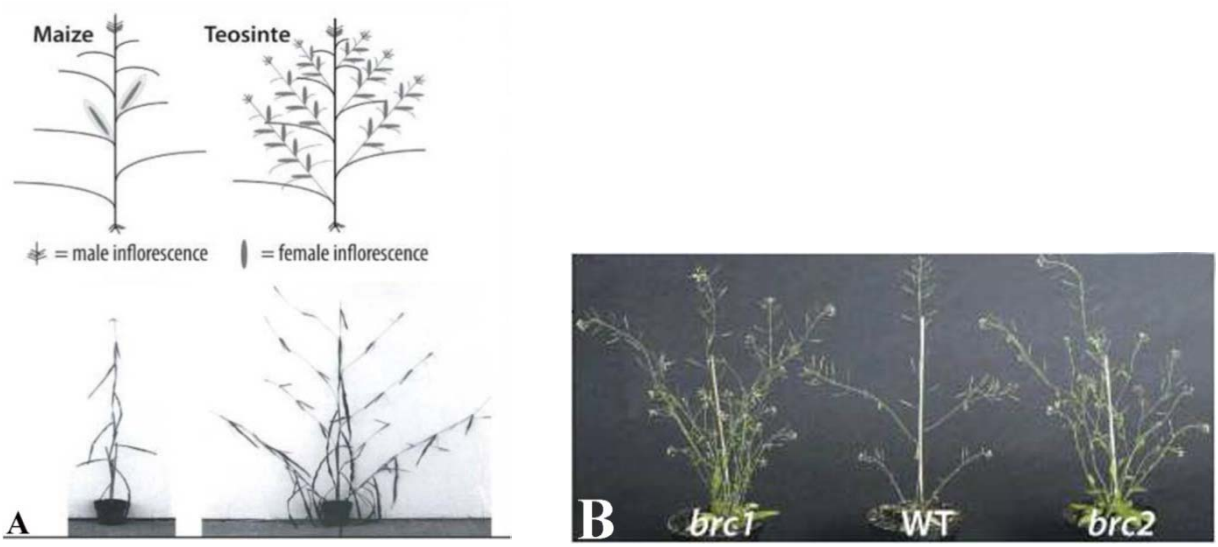

Figure 1-11 Branching morphologies of maize (Zea mays) and *Arabidopsis branched1* (*brc1)* and *branched2* (*brc2*) mutant phenotypes.
A: Upper row, (left) versus its ancestor teosinte (right); lower row, segregation of form among recombinant inbred progeny derived from maize– teosinte hybridization that are homozygous for maize (left) or teosinte (right) chromosomal segments containing the major quantitative trait loci (QTL) for branching with the TEOSINTE BRANCHED1 (TB1) gene. (Deobley et al., 1997), B: Arabidopsis branched1 (*brc1)* and branched2 (*brc2*) mutant phenotypes (Aguilar-Martinez et al., 2007).

of modern maize from its wild teosinte ancestor (Doebley et al., 1995; Deobley et al., 1997). Overexpression of the *TB1* gene suppresses lateral branching and contributes to a more compact plant form suitable to cultivation under a high-density crop environment (Figure 1-12). *TB1* orthologs with similar phenotypic effects have been found in rice (*OsTB1*) and Arabidopsis (*BRANCHED1* and *BRANCHED2*), (Figure 1-12), (Takeda et al., 2003; Aguilar-Martinez et al., 2007).

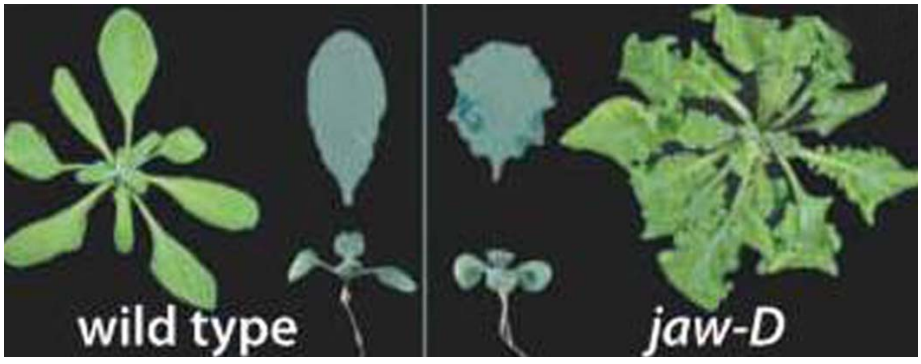

Figure 1-12 *Arabidopsis jaw* miRNA mutant phenotypes.
The wild type is shown on the left, and the mutant on the right (Palatnik et al., 2003).

In *Antirrhinum*, the *CINCINNATA* (*CIN*) gene encodes a TCP domain transcription factor that controls leaf curvature and therefore surface features (Crawford et al., 2004). Plants bearing homozygous *cin* alleles show excessive curvature, particularly in the marginal regions, resulting from excessive uncontrolled cell growth. Developing leaves in *cin* mutants suffer from a delay in cell division arrest, resulting in an excess of cells, causing curvatures in the leaf surface. A similar effect is observed in *Arabidopsis*. *thaliana* (Figure 1-12). Activation tagging of microRNA159/319 in the *jaw* mutant is a near phenocopy of the *cin* mutant in snapdragon (*Antirrhinum majus*), (Palatnik et al., 2003). The phenotypic effect is a result of miR159/319-mediated cleavage of TCP4 mRNA. A TCP gene also controls development of compound leaves in tomato. Gain-of-function mutations in the *LANCEOLATA* (*LA*) gene render *LA* mRNA resistant to degradation by miR159/319 (Ori et al., 2007). The elevated *LA* transcript abundance leads to precocious differentiation of the leaf margin and precludes compound leaf development.

1.2.3 Growth-regulating factor (*GRF*) and ANGUSTIFOLIA act together in control of leaf size and shape

Growth-regulating factor (*GRF*) genes represent a small transcription factor gene family in plants that control leaf size and relative lateral to longitudinal dimensions via control of cell proliferation. The founding member of the gene family, *OsGRF1*, was found in rice; it was induced by GA and is highly expressed in rapidly elongating stems (van der Knaap et al., 2000). The *Arabidopsis GRF* gene family compromises nine members. Most of the *AtGRF* genes are strongly expressed in actively growing and developing tissues, such as shoot tips, flower buds and roots but weakly in mature stem and leaf tissues. In *Arabidopsis*, four members of the family (*GRF1*, *GRF2, GRF3*, and *GRF5*) were found to have strong growth promoting effects on both leaves and cotyledons (Kim et al., 2003). Triple insertional knockout mutants of *GRF1–3* have smaller leaves and cotyledons, while single mutants have no apparent phenotype. By contrast, a single knockout of *GRF5* exhibits a narrow leaf phenotype that is associated with a decrease in cell numbers (Horiguchi et al., 2005). While overexpression of *AtGRF1* and *AtGRF2* resulted in larger leaves and cotyledons, as well as in delayed bolting of the inflorescence stem when compared to wild-type plants. Using the yeast two hybrid system it was shown that GRF protein family members can interact with ANGUSTIFOLIA3 (*AN3*)/*GRF-INTERACTING FACTOR1* (*AtGIF1*), (Busov et al., 2008). Modification of *AN3* expression seems to have phenotypic effects similar to that for *GRF*, suggesting that the two proteins may act together to control the development of leaf size and shape. Overexpression of *AN3* in transgenic plants induces large leaves, while its knockout results in small, narrow leaves (Busov et al., 2008).

1.2.4 GRAS and MYB proteins control branching

Shoot branching is initiated during postembryonic development by the formation of secondary meristems. These new meristems, which are established between the stem and leaf primordia, develop into vegetative branches or flowers. Thus, the number of axillary meristems has a major impact on plant architecture and reproductive success .Molecular and genetic analyses have shown that control of branching involves at least two steps, the formation of the axillary meristem and

outgrowth of the axillary bud (Schmitz et al., 2002). The tomato genes *BLIND* (*Bl*), which encodes a MYB-domain transcription factor, and *LATERAL SUPPRESSOR* (*LS*), which encodes a GRAS-domain transcription factor, control the initiation of lateral meristems (Schumacher et al., 1999; Schmitz et al., 2002). Studies of Ls homologs from rice (*MONOCULM1* (*MOC1*); (Li et al., 2003) and Arabidopsis (*LATERAL SUPPRESSOR* (*LAS*) , (Greb et al., 2003) as well as Bl homologs from Arabidopsis (*REGULATOR OF AXILLARY MERISTEMS* (*RAX*) *1*/*2*/*3*; (Keller et al., 2006; Muller et al., 2006) support the idea that these are key regulators of axillary meristems conserved over large evolutionary distances. *LS*/*LAS* and *Bl*/*RAX1* appear to act in separate pathways and have partially redundant functions in axillary meristem initiation and maintenance. There are, however, also important differences among the homologs.

For example Bl regulates axillary meristem initiation during both vegetative and reproductive development, whereas *RAX1*/*2*/*3* regulates branching along overlapping zones of the shoot, with RAX1 acting early in vegetative development and *RAX2*/*3* primarily acting later during inflorescence development. *RAX1* also appears to affect the timing of the floral transition by modulating GA concentrations in the shoot apex.

1.2.5 TERMINAL FLOWER1 (TFL1) and shoot architecture

The Arabidopsis gene *TFL1* controls shoot meristem identity throughout the plant life cycle, and encodes a putative signal transduction protein with homology to mammalian phosphatidylethanolamine-binding proteins (Bradley et al., 1997). Overexpression of *TFL1* results in increased vegetative growth, a larger and highly branched inflorescence, and delayed flower formation (Ratcliffe et al., 1999). By contrast, *tfl1* mutants have a short vegetative phase during which they produce few leaves and branches, and the normally indeterminate inflorescence meristem forms a terminal flower (Shannon and Meeks-Wagner, 1991). Natural and induced mutations in the pea *TFL1* homolog *LATE FLOWERING* (*LF*) have been important for pea domestication (Weller et al., 2007). A major domestication trait in tomato was produced by a recessive mutation in the tomato *TFL1* homolog *SELF-PRUNING* (*SP*), (Pnueli et al., 1998). The *sp* allele causes an accelerated termination of sympodial units into inflorescences, resulting in a bushy, compact form and nearly homogeneous sized fruits.

1.3 Cell cycle genes

The cell cycle is obviously necessary for generating the cells that build organs and organisms; bigger plants and organs are generally built of more cells (Meyerowitz, 1997); Early experiments showed that arresting cell division by gamma irradiation of wheat seedlings had little effect on final growth and development (Haber, 1962).The molecular controllers determining progression through the transitions in cell cycle (e.g. G1/S and G2/M transitions) are represented by heteromeric cyclin-dependent kinases (CDKs) with their regulatory subunits, the activating unit is known as cyclin, and the inhibitory unit as cyclin-dependent kinase inhibitor (CKI/KRP), (Dewitte and Murray, 2003; Verkest et al., 2005; Inze and Veylder, 2006).

1.3.1 Cell proliferation

Results from experiments that directly slowed the rate of cell cycling have produced variable results. In many cases, effective decreases in cell proliferation resulted in fewer cells, but compensatory increases in cell size reduced most of the impact on final size and form (Doonan, 2000; Inze and Veylder, 2006). For example, expression of a dominant negative form of CDKA;1 in transgenic tobacco resulted in a block of G1/S transition and decreased cell proliferation; however, it was compensated by larger cell sizes, resulting in normal growth and development (Hemerly et al., 1995). By contrast, overexpression of any of the *CKI*/*KRP* genes in *Arabidopsis* resulted in cell cycle retardation and fewer cells and, despite partial compensation through increases in cell size, transgenic plants were severely dwarfed, with most organs reduced in size. There were also modifications in plant morphology, such as in the shape and serration of leaves and petals (Wang et al., 2000; De Veylder et al., 2001). Transgenic plants with increased cell cycling via induction of faster G1/S transitions have increased growth rates in roots and/or shoots, but with no effects on overall plant stature. For example, overexpression of *CYCD2; 1* in transgenic tobacco increased shoot growth and accelerated development (Cockcroft et al., 2000). Overexpression of B-type cyclins (*CYCB1*; 1 and *CYCB2; 2*) increased the rate of root growth (Doerner et al., 1996; Lee et al., 2003).

1.3.2 Incomplete cell cycles: endoreduplication and growth

In plants, increases in nuclear size caused by polyploidization are positively correlated with cell size, and consequently with organ and organism size (Kondorosi et al., 2000) . Therefore, genes that regulate endoreduplication have been viewed as potential targets for modifying cell size and consequently plant stature. In many of these manipulations increased nuclear DNA content was observed, but this was likely a result of compensatory mechanisms; the final stature and form were not or only slightly changed (Inze and Veylder, 2006). For example, KRP2, an inhibitor of CDKA1; 1, controls the onset of the endoreduplication cycle in *Arabidopsis* (Verkest et al., 2005). Transgenic plants overexpressing KRP2 under the 35S promoter showed a dose-dependent response, with the highly expressing lines having no effect on the level of endoreduplication and ploidy, and the lines with low transgene expression showed higher levels of endoreduplication and ploidy in leaves. The overall size and form of transgenic plants were not changed. Expression of KRP2 under the SHOOT MERISTEMLESS (STM) gene promoter, which drives expression in mitotically active cells, increased endoreduplication and ploidy levels in leaf cells. The total size of transgenic plants was slightly decreased because of mitosis inhibition, but the resulting decrease in cell number was almost fully compensated by increases in cell size. Another well-documented regulator of endoreduplication is the cell cycle switch 52 (CCS52), isolated from Medicago and playing a role in cell enlargement during nodule formation (Cebolla et al., 1999; Vinardell et al., 2003). Likely because overexpression of *CCS52* causes embryonic lethality, no transgenic plants overexpressing the protein were recovered. Antisense-mediated down regulation resulted in wild-type-like plants that were somewhat slender, a result of the formation of fewer side branches. A DP-E2F-like1 (DEL1) protein with an unknown molecular role seems to be negatively regulating the onset of endoreduplication (Vlieghe et al., 2005).

Although transgenic plants with down- or up-regulation of *DEL1* predictably changed the ploidy level, transgenics were phenotypically similar to wild-type plants.

1.4 Cytoskeleton organizing genes

Plants control the direction of cell expansion as a way of shaping growth. Since their discovery in plants 40 years ago, cytoskeleton microtubules (MT) have been suspected of forming a template that helps to regulate the direction of growth. The detailed mechanism, however, has been elusive, especially as plants lack a microtubule-organizing centre.

In contrast to animals, fungi and protists in land plants one of the main factors which affect the establishment of division planes is the formation of transient cortical ring of MTs that precisely foretells the position of the cell division planes at the G2/prophase transition. During interphase, arrays of parallel MTs encircle the cell at the cortex. The positioning of MTs within these cortical arrays appears to involve both MT dynamicity and translocation. To understand the molecular mechanisms underlying MT arrangements, mutant impaired in MT functions are essential and a number of proteins involved in MT organization or dynamics have been identified.

Arabidopsis *botero1* mutant (which also is allelic to the *fra2* mutant), (Zhong et al., 2001), which displays incorrect orientation of interphase cortical MTs and defects in anisotropic growth in root tip cells (Bichet et al., 2001). The *FRA2* gene encodes a protein with high similarity to the sea urchin p60 subunit of katanin, which is known to be involved in MT severing (Mc Clinton and Sung, 1997; Burk et al., 2001).

The *Arabidopsis* temperature- sensitive *mor1* mutation causes cortical MT shortening and disorganization concomitant with isotropic cell expansion and left-handed organ twisting (Whittington et al., 2001), (Figure 1-13). The *MOR1* gene encodes a protein similar to a family of MT-associated proteins from mammals and fungi (Whittington et al., 2001).

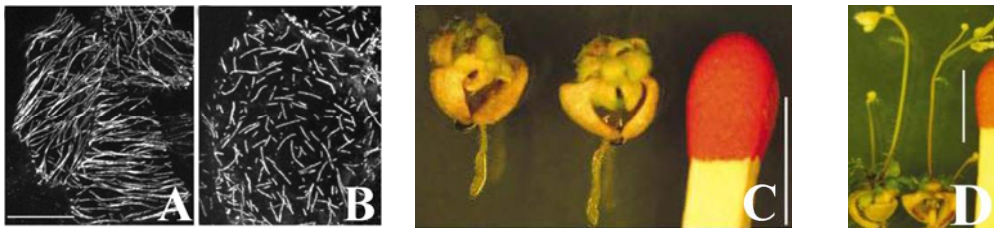

Figure 1-13 Mutations in the *MOR1* gene cause temperature-dependent microtubule disruption.
Anti-tubulin immunofuorescence was used to label cortical microtubules in epidermal cells of the first true leaf of 21-day-old seedlings after incubating seedlings at 29 8C for 2 hours before fixation. A,wild type. B,*mor1-1* homozygote. Scale bar, 25mm.C and D morphological consequences of *mor1*'s microtubule disruption. C, cultured for 4 weeks at 31°C, then 1 week at 21°C, *mor1-1* (left) and *mor1-2* (right) plants are severely stunted, show radially swollen and short organs and do not produce flowers. Scale bar, 5 mm. D, After culture at 31°C for 2 weeks followed by 3 weeks at 21°C, latent ability to bloom is triggered in both *mor1-1* (left) and *mor1-2* (right) mutants. Scale bar, 5 mm.

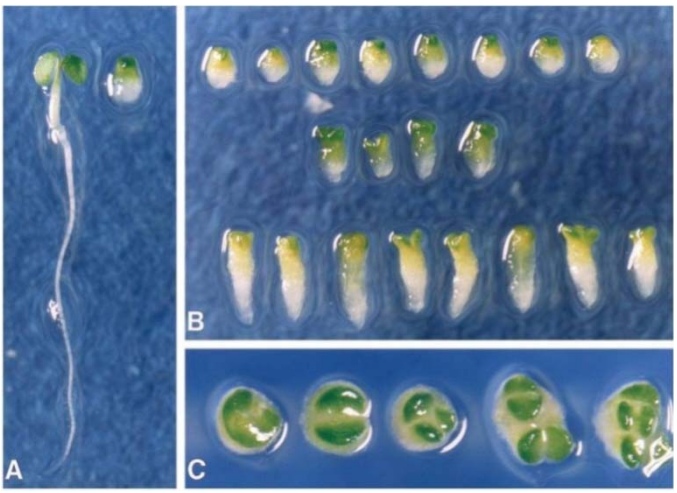

Figure 1-14 Seedling phenotype of the *fass* mutants.
A, strong allele *fass*R226-32 (right) showing extreme compression of all body elements; wild-type on the left. Colours indicate orientation in the mutant: the dark green at the apical end represents the cotyledons, the light-green region corresponds to the hypocotyl ending in a broad, white root end (9X). B, Comparison of homozygous strong (*fs*R226-32/*fs*R226-32), trans-heterozygous (*fs*R226-32/*fs*U93-11) and homozygous weak (*fs*U93-11/ *fs*U93-11) *fass* seedlings. C, Cotyledon number variation of *fass* seedlings (allele *fs* R2-3, from left to right, one to five cotyledons). Note the π and pairwise arrangement in seedlings with three or more cotyledons respectively. Figure from (Torres-Ruiz and Jurgens, 1994).

The *Arabidopsis zwichel* trichome-branching mutation affects the kinesin-like calmodulin binding protein (Oppenheimer et al., 1997). This MT motor protein is proposed to provide the MT stability needed for trichome branch initiation (Mathur and Chua, 2000). The maize *tangled1* mutant has an altered cell division pattern associated with defective PPB positioning and phragmoplast guidance (Cleary and Smith, 1998). The *TANGLED1* gene was cloned recently and was found to encode a MT-associated protein (Smith et al., 2001).

Arabidopsis spiral mutants, which exhibit righthanded twisting of organs associated with defects in cell growth anisotropy, cortical MTs form left-handed helices instead of transverse arrays (Furutani et al., 2000) . The *SPIRAL1* and *SPIRAL2* genes define two novel plant-specific gene families involved in cortical MT organization (Furutani et al., 2000).

The *Arabidopsis fass*/*tonneau* mutants affecting seedling body organization (Figure 1-14), (Mayer et al., 1991; Torres-Ruiz and Jurgens, 1994; Trass et al., 1995). *fass* seedlings are strongly compressed in the apical-basal axis and enlarged circumferentially, notably in the hypocotyls (Figure 1-14, A). Depending on the width of the hypocotyl, *fass* seedlings may have up to three supernumerary cotyledons (Figure 1-14, C), . Mutations at this locus drastically change plant shape, resulting in thick, dwarf seedlings and plantlets. However, the general body pattern (i.e., the number and relative positions of organs) is not altered, and mutants eventually produce highly compressed inflorescences when grown in vitro (Mayer et al., 1991; Torres-Ruiz and Jurgens, 1994; Trass et al., 1995). Mutants reach a maximum height of 1.5 to 3 cm at maturity for strong and weak alleles, respectively (Figure

1-15). Some almost morphologically normal, although sterile, flowers are observed in weak alleles (Figure 1-15, E to G), (Camilleri et al., 2002).

In these mutants, both the arrangement of interphase cortical MTs and preprophase band (PPB) formation are affected (Trass et al., 1995; Mc Clinton and Sung, 1997). At the cellular level, *ton* mutant is altered markedly in cell size, shape, and arrangement. This appears to be related to a defect in cell elongation and a random orientation of division planes. Cell differentiation seems mostly unaffected, and most cell types are present, including cell structures such as stomata that result from asymmetrical divisions. Cells of *ton* mutant have abnormal organization of the interphase cortical cytoskeleton and are unable to form PPBs (Trass et al., 1995; Mc Clinton and Sung, 1997). In interphase cells, cortical MTs most often are arranged randomly instead of forming transverse regular arrays, which are normally associated with cell elongation in plants. Noncortical MTs seem to be unaffected. Thus, the *ton* mutations uncouple histogenesis (oriented cell divisions and cell shape changes) and morphogenesis from organogenesis (Lloyd, 1996).

Camilleri *et al*. in 2002 have shown the TON2 protein has strong similarities to a regulatory subunit of PP2A and interacts with an *Arabidopsis* type A subunit of PP2A in the yeast two-hybrid system. The C-terminal part of the protein is necessary for interaction with other subunits. And likely functions as a regulatory subunit of type 2A protein phosphatase (PP2A) and probably involved in phosphorylation cascades that control the dynamic organization of the cortical cytoskeleton in plant cell (Camilleri et al., 2002).

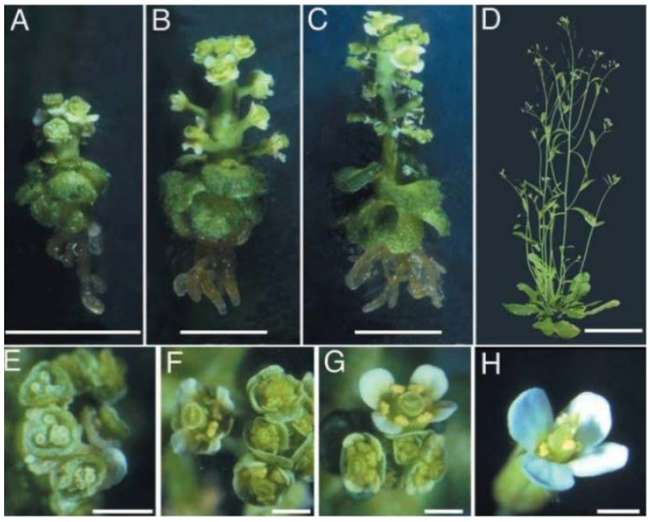

Figure 1-15 Phenotypes of *ton=fass* mutant plants.
Photographs showing strong (A, ton2-13) and weak (B, ton2-12; C, ton2-14) alleles of the ton2 mutation 6.5 weeks after germination, compared with wild-type Arabidopsis grown in the greenhouse D, Flowers of mutant plants are shown in E, (ton2-13); F,(ton2-12), and G, (ton2-14), and a wild-type flower is shown in H. Bars = 5 mm in A to C, 5 cm in D, and 1 mm in E to H (Camilleri et al., 2002).

1.5 Genes involved in cell wall components and related enzymes biosynthesis and function

The architecture, mechanism, and function of plants depend crucially on the structure of the cell wall. The wall is secreted and assembled as a complex structure that varies in form and composition as the cell differentiates. Primary cell walls are synthesized in actively growing cells, and secondary cell walls are deposited in certain cells, such as xylem vessel elements and sclerenchyma, after cell expansion ceases that elicit the production of defense compounds (phytoalexins) in the plant. Similarly, fungal pectinase releases biologically active oligosaccharins from the plant cell wall. Therefore, cell wall represent the unique type of extracellular matrix with both structural and growth regulating function. The presence of a rigid cell wall correlates with a mode of developmental where planes of cell divisions and the dimensions of subsequent cell expansion determine the size and shapes of indivijual cells and the complex tissues and organs which they are a part (Taiz and Zeiger, 1998) .

In study to analyze the synthesis, struture and function of the plant cell wall by genetic approach, several chemically mutagenised *Arabidopsis* lines were screened for changes in the monosaccharide composition of hydrolyzed cell wall material (Reiter et al., 1997). One screening procedure for identification *Arabidopsis* cell wall mutants, identified 23 mutant lines representing 11 different loci designated *mur1* to *mur11*. The *mur* lines fall into essentially three groups:

- Complete absence of a monosaccharide
- Significant reduction in the amount of a single monosaccharide
- Complex alterations in the relative amouns of the several monosaccharides.

All mutants in the first category represent alleles of the *mur1* locus and are deficient the *de novo* synthesis of fucose. Mutants with redution in a single monosaccharide have been identified for fucose (*mur2*, *mur3*), arabinose (*mur4*, *mur5*, *mur6*, *mur7*) and rhamnose (*mur8*). Mutants with complex changes in monosaccharide composition are represented by the *mur9*, *mur10* and *mur11*. Most of the mutant lines did not show morphological or physiological alterations. However, lines *mur1*, *mur9* and

1-16 A, growth habit of mutant lines *mur9* and *mur10* in comparison with wild type plant.Scale bar: 2cm. B, growth habit of *mur1mur4* double mutant in late flowering stage, figures taken from (Reiter et al., 1997).

mur10 cosegregated with reduced vigor or dwarfism of the plants (Reiter et al., 1997).

Arabidopsis lines carrying tight *mur1 and mur4* alleles were slightly dwarfed and showed considerable brittleness in elongating inflorescence stems (1-16, B). As shown in (1-16, A) plants carring *mur9* mutation grew very slowly during their rosette stage. Most of the seedling died early during development . But plants surviving to bolting stage developed normal inflorescence. The two *mur10* lines were characterized by slow growth, dark green leaves (Reiter et al., 1997), (1-16, A).

This example and other studies are clearly indicating to role of plant cell walls, their component, composition and structure in plant develpoment, form and stature.

In this study I have molecularly analyzed two *Arabidopsis thaliana* morphological and developmental mutants. The results of this study have shown that in the "*pgase*" mutant a T-DNA insertion in *Arabidopsis* polygalacturonases family member ,At3g07970, cause morphological defects in plant development. This insertion resulted in a mutant which was termed "*pgase*" and showed extreme susceptibility to biotic and abiotic stresses. In the "*bushy-ff*" mutant we have shown two independent mutations in the cortical microtubule organizing protein FASS with an *F-box* At1g77000 protein results in morphologically affected phenotype, this mutant termed so according to the plant appearance and molecular basis. Moreovre, we have showed that genetic and physical interaction of these proteins are required for *Arabidopsis* normal development.

2 MATERIALS AND METHODS

2.1 Organisms

2.1.1 Plants

Arabidopsis thaliana ecotype Columbia (Col-0) plants were used in this study. The seeds were gotten from NASC (Nottingham Arabidopsis Stock Centre). Mutant lines which were used in this study are listed in the following table.

2.1.2 Bacteria

2.1.2.1 Escherichia coli strains

DH5α. F-, Lambda-, recA1, endA1, hsdR17 (rK-, mK+), (lacZYA-argF), supE44, U169,Φ80dlacZ . M15, thi-1, gyrA96, relA1 (Hanahan, 1983). This bacterial strain possesses a modified recombination system (recA1), which results in reduced recombination probability, and lacks endonuclease (endA1). It was therefore used in the cloning experiments. ER2566: New England BioLabs (Frankfurt).

XL1 Blue. endA1 gyrA96(nalR) thi-1 recA1 relA1 lac glnV44 F'[::Tn10 proAB+ lacIqΔ(lacZ)M15] hsdR17(rK- mK+). This bacterium carries nalidixic acid resistant and tetracycline resistant (carried on the F plasmid). Genes listed signify mutant alleles. Genes on the F´ episome, however, are wild-type unless indicated otherwise.200138: Stratagene (USA).

BL21. (DE3). F– ompT gal dcm lon hsdSB (rB- mB-), lambda; (DE3) an *E. coli* B strain with DE3, a lambda; prophage carrying the T7 RNA polymerase gene and lacIq. Derived from B834 (Wood, 1996) by transducing to Met+. See the original studier paper (Studier and Moffatt, 1986) for more details. We used it for protein expression. B 2935: Sigma (USA). DB3.1. Strep 50R DB3.1 cells (containing a gyrA mutation) allow propagation of the Gateway® vectors containing the ccdB gene. 11782-018: Invitrogen

2.1.2.2 Hyaloperonospora arabidopsidis

Two different isolates of this pathogen (NOCO and WELA) which were described and used by Hermanns et al., (Hermanns et al., 2003), were used in this study.

2.1.2.3 Agrobacterium tumefacien strain

GV3101 (pMP90RK): Gmr, Kmr, Rifr (Koncz and Schell, 1986). This Agrobacterium strain contains a non-oncogenic Ti plasmid pMP90RK that represents one component of the binary vector system described by the above authors. This plasmid contains the vir-region as well as the genes for gentamycin and kanamycin resistances. After introduction of derivatives of the plasmid pS, this bacterial strain was used for the transformation of *A. thaliana* plants.

2.1.3 Yeast (*Saccharomyses cerevisiae*)

Y190 was used in Gal4 two-hybrid system. It is deficient for ADE, LEU,TRP and HIS and can not grow on minimal medium lacking one of those nutrients unless the corresponding functional genes are

introduced by transformation or mating (Flick and Johnston, 1990; Harper et al., 1993). 630445:Clontech (USA)

Table 2-1 Mutant and transgenic *Arabidopsis* lines used in this study.

Plant line	Accession	Description	Original source
"*bushy-ff*"	Col-0	T-DNA	Laboratory BioIII, RWTH- Aachen
"*pgase*"	Ta-0	T-DNA	Laboratory BioIII, RWTH- Aachen
*ton*2-5	Col-0	T-DNA	(Camilleri et al., 2002)
f-box At1g77000 knock out	Col-0	SALK- 045957 (T-DNA)	NASC (Nottingham Arabidopsis Stock Centre)
f-box At1g77000 knock out	Col-0	SALK-070175 (T-DNA)	NASC (Nottingham Arabidopsis Stock Centre)
pgase At3g0970 knock out	Col-0	GABI-Kat 058B07-016087 (T-DNA)	Weisshaar B. et al., Max-Planck-Institut für Zuechtungsforschung
f-box At1g77000 knock down	Col-0	T-DNA	This study
At5g18580 (*fass*) knock down	Col-0	T-DNA	This study

2.2 Vector

The following vectors which were listed in (Table 2-2), were provided from different sources, and used during this study. The physical map of these vectors were shown in (Figure 2-1- Figure 2-10).

Table 2-2 List of the vectors which were used through the molecular analysis of the developmental mutants. Related plasmid maps were shown in next figures (Figure 2-1 -Figure 2-10).

Name of plasmid	Backbone	Cloning	Marker
pGINBA+ *F-box* At1g77000 promoter	PGINBA (HAUSMANN,L; TÖPFER, R. GenBank Acc.-No. AY234330) Acc.-No. AY234330)	*F-box* At1g77000 promoter cloned between *Cla*I and *Xho*I	Amp^R in *E.coli*
F-box At1g77000 Promoter + GUS (Figure 2-1)	pLH7000 (HAUSMANN,L; TÖPFER, R. GenBank Acc.-No. AY234330)	*F-box* At1g77000 promoter+ GUS cloned between *Sfi*I sites	Amp^R in *E.coli*; $Carb^R$ in *Agro*; $BASTA^R$ in plants
35S:: Δ *FASS* CDS (Figure 2-2)	pJawohl3-RNAi (Ülker, Max-Planck-Institute, Cologne)	Truncated version of *FASS* CDS cloned between *Nco*I and *Spe*I .	Amp^R in *E.coli*; $Carb^R$ in *Agro* ; $BASTA^R$ in plants
35S::*FASS* full CDS (Figure 2-3)	pJawohl3-RNAi (Ülker, Max-Planck-Institute, Cologne)	CDS of *FASS* cloned between *Nco*I and *Spe*I .	Amp^R in *E.coli*; $Carb^R$ in *Agro* ; $BASTA^R$ in plants
35S::*PGase* At3g07970 CDS (Figure 2-4)	pJawohl3-RNAi (Ülker, Max-Planck-Institute, Cologne)	CDS of *PGase* At3g07970 cloned between *Bam*HI and *Eco*RI.	Amp^R in *E.coli*; $Carb^R$ in *Agro* ; $BASTA^R$ in plants
PGWB2+ *F-box* At1g77000 CDS (Figure 2-5)	PGWB2 (Nakagawa et al., 2007)	CDS of *F-box* At1g77000 cloned between Gateway att1,att2 sites	Hyg^R and Kan^R in *E.coli*; Hyg^R and Kan^R in *Agro*; Hyg^R or Kan^R in plants
PGWB6+*F-box* At1g77000 CDS (Figure 2-6)	PGWB6 (Nakagawa et al., 2007)	CDS of *F-box* At1g77000 cloned between Gateway att1,att2 sites	Hyg^R and Kan^R in *E.coli*; Hyg^R and Kan^R in *Agro*; Hyg^R or Kan^R in plants
Yeast-two-hybrid *FASS* prey vector (Figure 2-8)	pGADT7 (Clontech) (Chien et al., 1991)	CDS of *FASS* cloned between *Eco*RI and *Cla*I sites	Amp^R in *E.coli*; Leu seletion marker in yeast
Yeast-two-hybrid *F-box* At1g77000 prey vector (Figure 2-7)	pGADT7 (Clontech) (Chien et al., 1991)	CDS of *F-box* At1g77000 cloned between *Nde*I and *Bam*HI sites	Amp^R in *E.coli*; Leu seletion marker in yeast
Yeast-two-hybrid *FASS* bait vector (Figure 2-10)	pGBKT7 (Clontech) (Louret and al, 1997)	CDS of *FASS* cloned between *Nco*I and *Eco*RI sites	Kan^R in *E.coli*; Trp seletion marker in yeast
Yeast-two-hybrid *F-box* At1g77000 bait vector (Figure 2-9)	pGBKT7 (Clontech) (Louret and al, 1997)	CDS of *F-box* At1g77000 cloned between *Nde*I and *Bam*HI sites	Kan^R in *E.coli*; Trp seletion marker in yeast

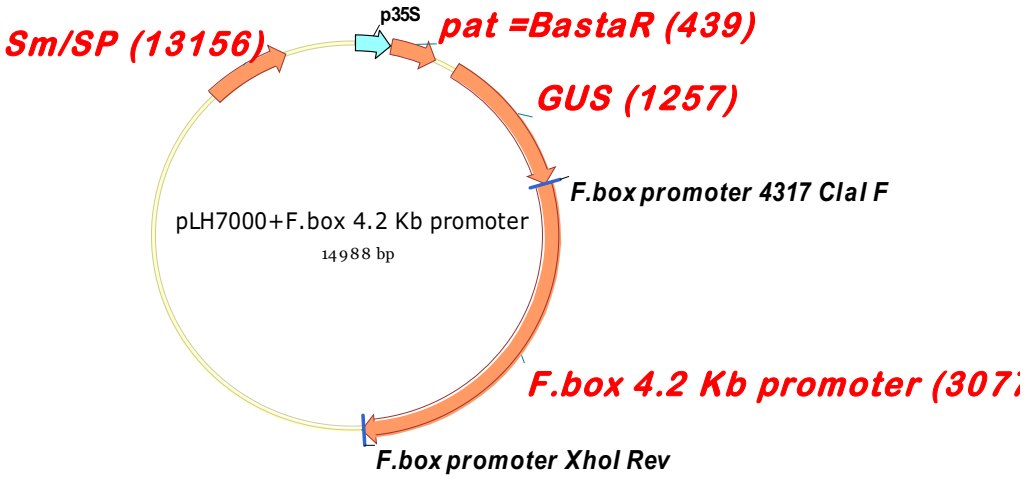

Figure 2-1 Recombinant pLH7000 +*F-box* At1g77000 promoter vector map.
The 4,2 kb *F-box* At1g77000 promoter sequence was cloned upstream of GUS via *Cla*I and *Xho*I the restriction sites. Sm/SP: spectinomycin resistance gene for selection in *E. coli* and *Agrobacterium*. Pat, BASTA herbicide resistance for selection in plants under the control of 35S promoter and terminator.

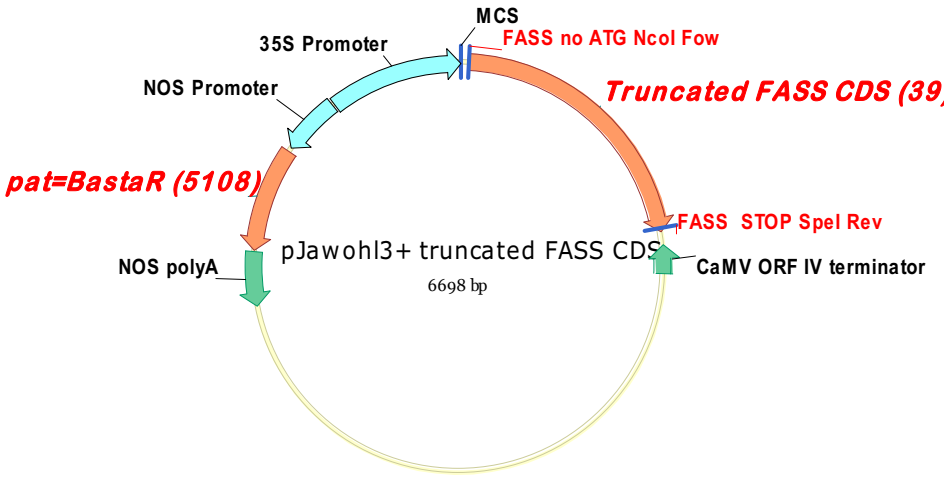

Figure 2-2 Plasmid map of recombinant pJawohl3 with Δ *FASS* CDS.
The CDS of *FASS* was cloned between *Nco*I and *Spe*I restriction sites under the control of the 35 CaMV promoter and the resistance gene to the herbicide BASTA in planta , ampicillin resistance in *E. coli* and carbenicillin resistance in *Agrobacterium*.

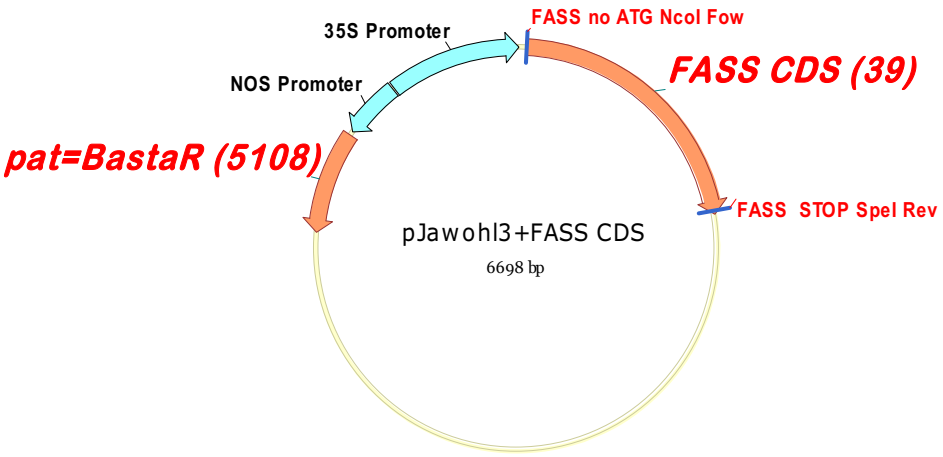

Figure 2-3 Plasmid map of recombinant pJawohl3 with *FASS* CDS.
The CDS Of *FASS* was cloned between *Nco*I and *Spe*I restriction sites under the control of the 35 CaMV promoter and the resistance gene to the herbicide BASTA in planta , ampicillin resistance in *E. coli* and carbenicillin resistance in *Agrobacterium*.

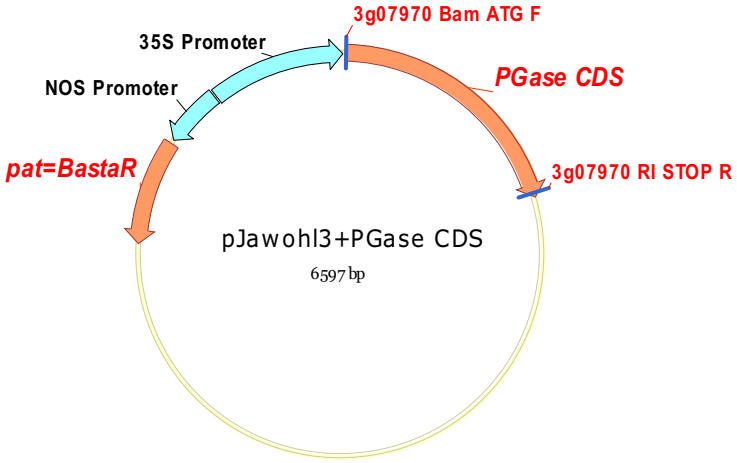

Figure 2-4 Plasmid map of recombinant pJawohl3 with *PGase* At3g07970 CDS.
The CDS of *PGase* At3g07970 was cloned between *Bam*HI and *Eco*RI restriction sites under the control of the 35 CaMV promoter and the resistance gene to the herbicide BASTA in planta , ampicillin resistance in *E. coli* and carbenicillin resistance in *Agrobacterium*.

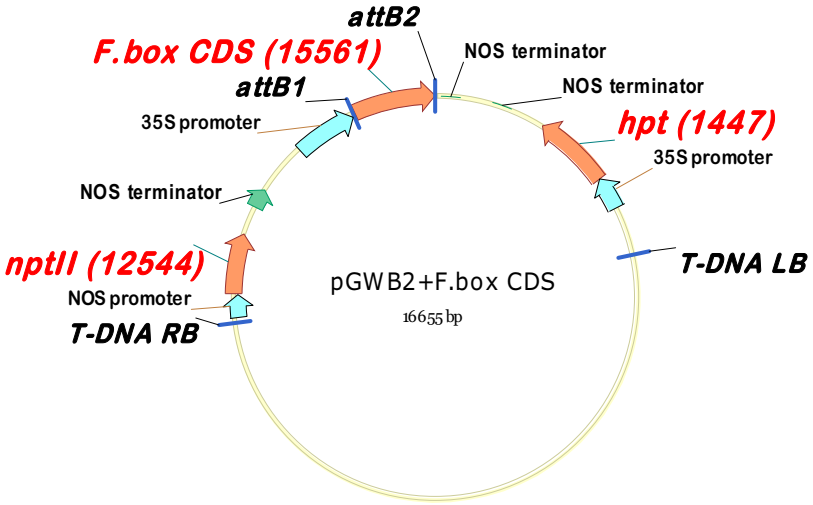

Figure 2-5 Plasmid map of recombinant pGWB2 with *F-box* At1g77000 CDS.
The CDS of *F-box* was cloned between attB1 and attB2 sites under the control of 35 CaMV. and the resistance gene to the Hygromycine / Kanomycine in planta , Hygromycine , Kanomycine resistance in *E. coli* and Hygromycine , Kanomycine resistance in *Agrobacterium*.

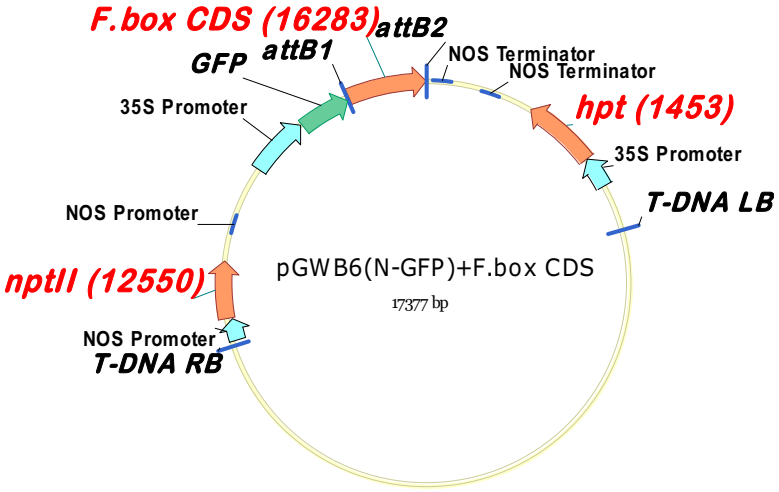

Figure 2-6 Plasmid map of recombinant pGWB6 with *F-box* At1g77000 CDS.
The CDS of *F-box* was cloned between attB1 and attB2 sites under the control of 35 CaMV, downstream of Green Fluorescence Protein (GFP) CDS, with the resistance gene to the Hygromycine/Kanomycine in planta , Hygromycine , Kanomycine resistance in *E. coli* and Hygromycine , Kanomycine resistance in *Agrobacterium*.

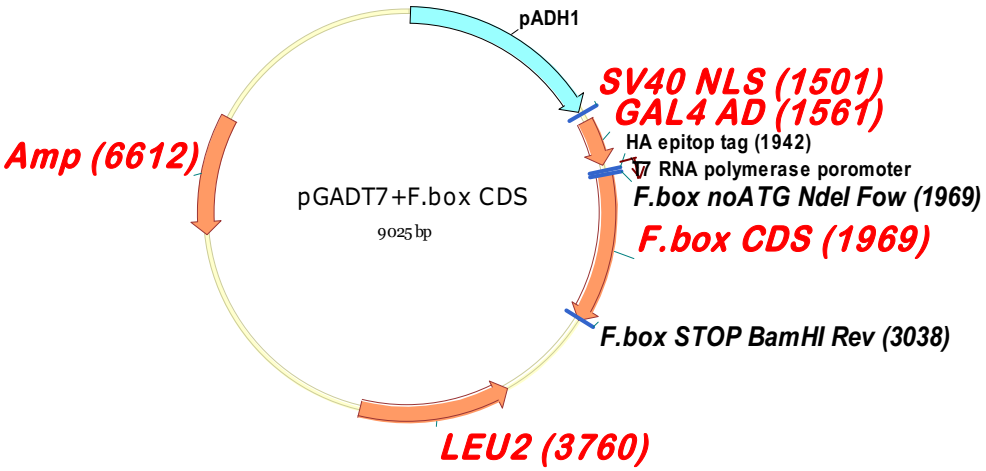

Figure 2-7 Plasmid map of recombinant pGADT7 with *F-box* At1g77000 CDS.
pGADT7 is used to generate fusions of the GAL4 AD protein with target or prey protein. Fusion protein expression is under the control of strong yeast ADH1 promoter. The LEU2 transformation marker is used for selection in yeast and Ampiciline resistance to *E.coli*.

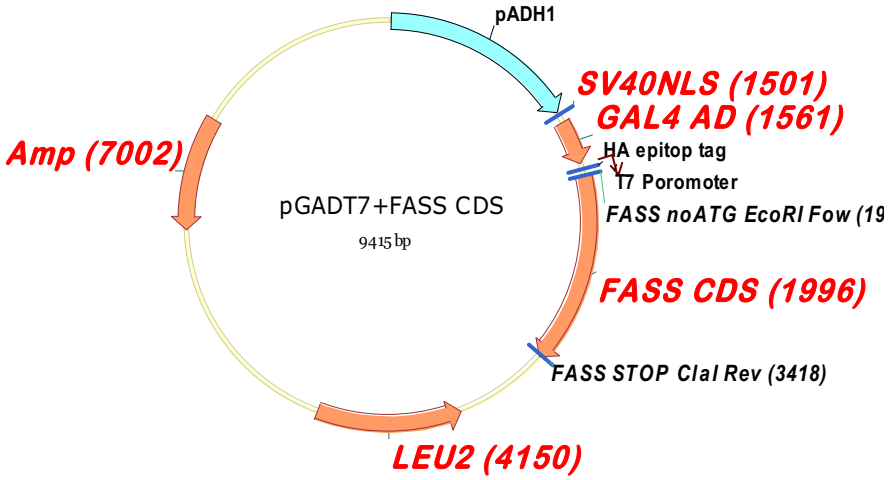

Figure 2-8 Plasmid map of recombinant pGADT7 with *FASS* CDS.
pGADT7 is used to generate fusions of the GAL4 AD protein with target or prey protein. Fusion protein expression is under the control of strong yeast ADH1 promoter. The LEU2 transformation marker is used for selection in yeast and Ampiciline resistance to *E.coli*.

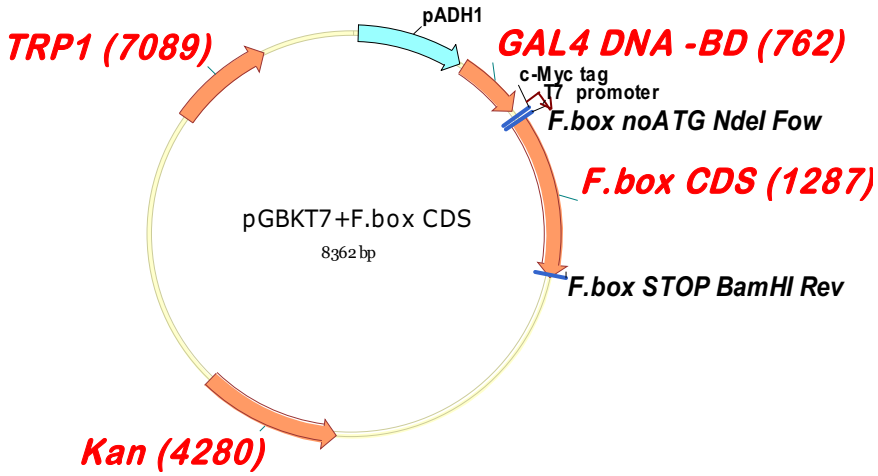

Figure 2-9 Plasmid map of recombinant pGBKT7 with *F-box* At1g77000 CDS.
pGBKT7 is used to generate fusions of the GAL4 DNA-BD protein with a target or bait protein. Fusion protein expression is controlled by the strong yeast ADH1 promoter. The TRP1 transformation marker is used for selection in yeast and Kanomycine resistance to *E.coli*.

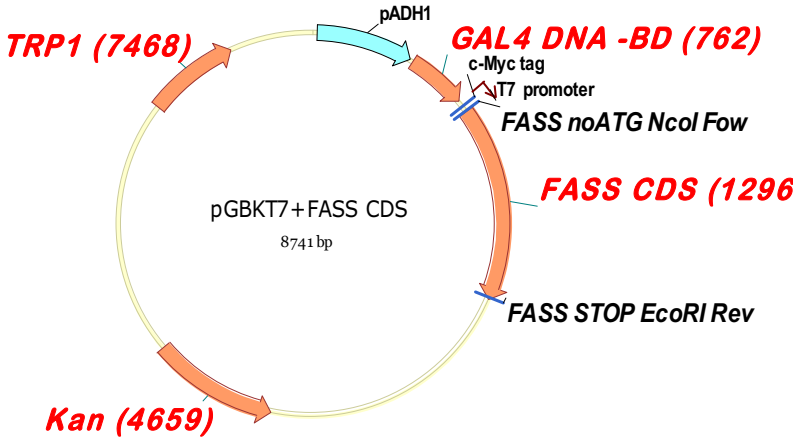

Figure 2-10 Plasmid map of recombinant pGBKT7 with *FASS* CDS.
pGBKT7 is used to generate fusions of the GAL4 DNA-BD protein with a target or bait protein. Fusion protein expression is controlled by the strong yeast ADH1 promoter. The TRP1 transformation marker is used for selection in yeast and Kanomycine resistance to *E.coli*.

2.3 Synthetic Oligonucleotides

The following primers from Sigma were used for cloning and sequencing of the genes required for the molecular analysis of the developmental mutants.

Table 2-3 List of the primers used throughout this work. Primers that were used during this work were described in detail below.

No.	Name of primer	Sequence
1	*F-box* 6941 intron1 forward	ATGCCTGGTGATTGAAAGAGTC
2	*F-box* 6634 exon 4 qRT forward	AAGGAAAATTCGATGAAGAAGGAC
3	*F-box* 6801 exon 4 qRT reverse	GAGCTTGAAGGATACAAGCACAAT
4	*F-box* 6524 exon 4 qRT forward	CACTTGAGGTCATTGGGGTTATAC
5	*F-box* 6690 exon 4 qRT reverse	CTTGAACAGCTGAAGGTGTTAGGT
6	*F-box* 5890 exon 2 qRT reverse	TACGAATTTGGGAGCAAGAGATAG
7	*F-box* 5405 exon 1 qRT reverse	GATGGAAGGAGTTTTGATCTCTGA
8	*F-box* 560 forward	CATTGCAGGCTATTGGAGAA
9	*F-box* 626 reverse	TATTCTCACACCATCCCAAGTT
10	*F-box*4458 *Cla*I forward	AAATCGATAAACAAGAAAATGGGCTGAGAA
11	*F-box* 4317 *Cla*I forward	ATCGATCGATGAGTTTTTTCTGCATCTTC
12	*F-box* 4458 forward	AAACAAGAAAATGGGCTGAGAA
13	*F-box* XhoI reverse	TTCTCGAGCCTTGAAGCGGTTTCTTTGATTC
14	*F-box* 4406 forward	CCGTTAGTCGACGAAGAAACTC
15	*F-box* exon 1 reverse	AGTCCGATCATCAACAAGGTTT
16	*F-box* 750 forward	AAAAGAGTCGTCGAATTTGGAA
17	*F-box* ATG GW forward	AAAAAGCAGGCTCCATGGTGAGTGAAGGAGCAACAA
18	*F-box* no ATG *Nde*I forward	AAACATATGGTGAGTGAAGGAGCAACAAGA
19	*F-box* STOP *Bam*HI reverse	AAGGATCCTCAATGCGCCGGGTGAGGGTA
20	*F-box* no ATG GW forward	AAAAAGCAGGCTCCGTGAGTGAAGGAGCAACAAGAA
21	*F-box* STOP GW reverse	AGAAAGCTGGGTATCAATGCGCCGGGGTGAGGGTAA
22	*F-box* no STOP GW reverse	AGAAAGCTGGGTAATGCGCCGGGTG AGGGTAAACG
23	*FASS* Promoter forward	GTTCTTCCCGAGACTTTGTCAGGT
24	*FASS* Promoter Nest forward	TTGAAGTTTGAAGCTTGGATCTCG
25	*FASS* intron 1 revrse	ACAGACTGTCCCAACAACCAAAAC
26	*FASS* exon 2 reverse	CGAGCAAGATTCTCTTCGTCTCAA
27	*FASS* exon 7 forward	TCCCTAATCTGGCACAACTGAGAG
28	*FASS* exon 8 reverse	GCAATTCCATTAGTTCCTGCAGAC
29	*FASS Nco*I no ATG forward	TCCATGGCCTATAGCGGATCTAGCGATGGT
30	*FASS* exon 11 reverse	CAGCAGTAGTGAGAAAGCCTCTCC
31	*FASS* 3`UTR reverse	AGCCATTTCATTAAACGTCACCAA
32	*FASS* exon 11 forward	GGTAAAATCGTGGCAGGCAATTC
33	*FASS* exon 10 forward	GCTGATGGGACCCTAACTGAGATT
34	*FASS* 5` UTR forward	CAGTTCCTGGTTCAGTCTCACCAT
35	*FASS* STOP *Spe*I reverse	GACTAGTTCACTGAGACTCTTCCTCAGGT
36	*FASS* STOP *EcoR*I reverse	AAGAATTCTCACTGAGACTCTTCCTCAGG
37	*FASS* no ATG *Eco*RI forward	AAGAATTCTATAGCGGATCTAGCGATGGT
38	*FASS* no ATG *Nco*I forward	AACCATGGCTTATAGCGGATCTAGCGATGGT

39	*FASS* STOP *Cla*I reverse	AAAATCGATTCACTGAGACTCTTCCTCAGG
40	*PGase* exon 3 reverse	GAACACAATCCAATGCCTACGTTC
41	*PGase* exon 7/8 forwaed	AAGACTTGGCAGGGAGGACATGGA
42	*PGase* exon 9/8 reverse	TACCGCGGATTTCTGTTCGGGGCA
43	*PGase* exon 1 reverse	TTTAGCACCGAAAGTGTTGACGTT
44	*PGase* exon 1 Nest reverse	ATTGTGACCATGTTGATGTTGTCG
45	*PGase* 3`UTR reverse	TTTTTCTTGGGGATCAAAAGTGA
46	*PGase Bam*HI ATG forward	TGGATCCATGTATGAAAAGATCATAATCTTA
47	*PGase Eco*RI STOP reverse	TGAATTCTCAAGTGCAAAGAGGAGAAACATT
48	"*pgase*" mutant verification forwaed	CTATGAGGATGTAAATGCGGCTTG
49	"*pgase*" mutant verification Nest forward	CAGGCATACAACATGACGTCAAAA
50	pCHF1 LB out	CGCTTGGTGCTTATGTGATCTA
51	pCHF1 LB out Nest	TCGACATCGAGTTTCTCATAA
52	pCHF1 LB out Nest 2	GGTTCTTATAGGGTTTCCTCA
53	pCHF1 RB out	GTTACCCAACTTAATCGCCTTG
54	pCHF1 RB out Nest	AGCTTGGATCAGATTGTCGTTT
55	Genome Walker Long Adaptor	GTAATACGACTCACTATAGGGCACGGTGGTCGACGGCCCGGG
56	Actin RT-PCR forward	TCGGTGGTTCCATTGTTGCT
57	Actin RT-PCR reverse	GCTTTTTAAGCCTTTGATCTTGAGAG
58	Actin 2 exon1/2 forward	CGTACAACCGGTTTGTGCTGGATT
59	Salk T-DNA LB	TCGCCAGCTGGCGTAATAGCGAAGAG
60	Salk T-DNA LB nested	CTCCCTTTAGGGTTCCGATTTAGT
61	GABI-Kat LB forward primer	GTTTCTCATCTAAGCCCCCATTTG
62	GABI-Kat LB nested forward primer	TAACGCTGCGGACATCTACATTTT
63	*COR78* forward	GCGAAATTTCCAGGTGAATGAG
64	*COR78* reverse	CGATGGGCTTTGGTAGTGAATC

2.4 Seed Cultivation

Seeds were cultivated on a mixture of 3 times Einheitserde VM and 1 times sand. Plants were grown under 150µ Einsteins m^{-2} s^{-1} in 8.5 hours light/15.5 hours dark cycles with 18-20 °C.

2.4.1 Seed sterilization:

- Add 1ml ethanol (70 %), rotate them for 5 minutes
- Spin (short), remove ethanol
- Add 1 ml ethanol (95 %), let sit for 2 minutes
- Spin (short), remove ethanol
- Wash 3 times with sterile water
- Plate on MS media
- Store for 2 days at 4°C (dark)
- Transfer to growth chamber

2.4.2 Murashige & Skoog Salt Mixture medium (1 L)

- Take 0.22 % MS (Murashige & Skoog Salt Mixture, powder, Gibco Corporation)
- Add 8 g agar
- Fill to 1000 ml with ddH2O
- Autoclave (~20min)
- Cool to ~60°C
- Pour to plates

2.5 Molecular methods

2.5.1 Isolation of plasmid DNA

Plasmid mini and maxi prep kits (Peqlab and Invitrogen) were used to isolate plasmid DNA from transformed DH5α and XL1Blue bacteria (competent *E. coli* strain) that were transformed with different constructs according to the instructions provided with these kits. For verification of quality and quantity, 2-5 µl of the total DNA eluate were visualized on a 1% (w/v) agarose gel containing ethidium bromide.

2.5.2 Isolation of plant genomic DNA

2.5.2.1 Genomic DNA extraction from plants for Southern blot and Genome Walker analysis

Materials:

- Extraction buffer: 100 mM TRIS-HCl pH 8,5; 100 mM NaCl; 10 mM EDTA
- pH 8,0; 2% (W/v) SDS
- 1 x TE: 10 mM TRIS-HCl pH 8,0; 1 mM EDTA pH 8,0
- 3M Natrium-acetat pH 5,2
- 70 % ethanol
- 100% ethanol
- Chloroform = Chloroform : Isoamylalcohol 24:1
- Phenol: Chloroform : Isoamylalcohol (25:24:1)

Procedure:

- Grind 4x 0.25 g of young (!) leaves in liquid N2 to very fine powder
- Add 0.7 ml extraction-buffer to 2 ml Eppi on ice, transfer leaf poweder to Eppi and immediately mix by shaking
- Add 0.7 ml Phenol/ Chloroform/Isoamylalcohol and vortex 1 minute
- Separate phases by centrifugation at 4°C for 3 minutes at 15,300 rpm.
- Transfer upper aqueous phase in new Eppi, add 0.7 ml Chloroform/Isoamylalcohol and vortex 1 minute

- Transfer upper aqueous phase in new Eppi, add 0.7 ml Chloroform/Isoamylalcohol and vortex 1 minute
- Separate phases by centrifugation at 4°C for 3 minutes at 15,300 rpm.
- Transfer upper aqueous phase in new Eppi and add 1/10 Vol 3 M NaAc, pH: 5,2 (greenish solution turns violett-colorless) and add 2 volume 100 % ethanol
- Pellet DNA by centrifugation at 4°C for 10 miutes at 15,300 rpm.
- Resuspend PEL in 550µl 1x TE (if necessary warm to 65°C)
- Add 5 µl RNase A (10 mg ml^{-1}), incubate 1 hour at 37°C
- Extract with 200µl Phenol/Chloroform/Isoamylalcohol
- Separate phases by centrifugation at 4°C for 3 minutes at 15,300 rpm.
- Do 200 µl Chloroform/Isoamylalcohol extractions until no interphase is visible
- Transfer upper aqueous phase in new Eppi and add 1/10 Vol 3 M NaAc pH 5,2 and add 2 volume 100 % ethanol
- Resuspend DNA PEL in minimal volume of TE (ca. 30µl); check 1 µl on agarose gel

2.5.2.2 Genomic DNA extraction from plants (Quick prep for PCR)

Materials:

Buffer A: 10 M NaOH stock 20%Tween 20 stock dilute 1:10 for working concentration

Buffer B: 100 mM Tris-HCl (not normal Tris!) 2mM EDTA pH is 2.0 (adjust with HCl)

Procedure:

- Make fresh buffer A (5ml per 96 well plate:50 µl Tween-stock+4.45 ml H2O)
- Heat up PCR machine to 95°C Punch out a leaf disc from 1 young and green leaf with lid of 200 µl PCR tube (30mm^2/plant, rosette stage)
- Add 50 µl buffer A to each well and add 50 µl buffer B (not diluted) to each well, mix at moderate speed
- Spin down shortly
- Use 1-2 µl for PCR (in 25 to 50 µl volume)

2.5.3 Isolation of DNA fragments from agarose gel

To isolate DNA fragments (70 bp - 10 kb) from agarose gels, the Peqlab gel extraction kit was employed according to the manufacturer's instruction.

2.5.4 Polymerase chain reaction (PCR)

Polymerase chain reaction (PCR) is a method for enzymatic amplification and modification of a target DNA sequence flanked by two known sequences. PCR reactions were performed essentially as described in Sambrook and Russel (Sambrook and Russel, 2002). For special proofreading Taq polymerases the company recommended procedure were followed.

2.5.5 Reverse transcription-polymerase chain reaction (RT-PCR)

RT-PCR was carried out in two steps. Revert Aid^{H} Minus M-MuLV Reverse Transcriptase (Fermenats, EP0441) was used for first strand cDNA synthesis:

- Take 1µg template total RNA
- Add 1µl primer dT18 (0.5 µg/µl)
- Add deionized wtare (nuclease free) up to 12 µl
- Mix gently and spin down for 3-5 seconds
- Incubate the mixture at 70°C for 5 minutes chill on ice and collect drops by brief centrifugation
- Keep mixture on ice , add 4 µl 5X reaction buffer , µl Ribonuclease inhibitor (20 U/ µl) and 2 µl dNTP mix (10 mM) Mix gently and collect drops by brief centrifugation.Incubate samples at 37°C for 5 minutes
- Add 1 µl Revert Aid H Minus M-MuLV Reverse Transcriptase (200U/µl)
- Incubate the mixture at 42°C for 60 minutes
- Stop the reaction by heating at 70°C for 10 minutes
- Chill on ice

For subsequent normal PCR, 1 µl of the above RT-reaction product was used as cDNA template. As template total RNA for the reverse transcription reaction was not DNase treated a control reaction for each RNA preparation was performed in which the reverse transcription reaction was incubated without reverse transcriptase enzyme (enzyme replaced by equal volume of DEPC-water) to check in the following PCR for contamination by genomic DNA.

2.5.6 Semi quantitative reverse transcription polymerase chain reaction (SQ RT-PCR)

- Mesure RNA in photometer
- Do reverse transcription reaction (as described above) with equal quantities of RNA
- Run test PCR (94°C for 1:30; 94°C for 0:30; 55°C for 0:30;72°C for 0:30) with actin oligos; remove samples after 20,23, and 25 cycles; this should allow to adjust relative amount of cDNA for “real” PCR

2.5.7 Asymmetric interlaced (=TAIL) PCR

Adaptor ligation PCR is a simple method for finding unknown genomic DNA sequence adjacent to a known sequence such as a T-DNA (Siebert et al., 1995).

- Extract genomic DNA from plants, concentrate gDNA to high quantity
- Digest seperate aliquots of gDNA completely and partially with different restriction enzymes (5µg gDNA for each digestion reaction, for complete digestion 1.5 hours at 37°C and for partial digestion 20 minutes at 37°C)
- Inactivate digestion reaction by incubating at 65°C for 10 minutes

- Run a small aliquot of each digestion reaction on 0.7% agarose gel (10 minutes - 40V ,1,5 hours - 150V)
- Do the fill- in reaction for digested gDNA with 0.4µl dNTP and 2µl Klenow-fragment for those enzymes which produce sticky ends (*Hae*III produce blunt ends)
- Ligate the adaptors to digested gDNA
- Mix long and short adaptor in small quantity
- Incubate at 80°C in water bath for 30 minutes
- Turn of f water bath, leave the sample there to cooling
- Take 10 µl digested DNA, 4µl from mixed Adaptors, 2µl PEG 8000, 2µl T4-ligase buffer and 2µl T4-ligase
- Put ligation reactions at 16°C for 12h and 70°C for 5minutes
- Add 60µl 1mM TE to each ligation reaction
- Run 1st PCR with adaptor (AP1) ,T-DNA oligos and ligation mixture as a template (7 cycles: 94°C for 5:00, 94°C for 0:25, 72°C for 3:00**;** 32 cycles: 94°C for 0:25, 67°C for 3:00, 67°C for 5:00, 4°C for ever)
- Run 2nd PCR with AP2 and T-DNA nested oligos, take 1µl from first PCR product as a template for second PCR (5 cycles:94°C for 5:00, 94°C for 0:25, 72°C for 3:00**;** 30 cycles: 94°C for 0:25, 67°C for 3:00, 67°C for 5:00, 4°C for ever)
- Test PCR products on an agarose gel
- Clone and analyze major PCR products

2.5.8 Restriction enzyme digestion

Restriction and ligation reactions were performed essentially as described in Sambrook and Russel (Sambrook and Russel, 2002).

2.5.9 DNA sequencing

Some sequencing reactions were kindly performed by Jost Muth and colleagues at the Institute of Molecular Biotechnology, RWTH Aachen. 20 pmol of the used primers were added to 1.2- 1.5 µg of plasmid DNA and sequencing reactions were performed using the di-desoxy chain termination method with labeled nucleotides and a cycle sequencing protocol (Sanger et al., 1997). And another sequencing reactions were performed by Seqlab company.

2.5.10 Isolation of total RNA from plant leaves (Sauerbruun and Schlaich, 2004)

Materials:

- TRI-REAGENT: 0.4 M ammonium thiocyanate, 0.8M guanidinium thiocyanate, 0.1M Na-acetate, 5 % (v/v) glycerol, 38 % (v/v) acidic phenol, adjust pH to 5 with glacial acetic acid
- Phenol (TRIS pH 8,0 equilibrated)
- Chloroform / Isoamylalcohol 24:1
- 100% ethanol

- Na-acetate 3 M (preprared with RNase free water)
- RNase-free water

Procedure:

- place frozen (-70°C) leaf tissue in 1.5ml tubes and in liquid nitrogen
- To one and a half to two *Arabidopsis* leaves add 650 µl TRI-Reagent (0.4M ammonium thiocyanate/0.8M guanidinium thiocyanate/0.1M Na-acetate/5% (v/v) glycerol/38% (v/v) water-saturated phenol, adjust pH to 5 with glacial acetic acid; depending on the leaf size; too much tissue causes problems with polysaccharides. It may be helpful to use more TRI-Reagent in this case.
- Thoroughly (no more clumps) homogenize the leaves with a drilling machine supplemented with a Teflon tip (it is worthwhile to do a first homogenization step with frozen tissue by crushing the leaf tissue once with the tip, then add the TRI-Reagent)
- Add another 350 µl of TRI-Reagent
- Vortex and keep at room temperature for at least 10 minutes (start to count from the last tissue sample)
- Add 100 µl of bromchloropropane and vortex for exactly 10 seconds
- Keep at room temprature for 10 minutes
- Spin for 10 minutes at 14000 rpm and 4°C in a microfuge
- Transfer the upper, aqueous phase to a new tube
- Extract aqueous phase again with bromchloropropane
- To the aqueous phase, add an equal volume of isopropanol
- Mix and precipitate the RNA for 15 minutes at room temprature
- Spin for 10 minutes at 4°C and 14000 rpm in a microfuge
- Decant supernatant
- Wash pellet with 70% ethanol
- Decant supernatant, dry pellet and dissolve in 10-25 µl of RNase-free water
- Store at –70°C (or at –20°C)
- Determine OD_{260} by adding 2 µl of the RNA soln to 1 ml of RNase-free water. 1 OD_{260} equals to about 40 µg RNA/ml. Determine RNA concentration of each sample and set to a same concentration by dilution with water
- Run a 1% (w/v) TAE/agarose test gel at 5V/cm with 1 µl RNA supplemented with 1 µl formamide (containing a small amount of bromphenol blue) and make RNA visible by ethidium bromide staining

2.5.11 Northern blot

Materials:

- 10x MOPS buffer: 200 mM MOPS; 50 mM sodium acetate; 10 mM EDTA; adjust pH to 7.0 with NaOH

- 20 x SSC: 3.0 M NaCl ; 0.3 M Citric acid- mono hydrate: adjust pH to 7.0 with NaOH
- 37% Formaldehyde
- Ethidium bromide
- 2x RNA loading buffer (MBI Fermentas, St. Leon-Rot, Germany)
- RNase-free water
- Agarose
- 3MM Whatman paper
- Nylon membrane
- Paper towels
- Stratalinker at "AUTO" setting

Procedure:

- Dry 20 µg total RNA per lane in speedvac (for 4 lanes take 80 µg total RNA)
- Dissolve dried RNA in 10 µl RNase-free water and 10 µl 2x RNA loading buffer by Incubating at 65°C shaking for 10 minutes (for 4 lanes take 42 µl RNase-free water and 43µl 2x RNA loading buffer
- Load 20 µg RNA (=20µl) on a 1% Agarose gel (dissolve 1.6 g Agarose by boiling in 16 ml 10x MOPS buffer + 130 ml RNase-free water; after cooling to 55°C add 17.5 ml 37% Formaldehyde and 150 µg Ethidium bromide (both are toxic: use gloves and do everything under the fume hood!!!) (Do not need to Ethidium bromide because add it to loading buffer)
- Run gel with 3V per cm^{-2} in 1x MOPS buffer until fast blue dye migrated about 7 cm
- Take a picture of gel on UV-plate after running
- Place 2 of 3 MM whatman papers on the paper bridge and wet them completely and flat them carefully, and upset gel on it, float the nitrocellulose filter on surface of dish that gel placed into it, place 3MM whatman paper (membrane touch completely they have to be wet with 6xSSC, make sure no air bubbles between them and gel
- Transfer RNA onto positively charged nylon membrane using RNase-free 6xSSC for more than 16 hours
- Cross-link RNA to membrane using Stratalinker at "AUTO" setting
- Staining membrane with methylene blue (with shaker 1-2 minutes, and washing with destilled water 3 times until background be white and mark ladder
- Put in a plastic packet
- Store membrane until use (short-term) at +4°C slightly moistened with RNase-free, sterile 6xSSC, or store membrane in –20 °C for longer time

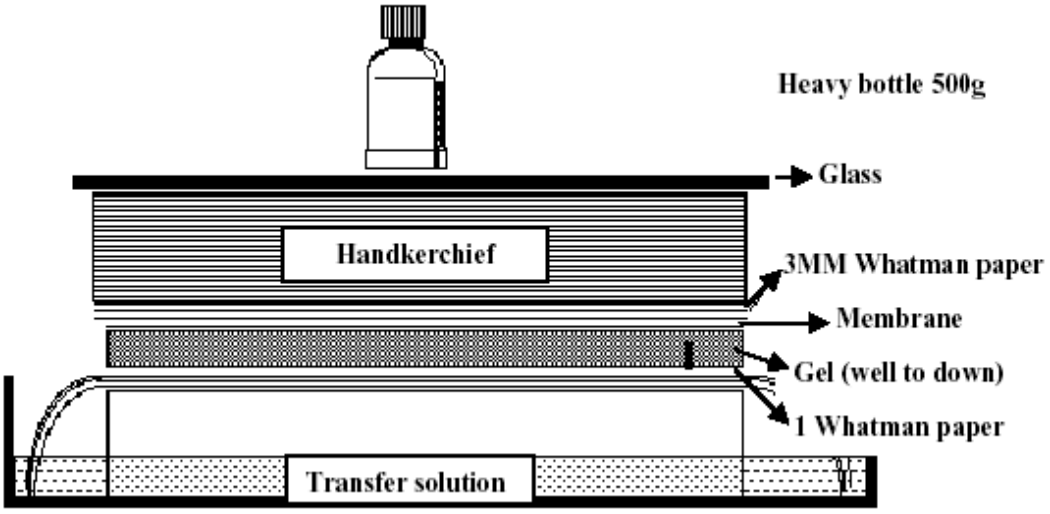

Figure 2-11. Schematic represenation of northern blot experiment performance, required components and the order of components position.

2.6 Microbiological methods

2.6.1 Culture of bacteria

2.6.1.1 Culture of Pseudomonas syringae

Materials:

KB:

- 20 g L^{-1} Peptone (proteose);
- 1,59 g L^{-1} K_2HPO_4;
- 10 ml L^{-1} (=12 g) Glycerol;
- 15 g L^{-1} agar for solid medium;
- PH should be adjusted to 7,2 with 1 ml 5% H3PO4;
- Sterilize by autoclaving for 20 minutes

Procedure:

- Melt KB solid medium in microwave
- Add appropriate antibiotic to the medium (37 °C)
- Pour medium in two small plates
- Inoculate plates with bacteria kept in –80 °C freezer
- Incubate at 28 °C for two days

- Pour 10 ml of liquid medium in bottles
- Add 10 µl Tet and 10 µl Rif to both of plates
- Place on shaker at 28 ° C overnight
- Centrifuge 15 minutes at 28 °C, 5000 – 6000 rpm.
- Throw supernatant away
- Resuspend pellet in 10 mM $MgCl_2$ with loop (10 ml of the same medium volume)
- Dilute them 1/10 with $MgCl_2$, if they have high concentration (spectrophotometer can read a range between, 0,1 – 0,5)
- Measure CFU (colony forming per unit) with spectrophotometer
- Dilute solution to 3 forms: 5 × 107 , 5 × 106 , 5 × 105 (need 1,5 ml per pot)
- Infiltrate plants

2.6.1.2 Infiltration of P. syringae

- Take six weeks old plants from growth chamber and label the best leaves.
- Spray on them with tap water
- Spray on the lid of tray
- Close the lid of tray
- Wait 30 minutes
- Infiltrate from the lowest concentration at first with syringe
- Dry the back of leaves
- Put them in growth chamber

2.6.1.3 Infection of plants with Hyaloperonopsora arabidopsidis

Infection of plants with different isolates of this pathogen was performed kindly with M.Hermanns as described in (Hermanns et al., 2003).

2.6.1.4 Culture of Escherichia coli

Materials:

LB:

- 10 g L^{-1} Bacto-Tryptone;
- 5 g L^{-1} Bacto-Yeast extract;
- 10 g L^{-1} NaCl;
- distilled H_2O to make a final volume of 1 L;
- PH should be adjusted to 7.0 with 5 N NaOH (0.2 ml);
- Sterilize by autoclaving for 20 minutes

Procedure:

E. coli was cultured in LB medium on a platform shaker at 37°C.

2.6.1.5 Culture of Agrobacterium tumefaciens

Materials:

YEP:

- 10 g L^{-1} peptone;
- 10 g L^{-1} yeast extract;
- 5 g L^{-1} NaCl;
- 15 g L^{-1} agar solid medium;
- PH should be adjusted to 7,0 with 1 ml 5N NaOH;
- Sterilize by autoclaving for 20 minutes

Procedure:

A. tumefaciens was culture in YEB medium at 28°C.

2.6.2 Transformation of bacteria

2.6.2.1 Making and transformation of electrocompetent E. coli

Materials:

2xYT:

- 16 g L^{-1} tryptone;
- 10 g L^{-1} yeast extract;
- 5 g L^{-1} NaCl;
- pH should be adjusted to 7 with 3 ml 1 N NaOH;
- 15 g L^{-1} agar for solid medium;
- Sterile 10% glycerol
- Sterile water
- Sterilize by autoclaving for 20 minutes

Procedure:

- Add about 2 ml of 2xYT medium to sterile glass tube under sterile conditions
- Add a small loop of *E. coli* from –80°C stock (thaw frozen culture only partially with hand and return quickly to –80°C freezer)
- Allow bacteria to grow overnight at 37°C shaking at 200 - 220 rpm
- Dilute overnight culture at least 1:100 under sterile conditions in fresh medium (add about 2 ml overnight culture to 200 ml fresh medium in 1L Erlenmeyer flask)
- Measure OD_{600} nm (1= $1*10^{6}$) before placing culture in 37°C shaker
- Precool Heraeus centrifuge to 4°C

- When OD_{600} nm reaches 0.5 (approx. 2 hours), place Erlenmeyer flask in ice-water for 10 minutes
- Harvest bacteria in cool Heraeus centrifuge for 5 minutes with 3,500 rpm at 4°C
- Discard supernatant (SUP) and carefully resuspend *E. coli* pellet (PEL) with a sterile plastic loop in 200 ml ice-cold sterile 10% glycerol, so that no clumps are left.
- Harvest bacteria in Heraeus centrifuge for 5 minutes with 3,500 rpm at 4°C
- Discard SUP and carefully resuspend PEL with a sterile plastic loop in 100 ml ice-cold sterile 10% glycerol, so that no clumps are left
- Harvest bacteria in Heraeus centrifuge for 5 minutes with 3,500 rpm at 4°C
- Discard SUP and carefully resuspend PEL with a sterile plastic loop in 5 ml ice-cold sterile 10% glycerol, so that no clumps are left
- Harvest bacteria in Heraeus centrifuge for 5 minutes with 3,500 rpm at 4°C
- Discard SUP and carefully resuspend PEL with a sterile plastic loop in remaining, so that no clumps are left
- Keep solution of competent *E. coli* on ice
- Place electroporation cuvettes on ice
- Add 45 µl of competent *E. coli* to plasmid DNA
- Incubate on ice for approx. 5 minutes
- Switch on electroporation apparatus
- Change setting to Ec2 (with arrow up button)
- Transfer *E. coli* with plasmid to electroporation cuvette, wipe cuvette with dry paper insert into sledge and press the "pulse" button (time constant should be around 5.8 ms)
- Immediately after the pulse add approx. 1 ml of ice-cold SOC- or 2xYT-medium to cells
- Collect them from the cuvette with sterile pasteur pipette and transfer them back into Eppi tube
- Rotate tube for about 1 hour at room temprature on the wheel
- Plate 100 µl of electroporated *E. coli* on solid medium containing antibiotic
- Collect remaining approx. 900 µl of *E. coli* by centrifugation at 7,000 rpm for 1 minute
- Discard most of the SUP and resuspend PEL in remaining 50 – 100 µl
- Plate this onto solid medium containing antibiotics

2.6.2.2 Making and transformation of chemically competent E. coli

Materials:

TB-JAP:

- 10 mM PIPES;

- 15 mM $CaCl_2$ $2H_2O$;
- 250 mM KCl;
- Adjust pH to 6.7 (KOH);
- 55 mM $MnCl_2$; filter sterilize (forms brown precipitate when autoclaved or stored for longer times at –20°C; then it is not good anymore and has to be discarded!)

Procedure:

- Start from single colony a 2.5 ml LB (for XL1 Blue with Tet^{30}; for MC1061 no antibiotic!) overnight culture at 37°C. Precool centrifuges and rotors
- Inoculate 250 ml LB (for XL1 Blue with Tet^{30}; for MC1061 no antibiotic!) with o/n culture and grow at 18°C (!) until OD_{600} of 0.6. Chill bacterial culture for 10 minutes in ice water.
- Harvest bacteria at 4°C in sterile 50 ml blue cap tubes (4°C cold Heraeus: 2500x g, for 5 minutes)
- Resuspend bacterial pellet in 100 ml ice cold, sterile TB-JAP to which 2 ml DMSO have been added
- Keep on ice for 5 minutes
- Harvest bacteria at 2500x *g*, for 5 minutes in 4°C cold Heraeus
- Resuspend bacterial pellet in 18.6 ml ice cold TB-JAP to which 1.4 ml DMSO have been added
- Keep on ice for 5 minutes
- In cold room dispense 100 µl aliquots into sterile tubes and immediately freeze in liquid nitrogen
- Store at –80°C (Inoue et al., 1990).

2.6.2.3 Making of and transformation of chemical competent Agrobacterium cells

Materials:

- YEP medium
- Sterile 10% glycerol

Procedure:

- Grow 2 ml culture of Agro strain GV3101+pRK in YEP $+Rif^{100}$ $+Kan^{50}$ overnight at 28° shaking
- Inoculate 100 ml YEP + Rif^{100} $+Kan^{50}$ with 1 ml of over-night culture; shake at 250 rpm, 28°C until OD_{600} reaches 1-1,5 (might be 16-24 h)
- Chill cells in ice-water for 10 minutes
- Harvest cells in Heraeus centrifuge at 3500 rpm 4°C for 5 minutes

- Resuspend cell PEL in 100 ml ice-cold sterile 10% glycerol
- Harvest cells in Heraeus centrifuge at 3500 rpm 4°C for 5 minutes
- Resuspend cell PEL in 10 ml ice-cold sterile 10% glycerol
- Harvest cells in Heraeus centrifuge at 3500 rpm 4°C for 5 minutes
- Resuspend cell PEL in 500 µl ice-cold sterile 10% glycerol
- Aliquot 50 µl into cooled Eppi tubes and freeze in liquid N2
- Add 1µg of T-DNA plasmid to thawed cells
- Let sit on ice for 3 minutes
- Electroporate (2,5 kV, 200 Ohm, 25 µF) in 0.2 mm gap cuvettes (time constant should be around 6,3)
- Add immediately 1 ml of YEP and incubate cells for 1 hour on wheel after pulsing
- Plate 50–100 µl on YEP containing Rif, Kan (and appropriate antibiotic for new plasmid)
- Incubate plates for 2- 3 days at 28°C until colonies appear

2.6.3 Gateway Technology to clone DNA sequences for functional analysis and expression

2.6.3.1 BP Recombination

Reaction:

Perform a BP recombination reaction between an attB-flanked DNA fragment and an attP-containing donor vector to generate an entry clone.

Add the following components to a 1.5 ml microcentrifuge tube at room temperature and mix:

- 1-10 µl, attB-PCR product or linearized attB expression clone (40-100 fmol)
- 2 µl, pDONR™ vector (supercoiled, 150 ng/µl)
- 4 µl, 5X BP Clonase™ reaction buffer
- Add X µl TE Buffer, which total volume reaches 16 µl, pH 8.0
- Vortex BP Clonase™ enzyme mix briefly
- Add 4 µl to the components above and mix well by vortexing briefly twice.
- Incubate reaction at 25°C for 1 hour
- Add 2 µl of 2 µg/µl Proteinase K solution and incubate at 37°C for 10 minutes.
- Transform competent E. coli and select for the appropriate antibiotic-resistant entry clones

2.6.3.2 LR Recombination

Reaction:

Perform an LR recombination reaction between an attL-containing entry clone and an attR-containing destination vector to generate an expression clone.

Add the following components to a 1.5 ml microcentrifuge tube at room temperature and mix:

- 1-10 µl, Entry clone (supercoiled, 100-300 ng)
- 2 µl, Destination vector (supercoiled, 150 ng/µl)
- 4 µl, 5X LR Clonase™ reaction buffer
- Add X µl TE Buffer, which total volume reaches 16 µl, pH 8.0
- Vortex LR Clonase™ enzyme mix briefly
- Add 4 µl to the components above and mix well by vortexing briefly twice
- Incubate reaction at 25°C for 1 hour
- Add 2 µl of 2 µg/µl Proteinase K solution and incubate at 37°C for 10 minutes
- Transform competent *E. coli* and select for the appropriate antibiotic-resistant expressio clones

2.7 Biochemical methods

2.7.1 Extraction of proteins from plant leaves

- Ground frozen leaves in liquid nitrogen to a fine powder with a mortar and pestles
- Add the same amount of 2 x SDS sample buffer
- Spin down (30000 x g) at 4°C for 15 minutes
- Take supernatant and discard PEL

2.7.2 Determination of protein concentrations in leaf extracts (Bradford, 1976)

Materials:

- Bradford reagent: 100 mg L^{-1}
- Coomassie Brilliant Blue G 250; 50mg L^{-1}
- Ethanol 96% (v/v); 100 mg L^{-1} phosphoric acid 85% (v/v)
- Bovine serum albumin pH 7.0 (Serva)

Procedure:

- Mix 2 µl of leaf protein with 1 ml of Bradford reagent
- Incubate 15 minutes at RT
- Measure the basic extinction, against a reagent blank prepared from 2 µl of the corresponding extraction buffer and 1 ml of Bradford reagent at 595 nm wave length
- Draw a standard curve in a range between 1 and 10 µg protein using Bovine serum albumin pH 7.0 (Serva)

2.7.3 SDS-Polyacrylamide Gel electrophoresis

Materials: 5X Running buffer:

- 15 g Tris Base;
- 72 g Glycine;
- 5 g SDS;
- pH shoiul be adjusted to 8.3 (1 liter)

Procedure:

- Make SDS-polyacrylamide gels (for the stacking gel: 5 % (w/v) acrylamide/bisacrylamide 29:1, 0.125 M Tris/HCl, pH 6.8; for the separating gel: 10 % (w/v) acrylamide/bisacrylamide 29:1, 0.375 M Tris/HCl, pH 8.8), (Laemmli, 1970).
- Mix protein sample with 2 x SDS sample buffer
- Boil at 95°C for 5 minutes
- Chill on ice and spin down for 5 seconds
- Harvest supernatant as protein sample
- Load into submerged wells
- Run SDS-PAGE gel with 1 x SDS-PGAE electrophoresis buffer for 120 minutes at 120 V/cm
- Stain it with Coomassie Berilliant Blue (2-7-4) or transfer onto a nitrocellulose membrane for western blot analysis (2-7-5), (Ausubel et al., 1994).

Table 2-4 SDS-PAGE separating gels (12 ml=sufficient for 2 mini-gels with 1mm spacer).

Mterials/Gel%	7.5%	10%	12%	15%	20%
H_2O	4.83 ml	3.96 ml	3.38 ml	2.53 ml	1.1 ml
4X Seperating gel buffer(1M Tris pH 8.8, 0.4% SDS)	2.87 ml	2.87 ml	2.87 ml	2.87 ml	2.87 ml
2% PAA	1.8 ml	1.8 ml	1.8 ml	1.8 ml	1.8 ml
40% Acrylamid	2 ml	2.87 ml	3.45 ml	4.3 ml	5.75 ml
10% Ammoniumpersulafte (APS)	50 ml	50 ml	50 ml	50 ml	50 ml
TEMED	25 µl	25 µl	25 µl	25 µl	25 µl

Table 2-5 SDS-PAGE stacking gel.

Mterials/Gel%	5%
H_2O	3.86 ml
4X Stacking gel buffer (1M Tris pH 6.8, 0.4 % SDS)	0.85 ml
40% acryamid/0.8% bisacrylamid	0.59 ml
10% Ammoniumpersulafte (APS)	30 µl
TEMED	30 µl
Bromophenolblue	10 µl

2.7.4 Rapid ethanol-based Coomassie Blue staining of SDS-polyacrylamide gels

Materials:

- Low-toxicity staining solution: 0.25g Coomassie Blue R-250; 100 ml ethanol; 100 ml water
- Stir until dye is completely dissolved, about one hour
- Add 25 ml acetic acid and make to 250 ml with water
- Store at room temperature in a dark bottle. The final solution is 0.1% Coomassie Blue, 10% acetic acid, 40% ethanol
- Destaining solution: 400 ml ethanol; 100 ml acetic acid; make to 1000 ml with water
- Store at room temperature

Procedure:

- Place minigel in a loosely covered glass or microwaveable plastic (e.g. tupperware) container, ideally on top of plastic mesh if available
- Cover gel with 250 ml of staining solution
- Microwave loosely covered gel/stain on high for approximately 2 minutes or until the solution just begins to boil. (Gels of 10-12% acrylamide are quite robust and will not be damaged even if the solution is boiled for a few minutes)
- Place the loosely covered gel/stain container on a slow shaker or simply leave on the bench for 15-60 minutes. It is usually possible to discern bands after as little as 15 minutes
- Remove stain from the container (it can be reused many times) and rinse the gel and gel container with water to remove excess staining solution
- Cover gel with 200-250 ml of destaining solution (staining solution minus dye)
- Microwave on high for approximately 2 minutes or until the solution just begins to boil
- Place the loosely covered gel/stain container on a slow shaker or simply leave on the bench for 1-24 hours. For rapid destaining, change the destaining solution after one hour and microwave. One to three changes are usually sufficient to visualize bands with a clear background (2-4 hours total destaining time). For overnight destaining, place one large or several small crumpled Kimwipe tissues in the destaining solution to bind up dye, and agitate on a slow shaker
- Destained gels are rinsed throroughly with and stored in distilled water. Rinsed gels can be immediately dried in a membrane air-dryer for longer term preservation

2.7.5 Western blot (Wet blotting)

Materials:

- Ponceau solution (RT): 0,2% Ponceau S in 3% TCA

- 10 x TBS (RT): 87.7 g NaCl (1.5 M) + 60.5 g Tris/HCl (500 mM) total volume 1 L pH 7.5
- 10 x blotting buffer (RT): 144 g Glycine (1.92 M) + 30 g Tris (250 mM) + 10 ml 20 % SDS (0.2 %)
- Tris-Buffered Saline Tween-20 (TBST)
- Dissolve 8.8 g of NaCl, 0.2 g of KCl, and 3 g of Tris base in 800 ml of distilled H_2O
- Add 500 ul of Tween-20
- Adjust the pH to 7.4 with HCl
- Add distilled H_2O to 1L
- Sterilize by autoclaving

Procedure:

- Remove separating gel
- Wet 4 blotting papers and Nitrocellulose membrane and sponges in 1x blotting buffer (mix 100 ml 10x blotting buffer + 100 ml methanol and 800 ml d H2O) and wet them completely)
- Place sponge on plastic support
- Place 2 blotting papers on the sponge on the black support (negative bar)
- Place gel on the papers without air bubbles (!) and smooth it
- Mark nitrocellulose membrane to detect the sample direction and put on the gel
- To remove air bubbles roll it with pipet
- Place 2 blotting papers on sandwich and remove the bubbles
- Close sandwich carefully
- Push sandwich in the tank in which an ice block was placed before (lid of sandwich up). If protein of interest is of low molecular weight, adjust power supply to 300 mA for 90 minutes
- Stain membrane with Ponceau S solution, to see the bands; destain with bidest
- Transfer membrane to 10-15 ml of 1xTBST or 1xPBST + 5% milk for 30 minutes to 2 hours to block the membrane at room temperature (if background is high try blocking at 37°C)
- Add 0,2 to 0,5 µl primary (specific) antibody and incubate it for 1.5 to 2 hours at room temprature or overnight at 4°C on rocking platform
- Wash 5 times with plenty 1xTBST or PBST each time 5-10 minutes
- Place membrane in 10-15 ml of 1xTBST + 5% milk and add secondary antibody conjugate (HRP=horseradish peroxidase) in our case anti rabbit IgG peroxidase
- Incubate 45 minutes to 2 hours at room temprature on rocking platform
- Wash 5 times with plenty of 1xTBST or PBST each time 5-10 minutes

2.7.6 Protein interaction using GAL4 Yeast-two-hybrid systems

This assay is based on the fact that the eukaryotic transcriptional regulator GAL4 is composed of physically separable, functionally independent domains: one acts as the DNA–Binding domain while

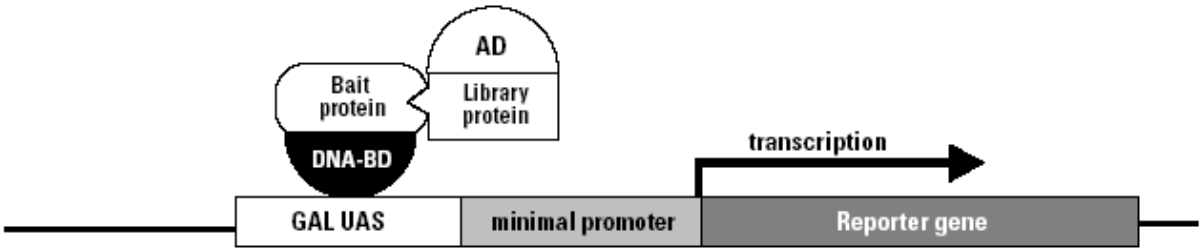

Figure 2-12 Schematic diagram of the Matchmaker GAL4 two-hybrid system.
The DNA-BD is amino acids 1–147 of the yeast GAL4 protein, which binds to the GAL UAS upstream of the reporter genes. The AD is amino acids 768–881 of the GAL4 protein and functions as a transcriptional activator. The reporter genes (HIS3 and lacZ) are integrated in theY190 genome.

the other functions as the transcriptional activation domain (Figure 2-12). The DNA–binding domain (DNA-BD) localizes the transcriptional factor to specific DNA sequences present in the upstream region of the GAL1 gene that is regulated by this factor, while the activation domain (AD) directs the RNA polymerase II complex to transcribe the gene downstream of the DNA binding site. Both domains are required for normal activation function, and normally two domains are part of the same protein. The yeast strain Y190 contains a reporter gene to detect interaction between two fusion proteins, the HIS3 gene under the control of GAL1 UAS and a minimal promoter containing both HIS3 TATA boxes (TC+TR , Flick and Johnston,1990). The result is high-level expression (due to the GAL1 UAS) when induced by a positive two-hybrid interaction. In addition, it contains the lacZ gene as reporter, also under the control of GAL1 UAS and GAL1 promoter.

2.7.7 Yeast cell protein extraction procedure

Materials:

Yeast medium:

- 1.7 g L^{-1} YNB (yeast nitrogene base); 5g L^{-1} $(NH_4)_2SO_4$; 20 g L^{-1}; Glucose; 0.7 g L^{-1};
- CSM (complement suplement mixture);
- For solid medium 18 g L^{-1} agar ;
- For Gal gene activation instead of glucose: 5 g L^{-1} D- raffinose and 10 g L^{-1} galactose.

Procedure:

- Choose singles colonies and streak them on ¼ of a petridish therefore you propagate a single colony
- Take each of them from dish and grow ~ 50 ml culture overnight in proper medium
- Harvest yeast cell in 20 OD_{600} (for example: dilute 1/10 and measure OD_{600} =0.083 , multiple to 10 = 0.83, divide 20 to 0.83 = 23) by centrifugation in 3000 rpm, 3 minutes in Heraeus centrifuge machine
- Transfer into 2 ml safe lid Eppendorf (with a extra part in lead that it make easy open and close the lid) with ~ 1 ml H_2O
- Spin for 10 seconds, Eppendorf centrifuge with maximum speed
- Suck off water

- Add 400 µl 2 x SDS gel loading buffer :
- Add glass beads (~ ¾ volumes)
- Vortex 1 minutes
- Boil for 2 minutes at 95°C and vortex and repeat it (4 minutes boiling)
- Spin for 10 seconds , Eppendorf centrifuge, maximum speed
- Transfer supernatant with 100 µl micropipet to new tube
- Ready to be loaded on the SDS gel or keep in –20 °C

2.7.8 Yeast plasmid extraction

Materials:

- Lysis buffer: 100 mM NaCl; 10 mM TRIS pH8.0; 1 mM EDTA; 0.1% SDS.
- Phenol: $CHCl_3$: Isoamylalcohol 25: 24: 1.

Procedure:

- Pick a 2-3 mm yeast colony into 200 µl lysis buffer
- Add an equal volume of glass beads
- Vortex vigorously for 1-2 minutes
- Extract with phenol: CHCl3: Isoamylalcohol
- Extract with $CHCl_3$
- Precipitate DAN with ethanol
- Wash once with 80% ethanol
- Resuspend in about 80 µl TE
- Use 5 µl for PCR or 2 µl to transform *E.coli*

2.7.9 Yeast transformation

Materials:

- 0,1 M Lithium acetate
- 1 M lithium acetate
- 50 % PEG
- Fish sperm DNA (HSP)

Procedure:

- Add yeast to 5 ml YPD medium in 100 ml Erlenmeyer flask, incubate it overnight in 28°C
- Measure OD_{600}=0.2-0.3 increase medium to 50 ml, incubate 2 hours at 28 °C until OD_{600} reaches to 0.6
- Pour them to sterile 50 ml Falkon tube and spin it at room temprature for 5 minutes at 2000 rpm.

- Throw away supernatant and wash pellet with 50 ml bidest autoclaved water and spin for 5 minutes at room temprature in 2000 rpm.
- Take the cell in 1 ml 0,1 M Lithium acetate in sterile 1.5 Eppendorf tube
- Spin 15 seconds at room temprature in 14000 rpm.
- Throw away supernatant and resuspend pellet with 400 µl 0.1 M Lithium acetate by
- pipet, vortex shortly
- Take 50 µl cell suspension, centrifuge shortly, throw away supernatant
- Add: 240 µl PEG (50 % polyethylene glycol), 36 µl 1M Lithium acetate, 10 µl Fish sperm-DNA (10 mg ml^{-1}), X µl plasmid (1µg/partner), X µl sterile water to total volume 60 µl
- Incubate 1 minute at room temprature, then vortex
- Incubate 30 minutes at 28 °C on rotator
- Add 36 µl sterile water incubate 15 minutes at 42 °C
- Spin 15 seconds at room temprature with 6000 rpm.
- Aliquote them in 200 µl parts
- Strike 100 µl of them on each plate

2.8 Histochemical analyses

2.8.1 GUS staining protocol (Protz, RWTH Aachen)

Materials:

- Staining solution: 500 mg l^{-1} X-Glucuronide (solve in 5 ml dimethyfromamid), 50 mM sodium phosphate buffer (pH 7.0)
- Fixation solution: 3.0% formaldehyd; 0.3 M mannitol; 10 mM MES; (pH 5.6)

Procedure:

- Cut the tissue and fix them into fixation solution for 45 minutes
- Wash tissue two times with 50mM sodium phosphate buffer
- Incubate overnight into staining solution (Incubation time depends on to promoter)
- Destaining with 70% etanol until chlorophyll is washed (It lasts for 2 weeks)

2.8.2 Staining of the *Hyaloperonospora.arabidopsidis* infected leaves

The staining of the infected leaves on day 3 after inoculation of the plants was performed according to the procedure described in (Keogh et al., 1980).

2.9 Generation and characterization of transgenic plants

2.9.1 Transformation of *Arabidopsis* plants through *Agrobacterium*-mediated floral dip transformation

- Grow 2 – 4 plants per 25 cm^2 pot at 24°C day (150 µ Einsteins m^{-2} s^{-1})/ 20°C night, 18 hours light
- When most plants have first inflorescence, clip it
- Allow secondary inflorescence to regrow for 4 – 8 days (until 1 – 10 cm tall)
- Grow *Agrobacterium* culture for at least 48 hours at 25°C- 28°C until OD_{600} of at least 2
- Dilute bacteria into 5% sucrose; 0.04% Silwet L-77 to OD_{600} 0.8
- Submerge aerial parts of *Arabidopsis* into *Agrobacterium* solution for 3 – 10 minutes
- Spray *Arabidopsis* inflorescences with left over bacteria until really wet. Return *Arabidopsis* into 16°C dark chamber covered with plastic dome for 16- 24 h.
- Return plants to regular growth conditions and harvest seeds from brown dried siliques (Clough and Bent, 1998).

2.9.2 Selection of the transgenic plants

- Sterilized seeds and cultivated on selective medium
- Select resistance plants seedling to proper antibiotic or BASTA and transplant them
- Harvest the seeds from resistance and cultivate them in next generation (30 plants)
- Select plants that show 3:1 resistance to sensitive segregation proporation (10 plants)
- Cultivate half of the seeds form above mentioned 10 plants and look for homozygous plants
- Select 3-4 homozygous plants and test them with molecular method

2.9.3 Crossing *Arabidopsis* plants (flower emasculation and flower preparation for fertilization)

Prior to performing the experiments, maturing flowers must be present in the bolting *Arabidopsis* plants.

- Preparation of recipient flower (ovary). The objective is to remove all the flower parts except the ovary
- Choose an inflorescence and remove all the flowers that are too young (too small) and the ones that already show white petals (opening flowers will tend to have started self-fertilization)
- Cut both too young and too old flowers from inflorescence, leaving 3-10 flowers in the middle
- Cut of all other plant parts in the immediate vicinity, especially cliques. The idea is to have as free a work environment as possible

- While cutting parts of from flowers, DO NOT tare parts off. Flowers are delicate and be easily damaged. Practice will give a good feel for how much they can take
- In between flowers, clean forceps by dipping them in 95% ethanol followed by distilled water
- Use a Kim-wipe as surface while viewing the flowers on a dissecting scope. This helps in holding the flower parts to the paper and not the forceps
- Obtain pollen by getting fully mature flowers and removing the stamens. Use these stamens to brush the prepared ovaries. Repeat this at least twice to make sure there is plenty of pollen at the tip of the flower. This should be evident when looking at the ovaries through the a dissecting scope as the pollen looks like a grainy brownish surface on top of the green ovary
- Label the cross accordingly
- Leave ovaries developing until they start yellowing before harvesting. If too dry, they may shed their seeds

3 RESULTS

3.1 "*pgase*" mutant

3.1.1 Isolation of "*pgase*" mutant

An independent randomly occurring mutant was isolated after the generation of *Arabidopsis* transgenic lines in the Ta-0 accession in our lab. This mutant showed striking morphological alterations as compared to wildtype plants and was called the polygalacturonase (*pgase*) mutant since the molecular analysis results indicated an insertion of the T-DNA in the At3g07970 locus which encodes a putative polygalacturonase (PGase; see below for details). In the "*pgase*" mutant the total size of plant in diameter and height was smaller than Ta-0 plants. The leaves were somewhat twisted. Mature plants could reach a maximum height of ~20cm, while wild-type plants could reach more than ~40cm (Figure 3-1).

Figure 3-1 Morphology of the "*pgase*" mutant in comparison to Ta-0.
A: 6.5 weeks old "*pgase*" mutant compared to a Ta-0 plant of the same age grown in short day conditon; B: 4.5 weeks old "*pgase*" mutant and C: 3 weeks old "*pgase*" mutant grown in long day condition. Bars are given for size reference.

To find out whether the reduced total size in the "*pgase*" mutant, resulted from smaller cell size or lower number of cells, microscopic analysis was performed. For this purpose, roots of Ta-0 and "*pgase*" plants were stained with trypan-blue and the size of root epidermal cells was analysed. Measuring 100 root epidermal cells revealed that the epidermal cell-size of the "*pgase*" mutant was 15% smaller than Col-0 cell size (Figure 3-2).

Further microscopic analysis showed that in Ta-0 the root/hypocotyl transition zone width is 12% wider than in the "*pgase*" mutant and there were not too much differences in the length of elongation zone (Figure 3-3 and Figure 3-4).

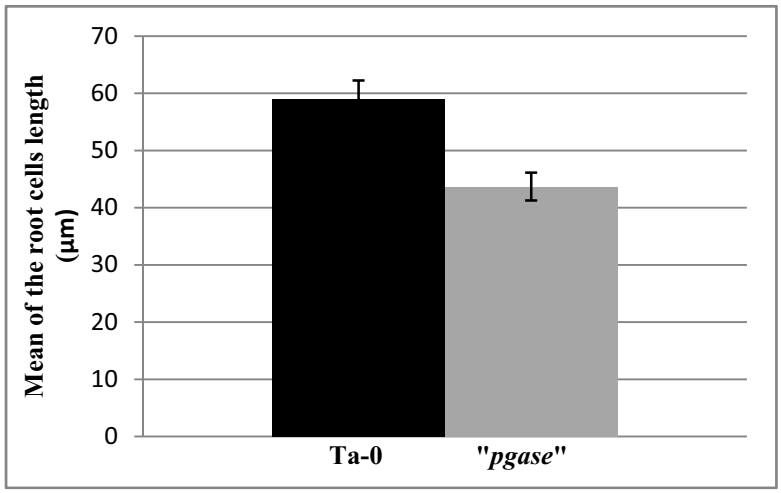

Figure 3-2 .The length of Ta-0 and "*pgase*" root cells.
Ta-0 and "*pgase*" plants were grown on MS agar for two weeks, roots stained with trypan blue and the length of root cells were measured with the "Diskus" software.

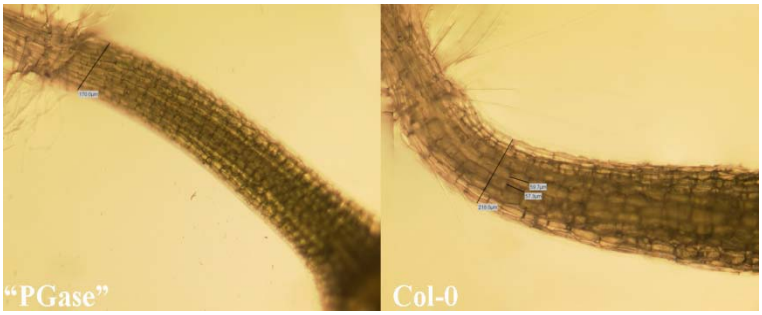

Figure 3-3 Comparison the size of "*pgase*" and Ta-0 elongation zone.
Ta-0 and "*pgase*" plants were grown on MS agar for two weeks and roots stained with trypan blue. Micrographs were taken and cell size was measured in the elongation zone using the "Diskus" software.

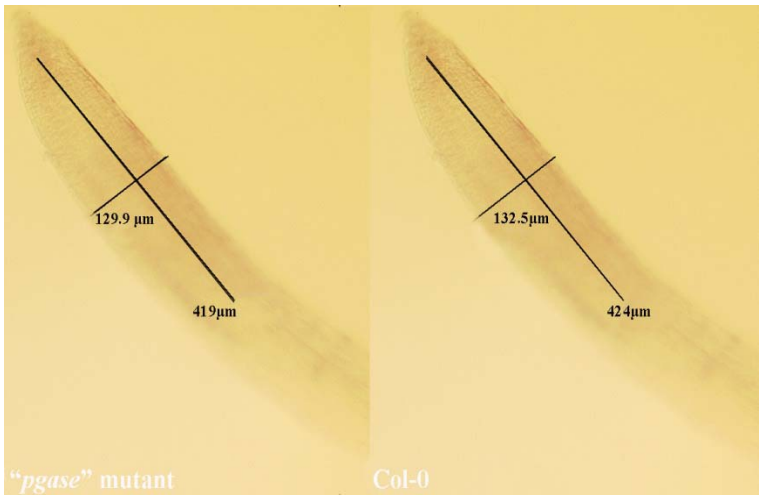

Figure 3-4. Comparison the width of "*pgase*" and Ta-0 root/hypocotyls in the transition zone.
Ta-0 and "*pgase*" plants were grown on MS agar for two weeks and roots stained with trypan blue. Micrographs were taken and cell size was measured in the transition zone using the "Diskus" software.

To get more precise information about the cellular alterations occurring in *"pgase"* plants, scanning electron microscopy (SEM) analysis was also kindly performed on "*pgase*" plants by Dr. E. Schmelzer. SEM analysis revealed some defects in the *"pgase"* mutant. First of all, the number of the thricomes in "*pgase*" and GABI-Kat KO line were 30% less than trichome numbers in wild-type plants (Figure 3-5, A-C), but actually the shape and branch number of thricomes was not affected (Figure 3-5, D-F). Secound, the epidermal cells in "*pgase*" and GABI-Kat KO line were more serrated in compare to WT epidermal cells (Figure 3-5, G-I). Third the number of guard cells in "*pgase*" and GABI kat KO mutants were less than WT but the shaping of them was not affected (Figure 3-5, G-I). Fourth, the mesophyl cells of "*pgase*" and GABI-Kat KO had less layers in compare to WT mesophyl cells (Figure 3-5, J-O), which this is consistent with the notion that the leaves of "*pgase*" and GABI-Kat KO were thinner than WT leaves.

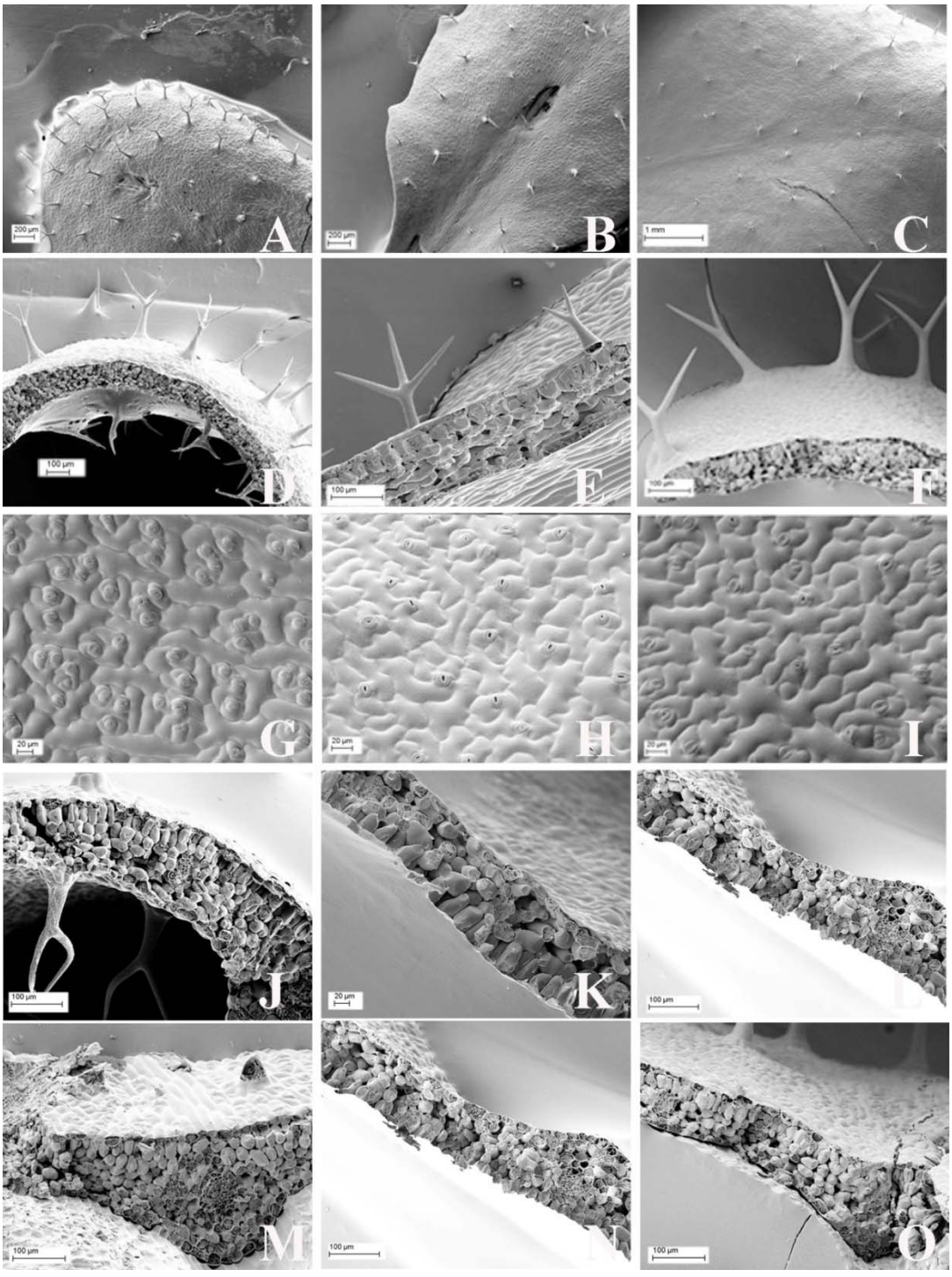

Figure 3-5 Scanning electron microscopic (SEM) analysis of the *"pgase"* and GABI-Kat KO plants.
A, D, G, J, M and P: Ta-0; B, E, H, K, N and Q: "*pgase*" ; C, F, I, L, O and R: GABI-Kat knock out line. A-C: number of thricomes; D-F: shape of thricomes; G-I shape of epidermal cells and number of stomata cells on epidermis; J-L: leaves mesophyll cells viewed as freeze fractions; M-O: mesophyll cells around vascular bundle area viewed as freeze fraction. SEM analysis results revealed some defects in these mutants including: number of the thicomes and guard cells, shape of leaves epidermal cells, the layers of mesophyll cells.Molecular analysis of the *"pgase"* mutant.

The altered morphology of "*pgase*" mutant persuaded us to investigate the molecular basis of this mutant. Since the "*pgase*" mutant phenotype was linked to the Gentamycine selection marker associated with the T-DNA used to generate the transgenic line, we speculated that integration of the T-DNA is responsible for causing the morphological phenotype. Thus, we wanted to characterize the T-DNA integration site in the plant nuclear genome. Therefore, thermal asymmetric interlaced (=TAIL) PCR was employed. To this end, large quantities of high quality plant genomic DNA (gDNA) was extracted from leaves of the "*pgase*" plants. Aliquots of the gDNA were digested to completion with the restriction enzymes *Eco*RI, *Bam*HI, *Hin*dIII. After checking a small aliquot of digested gDNA on an agarose gel to control that digestion has worked properly (Figure 3-6, A), the remaining digested gDNA was blunted with Klenow and the adaptors were ligated to the ends of the digested gDNA fragments. Subsequently, nested PCR with T-DNA specific oligos and adaptor-specific oligos was performed. Nested PCR with a T-DNA left border (LB) oligo and an adaptor oligo yielded a PCR band that was purified and sequenced. Sequence analysis revealed that the T-DNA was integrated 371 nucleotides upstream from the start codon in the promoter region of At3g07970 (Figure 3-6, B, C). This gene is annotated as encoding for a putative polygalacturonase/pectinase in *Arabidopsis* which plays a role in carbohydrate metabolic process.

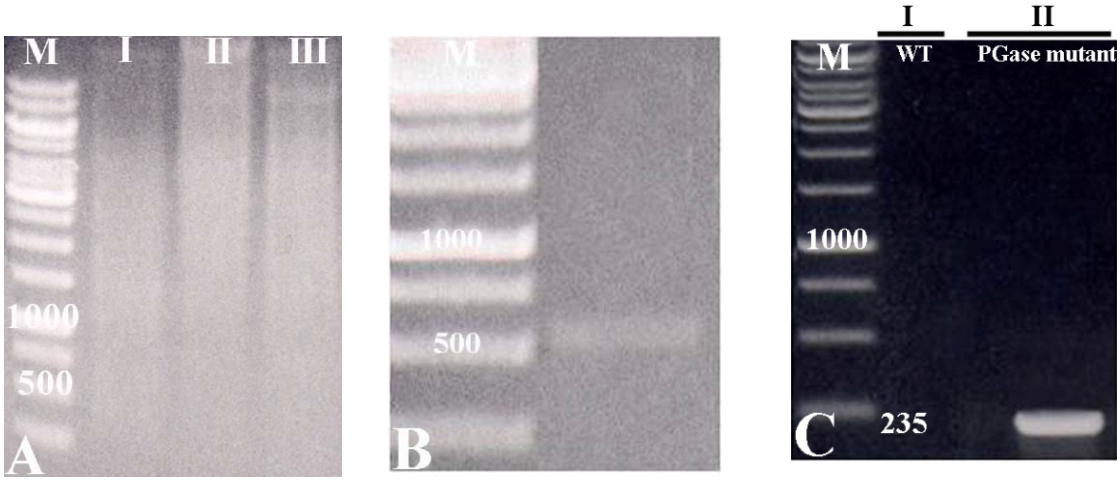

Figure 3-6 Analysis of the T-DNA integration site in the "*pgase*" mutant.
A, genomic DNA which was digested with: I, *Eco*RI; II, *Bam*HI; III, *Hin*dIII respectively. B: Nested PCR with T-DNA LB and adapter oligo. C: PCR with T-DNA- and *PGase* -specific oligos. I, PCR with T-DNA LB nested (Table 2-3- 51) and *PGase* specific (Table 2-3-48) oligos in Col-0 and II, PCR with same oligos in "*pgase*" mutant.

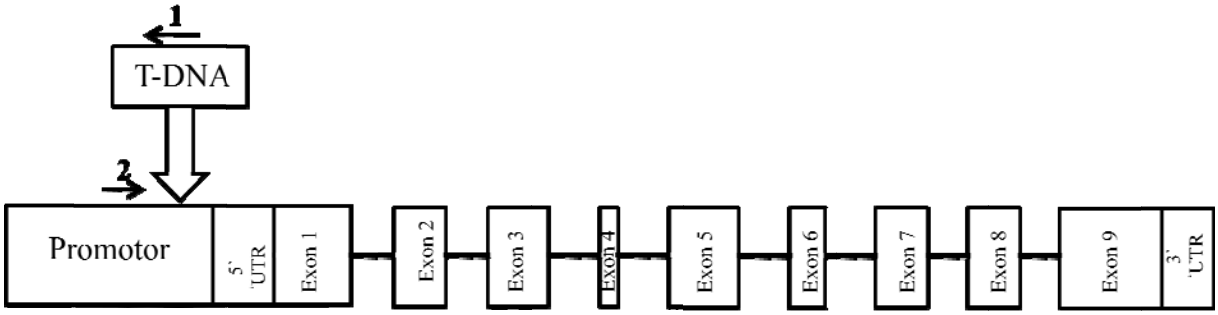

Figure 3-7.Genomic organization of the T-DNA integration site in the "*pgase*" mutant.
In the *"pgase"* mutant the T-DNA was inserted 371 nucleotides upstream of the translational start codon of *PGase* locus. 1: T-DNA LB reverse and 2: *PGase* promoter verification forward oligo.

3.1.2 The T-DNA insertion in the"*PGase*" At3g07970 was responsible for morphological phenotype in the "*pgase*" mutant

To test the hypothesis whether really the T-DNA insertion in the promoter of the *PGase* At3g07970 gene was responsible for the altered phenotype in the "*pgase*" mutant, other independent T-DNA insertion lines predicted to reside within the At3g07970 locus were obtained from the GABI-Kat collection in the Col-0 background. The T-DNA of GABI-Kat line 058B07 was predicted to be inserted in the first exon of *PGase* At3g07970. To verify the suggested T-DNA insertion in exon1 genomic DNA was extracted from this line and used as a template for PCR with *PGase* and T-DNA-specific primers (Table 2-3, 43 and 62). By sequencing the PCR bands raised from lines 7 and 8 we found that the T-DNA of line 058B07 line was integrated in the exon 1, specifically 5 base pairs (bp) after the predicted ATG start codon of *PGase* At3g07970 gene.

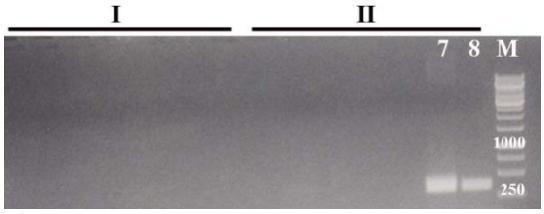

Figure 3-8. PCR analysis to detect T-DNA in GABI-Kat *pgase* knock out line 058B07.
gDNA extracted from leaves of predicted knockout *PGase* plants was used as a template. I: PCR with GABI-Kat LB forward and *PGase* exon 3 reverse primer. II: PCR with GABI-Kat LB nested forward primer and *PGase* exon 1 reverse primer. Results of these PCRs identified lines 7 and 8 as GABI-Kat *pgase* knock out carrying the T-DNA in the first exon of the *PGase* At3g07970 gene.

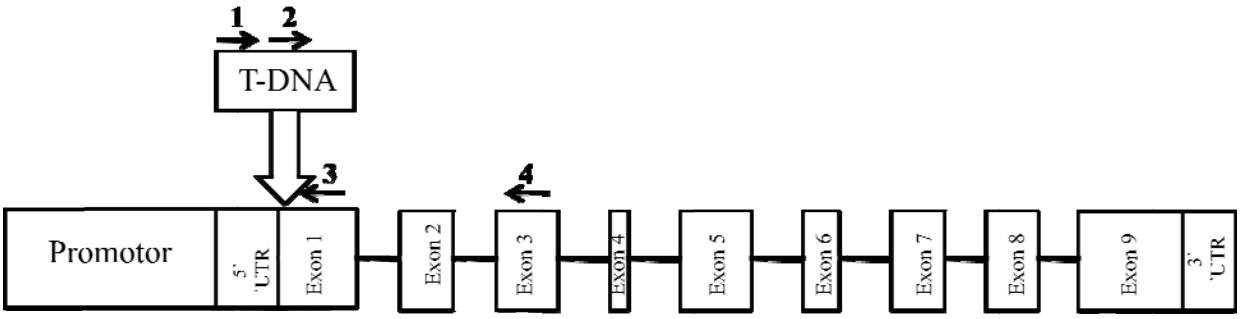

Figure 3-9 Genomic organization of the At3g07970 locus in GABI-Kat line 058B07.
PCR analysis using oligos 1: GABI-Kat LB forward primer, 2: GABI-Kat LB nested forward primer, 3: *PGase* exon 1 reverse primer, 4: *PGase* exon 3 reverse primer and subsequent sequencing revealed that the T-DNA was inserted 5 bp after the start codon in the first exon of the *PGase* At3g07970 gene.

Figure 3-10 Morphology of the 4 weeks old GABI-Kat T-DNA insertion line in At3g07970 in Col-0 background grown in short day condition which phenocopy the "*pgase*" mutant phenotype.
A: Col-0; B: line 058B07; C: "*pgase*" mutant in Ta-0 background. This GABI-Kat *PGase* knock out line has a T-DNA insertion 5 nucleotides downstream of the ATG, while the "*pgase*" mutant has the T-DNA insertion 376 nucleotides upstream of the ATG.

This molecularly analyzed *pgase* knock out line from GABI-Kat collection displayed a phenotype indistinguishable from the initially characterized "*pgase*" mutant (Figure 3-10). Therefore, our hypothesis that the T-DNA insertion in the *PGase* gene is the reason for the phenotype in the "*pgase*" mutant was corroborated.

We performed molecular analysis on the "*pgase*" mutant (in Ta-0) and GABI-Kat *pgase* knock out line to test the *PGase* mRNA expression level with semi quantitative RT-PCR. Results indicated that both "*pgase*" knock out lines, the one in Ta-0 and the other in Col-0 background express *PGase* at relative to the wild type very low and comparable levels (Figure 3-11).

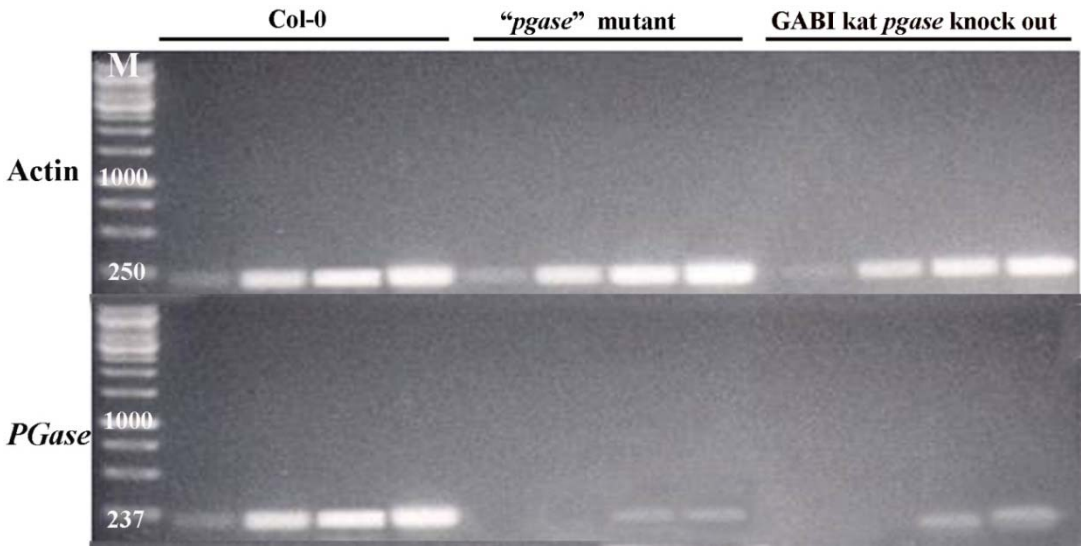

Figure 3-11 Expression analysis of *PGase* in "*pgase*" mutant and GABI-Kat T-DNA insertion line of At3g07970 .
1 µg total RNA which was extracted from Col-0, "*pgase*" mutant and GABI-Kat *pgase* knock out plants and used for making cDNA which served as a template in semi quantitative RT-PCR analysis. Actin: Semi quantitative RT-PCR as a cDNA input control with actin specific oligos: (Table 2-3, 56 and 57) in Col; "*pgase*" mutant and GABI-Kat *pgase* knock out line. *PGase*: Semi quantitative RT-PCR to test expression of PGase mRNA with *PGase* specific oligos (Table 2-3, 46 and 43) oligos in Col; "*pgase*" mutant and GABI-Kat *pgase* knock out . Lanes 1, 2, 3 and 4 correspond to PCR cycle 23, 25, 27 and 30. M= molecular weight marker with 237 and 250 bp band indicated.

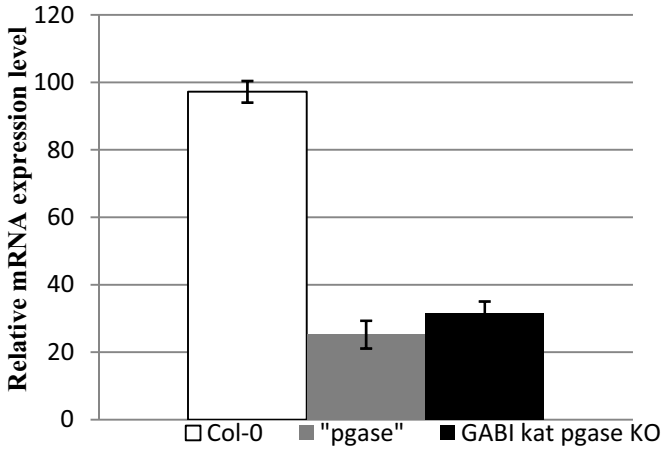

Figure 3-12 Quantitation of semi quantitative RT-PCR analysis related to mRNA expression level of *PGase* in Col, "*pgase*" mutant and GABI-Kat *pgase* knock out line.
RNA expression levels are expressed as relative to actin control and RT-PCRs data at cycle 27 have been shown.

After standardization of actin PCR bands with the described procedure in 3-2-4, it was found that the expression of *PGase* At3g07970 in Col-0 is 4.65 X more than in the "*pgase*"mutant and 3.56 X more than in the GABI-Kat *pgase* mutant.

3.1.3 Complementation of the *"pgase"* mutant phenotype with over expression of *PGase* At3g07970 CDS

The perception of the very similar phenotype in the GABI-Kat *pgase* knock out mutant (which was in the Col-0 background) with our isolated "*pgase*" mutant (in Ta-0), prompted us to test the complementation of "*pgase*" mutant phenotype with the *PGase* CDS.Therefore, lines constitutively expressing *PGase* (35S::*PGase* At3g07970) were generated in the screened homozygous "*pgase*" lines (Figure 3-13) and Col-0 background . To this end, the *PGase* coding sequence from cDNA was cloned into the binary vector pJawohl3 downstream of the strong 35S CaMV promoter (Figure 2-4). The sequence of the recombinant plasmid was confirmed and the recombinant plasmid was transformed into Col-0 and homozygous "*pgase*" plants by the floral dip method (Clough and Bent, 1998). All transformed selected T_1 plants were wild-type looking plants (Figure 3-14). Over-expressing "*PGase*" lines 13 and 16 in the "*pgase*" background were chosen in the T_2 generation based on their segregation of 52:150 dead (susceptible): alive (resistant) to the BASTA herbicide which showed they carried one insertion. The 3 out of 4 plants which were resistant (alive) in the T_2 generation displayed normal Col-0 phenotype (Figure 3-14), which means that in the "*pgase*" over-expression of *PGase* coding sequence could complement the phenotype of this mutant. 23 out of 92 (in line13) and 25 out of 100 (in line 16) displayed "*pgase*" phenotype when a defined number of T_2 seeds of these lines were sowed on soil without any selection (consistent with ¼ of plants being non-transformed plants). In T_3, lines 13 and 16 displayed 100% plants with Col-0 looking phenotype.

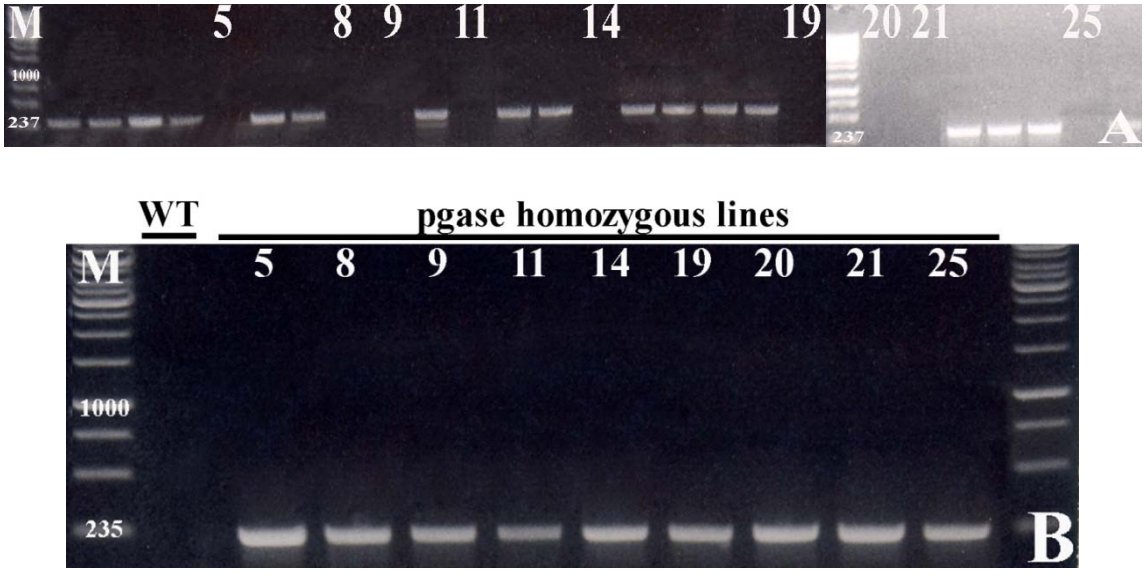

Figure 3-13 PCR analysis related to isolation "*pgase*" T_2 homozygous lines.
A, wild-type PCR with *PGase* specific (Table 2-3, 48 and 43) oligos for screening "*pgase*" homozygous lines in T_2 generation. B, FST-PCR with T-DNA LB nested and *PGase* specific (Table 2-3, 48) oligos in Col-0 and "*pgase*" homozygous lines which did not produced PCR band in wild-type PCR (Figure A). Numbers indicates to line number.

Figure 3-14 Over expression of *PGase* At3g07970 plants in "*pgase*" background.
A, Selection of T_1 over-expression *PGase* At3g07970plants in *"pgase"* background with resistance to BASTA herbicide. B, T_2 generation of *PGase* over- expression line 13 plants in *"pgase"* background (*"pgase"*+pJawoh3+*PGase* At3g07970 CDS), on soil without any selection, which 69 out of 92 plants show WT normal looking like phenotype and 23 out of 92 plants (circled) display *"pgase"* phenotype.

Over-expressing *PGase* At3g07970 lines were selected in the T_3 generation for homozygosity (plants that no longer segregate for the BASTA-resistance marker) and the RNA levels of the *PGase* At3g07970 gene were analyzed by semi quantitative RT-PCR. Semi quantitative RT-PCR analysis with *PGase*-specific oligos (Table 2-3, 46 and 43) confirmed over-expression of *PGase* At3g07970 in lines 13 and 16 (Figure 3-15).

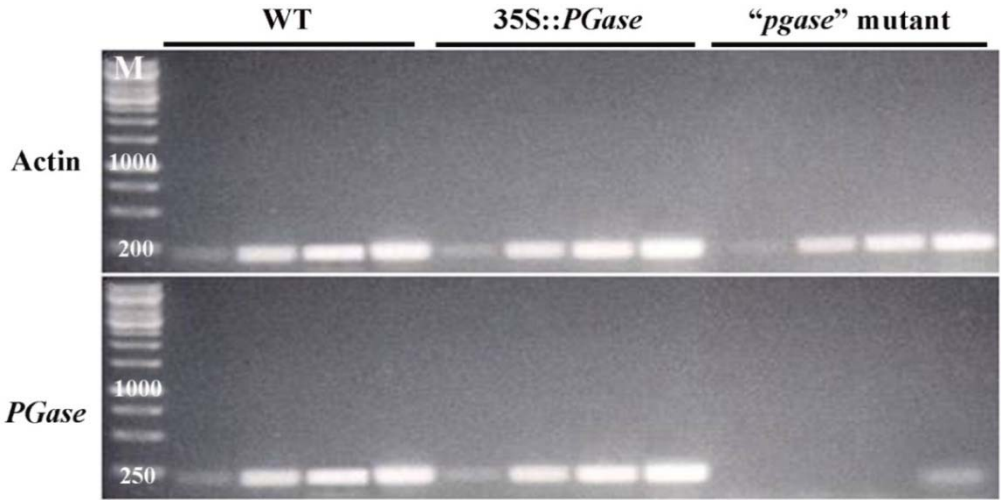

Figure 3-15 Expression analysis of *PGase* in 35S::*PGase* line 16.
Semi quantitative RT-PCR analysis with 1 µg total RNA which were extracted from Col-0, 35S::*PGase* and "*pgase*" plants and used for making cDNA which served as a template in semi quantitative RT-PCR analysis. Actin, Semi quantitative RT-PCR for actin expression with actin specific (Table 2-3, 56 and 57) oligos in Col; 35S::*PGase* line 16 and *"pgase"* mutant. *PGase* : Semi quantitative RT-PCR for expression of *PGase* mRNA with *PGase* specific (Table 2-3, 46 and 43) oligos in Col; 35S::*PGase* line 16 and *"pgase"* mutant. Lanes 1, 2, 3 and 4 correspond to PCR cycle 23, 25, 27 and 30. M= molecular weight marker with 250 and 1000 bp band indicated.

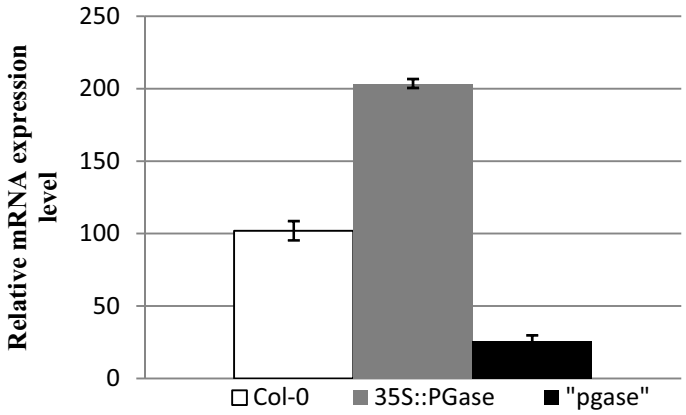

Figure 3-16 Quantitation of semi quantitative RT-PCR analysis related to mRNA expression level of *PGase* At3g07970 in Col-0, 35S::*PGase* and the "*pgase*" mutant.
RNA expression levels are expressed as relative to actin control and RT-PCRs data at cycle 27 have been shown.

After standardization of actin PCR bands with the described procedure in 3-2-4, was calculated the expression of *PGase* in 35S::*PGase* At3g07970 is 2.04 X more than in Col-0 and 9.4 X more than in "*pgase*" plants (Figure 3-16).

3.1.4 *PGase* At3g07970 is expressed in stems, roots and slightly in leaves and flowers

To study organ specific expression of the *PGase* At3g07970 gene, total RNA of Col-0 organs including roots, leaves, stems and flowers were extracted. cDNAs were prepared from extracted RNA and used as a template for semi quantitative RT-PCR analysis. Results of RT-PCR analysis showed that *PGase* At3g07970 had generally low mRNA levels and was expressed mostly in roots and stems and in very low amounts expression could be detected in leaves and flowers of Col-0 (Figure 3-17and Figure 3-18).

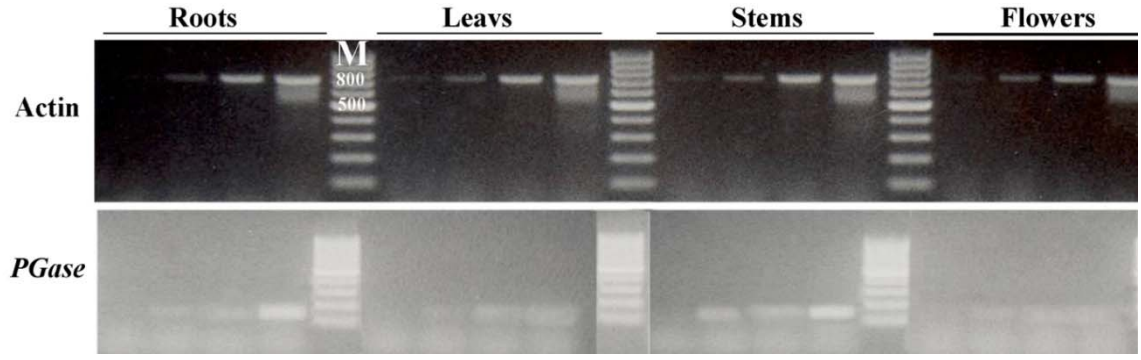

Figure 3-17 Semi quantitative RT-PCR analysis of *PGase* At3g07970 gene expression in different organ of plant including roots, leaves, stems and flowers respectively.
Actin: Semi quantitative RT-PCR with Actin specific (Table 2-3, 57 and 58) oligos ; *PGase*: Semi quantitative RT-PCR with *PGase* specific (Table 2-3, 41 and 42) oligos RT-PCRs. Lanes 1, 2, 3 and 4 correspond to PCR cycle 23, 25, 27 and 30. M= molecular weight marker with 500 and 800 bp band indicated.RNA expression levels are expressed as relative to actin control and data were shown at cycle 27.

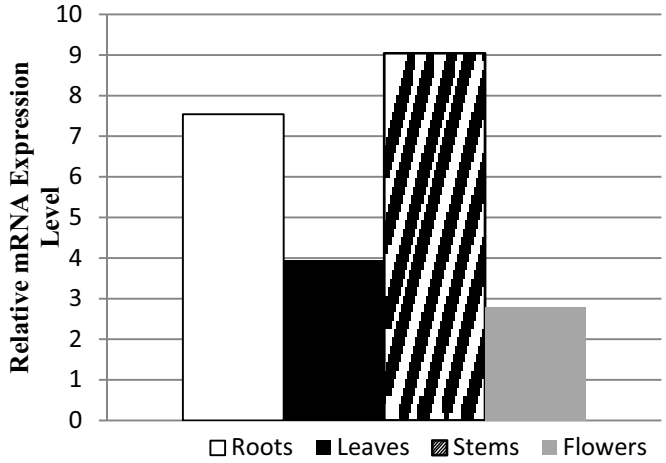

Figure 3-18 Quantitation of semi quantitative RT-PCR analysis of *PGase* At3g07970 gene expression in different organ of plant including roots, leaves, stems and flowers respectively.
RT-PCRs data have been shown at cycle 27. RNA expression levels are expressed as relative to actin control.

3.1.5 Interaction of "*pgase*" knocks out mutants and *Hyaloperonospora arabidopsidis*

To study the interaction between the "*pgase*" mutants ("*pgase*" mutant in Ta-0 background and GABI-Kat "*pgase*" in Col-0 background) with plant pathogens, we studied the interaction of oomycete *Hyaloperonospora arabidopsidis* (formerly *Peronospora parasitica*) with the "*pgase*" mutants. To this end, the leaves of three weeks old "*pgase*" mutant, GABI-Kat "*pgase*", Col-0, Ta-0, "*pgase*" in Ta and *eds*1 genotypes were inoculated with the NOCO isolate of *H. parasitica* (Combination of Col-0 accession with NOCO is a compatible interaction while combination of Ta-0 accession with NOCO is an incompatible interaction). The responses of the "*pgase*" mutants were compared with those which were observed in Col-0, Ta and *eds*1 genotypes .Three days after inoculation of leaves with the conidiospores of pathogen, the mass of grown hyphae within the leaves was assessed by trypan blue staining of detached leaves. As shown in Figure 3-19, in the "*pgase*" mutant in the Ta-0 background, no hyphal growth was detected on day 3 after inoculation. But we found that the mass of the hyphae which appeared in the inoculated leaves of the GABI-Kat "*pgase*" mutant with NOCO on day 3 was more or less identical to the hyphal mass which appeared in *eds*1 mutant (Figure 3-19). Thus, in both these genotypes much more hyphae were observed as in Col-0. On day seven after inoculation, the emerged conidiospores were counted. For counting of the conidiospores, same number of leaves from different genotypes was taken, washed in sterile water and were counted under microscope on a graded glass slide. The number of the conidiospores counted in the GABI-Kat "*pgase*" mutant was statistically similar to the counted conidiospores in the *eds*1 muatnt (Figure 3-20). The numbers of both lines was much more than the conidiospore numbers of Col-0.This experiment was repeated for three times and same results were recorded.

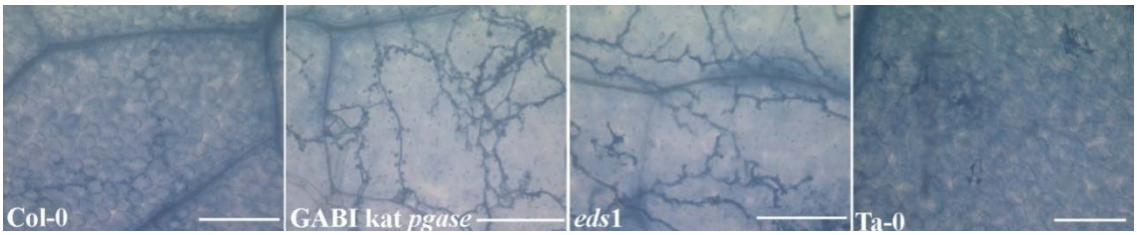

Figure 3-19 Trypan blue stained leaves on day three after inoculation with *Hyaloperonospora arabidopsidis* (NOCO). The mass of hyphae in the GABI-Kat *pgase* mutant was more or less identical with *eds*1 and much more than in Col-0 and no hyphae were detected in the "*pgase*" mutant in the Ta-0 background.

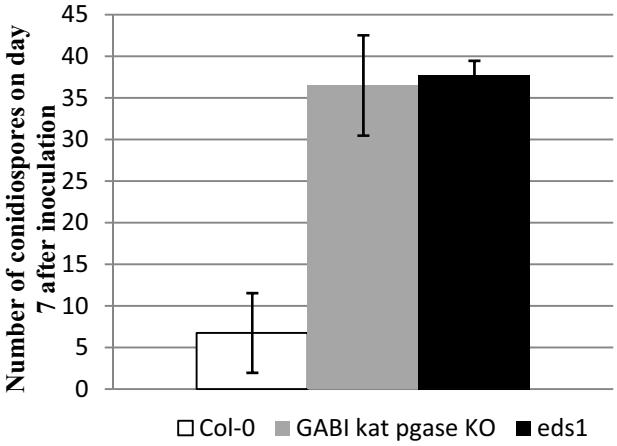

Figure 3-20 Number of conidiospores on day 7 after inoculation.
The emerged conidiospores on the GABI-Kat "*pgase*" mutant were quite similar to the amount of conidiospores which were emerged on *eds*1 and seven times more than emerged conidiospores on Col-0.

Since *eds*1 mutant was identified as a super susceptible mutant to infection with *Hyaloperonospora arabidopsidis* (NOCO race). Therefore the inoculated *eds*1 plants can give rise to conidiospores already 5 days after inoculation, in contrast to Col-0. To test the response of susceptible GABI-Kat *pgase* mutant on day 5 after inoculation, infected GABI-Kat, *eds*1 and Col-0 plants were brought into sporulation inducing conditions. It was observed that the GABI-Kat *pgase* mutant, like the *eds*1 mutant allowed sporulation at this time point while Col-0 did not. The amount of produced conidiospores on the leaves of both mutants were statistically similar(Figure 3-21).

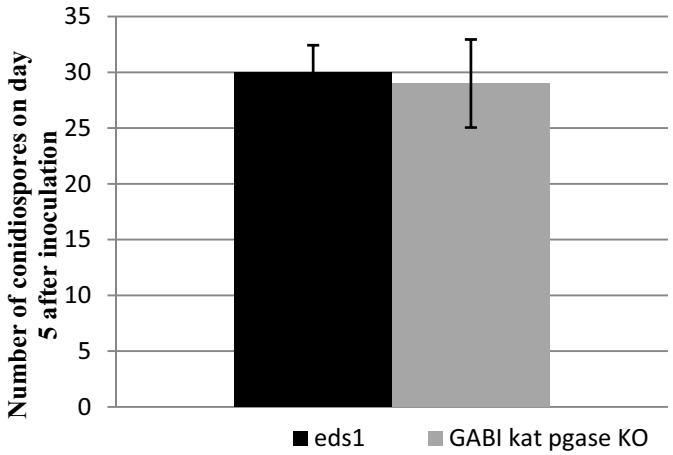

Figure 3-21 Number of conidiospores found on pgase, *eds*1 and Col-0 plants five days after inoculation.
The emerged conidispores on the GABI-Kat "*pgase*" mutant was similar to amount of conidiospores which were emerged on *eds*1 mutant.

3.1.6 "*pgase*" mutants was susceptible to cold stress

To study the behavior of the "*pgase*" mutants in response to cold stress, 3 weeks old "*pgase*" mutant, GABI-Kat *pgase* knock out mutant, Col-0, Ta-0 and complemented "*pgase*" mutant with "*PGase*" CDS were treated with +4°C in a light cabinet for about 20 hours and then transferred back to normal conditions, *i.e.* 22°C. As shown in (Figure 3-22, A and B) both "*pgase*" mutants (in Col-0 and Ta-0 backgrounds) produced severe susceptible symptoms during the 20 hours and 48 hours after being returned to 22°C they were dead while the control genotypes did not produce any symptoms in the same condition (Figure 3-22, A and B). The response of complemented "*pgase*" mutant with "*PGase*" CDS was similar with Col-0 and Ta-0 plants. Since BTH is known as an inducer of plant basic resistance to different abiotic stresses, I attempted to study the effect of BTH on the "*pgase*" mutant. Thus, three days before cold-treatment plants were sprayed with 100µM BTH, then treated with +4°C and it was observed that BTH could not improve the susceptibility of the " *pgase*" mutants to cold stress.

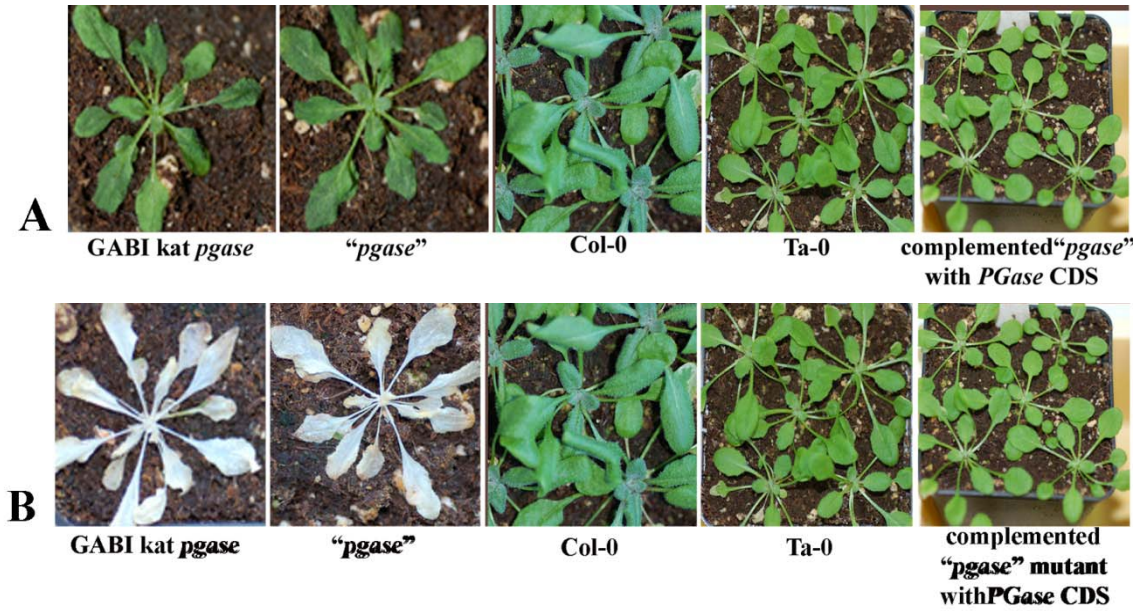

Figure 3-22 Response of "*pgase*" and GABI-Kat *pgase* mutants to cold stress in comparison to Col-0, Ta-0 and complemented "*pgase*" mutant as control plants.
A: after 20 hours incubation in +4°C, B: 48 hours after taking the plants from +4°C.

Since the "*pgase*" knock out mutant showed a severe cold-sensitive phenotype we decided to study the relation of *PGase* and cold regulated genes (*COR78*). For this purpose, the leaf samples were harvested at t=0, 4, 8, 24 and 48 hours past cold treatment (hpt). Total RNA was extracted from the leaves, cDNA was prepared and semi quantitative RT-PCR analysis was performed. Results of RT-PCR analysis indicated that in Col-0 *COR78* and *PGase* At3g07970 started to induce 8 hpt (Figure 3-23) and in t=24 their expression had reached a maximum level. Interestingly, semi quantitative RT-PCR analysis with "*pgase*" mutants RNAs, showed that cold regulated gene (*COR78*) was not induced in these lines (Figure 3-25) while the induction pattern of *PGase* At3g07970 and *COR78* in the complemented "*pgase*" line were identical with Col-0 (Figure 3-24).

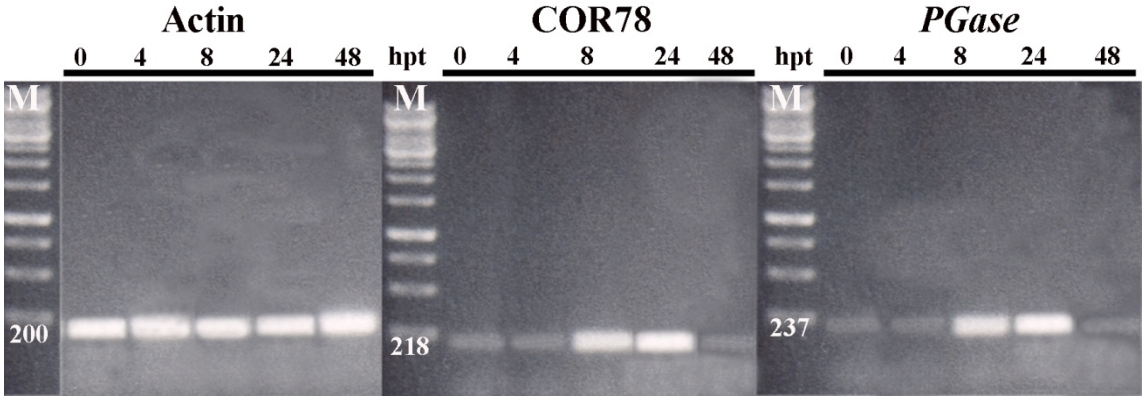

Figure 3-23 Expression analysis of *COR78* and *PGase* At3g07970 in Col-0 plant in response to cold stress.
Semi quantitative RT-PCR analysis with 1 µg total RNA which were extracted from Col-0 plants and used for making cDNA which served as a template in semi quantitative RT-PCR analysis. Actin: Semi quantitative RT-PCR for actin expression with actin specific (Table 2-3, 56 and 57) oligos in Col, *PGase* : Semi quantitative RT-PCR for expression of *PGase* mRNA with *PGase* specific (Table 2-3, 46 and 43) oligos in Col, *COR78* : Semi quantitative RT-PCR for expression of *COR78* mRNA with *COR78* specific (Table 2-3, 63 and 64) oligos. Lanes 1, 2, 3, 4 and 5 correspond to PCR cycle 23, 25, 27, 30 and 33. M= molecular weight marker with 250 bp band indicated.

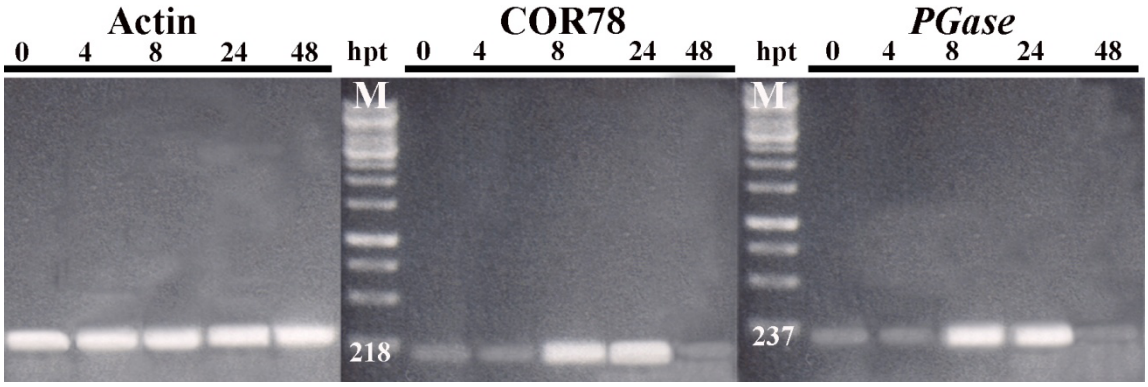

Figure 3-24 Expression analysis of *COR78* and *PGase* At3g07970 in complemented "*pgase*" mutant with *PGase* At3g07970 CDS in response to cold stress.
Semi quantitative RT-PCR analysis with 1 µg total RNA which were extracted from complemented "*pgase*" mutant and used for making cDNA which served as a template in semi quantitative RT-PCR analysis. Actin: Semi quantitative RT-PCR for actin expression with actin specific (Table 2-3, 56 and 57) oligos in Col, *PGase* : Semi quantitative RT-PCR for expression of *PGase* mRNA with *PGase* specific (Table 2-3, 46 and 43) oligos in complemented "*pgase*" mutant with *PGase* CDS, *COR78* : Semi quantitative RT-PCR for expression of *COR78* mRNA with *COR78* specific (Table 2-3, 63 and 64) oligos in complemented "*pgase*" mutant. Lanes 1, 2, 3, 4 and 5 correspond to PCR cycle 23, 25, 27, 30 and 33. M= molecular weight marker with 250 bp band indicated.

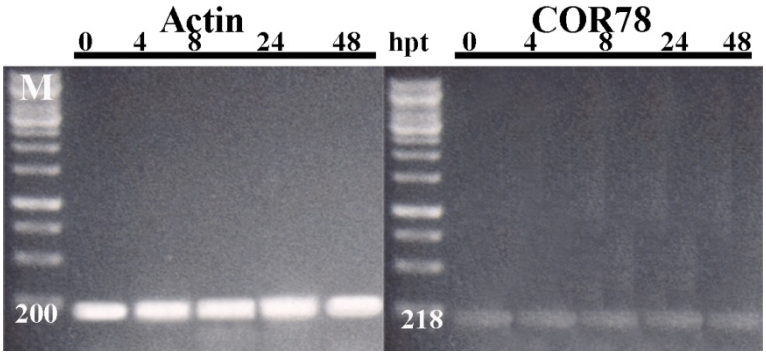

Figure 3-25 Expression analysis of *COR78* in "*pgase*" mutant in response to cold stress.
Semi quantitative RT-PCR analysis with 1 µg total RNA which were extracted from Col-0 plants and used for making cDNA which served as a template in semi quantitative RT-PCR analysis. Actin, Semi quantitative RT-PCR for actin expression with actin specific (Table 2-3, 56 and 57) oligos in "*pgase*" mutant. *COR78*: Semi quantitative RT-PCR for expression of *COR78* mRNA with *COR78* specific (Table 2-3, 63 and 64) oligos in "*pgase*" mutant. Lanes 1, 2, 3, 4 and 5 correspond to PCR cycle 23, 25, 27, 30 and 33. M= molecular weight marker with 250 bp band indicated.

3.1.7 "*pgase*" mutants were susceptible to heat shock

To study the behavior of the "*pgase*" mutants in response to heat shock, 3 weeks old "*pgase*" mutant, GABI-Kat *pgase* knock out mutant, Col-0, Ta-0 and complemented "*pgase*" mutant with 35S::*PGase* were treated with +48°C in a light cabinet for about 8 hours and then transferred into normal condition. Before placing the plants at 48°C they have been watered with 50°C warm water. As shown in (Figure 3-26) both "*pgase*" mutants (in Col-0 and Ta-0 backgrounds) withered 8 hours after incubation at 48°C while control genotypes did not produce any symptom in the same condition. The response of the complemented "*pgase*" mutant with 35S::*PGase* was similar to Col-0 and Ta-0 plants. Since BTH was known as an inducer of plant basic resistance to different abiotic stresses, I studied the effect of BTH on our susceptible "*pgase*" mutant Thus, three days before treating plants with +48°C, they were sprayed with 100µM BTH and three days later treated with +48°C. As shown in (Figure 3-27), BTH could improve the susceptibility of the "*pgase*" mutants in response to heat shock.

Figure 3-26 Response of GABI-Kat *pgase* and "*pgase*" mutants to heat shock (heat stress) in comparison to Col-0, Ta-0 and complemented "*pgase*" mutant as control plants 8 hours after incubation at 48°C.

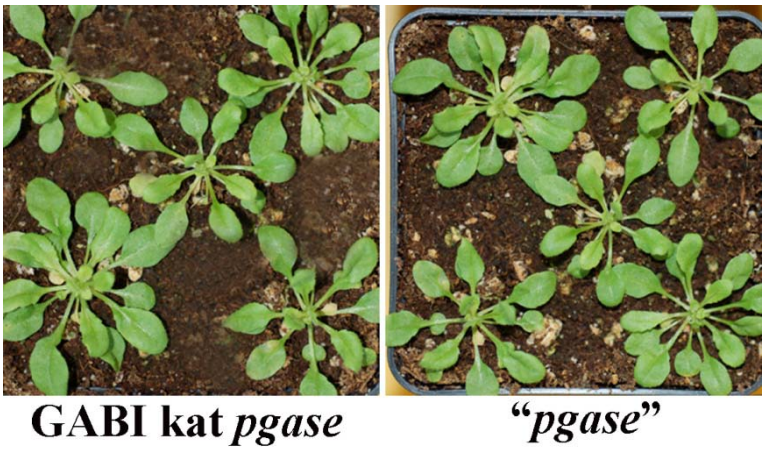

Figure 3-27 The improvement effect of BTH on the susceptibility of the GABI-Kat *pgase* knock out and *"pgase"* mutants. The plants were treated with 100µM BTH three days before heat stress and later treated with heat by putting the plants at +48°C.

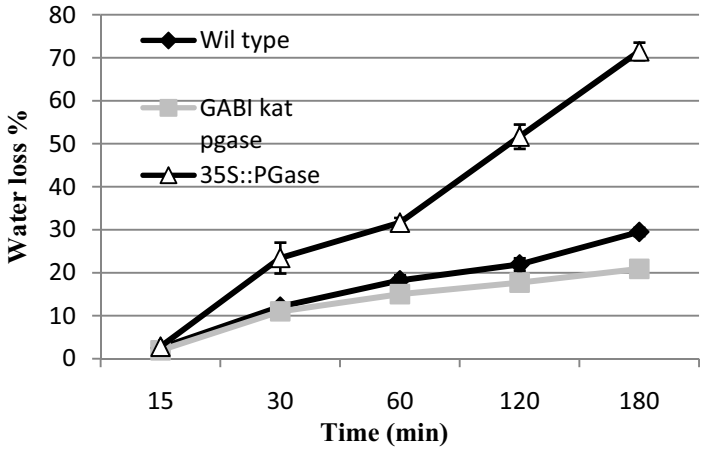

Figure 3-28 Rate of water loss from 35S::*PGase* At3g07970, GABI-Kat *"pgase"* and wild-type plants. Detached rosettes were weighed at the time intervals shown. The results are derived from three independent experiments and are shown with SE for the mean for each time point.

3.1.8 "*pgase*" mutants shows lower transpiration rates

To study the behavior of the "*pgase*" mutants in water loss and transpiration rate during drought period, water loss from detached leaves of 3 weeks old "*pgase*" mutant, GABI-Kat *pgase* knock out mutant, Col-0, Ta-0 and complemented "*pgase*" mutant with 35S::*PGase* were measured. For this purpose 3 weeks old plants grown on soil were dehydrated on Whatman 3 MM paper. And during the desiccation period the fresh weight (FW) of leaves were measured to estimate the water loss and transpiration rate. During the first minutes following the start of the treatment, the complemented "*pgase*" lines with *PGase* At3g07970 CDS , 35S::*PGase* At3g07970, showed a more rapid water loss than other control plants, such that almost 80% of the FW of leaves was lost within 3 hours following excision, whereas "*pgase*" lines leaves lost only 20% and other control plants leaves lost only 30% of their FW in the same period of time (Figure 3-28). Similar results were obtained from different homozygous complemented "*pgase*" lines with *PGase* CDS, 35S::*PGase* At3g07970, and "*pgase*" lines.

So, the identified "*pgase*" mutant in Ta-0 background displayed several morphological defects. The independent GABI-Kat line in Col-0 background which carried the insertion in the first exon of the *PGase* gene phenocopied the phenotype of the initionally characterized "*pgase*" mutant which the T-DNA was inserted in the promoter region of *PGase* in this line. Therefore, was concluded that the T-DNA insertion in the *PGase* locus which was annotated to encode a galacturonase is responsible for abnormal morphology of the "*pgase*" mutant and supersusceptibilty to biotic and abiotic stresses.This mutants displayed hypersusceptiblity to virulent *H. arabidopsidis* , susceptiblity to cold , heat stress, and surprisingly the mutants have showed lower transpiration rate which fit with the point that their epidermal cells contain lower guard cells compare to wild-type plants. And finally only heat stress can be alleviated by BTH pretreatment.

3.2 "*bushy-ff*" mutant

3.2.1 Isolation of the *Arabidopsis thaliana* developmental "*bushy-ff*" mutant

In the process of generating transgenic *Arabidopsis* lines, a randomly occurring mutant with a severe morphological phenotype was isolated. This plant was named "*bushy-ff*" according to the dramatically reduced plant size. "*bushy-ff*" plants are strongly compressed in all dimensions, plants reached a maximum height of ~2 to10 cm in maturity contrasting to approx. 30 cm of wild-type plants (Figure 3-29, A). The length of mature leaves of the "*bushy-ff*" mutant was ~2.5-times smaller compared to leaves of Col-0 (wild-type) plants . Also, as shown in (Figure 3-30), "*bushy-ff*" plants set flowers earlier approx. 12 days than Col-0 plants in short and long day conditions.

Reduced plant size can either be a result of smaller cell size or lower cell number. To understand which of these two reasons is the basis of the "*bushy-ff*" phenotype, microscopic analysis was performed. Measuring the length of 100 trypan blue-stained root cells of *"bushy-ff"* and Col-0 plants revealed that the size of the *"bushy-ff"* root cells was ~30 % smaller than Col-0 root cells (Figure 3-31). Microscopic investigations also suggested that the root/hypocotyl transition zone in Col-0 was ~35% wider than in *"bushy-ff"* (Figure 3-32) and the size of the elongation zone in *"bushy-ff"* was ~30% smaller than Col-0 plants (Figure 3-33).

Figure 3-29 Morphology of the *"bushy-ff"* mutant.
A and B: 4 weeks old "*bushy-ff*" and Col-0 plants; C and D: flowers from flowering "*bushy-ff*" plant; E: 6.5 weeks old "*bushy-ff*" plant after germination in comparison to Col-0 plants of the same age.

Figure 3-30 Early flowering phenotype of the "*bushy-ff*" mutant.
Col-0 (wild-type) and "*bushy-ff*" plants grown for five weeks in short day conditions, which in the "*bushy-ff*" mutant flowers were appeared while in same age Col-0 flowers not appeared . Bars are given for size reference.

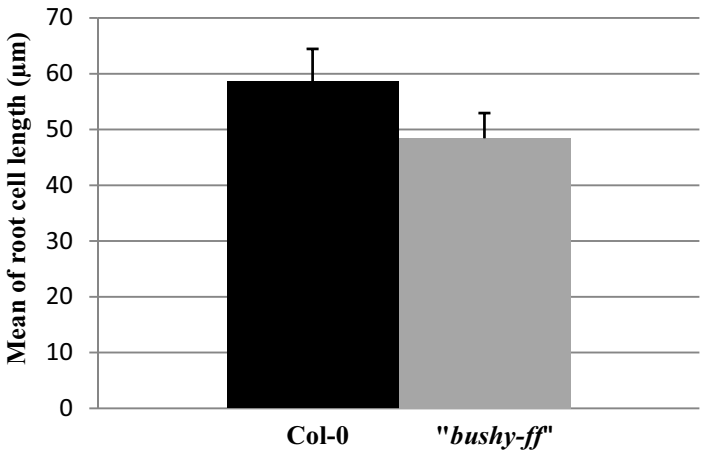

Figure 3-31 The length of Col-0 and the "*bushy-ff*" root cells.
Col-0 and "*bushy-ff*" plants were grown on MS agar for two weeks, roots stained with trypan blue and the length of root cells were measured with the "Diskus" software.

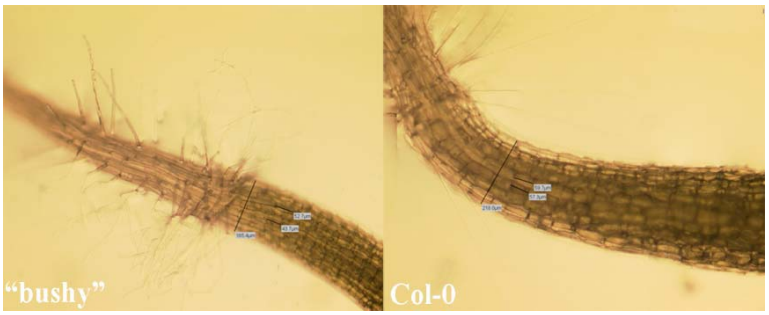

Figure 3-32 Comparison the width of "*bushy-ff*" and Col-0 root/hypocotyls in the transition zone.
Col-0 and "*bushy-ff*" plants were grown on MS agar for two weeks and roots stained with trypan blue. Micrographs were taken and cell size was measured in the transition zone using the "Diskus" software.

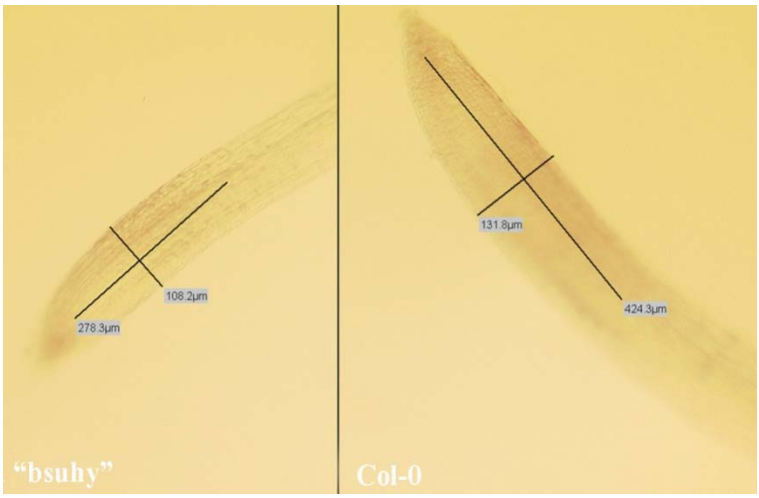

Figure 3-33 Comparison the size of *"bushy-ff"* and Col-0 elongation zone.
Col-0 and "*bushy-ff*" plants were grown on MS agar for two weeks and roots stained with trypan blue. Micrographs were taken and the size of elongation zone was measured using the "Diskus" software.

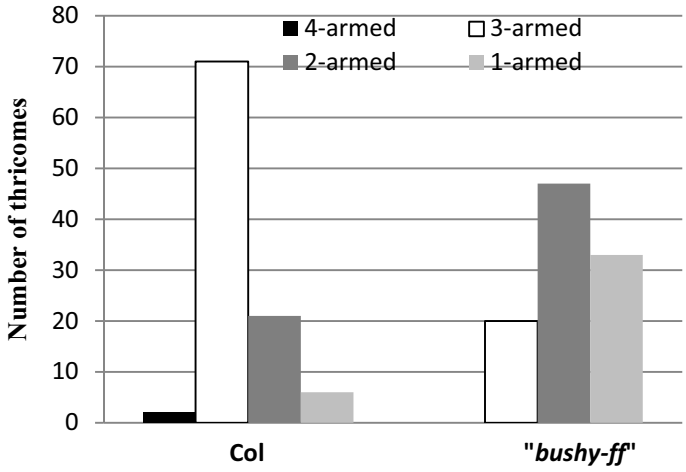

Figure 3-34 Frequency of the trichomes arm in Col-0 and "*bushy-ff*".
100 trichomes rosette from leaves of Col-0 and "*bushy-ff* were counted and percentage of each category were presented. Similar results were recorded in several independent repetitions.

To get more precise information about the cellular alterations occurring in *"bushy-ff"* plants, scanning electron microscopy (SEM) analysis was kindly performed by Dr. E. Schmelzer (MPI in Cologne). SEM analysis revealed multiple defects in the *"bushy-ff"* mutant. For example, the number of the trichomes in "*bushy-ff*" plants was altered, each "*bushy-ff*" with the number of total trichomes being 42 % less than Col-0 (Figure 3-34, A and E). In contrast to Col-0 plants in which ~71% of total trichomes are three-armed and juts ~21% of them are two-armed, in *"bushy-ff"* plants ~20% of trichomes were three-armed, ~47% two-armed and ~33% of trichomes were without branching (Figure 3-34) and (Figure 3-35 B, C, F and G). Furthermore, epidermal cell shape and stomata spacing in *"bushy-ff"* plants was different from Col-0 plants (Figure 3-35, D and H). Also, mesophyll differentiation into palisade and spongy mesophyll cells in *"bushy-ff"* was aberrant (Figure 3-35, I- P). Moreover, flowers in the *"bushy-ff"* mutant were another organ which was severely affected, as shown in (Figure 3-35, Q-T). The overall size of flowers was much smaller compared to Col-0 flowers and the stamens, sepals and petals of *"bushy-ff"* flowers were compressed in length (Figure 3-35, Q-T).These defects in flower morphology resulted in a ~ 40 reduction of seed production in the *"bushy-ff"* mutant.

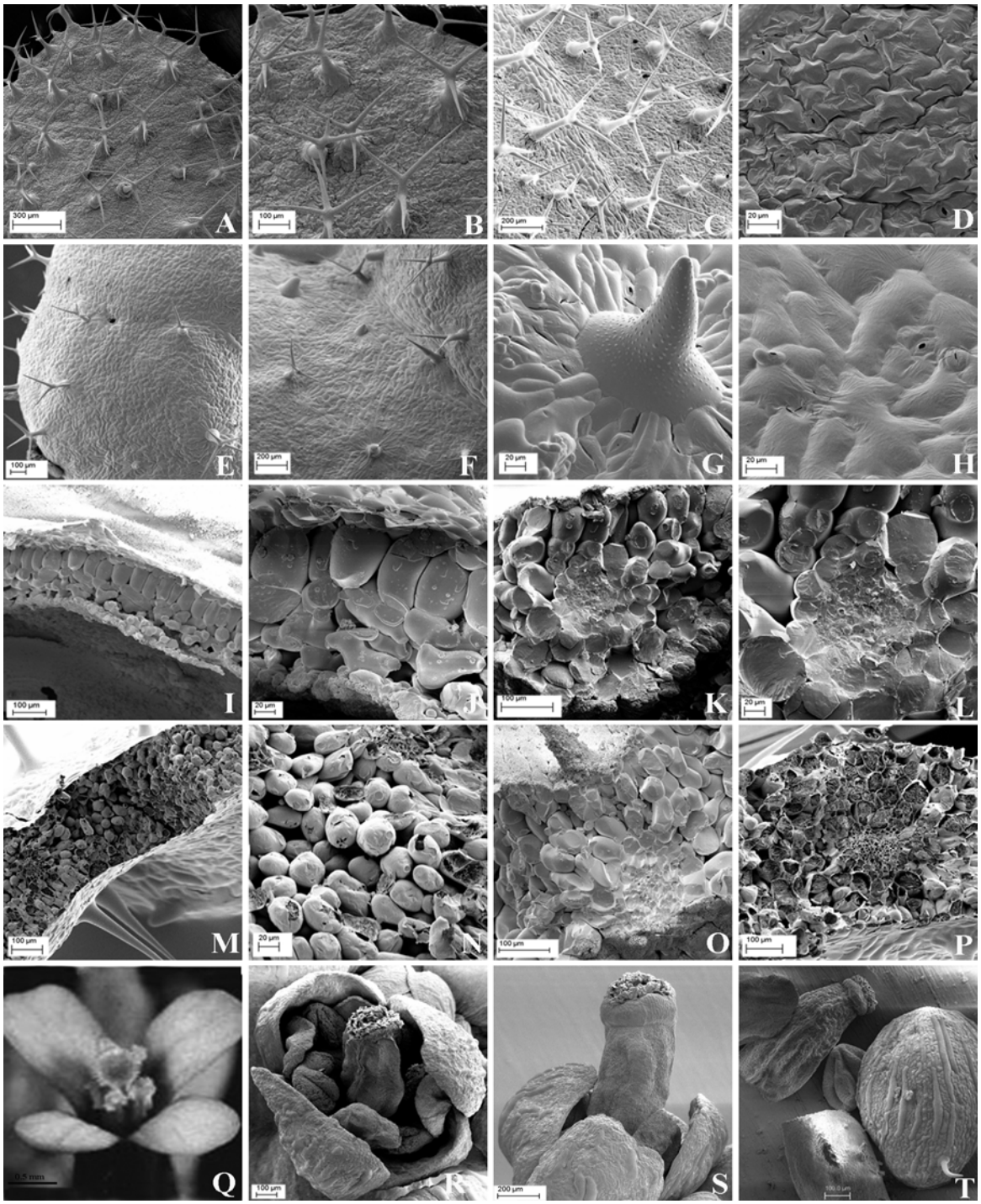

Figure 3-35 Scanning electron microscopic (SEM) analysis of the *"bushy-ff"* plants.
Leaves and flowers of Col-0 and *bushy-ff* plants of the same age and grown side-by-side were analysed by SEM. A-D: epidermis of Col-0, E-H: epidermis of "*bushy-ff*"; I-L: cross section of Col-0 leaf; M-P: cross section of "*bushy-ff*" leaf; Q: flower of Col-0; R-T: floral organs of *bushy-ff*. Bars are given in each figure for size comparison. SEM pictures are a courtesy of Dr. E. Schmelzer (MPI Cologne).

3.2.2 Response of "*bushy-ff*" mutant to *Hyaloperonospora arabidopsidis*

To study the interaction between the "*bushy-ff*" mutant with plant pathogens, we investigated the interaction of the oomycete *Hyaloperonospora arabidopsidis* (formerly *Peronospora parasitica*) with the "*bushy-ff*" mutant. To this end, the leaves of three weeks old "*bushy-ff*", Col-0 and *eds*1 plants were inoculated with the NOCO race of pathogen (Col-0 and NOCO form a compatible interaction). The responses of the "*bushy-ff*" mutant were compared with those observed in Col-0 and *eds*1 genotypes. Three days after inoculation of leaves with conidiospores, oomycete growth was assessed with trypan blue staining (Figure 3-36). As shown in (Figure 3-36), the mass of the hyphae which appeared in the inoculated leaves of the "*bushy-ff*" mutant was more or less identical to those which appeared in Col-0 and much less than the hyphae mass which appeared in the *eds*1 mutant. On day seven after inoculation, the emerged conidiospores on the leaves were counted. For counting of the conidiospores, same number of leaves from different genotypes was washed in sterile water and were counted under microscope on graded glass slide. Here again the number of the conidiospores which were counted in the "*bushy-ff*" mutant was quite similar to conidiospore numbers in Col-0 and much less than conidiospore numbers of *eds*1 mutant (*eds*1 was identified as a super susceptible mutant to *Hyaloperonospora arabidopsidis*, (Figure 3-37). This experiment was repeated three different times and same results were recorded.

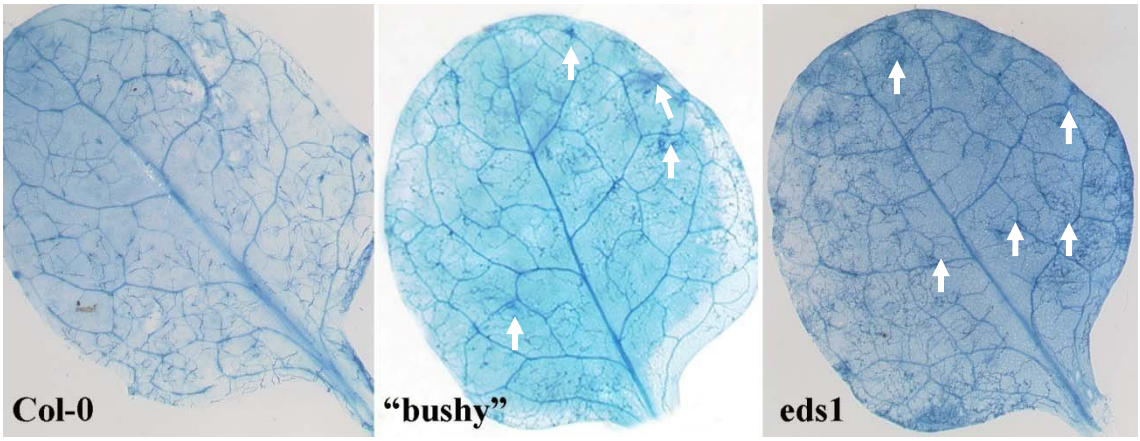

Figure 3-36 Growth of *H. arabidopsidis* in leaves of Col-0, "*bushy-ff*" and *eds1* plants.
Leaves of three week old plants were infected with a spore suspension and growth of the pathogen assessed three days later by trypan blue staining. The mass of hyphae in the "*bushy-ff*" mutant was more or less identical with hyphae mass in Col-0 and much less than hyphae mass in *eds*1 mutant.

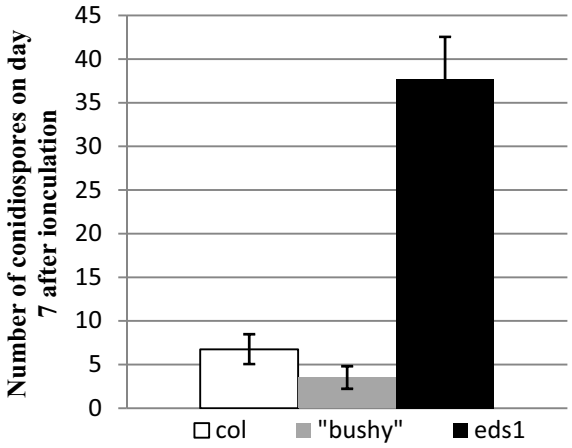

Figure 3-37 Number of conidiospores on day 7 after inoculation.
The emerged conidispores on the "*bushy-ff*" mutant was quite similar to amount of conidiospores which were emerged on Col-0 and less than emerged conidispores on *eds*1 mutant.

3.2.3 Molecular analysis of the *"bushy-ff"* mutant

The dramatic alterations displayed in all analyzed tissues of the "*bushy-ff*" mutant prompted us to investigate the molecular basis of the mutation causing this phenotype. Since the *"bushy-ff"* phenotype was linked to the Gentamycine selection marker associated with the T-DNA used to generate the line, we speculate that the T-DNA integration caused the *bushy-ff* phenotype. Thus, we wanted to characterize the T-DNA integration site in the plant nuclear genome. Thus, thermal asymmetric interlaced (=TAIL) PCR was employed. For this purpose large quantities of high quality plant genomic DNA (gDNA) was extracted from leaves of "*bushy-ff*" plants. Aliquots of the gDNA were digested to completion with the restriction enzymes *Eco*RI, *Bam*HI, *Hin*dIII and *Sal*I and partially digested with *Csp*6I and *Hae*III. After checking a small aliquot of digested gDNA on an agarose gel to control that digestion has worked properly (Figure 3-38, A), the remaining digested gDNA was blunted with Klenow and adaptors were ligated to the ends of the digested gDNA fragments. Subsequently, nested PCR with T-DNA specific oligos and adaptor-specific oligos was performed (See 2-5-7). Nested PCR with a T-DNA right border (RB) oligo and an adaptor oligo yielded a PCR band that was purified and sequenced. Sequence analysis revealed that the T-DNA was integrated in the promoter region of At1g77000. This gene is annotated as encoding an experimentally uncharacterized member of the F-box protein family in *Arabidopsis* (Figure 3-38, B and C).

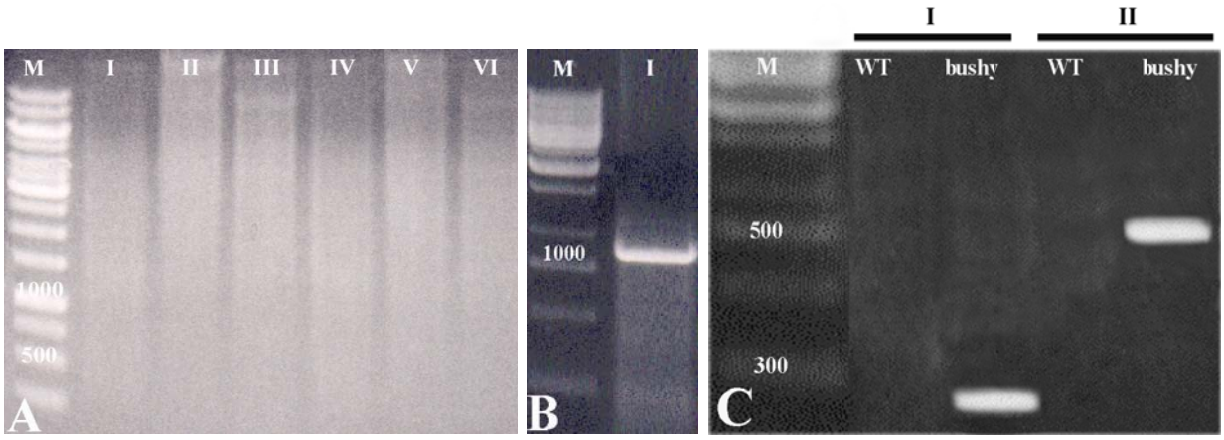

Figure 3-38 Analysis of the T-DNA integration site in the "*bushy-ff*" mutant.
A: Polaroid of genomic DNA which was digested with: I, *Eco*RI; II, *Bam*HI; III, *Hin*dIII; IV, *Sal*I; V, *Csp*6I and VI, *Hae*III respectively, separated by agarose gel electrophoresis and ethidium bromide-stained. B: Nested PCR with T-DNA RB and adapter oligo. C: PCR with T-DNA- and *F-box*-specific oligos. I, PCR with T-DNA RB nested (Table 2-3, 54) and *F-box* specific (Table 2-3, 15) oligos ; II, PCR with T-DNA LB nested (Table 2-3, 51) and *F-box* specific (Table 2-3, 16) oligos. M= molecular weight marker.

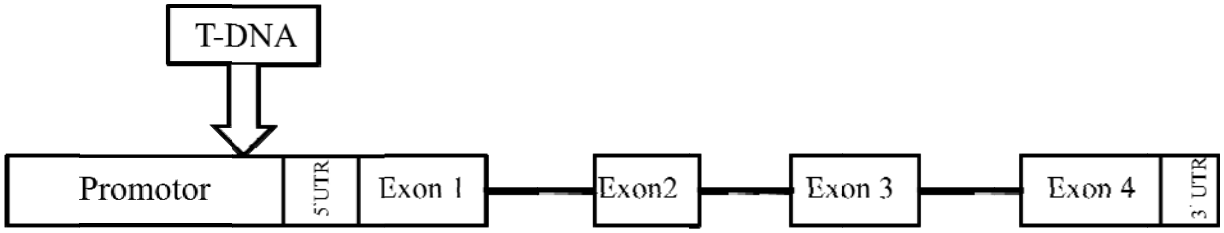

Figure 3-39 Genomic organization of the T-DNA integration site in the "*bushy-ff*" mutant.
The exon-intron structure of At1g77000 is shown along with the promoter, the 5' and 3' UTR. In the *"bushy-ff"* line the T-DNA was inserted 146 nucleotides upstream of the start codon *F-box* locus.

Additional PCRs with T-DNA primers and *F-box* At1g77000 specific primers confirmed the T-DNA integration and sequence analysis of the PCR bands placed the insertion 146 nucleotides upstream of the predicted ATG of At1g77000 (Figure 3-39). Furthermore, sequence analysis also indicated that eight nucleotides were missing in the "*bushy-ff*" genomic DNA due to the T-DNA integration event.

3.2.4 Is the T-DNA insertion in *F-box* At1g77000 gene responsible for the *"bushy-ff"* phenotype?

To test whether the T-DNA insertion in the promoter of the *F-box* At1g77000 gene is responsible for the "*bushy-ff*" phenotype, three further T-DNA insertion lines from the SALK collection were analysed which have a predicted insertion at various locations within the *F-box* At1g77000 locus. The T-DNA of SALK line 028396 was predicted to be inserted in the first exon of *F-box* At1g77000 while the T-DNAs of lines 070175 and 045957 ought to be inserted in the promoter region of *F-box* At1g77000. Since the two last lines had insertions similar to the insertion of the "*bushy-ff*" mutant, these two lines were molecularly analysed (Figure 3-40). To this end, genomic DNA was extracted from these lines and used as a template for PCR with *F-box* and T-DNA-specific primers (See Table 2-3 in Materials and Methods). By sequencing the PCR bands we have found that in both lines the T-DNA was integrated in the promoter region, specifically 243 base pairs (bp) before the predicted ATG start codon of *F-box* At1g77000 (Figure 3-41).

We performed molecular analysis on "*bushy-ff*" and *F-box* At1g77000 knock out plants with semi quantitative RT-PCR. PCR with actin oligos was carried out to show that an equal amount of cDNA was used in the PCR reactions. As shown in Figure 3-42 in RT-PCRs, with increasing PCR cycle numbers, the signals became stronger indicating the cycles chosen for analysis are within the dynamic range of PCR amplification and results indicated that *F-box* At1g77000 is expressed at low levels in "*bushy-ff*" and *f-box* At1g77000 knock out plants. The insertion of the T-DNA in promoter region in both lines reduced the expression and did not completely knock it out.

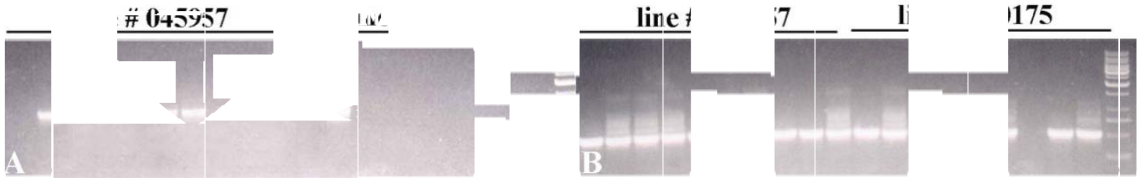

Figure 3-40 PCR analysis to detect the T-DNA in Salk knock out lines.
Genomic DNA was extracted from leaves of predicted *F-box* knock out plants and used as a template. A, PCR with Salk LB (Table 2-3, 59) and *F-box* specific (Table 2-3, 15) oligos for characterization of SALK line 045957 and PCR with same oligos for characterization of Salk line 070175. B, PCR with Salk LB nested (Table 2-3, 60) and *F-box* specific (Table 2-3, 15) oligos for characterization of Salk line 045975 and PCR with same oligos for characterization of Salk line 070175.

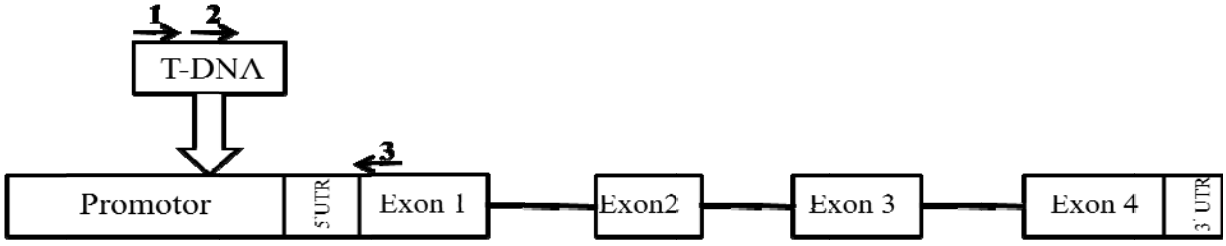

Figure 3-41 In SALK lines 070175 and 045957 the T-DNA was inserted 243 bp before the start codon in the promoter region of the *F-box* At1g77000 gene.
1: Salk LB forward primer; 2: Salk LB nested forward primer; 3: *F-box* exon 1 reverses primer.

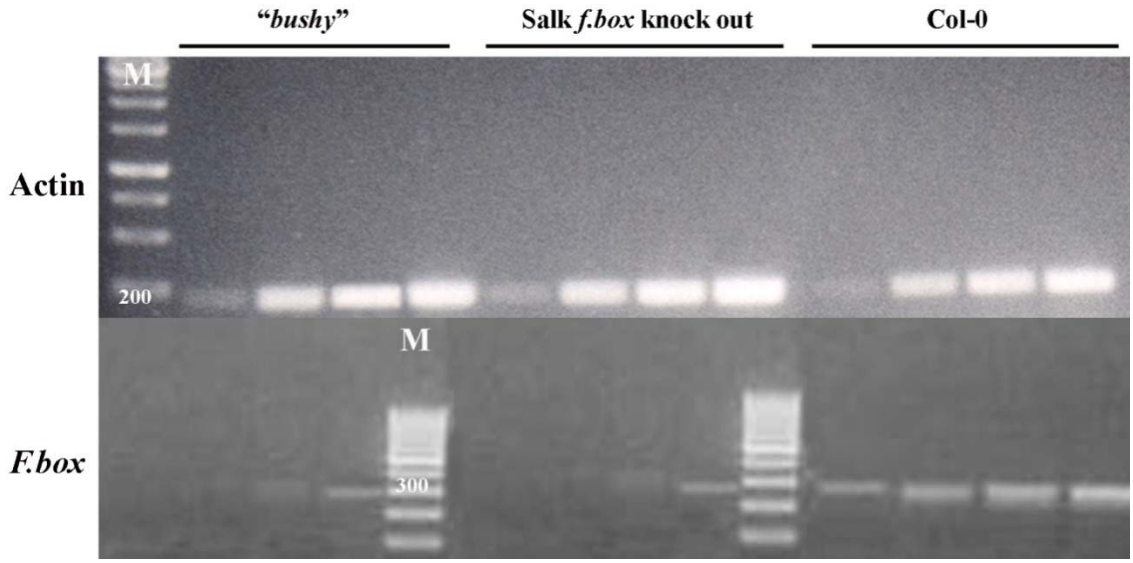

Figure 3-42 Expression analysis of *F-box* in the "*bushy-ff*", Salk T-DNA insertion lines of At1g77000 and Col-0.
Semi quantitative RT-PCR analysis with 1 µg total RNA which was extracted from Col-0, "*bushy-ff*" and Salk 070175 plants and used for making cDNA which served as a template in semi quantitative RT-PCR analysis. Actin: Semi quantitative RT-PCR as a cDNA input control with actin specific oligos: (Table 2-3, 56 and 57). F-box: Semi quantitative RT-PCR to test expression levels of *F-box* mRNA with *F-box* specific oligos (Table 2-3, 4 and 3). Lanes 1, 2, 3 and 4 correspond to PCR cycle 23, 25, 27 and 30. M= molecular weight marker with 200 and 300 bp band indicated.

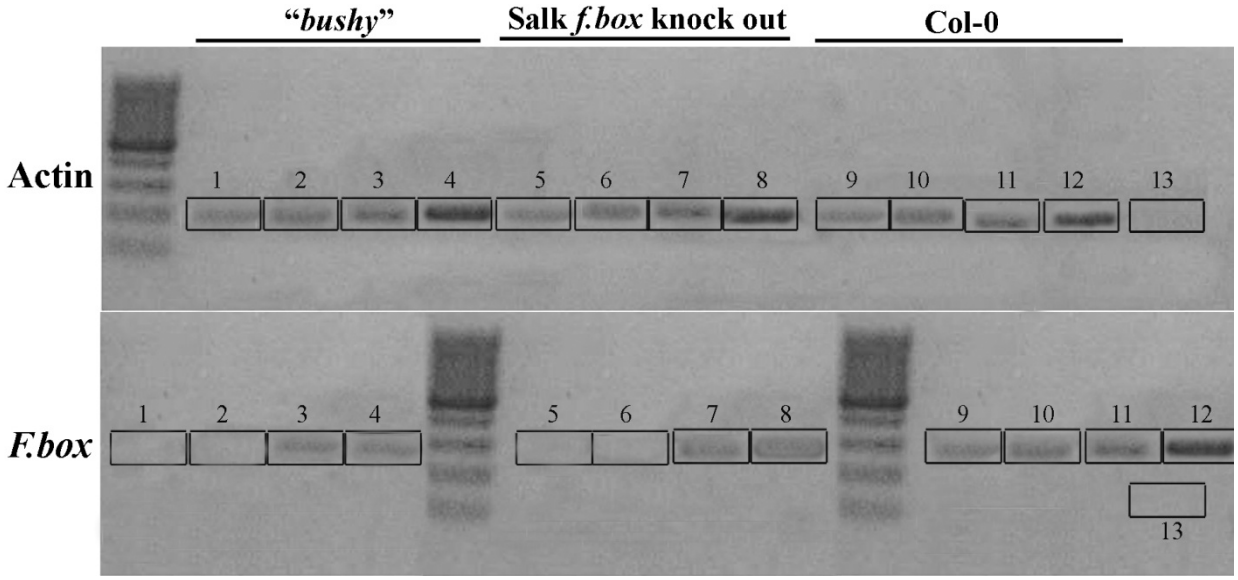

Figure 3-43 Quantitation of RT-PCR bands intensity with Aida Image analyser.
To quantitation of the RT-PCR bands intensity, the gel was scanned and the software counted the pixels of each RT-PCR bands in compare to background.

Table 3-1 Data related to quantitation of RT-PCR bands produced by Aida Image analyser software.

number	Integral-Bkg LAU	Integral/Area-Bkg LAU /mm^2	number	Integral-Bkg LAU	Integral/Area-Bkg LAU /mm^2
1	0	0	1	755.64	37.10385
2	0.07	0.006731	2	476.73	45.83942
3	226.98	21.825	3	632.25	60.79327
4	219.8	21.13462	4	755.64	72.65769
5	31.91	3.068269	5	371.67	35.7375
6	18.69	1.797115	6	479.62	46.11731
7	88.78	8.536538	7	629.73	60.55096
8	187.69	18.04712	8	746.53	71.78173
9	370.71	35.64519	9	391.15	37.61058
10	489	47.01923	10	503.1	48.375
11	600.95	57.78365	11	633.9	60.95192
12	717.35	68.97596	12	744.4	71.57692
13	0.0	0	13	0	0

Actin standardization (Normalization): For quantitation the pixel count values for actin and *F-box* At1g77000 PCR bands in the different genotypes were obtained and standardized to actin PCR bands. Thus, the actin Integral/Area-Background values (Table 3-1) of Salk *F-box* At1g77000 KO in cycle 29 (number 8=71.78173) was divided by the actin Integral/Area-Bgk value of Col-0 (number12=71.57692):

$$71.78173/71.57692=1.002$$

Now the *F-box* At1g77000 Integral/Area-Background values (Table 3-1) for Col-0 (12=68.9759) was multiplied with 1.002 for standardization:

$$68.97596 \times 1.002=69.11391$$

Then the *F-box* At1g77000 PCR values in different genotypes can be compared with each other:

$$69.11391/18.04712=3.74171\ X$$

So, according this calculation we could say that the expression of *F-box* At1g77000 in Col-0 is 3.74 X more than in Salk *F-box* At1g77000 mutant. With same procedure, we calculated that the expression of *F-box* At1g77000 in Col-0 is 3.23 X more than in the "*bushy-ff*" mutant (Figure 3-44).

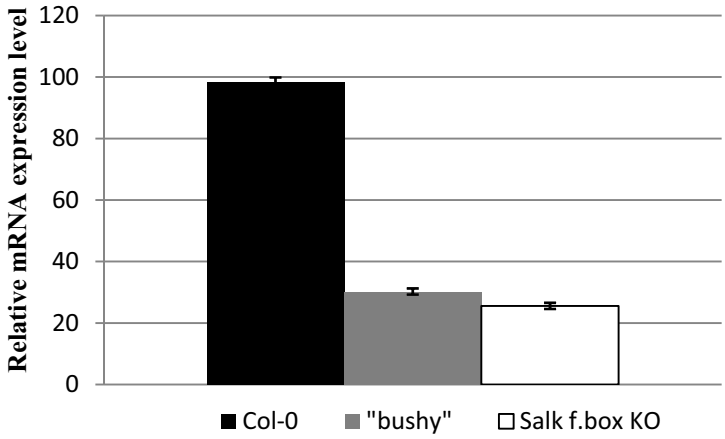

Figure 3-44 Quantitation of semi quantitative RT-PCR analysis of *F-box* At1g77000 gene expression in Salk f-*box* At1g77000 mutants and "*bushy-ff*" compared to *F-box* At1g77000 expression in Col-0 plants.
For quantitation the pixel count values for actin and *F-box* PCR bands in the different genotypes were obtained and standardized to actin PCR bands. Afterwards the *F-box* PCR values in different genotypes were compared with each other. RNA expression levels are expressed as relative to actin control and RT-PCRs data at cycle 27 have been shown.

Figure 3-45 Salk T-DNA insertion lines in At1g77000 did not phenocopy the "*bushy-ff*" phenotype.
Salk *f-box* At1g77000 knock out lines and "*bushy-ff*" grown five weeks in short day condition. Bars are given for size reference.

According to the hypothesis that a "mutation" in *F-box* At1g77000 is responsible for the "*bushy-ff*" phenotype", knock out *F-box* At1g77000 lines should display a similar phenotype as the "*bushy-ff*" mutant, but the Salk lines did not show any morphological phenotype, in contrast to the "*bushy-ff*" mutant (Figure 3-45).

Therefore, the presence of a second T-DNA in the "*bushy-ff*" line was suspected.

3.2.5 Detection of 2nd T-DNA in the *"bushy-ff"* line

Since the knock out *F-box* At1g77000 lines did not show morphological aberrations as were observed in "*bushy-ff*" plants, we considered it likely that there might be a second T-DNA insertion responsible for the "*bushy-ff*" phenotype. This was supported by segregation analyses, in which the Gentamycin marker did occur more frequently than expected for a single T-DNA insertion line. We addressed this question by Southern blot and another TAIL/adaptor ligation PCR. Despite several repetitions, the Southern blot experiments in this case were not successful, but using TAIL/adaptor ligation PCR, we could identify the presence of a 2nd T-DNA in the "*bushy-ff*" mutant (Figure 3-46, A). The 2nd T-DNA had integrated in an already characterized locus, 123 nucleotides upstream from the start codon the in the promoter region of At5g18580 (=*FASS/TON2*) (Torres-Ruiz and Jurgens, 1994; Camilleri et al., 2002), (Figure 3-46, B and Figure 3-47). Recessive mutations in the *FASS* gene cause a strong compression of the longitudinal axes of the plant body and of its organs throughout development. Mutations in *FASS* alter the pattern of cell division from the zygote without interfering with embryonic pattern formation. *fass* mutants can develop into tiny adult plants with all parts including floral organs (Figure 3-48). At the cellular level *fass* mutants affect cell elongation and the orientation of cell walls due to defects in cortical microtubule orientation but do not interfere with cell polarity as evidenced by the unequal division of the zygote (Torres-Ruiz and Jurgens, 1994; Camilleri et al., 2002). Moreover, FASS was shown to interact in an Y2H with a protein phosphatase (Camilleri et al., 2002).

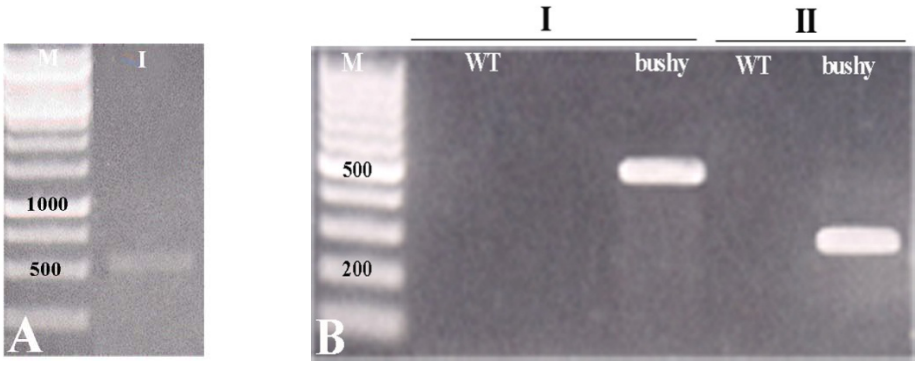

Figure 3-46 Molecular analysis with adaptor ligation PCR revealed presence of a second T-DNA in the "*bushy-ff*" mutant. A, I: PCR with AP2 and T-DNA LB nested oligos (Table 2-3, 55 and51). B, PCR with *FASS* - and T-DNA-specific oligos. I, PCR with FASS specific (Table 2-3, 26) and T-DNA LB (Table 2-3, 50) in Col-0 and "*bushy-ff*"; II, PCR with *FASS* specific (Table 2-3-26) and T-DNA LB nested (Table 2-3-51) oligos in Col-0 and "*bushy-ff*".

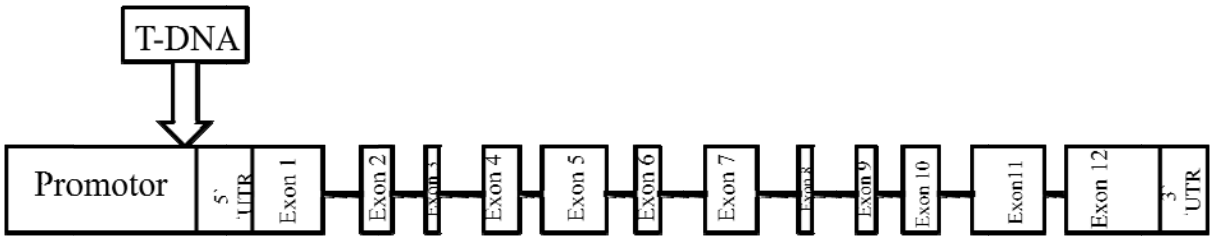

Figure 3-47 Genomic organization of the 2nd T-DNA integration site in the "*bushy-ff*" mutant.
In the *"bushy-ff"* line the 2nd T-DNA was inserted 123 nucleotides upstream of the start codon *FASS* locus.

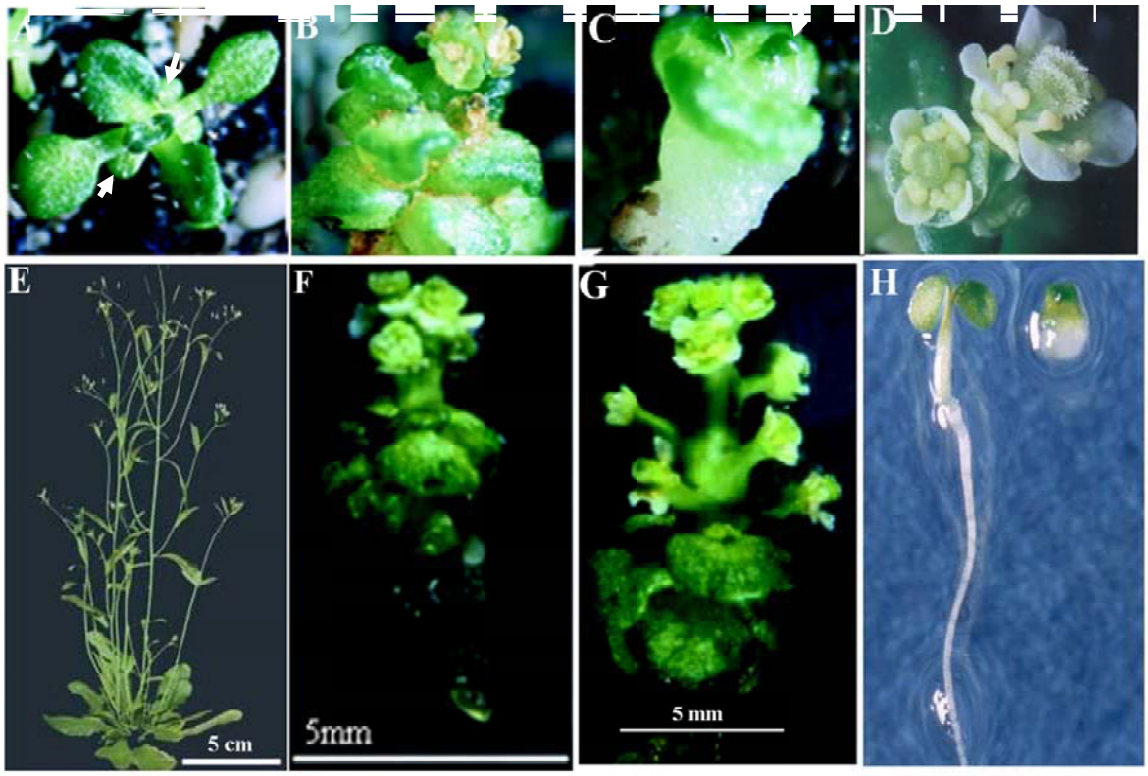

Figure 3-48 Morphology of mutants which carry mutations in the *FASS* gene.
A, Tricotyledoneous *fs* plants (weak allele) which cotyledons evenly spaced (arrowheads), and three staggered primary leaves; B, Adult plant with flowers (strong allele) ; C, Strong-phenotype seedling with emerging root (arrowhead) and primary leaves (arrows). D, Flower of weak (ton2-14) allele. E, wild-type seedling 6.5 weeks after germination, F and G strong (F: ton2-13) and weak (G: ton2-12) alleles of the ton2 mutation 6.5 weeks after germination (Figure reassembled from: (Torres-Ruiz and Jurgens, 1994; Camilleri et al., 2002).

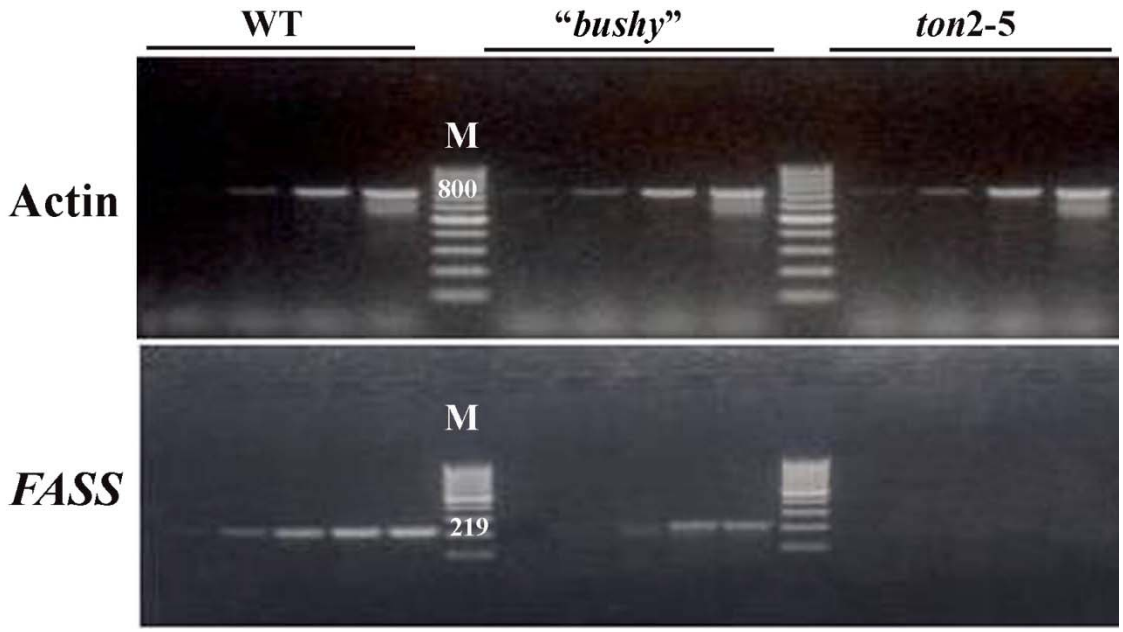

Figure 3-49 Expression analysis of *FASS* in Col-0, "*bushy-ff*" and *ton2-5* plants.
Semi quantitative RT-PCR analysis with 1 µg total RNA which was extracted from Col-0, "*bushy-ff*" and *ton2-5* plants and used for making cDNA as a template for semi quantitative RT-PCRs. Actin: Semi quantitative RT-PCR as a cDNA input control with actin specific oligos: (Table 2-3, 58 and 57) in Col-0; "*bushy-ff*" and *ton2-5* mutant. *FASS*: Semi quantitative RT-PCR to test expression levels of *FASS* mRNA with *FASS* specific (Table 2-3, 33 and 30) oligos in Col-0; "*bushy-ff*" and *ton*2-5 mutant. Lanes 1, 2, 3, 4 and 5 correspond to PCR cycle 23, 25, 27, 30 and 33. M= molecular weight marker with 800 and 219 bp band indicated.

We measured the expression levels of *FASS* RNA using semi-quantitative RT-PCR (Figure 3-49). After standardization of actin bands with the described procedure in 3-2-4 was calculated that the expression of *FASS* in Col-0 is 2.12 X more than in "*bushy-ff*" and 13X more than in *ton*2-5 mutants (Figure 3-50).

The "*bushy-ff*" phenotype resembled the published *fs* (=*ton*2-5) phenotype, both mutants were severely stunted. However as shown later in (Figure 3-51) they also had some differences. Also, with comparing *FASS* mRNA levels in the "*bushy-ff*" and *ton*2-5 mutant using semi-quantitative RT-PCR analysis, we found low expression levels of *FASS* in "*bushy-ff*", while in the *ton*2-5 mutant no expression of *FASS* could be detected. Therefore, so far we concluded that the "*bushy-ff*" phenotype was a consequence of a *FASS* knocks down mutation, while the *ton 2-5* mutant was a *FASS* knock out mutant (Figure 3-49 and Figure 3-50).

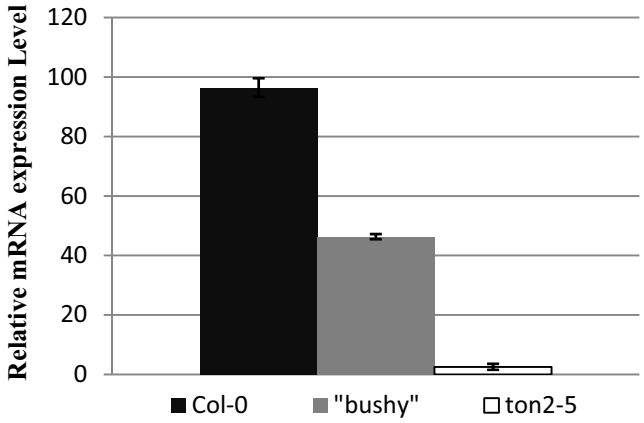

Figure 3-50 Quantitation of semi quantitative RT-PCR analysis of *FASS* gene expression in *ton2-5* and *"bushy-ff"* compared to *FASS* expression in Col-0 plants.
RNA expression levels are expressed as relative to actin control and RT-PCRs data at cycle 27 have been shown.

3.2.6 Is the *"bushy-ff"* mutant allelic to the *fass (=ton2)* mutant?

Our finding that "*bushy-ff*" contains two independent mutations, one in *F-box* At1g77000 locus and another in *FASS* locus and since "*bushy-ff*" mutant was partly similar in appearance to *fass* mutant, therefore this question was raised whether "*bushy-ff*" is allelic to *fass* or both of the occurred mutations are required for "*bushy-ff*" phenotype. This was particularly likely in view of the data that recessive mutations in the *FASS* gene cause a strong alteration in normal development due to abnormalities of the cortical microtubular cytoskeleton, as well as overall plant morphology (Torres-Ruiz and Jurgens, 1994; Camilleri et al., 2002). To answer this question, we phenotypically compared *fass* mutants which were kindly provided by Dr. Bouchez with the "*bushy-ff*" line. We compared the *fass* mutant with the "*bushy-ff*" and Col-0 plants at different stages of development (Figure 3-51). Apart from the fact, that both mutants were severely stunted, we found striking morphological differences between the two mutants and the Col-0. For example, as shown in Figure 3-51, the mutants are not morphologically similar in the seedling stage. At day 4 and 14, *fass* seedling were smaller in size than Col-0 and "*bushy-ff*" seedlings, while the overall size of "*bushy-ff*" seedlings at day 4 and 14 was quite similar to Col-0 seedlings. At day 14, the Col-0 and "*bushy-ff*" seedlings contained 2 cotyledons and 4 primary leaves, while in the *fass* seedling just two cotyledons had appeared. But these morphological differences could be a result of the different mutation sites in "*fass*" and "*bushy-ff*" (for example *ton2-5* has a nonsense mutation in exon8 of *FASS* (Camilleri et al., 2002) while the "*bushy-ff*" mutation had a T-DNA insertion occurring in the promoter). Although these evidences revealed differences between *ton2*-5, *fs* R325-23, *fs* R226-32 and "*bushy-ff*", but they were not a strong argument to claim "*bushy-ff*" is not allelic to *fass* mutant. Thus, we speculated genetic analyses should help resolve this question.

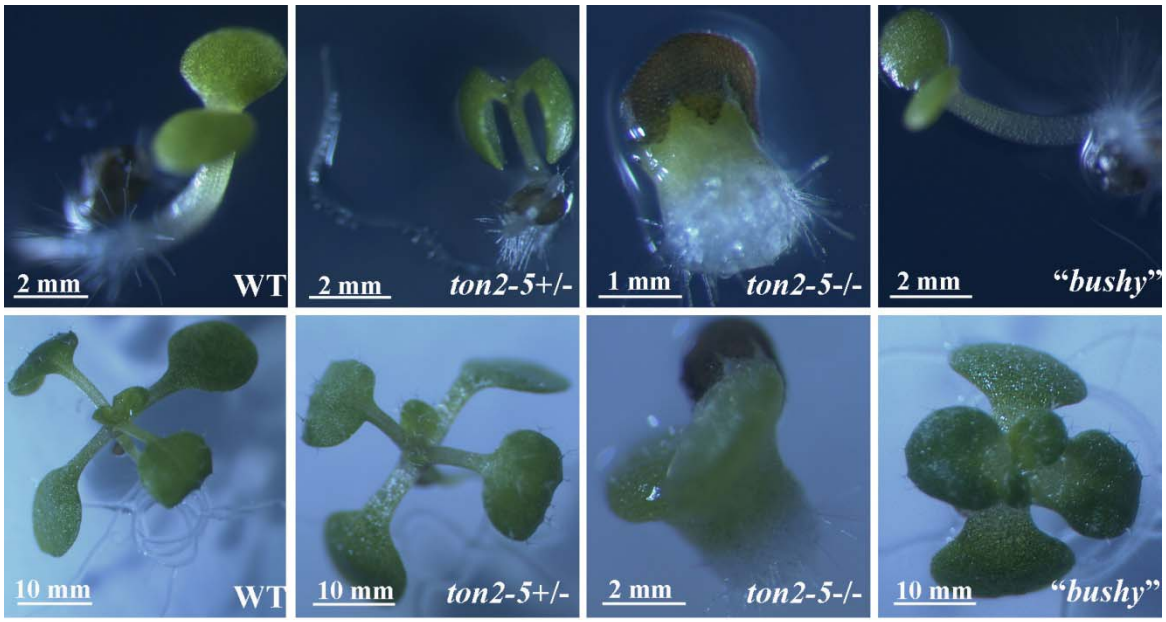

Figure 3-51 Comparison of Col-0, *ton2-5* and *"bushy-ff"* seedlings.
Top row: 4 days old seedlings, and low row: 2 weeks old seedlings grown on MS media. Bars are given for size reference.

Figure 3-52 Morphological appearance of plants in the F_2 generation of Col × "*bushy-ff*".
Three week old F_2 plants of a cross between Col and "*bushy-ff*" plants were analyzed. 6 out of 94 (1/16) plants show "*bushy-ff*" phenotype (circled).

3.2.7 Genetic cross of Col-0 × "*bushy-ff*" revealed "*bushy-ff*" phenotype is a result of two mutations

In order to test our hypothesis, that the two T-DNA insertions combined are required for the "*bushy-ff*" phenotype, we set up a cross between the "*bushy-ff*" mutant and Col-0 plants. Results of this cross revealed that the morphological phenotype of *"bushy-ff"* is a recessive trait, because in the F_1 generation of this cross 100% of plants were looking phenotypically like Col-0. And since in the F_2

generation of this cross 6 out of 94 (approx. 1/16) plants emerged as "*bushy-ff*" (Figure 3-52), it was supposed again that the "*bushy-ff*" phenotype is the result of two independent mutations.

To confirm the genetic results from the Col-0 × "*bushy-ff*" cross which were indicative of two independent mutations in the "*bushy-ff*" plants, the 6 phenotypically "*bushy-ff*" plants and 32 phenotypically Col-0 looking plants of the F_2 generation were molecularly characterized for carrying a T-DNA insertion in the *F-box* At1g77000 or *FASS* gene. To this end, genomic DNA of the plants was extracted and characterized by PCR. Flanking sequence tag PCRs (FST PCRs) with T-DNA-and gene-specific oligos (Figure 3-54 and Figure 3-55) showed the presence of both T-DNAs in the "*bushy-ff*" looking plants (Figure 3-53, A and B) and wild type PCRs with gene-specific oligos showed these lines were homozygous for the mutations since no PCR bands were obtained in contrast to the wild type control plants (Figure 3-53, C). Therefore we concluded that "*bushy-ff*" plants are homozygous knock down for *F-box* At1g77000 and *FASS* locus.

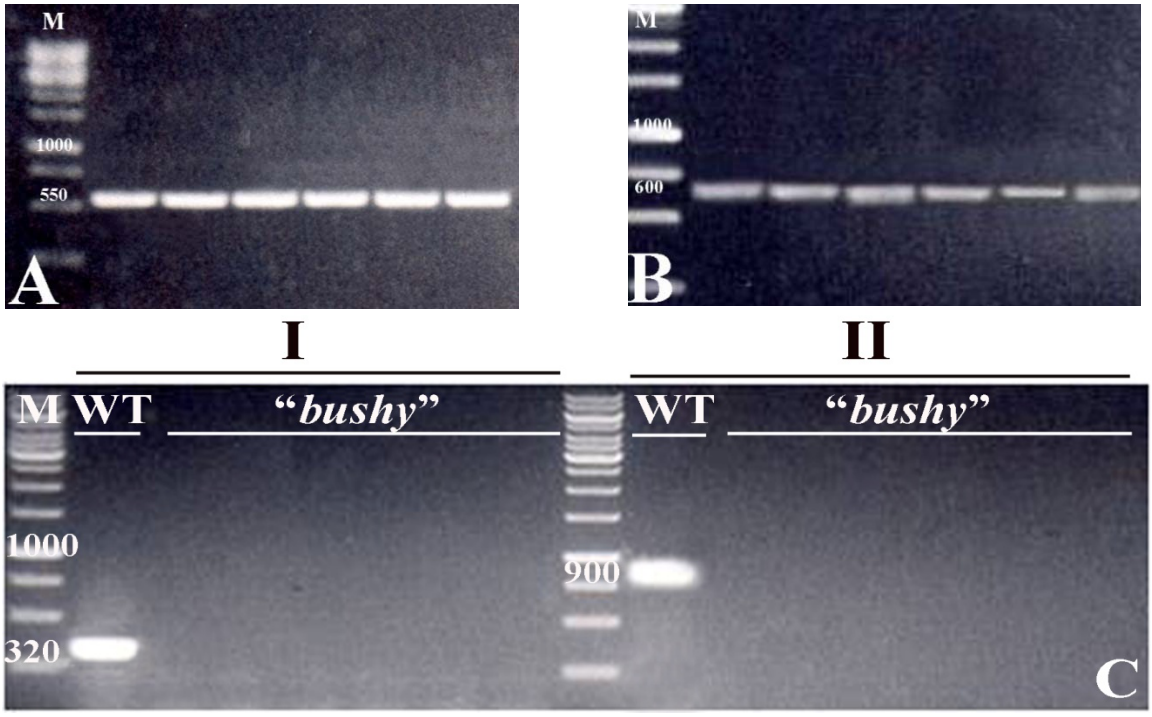

Figure 3-53 Genotyping F_2 "*bushy-ff*" looking plants.
From the 6 "*bushy-ff*" looking plants obtained in the F_2 generation, gDNA was extracted and used for PCR. A, FST PCR to show presence of T-DNA in *F-box* At1g77000 promoter with *F-box* specific (Table 2-3, 16) and T-DNA LB (Table 2-3, 50) oligos. B, FST PCR to show presence of T-DNA in promoter of *FASS* with T-DNA LB (Table 2-3, 50) and *FASS* specific (Table 2-3, 26) oligos. C, wild type PCR to analyse whether "*bushy-ff*" plants are homozygous knock down lines; I, with *FASS* specific (Table 2-3, 23 and 25) oligos; II, with *F-box* specific (Table 2-3, 16 and 15) oligos; in Col-0 and "*bushy-ff*" plants respectively.

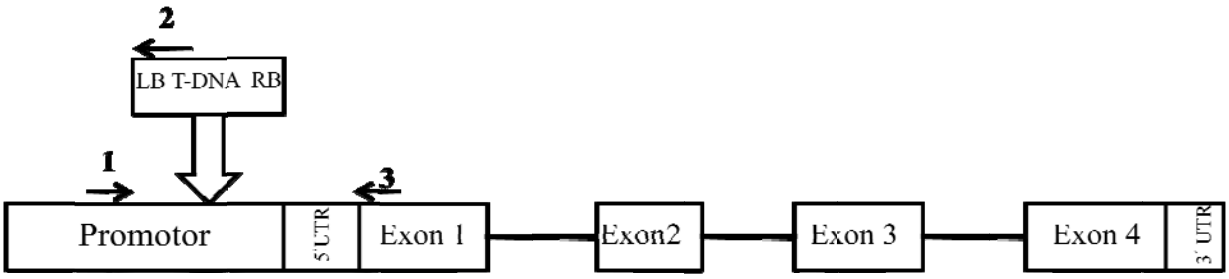

Figure 3-54 Schematic representation of *F-box* At1g77000 oligos used in the characterization of Col × "*bushy-ff*' plants. 1, *F-box* 750 forward and 2, T-DNA LB reverse oligos were used in the so called FST PCRs. 1 and 3, *F-box* exon 1 reverse oligos were used in so called WT PCRs.

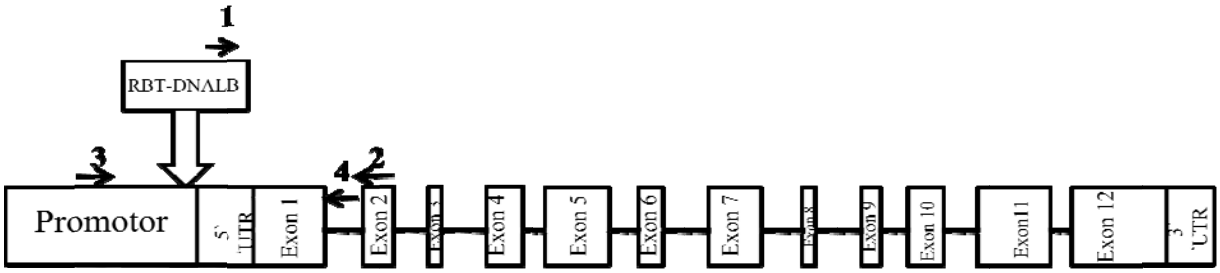

Figure 3-55 Schematic representation of *FASS* oligos used in the characterization of Col × "*bushy-ff*" plants. 1, T-DNA LB and 2, *FASS* exon 2 reverse ligos were used in the so called FST PCRs.3, *FASS* promoter forward and 4, *FASS* intron 1 reverse oligos were used in so called WT PCRs.

The characterization of the 32 Col-0 looking plants involved the same PCR reactions (Figure 3-56, A and B). These PCRs allowed to identify lines which had a single mutation for either the *F-box* At1g77000 or the *FASS* gene. FST-PCRs with *F-box* 750 forward and T-DNA LB oligos revealed that lines 6, 7, 18, 24 and 29 did not contain a T-DNA insertion in *F-box* At1g77000, but in the *FASS* gene (Figure 3-56, A). These results together revealed that lines 6, 7, 18, 24 and 29 only had a mutation in the *FASS* locus.

Conversely, lines 3, 5, 11, 13, 25 and 28 had only a T-DNA insertion in the *F-box* At1g77000 locus (Figure 3-56, B). These PCRs were repeated several times with independently prepared gDNA.

Line 26 did not produce any PCR band in both FST-PCRs which means this line does not carry any T-DNA and belonged to that 1 out of 16 plants which are genetically wild-type.

Together, we were not able to detect two T-DNA insertions in morphologically inconspicuous plants, thus we conclude that a combination of mutations in the *F-box* At1g77000 and the *FASS* gene are needed to cause the "*bushy-ff*" phenotype.

After the identification of single knock out lines (single *fass* knock down lines: 6, 7, 18, 24 and 29 and single *f-box* At1g77000 knock down lines: 3, 5, 11, 13, 25 and 28) we performed WT-PCRs to identify "homozygous" single knock down lines among the identified single T-DNA insertion lines. To this purpose, wild type PCRs with gene-specific oligos in each cases were performed (Figure 3-57) .To isolate *f-box* At1g77000 "homozygous" single knock down lines *F-box* 750 forward and exon 1 reverse oligos (Figure 3-57, I) and for isolate *fass* single homozygous knock down lines *FASS* Promoter forward and intron 1 reverse oligos were used (Figure 3-57 , II), (See Table 2-3 for used oligos). Results of these PCRs identified line 5 as a homozygous single *f-box* At1g77000 knock down line and line 24 as a homozygous single *fass* knock down line (Figure 3-57).

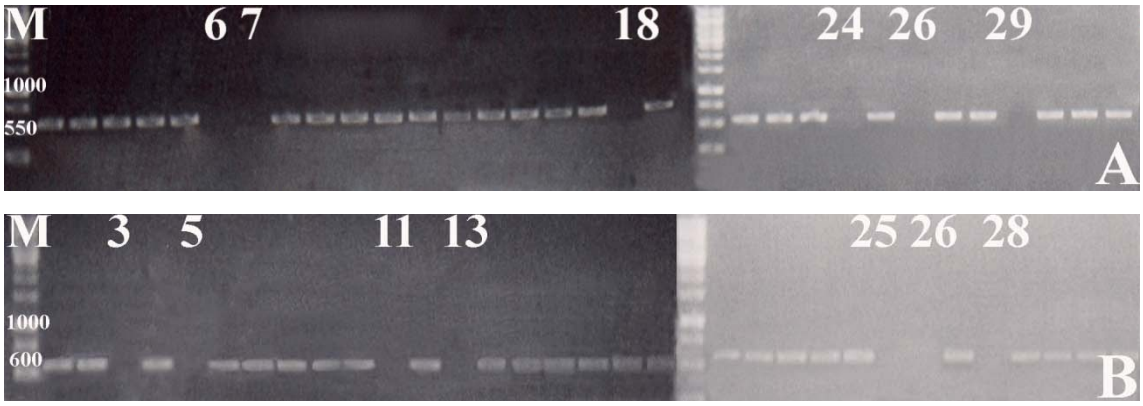

Figure 3-56 Genotyping wild-type looking plants.
From the 32 WT looking plants obtained in the F_2 generation, gDNA was extracted and used for PCR.A: FST-PCR with *F-box* specific (Table 2-3, 16) and T-DNA LB (Table 2-3, 50) oligos identified lines 6, 7, 18, 24 and 29 as lines which did not have a T-DNA insertion in the *F-box* At1g77000 gene. B: FST PCR with T-DNA LB (Table 2-3, 50) and *FASS* specific (Table 2-3, 26) oligos identified lines 3, 5, 11, 13, 25, and 28 which did not have mutation in *FASS* locus. Numbers indicates to line number. These characterization PCRs repeated several times with independent prepared gDNA and same PCR results were observed in all cases.

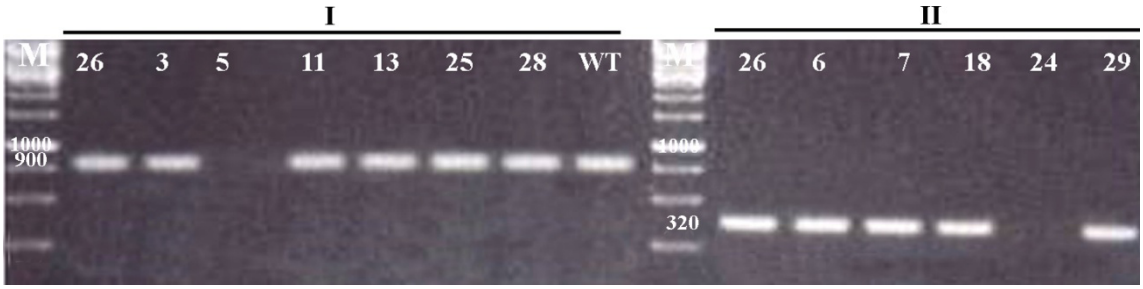

Figure 3-57 Screening for "homozygous" single mutant lines.
From the identified single T-DNA insertion lines obtained in the F_2 generation, gDNA was extracted and used for PCR. I, WT PCRs for isolating *f-box* single homozygous knock down lines with *F*-box specific (Table 2-3, 16 and 15) oligos. B, WT PCRs for isolating *fass* single homozygous knock down lines with *FASS* specific (Table 2-3, 23 and25) oligos.

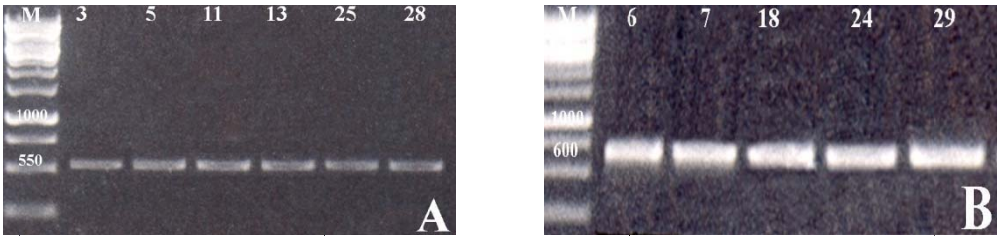

Figure 3-58 Confirmative FST-PCR results showed lines 3, 5, 11, 13, 25, and 28 were single *F-box* knock down and lines 6, 7, 18, 24 and 29 were single *FASS* knock down.
A, FST PCR with *F-box* specific (Table 2-3, 16) and T-DNA LB (Table 2-3, 50) oligos in lines 3, 5, 11, 13, 25, and 28 which did not produce band with *FASS* oligos, show the presence of the T-DNA in the promoter of *F-box* locus. B, FST PCR with T-DNA LB (Table 2-3, 50) and *FASS* specific (Table 2-3, 26) oligos in lines 6, 7, 18, 24 and 29 which did not produce band with *F-box* oligos, show the presence of T-DNA in *FASS* promoter. Numbers indicate line numbers.

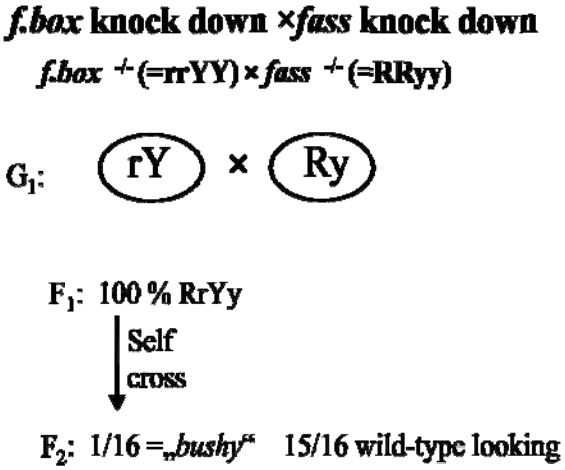

Figure 3-59 Schematic representation of the cross F-box-/- knock down×fass-/- knock down .
The F-box homozygous knock down line produced rY gametes (G1) and homozygous fass knock down mutants produced Ry G1. In F1 100 % of plants carried both mutations in F-box and FASS. Three independent F1 plants were followed in next generation

3.2.8 Genetic Cross of *f-box* At1g77000-/- knock down mutant × *fass*-/- knock down mutant

As mentioned before, results of Col × *"bushy-ff"* cross indicated that two independent mutations are required for the *"bushy-ff"* phenotype. To confirm our findings of the segregation of the "*bushy-ff*" phenotype another genetic cross was set up: the homozygous *F-box* At1g77000 knock down mutant, line 5, which was isolated among the F_2 generation of Col-0×"*bushy-ff*" cross (Figure 3-57), was crossed to the homozygous *fass* knock down mutant, line 24, (which this mutant also was isolated among the same source, see Figure 3-57) which should give rise in the F_2 generation to "*bushy-ff*" plants in a 15:1 ratio (Figure 3-59). Results of this cross reinforced our previous data which indicated that the "*bushy-ff*" phenotype is the result of two independent mutations, because in F_1 generation of this cross 100% of plants were wild-type looking (since phenotype of *"bushy-ff"* was recessive).Three independent F_1 plants were followed in the next generation. In F_2 generation of followed lines, ~1 out of 16 (11 out of 180 plants in line 1, 12 out of 190 plants in line 2 and 15 out of 242 plants in line 3)

were *"bushy-ff"* and ~15 out of 16 (169 out of 180 plants in line 1, 178 out of 190 plants in line 2 and 227 out of 242 plants in line 3) were wild-type looking (Figure 3-60, A and B).

All together our genetic data strongly supported the idea that the severe phenotype in the *"bushy-ff"* mutant was a result of both mutations in *F-box* At1g77000 and *FASS*. To understand whether, a specific mutation in *F-box* At1g77000 or *FASS* were necessary for arising this phenotype or any mutation in these genes could result in this kind of alteration in plant morphology, other genetic crosses between the lines which were allelic to our *F-box* At1g77000 knock down and *fass* knock

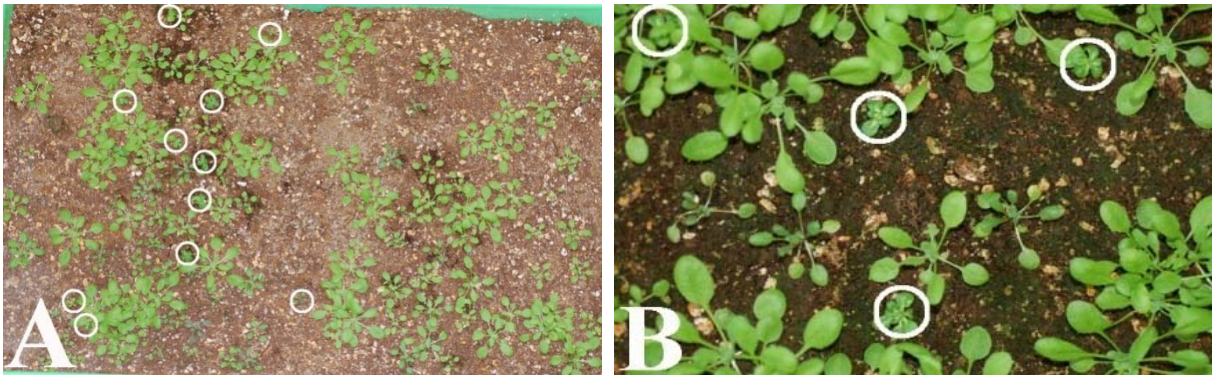

Figure 3-60 Segregation of the "*bushy-ff*" phenotype in the F_2 generation of the cross *f-box*$^{-/-}$ knock down× *fass*$^{-/-}$ knock down.
A, In F_2 generation line 1 displayed 11 out of 180 (~1 out of 16) plants with *"bushy-ff"* phenotype and 169 out of 180 (~15 out of 16) with wild-type looking phenotype. B, some of F_2 "*bushy-ff*" plants of line 1 with higher magnification.

down lines were performed.

3.2.9 Genetic cross of Salk *f-box* At1g77000 knock down$^{+/-}$ ×*fass* $^{-/-}$ knock down:

To address the question whether the "*bushy-ff*" phenotype is due to a combination of a particular set of mutations or whether the genetic interaction between *F-box* At1g77000 and *FASS* is irrespective of the mutant alleles, a cross between heterozygous Salk *f-box* At1g77000 knock down line and homozygous *fass* knock down mutant was performed. As mentioned before, we had isolated line 24 as a homozygous *fass* knock down mutant among the F_2 generation of Col-0×"*bushy-ff*" (Figure 3-52). Since the Salk *F-box* At1g77000 knock out line used in this cross was heterozygous, therefore in F_1 generation of this cross there were two groups of plants with different genotypes (Figure 3-61). 50 % of plants carried just one mutation in *FASS* locus and the other 50 % of plants (which were interesting for us) carried both mutations in *F-box* At1g77000 and *FASS*. A line which belonged to the latter 50 % group of plants which was genotypically shown to carry both mutations was identified by FST PCRs and was followed in the F_2 generation. When a defined number of F_2 seeds of the identified line were sowed on soil, it was recorded that 10 out of 160 plants (~1 out of 16) raised the "*bushy-ff*" phenotype and 150 out of 160 (~15 out of 16) showed wild-type looking phenotype (Figure 3-62, A and B). This indicated that the nature of the mutation in the *F-box* At1g77000 gene was not limited to the one discovered in the "*bushy-ff*" mutant.

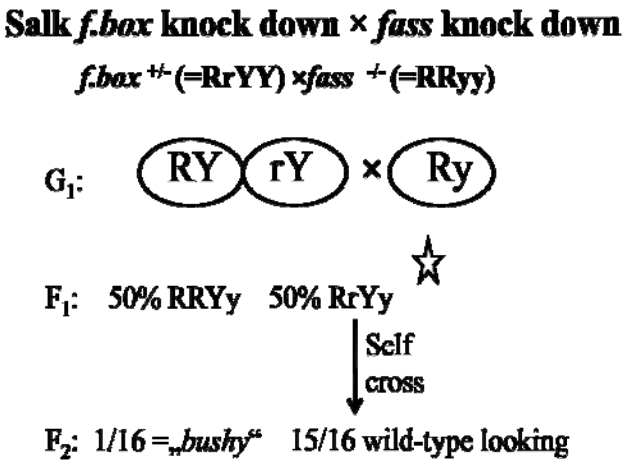

Figure 3-61 Schematic representation of the cross Salk f-*box* knock down$^{+/-}$ ×*fass* knock down$^{-/-}$.
The *f-box* At1g77000 heterozygous knock down line produced two different gametes: G_1 (RY and rY) while homozygous *fass* knock down produced one kind of G_1 (Ry). In F_1 50% of plants which were labelled with star in this figure carried both mutations in *F-box* and *FASS*. A line of this group was followed in F_2 generation.

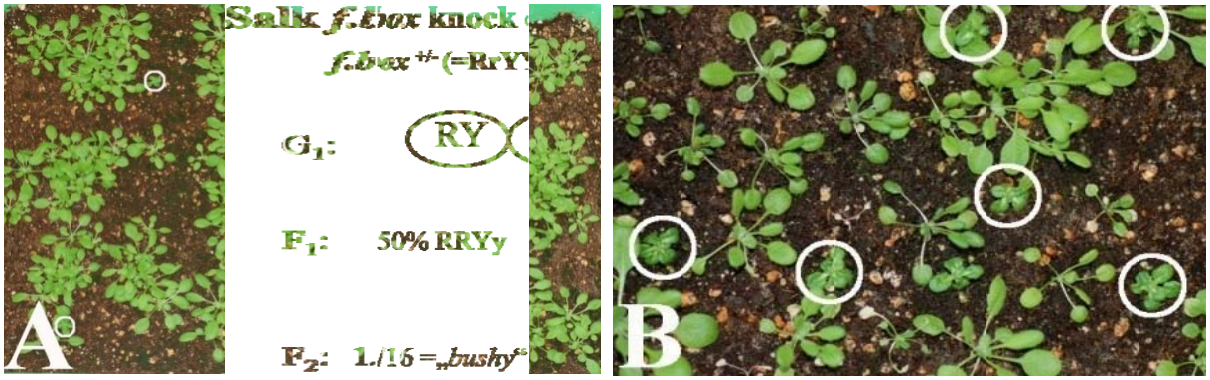

Figure 3-62 Segregation of the "*bushy-ff*" phenotype in the F_2 generation of the cross Salk *f-box* At1g77000 knock down$^{+/-}$ × *fass* knock down$^{-/-}$.
A, In F_2 generation of the identified line 10 out of 160 (~1 out of 16) plants were *"bushy-ff"* and 150 out of 160 (~15 out of 16) plants were wild-type looking .B, some of T_2 "*bushy-ff*" plants of identified line with higher magnification.

3.2.10 Cross of *F-box* At1g77000 knock down$^{-/-}$ mutant ×*ton2- 5* $^{+/-}$:

The reciprocal test aimed at the nature of the *fass* mutation. Thus, a third cross was performed between a homozygous *F-box* At1g77000 knock down line and a heterozygous *ton2-5* line. As mentioned before, we had isolated line 5 as a homozygous *F-box* At1g77000 knock down line in the F_2 generation of Col-0×"*bushy-ff*" (Figure 3-57).Since the *ton2*-5 mutant used in this cross was heterozygous, therefore in the F_1 generation of this cross 50% of plants are expected to carry just one mutation in the *F-box* At1g77000 locus and the other 50 % of plants (which were interesting for us) carried both mutations (Figure 3-63). A line which belonged to the latter 50% carrying both mutations was identified by FST PCRs and was followed in the F_2 generation. When a defined number of F_2 seeds of this line was sowed on soil, it was recorded that 100% of plants raised wild-type looking phenotype and none of the F_2 plants raised the "*bushy-ff*" phenotype (Figure 3-64). This indicated that the nature of the mutation in the *FASS* gene was specific to generate the *bushy-ff* phenotype.

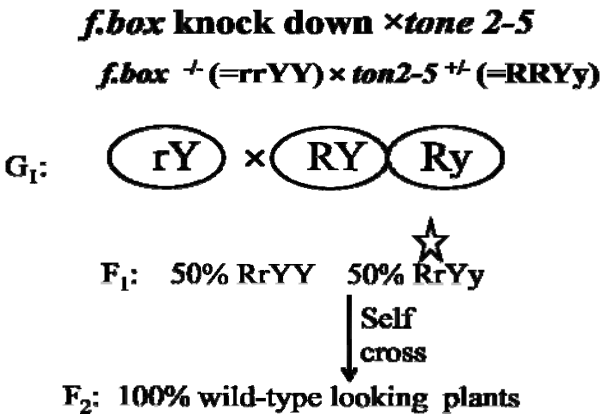

Figure 3-63 Schematic representation of the cross *f-box* knock down$^{-/-}$ ×*ton*2-5 $^{+/-}$ cross.
The *F-box* homozygous knock down line produced one kind G_1 (rY) while heterozygous *ton2-5* produced two different kinds of G_1 (RY and Ry). In F_1 50% of plants which were labelled with star in this figure carried both mutations in *F-box* At1g77000 and *FASS*. A line of this group was followed in F_2 generation.

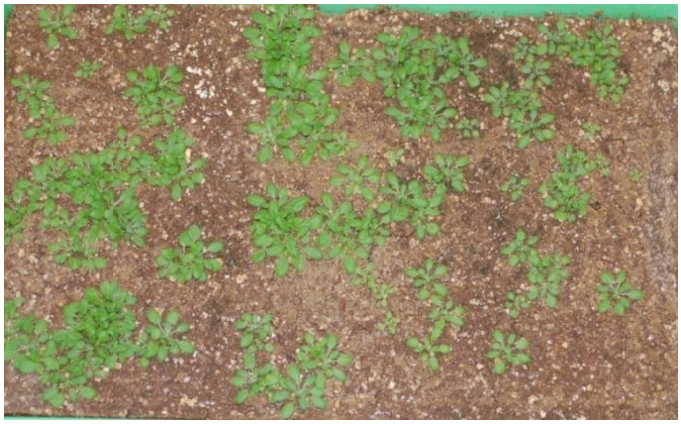

Figure 3-64 F2 generation of the cross *F-box* At1g77000 knock down mutant-/- ×ton 2-5 +/-.
F2 generation of the identified line of this cross were showed 100% plants with wild-type looking phenotype.

3.2.11 Genetic cross of Salk *F-box* At1g77000 knock down$^{+/-}$ mutant× *ton2-5* $^{+/-}$:

The last cross which was performed was the cross between Salk knock down mutant and *ton*2-5 mutant. Both of the lines used for this cross were heterozygous, therefore in F_1 there were four different group of genotypes, 25% of plant did not carry any mutation, 25 % carry a mutation only in *F-box* At1g77000 locus, 25 % carry a mutation only in *FASS* locus and just 25 % carried both mutations (Figure 3-65).The last 25 % of plants which genotypically carried both mutations were interesting for us. A line from this group of plants was identified with FST PCRs (Data not shown). This line was followed in the F_2 generation. When a defined number of F_2 seeds of this line were sowed on soil, it was recorded that 100% of plants raised wild-type looking phenotype and none of the F_2 plants raised the "*bushy-ff*" phenotype (Figure 3-66). This again, indicated that the nature of the mutation in the *FASS* gene was specific to generate the "*bushy-ff*" phenotype.

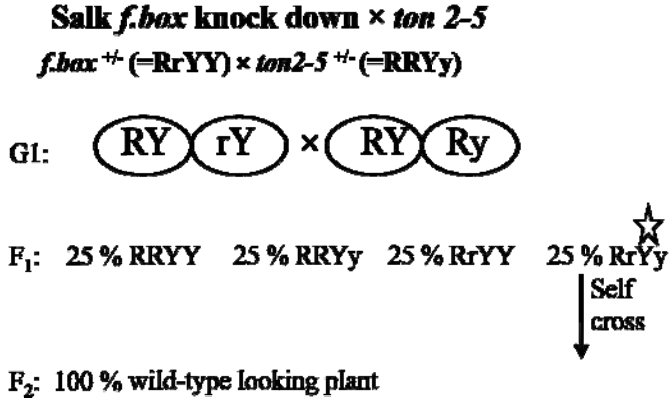

Figure 3-65 Schematic representation of the cross Salk *F-box* At1g77000 knock down$^{+/-}$ ×*ton*2-5$^{+/-}$cross.
The heterozygous *F-box* At1g77000 knock down line produced two different kinds of G_1 (RY and rY) and heterozygous *ton*2-5 mutant also produced two kinds of G_1 (RY and Ry).Therefore in F_1 just 25 % of plants which were labelled with star in this figure carried both mutations in *F-box* and *FASS*. A line of this group was followed in F_2 generation.

Figure 3-66 F_2 generation of the cross Salk *F-box* At1g77000 knock down mutant$^{+/-}$ ×*ton*2-5 $^{+/-}$.
F_2 generation of the identified line of this cross were showed 100% plants with wild-type looking phenotype.

3.2.12 Complementation of the "*bushy-ff*" phenotype with 35S:: *F-box* At1g77000

Our genetic analysis of the "*bushy-ff*" mutant suggested that constitutive expression of *F-box* At1g77000 should complement the "*bushy-ff*" phenotype. Therefore, lines constitutively expressing *F-box* At1g77000 (35S :: *F-box* At1g77000) were generated in the "*bushy-ff*" background. To this end, the coding sequence of *F-box* At1g77000 was amplified, so that Gateway attachment sites (attB1 and attB2) were fused to the end of the PCR band of *F-box* At1g77000 CDS. The PCR band was recombined into pDonor 201 and the sequence of the plasmid verified. The CDS of the *F-box* At1g77000 gene was recombined into destination vector, pGWB2 (Nakagawa et al., 2007), downstream of the strong 35S CaMV promoter through a LR reaction. The sequence of the plasmid was again verified. Finally the recombinant plasmid (Figure 2-5) was transformed into Col-0 and "*bushy-ff*" plants by the floral dip method (Clough and Bent, 1998). All transformed selected T_1 plants were wild-type looking plants (Figure 3-67, A).Transgenic lines 4 and 19 constitutively expressing the *F-box* At1g77000 gene in the "*bushy-ff*" background were chosen in the T_2 generation based on their segregation of 55:167 dead (susceptible): alive (resistant) to Kanamycin and Hygromycin selection indicating they carried one T-DNA. All resistant plants in the T_2 generation displayed normal Col-0 morphology, indicating that restoration of expression of *F-box* At1g77000 in "*bushy-ff*" could complement the "*bushy-ff*" phenotype. Further support for this claim stems from the following experiment: a small number of seeds of lines 4 and 19 (T_2 generation) were sowed on soil without antibiotic selection. As expected 24 out of 94 (in line 4) and 20 out of 80 (in line19) plants showed indeed the "*bushy-ff*" phenotype (consistent with ¼ of plants being non-transformed plants),(Figure

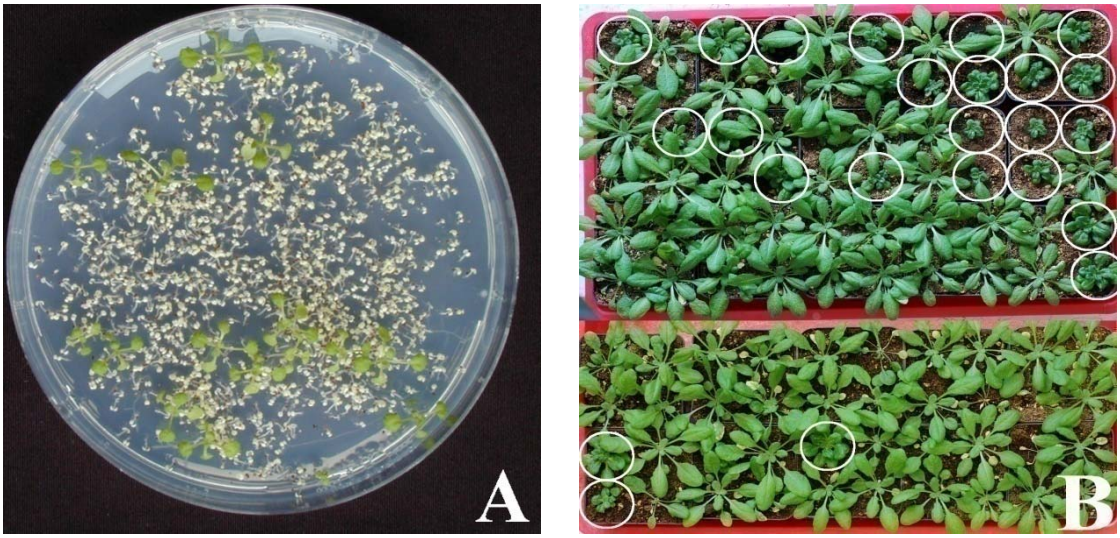

Figure 3-67 Over-expression of *F-box* At1g77000 in the "*bushy-ff*" background.
A, Selection of T_1 35S::*F-box* At1g77000plants on MS agar plates containing Kan^{50} and Hyg^{50}. B, T_2 plants of 35S::*F-box* At1g77000 line 4 in *"bushy-ff"* background ("*bushy-ff*"+pGWB2-*F-box* At1g77000 CDS) on soil without any selection, plants which are circled, displayed *"bushy-ff"* phenotype.

3-67, B). Consequently the segregation of lines 4 and 19 was followed in T_3, and 100% wild type normal phenotype displaying plants were observed.

Over-expression *F-box* At1g77000 lines in "*bushy-ff*" background were selected in the T_3 generation for homozygosity (plants that no longer segregate for the Kanamycin or Hygromycin-resistance marker) and the RNA levels of the *F-box* At1g77000 gene were analysed by semi quantitative RT-PCR. Semi quantitative RT-PCR analysis with *F-box* exon 4 6524 qRT forward and exon 4 6801 qRT reverse oligos confirmed over-expression of the *F-box* At1g77000 gene in lines 4 and 19 (Figure 3-68).

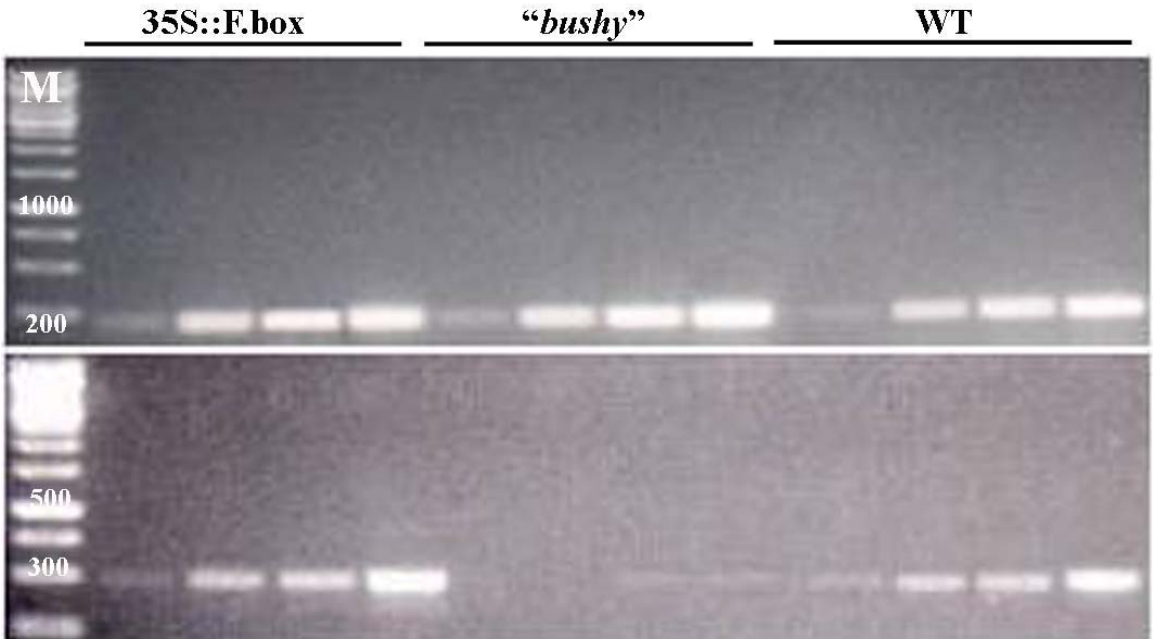

Figure 3-68 Expression analysis of *F-box* At1g77000 in 35S:: *F-box* At1g77000 line 19.
Semi quantitative RT-PCR analysis with 1 µg total RNA which was extracted from T_3 35S:: *F-box* At1g77000 plants, "*bushy-ff*" and Col-0 and was used for making cDNA as a template for semi quantitative RT-PCRs. Actin: Semi quantitative RT-PCR as a cDNA input control with actin specific oligos: (Table 2-3, 56 and 57) oligos in 35S:: *F-box* At1g77000 line 19; "*bushy-ff*" and Col-0. *F-box*: Semi quantitative RT-PCR to test expression of *F-box* mRNA with *F-box* specific (Table 2-3, 4 and 3) oligos in 35S:: *F-box* At1g77000 line 19; "*bushy-ff*" and Col-0. Lanes 1, 2, 3 and 4 correspond to PCR cycle 23, 25, 27 and 30. M= molecular weight marker with 200, 300 and 500 bp band indicated.

After standardization of Actin bands with the described procedure 3-2-4, I calculated that the expression of *F-box* At1g77000 in 35S::*F-box* At1g77000 is 2.6 X more than in Col-0 and 7.4 X more than in "*bushy-ff*"(Figure 3-69).

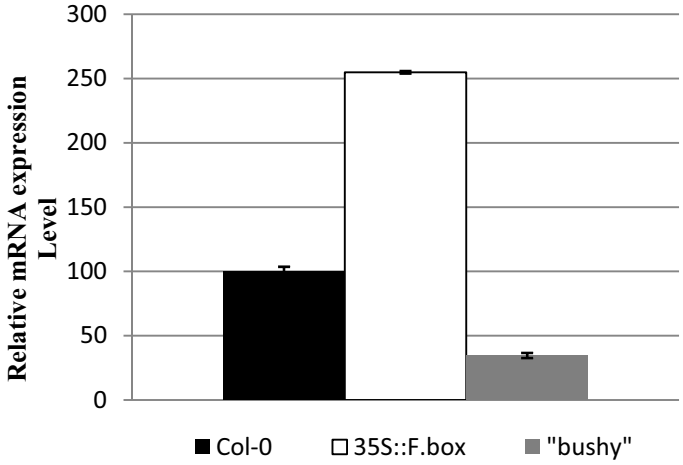

Figure 3-69 Quantitation of semi quantitative RT-PCR analysis of *F-box* At1g77000 gene expression in 35S:: F-box and "*bushy-ff*" compared to *F-box* At1g77000 expression in Col-0 plants.
RNA expression levels are expressed as relative to actin control and RT-PCRs data at cycle 27 have been shown.

3.2.13 Complementation of the "*bushy-ff*" phenotype with over-expression of *FASS*:

According to the genetic cross (Col×"*bushy-ff*") results which indicated that two independent mutations are required for the "*bushy-ff*" phenotype and since constitutive expression of *F-box* At1g77000 coding sequence could complement the "*bushy-ff*" phenotype, we wanted to examine whether the over-expression of *FASS* could also complement the "*bushy-ff*" phenotype. Therefore, the *FASS* coding sequence, which was amplified from cDNA, was cloned into the binary vector pJawohl3 downstream of the strong 35S CaMV promoter (Figure 2-3). The sequence of the recombinant plasmid was confirmed and the plasmid was transformed into Col-0 and *"bushy-ff"* plants by the floral dip method (Clough and Bent, 1998). All transformed T_1 plants were wild-type looking plants (Figure 3-70, A). Over-expressing *FASS* lines 2 and 9 in the "*bushy-ff*" background were chosen in the T_2 generation based on their segregation of 38:115 dead (susceptible): alive (resistant) to the BASTA herbicide which showed they carried one insertion. Here again, all plants which were resistant (alive) in the T_2 generation displayed normal Col-0 phenotype, which means that in "*bushy-ff*" over-expression of *FASS* coding sequence could complement the phenotype. When a defined number T_2 seeds of lines 2 and 9 were sowed on soil, 24 out of 96 (line 2) and 24 out of 98 (line 9) displayed the *"bushy-ff"* phenotype, consistent with ¼ of plants being non-transformed plants (Figure 3-70, B). In T_3, lines 2 and 9 displayed 100% plants with Col-0 looking phenotype.

Over-expressing *FASS* lines were selected in the T_3 generation for homozygosity (plants that no longer segregate for the BASTA-resistance marker) and with molecular analysis of the RNA levels by semi quantitative RT-PCR. Semi quantitative RT-PCR analysis with *FASS* oligos confirmed over-expression of FASS in lines 2 and 9 (Figure 3-71).

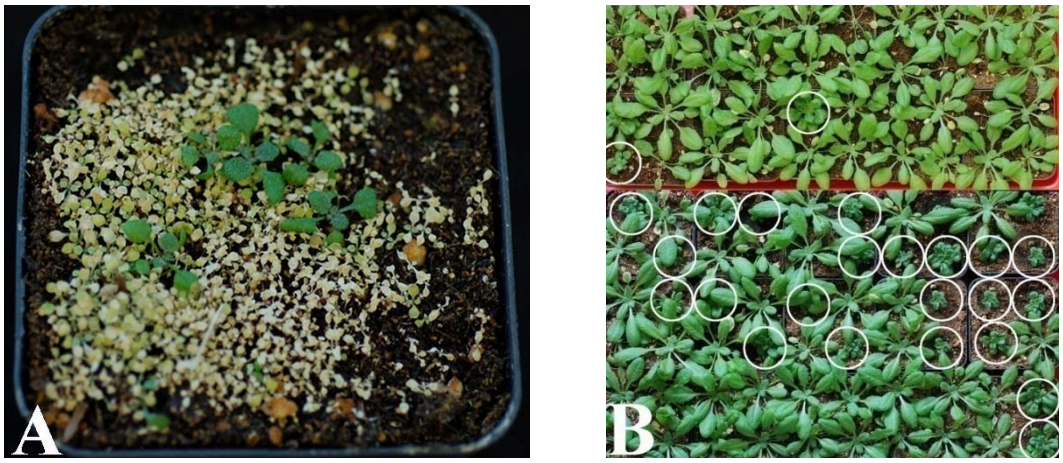

Figure 3-70 Over-expression *FASS* plants in "*bushy-ff*" background.
A, Selection of T_1 35S::*FASS* plants with resistance to the BASTA herbicide. B, T_2 generation of 35S::*FASS* line 9 in *"bushy-ff"* background (*"bushy-ff"*+pJawoh3+*FASS* CDS), on soil without any selection, plants which were circled, display the *"bushy-ff"* phenotype.

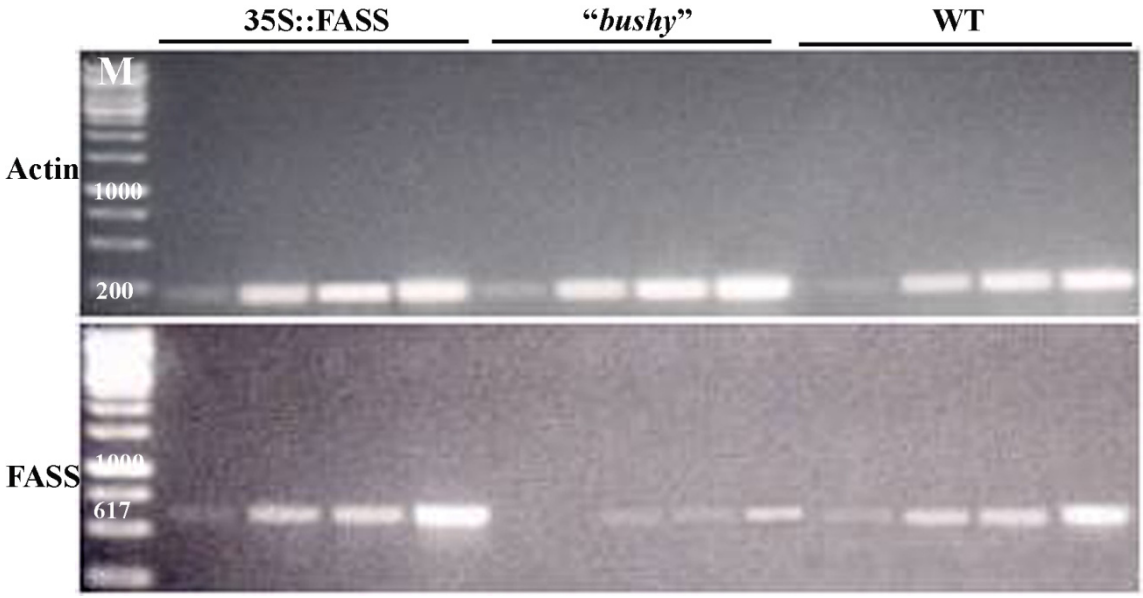

Figure 3-71 Expression analysis of *FASS* in 35S::*FASS* line 2.
Semi quantitative RT-PCR analysis with 1µg total RNA extracted from T3 35S::*FASS* plants, "*bushy-ff*" and Col-0 and was used for making cDNA as a template for semi quantitative RT-PCRs. Actin: Semi quantitative RT-PCR as a cDNA input control with actin specific oligos: (Table 2-3, 56 and 57) oligos in 35S::*FASS* line 2,"*bushy-ff*" and Col-0. *FASS* Semi quantitative RT-PCR to test the expression of FASS mRNA with *FASS* specific (Table 2-3, 33 and 31) oligos in 35S:: *FASS* line 2; "*bushy-ff*" and Col-0. Lanes 1, 2, 3 and 4 correspond to PCR cycle 23, 25, 27 and 30. M= molecular weight marker with 200, 617 and 1000 bp band indicated.

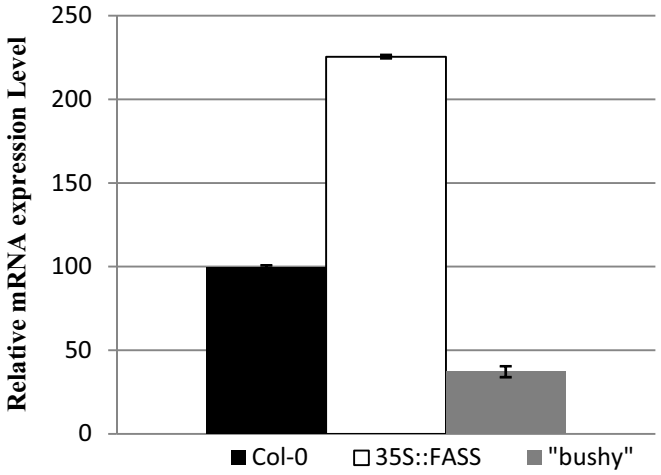

Figure 3-72 Quantitation of semi quantitative RT-PCR analysis of *FASS* gene expression in 35S::*FASS* and "*bushy-ff*" compared to *FASS* expression in Col-0 plants.
RNA expression levels are expressed as relative to actin control and RT-PCRs data at cycle 27 have been shown.

After standardization of actin bands with the described procedure 3-2-4, was calculated that the expression of *FASS* in 35S::*FASS* is 2.25 X more than in Col-0 and 5.63 X more than in "*bushy-ff*" (Figure 3-72).

3.2.14 Non complementation of the "*bushy-ff*" phenotype with truncated (Δ) version of *FASS* CDS:

In another attempt we have synthesized the *FASS* coding sequence from the cDNA library which was prepared from the extracted *Arabidopsis* leaves RNA. After sub cloning of this CDS in pGet1.2 and sequencing was revealed, this synthesized CDS from the reverse transcribed leaves RNA was 40 nucleotides shorter than full *FASS* CDS which was amplified from the related cDNA plasmid (Figure 3-73). Except those 40 missed nucleotides, the rest sequence of synthesized CDS was 100 % similar to data base annotated *FASS* CDS. To test whether this Δ *FASS* CDS version could also complement the "*bushy-ff*" phenotype as well as full *FASS* CDS, was cloned into the binary vector pJawohl3 downstream of the strong 35S CaMV promoter (Figure 2-2). The sequence of the recombinant plasmid was confirmed and the plasmid was transformed into *"bushy-ff"* plants by the floral dip method (Clough and Bent, 1998) .The transformed T_1 plants were selected according to their resistance to BASTA herbicide and was observed 100% of the resistant transformed T_1 plants in "*bushy-ff*" background raised again "*bushy-ff*" phenotype (Figure 3-74) in contrast to the phenotype of *FASS* over-expressing T_1 plants which were wild-type looking (Figure 3-70) .Here, the "*bushy-ff*" looking phenotype of the transformed T_1 plants indicated that, the Δ *FASS* CDS synthesized from the reverse transcribed leaves RNA could not complement the "*bushy-ff*" phenotype.

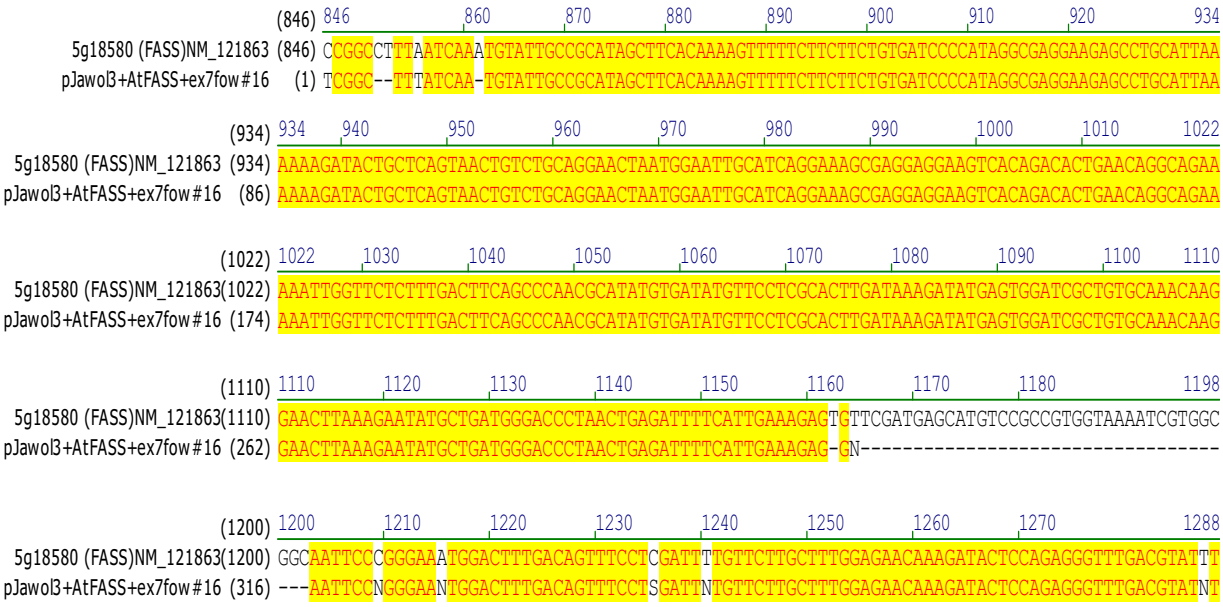

Figure 3-73 Alignment of *FASS* CDS with the synthesized Δ version of *FASS* CDS.
Alignment of data base annotated *FASS* CDS with the CDS which amplified from the reverse transcribed leaves RNA indicated synthesised CDS was 40 base pair (bp) shorter than full *FASS* CDS. Except than those 40 bp missed nucleotides (from 1163 to 1203 in picture) the rest sequence of synthesised Δ*FASS* CDS was correct.

Figure 3-74 Transformed T_1 "*bushy-ff*" plants with truncated *FASS* CDS.
Selection of T_1 transformed "*bushy-ff*" plants with Δ*FASS* CDS with resistance to the BASTA herbicide, short version of *FASS* CDS could not complemented the "*bushy-ff*" phenotype.

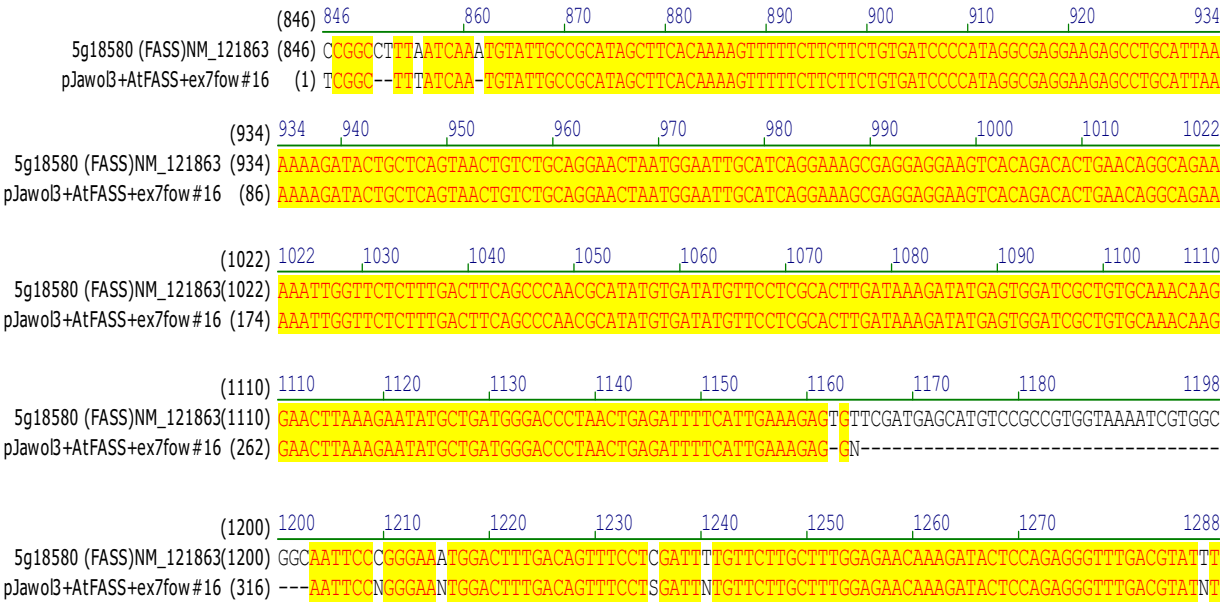

Figure 3-73 Alignment of *FASS* CDS with the synthesized Δ version of *FASS* CDS.
Alignment of data base annotated *FASS* CDS with the CDS which amplified from the reverse transcribed leaves RNA indicated synthesised CDS was 40 base pair (bp) shorter than full *FASS* CDS. Except than those 40 bp missed nucleotides (from 1163 to 1203 in picture) the rest sequence of synthesised Δ*FASS* CDS was correct.

Figure 3-74 Transformed T_1 "*bushy-ff*" plants with truncated *FASS* CDS.
Selection of T_1 transformed "*bushy-ff*" plants with Δ*FASS* CDS with resistance to the BASTA herbicide, short version of *FASS* CDS could not complemented the "*bushy-ff*" phenotype.

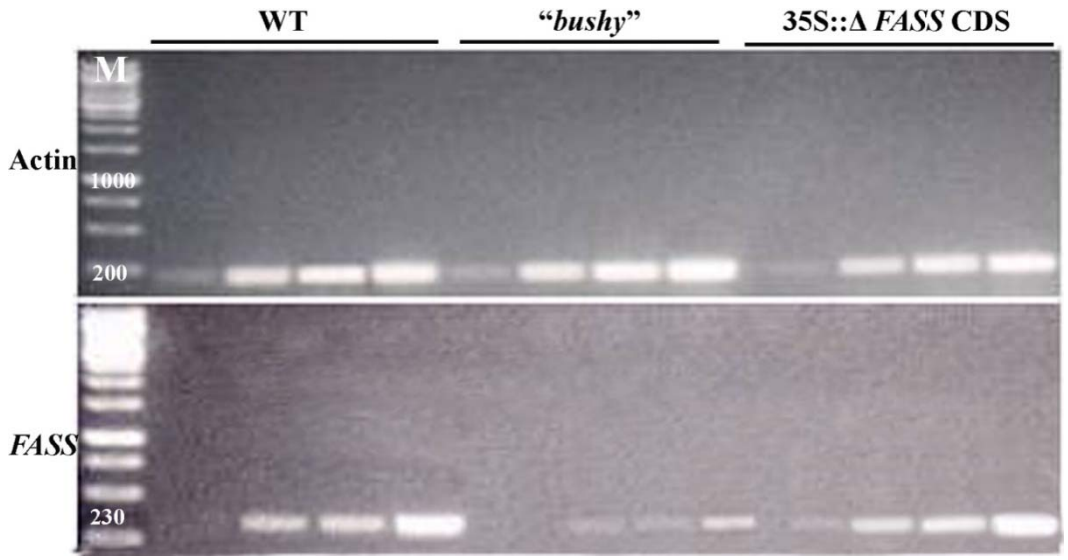

Figure 3-75 Expression analysis of *FASS* in 35S:: Δ *FASS* CDS plants.
Semi quantitative RT-PCR analysis with 1 µg total RNA which were extracted from 35S:: Δ *FASS* CDS ,"*bushy-ff*" and Col-0 plants and was used for making cDNA as a template for semi quantitative RT-PCR . Actin: Semi quantitative RT-PCR as a cDNA input control with actin specific (Table 2-3, 56 and 57) oligos in 35S:: Δ *FASS* ;"*bushy-ff*" and Col-0. *FASS*: Semi quantitative RT-PCR for expression of *FASS* mRNA with *FASS* specific (Table 2-3, 33 and 30) oligos in 35S:: Δ *FASS*; "*bushy-ff*" and Col. Lanes 1, 2, 3 and 4 correspond to PCR cycle 23, 25, 27 and 30. M= molecular weight marker with 200, 230 and 1000 bp band indicated.

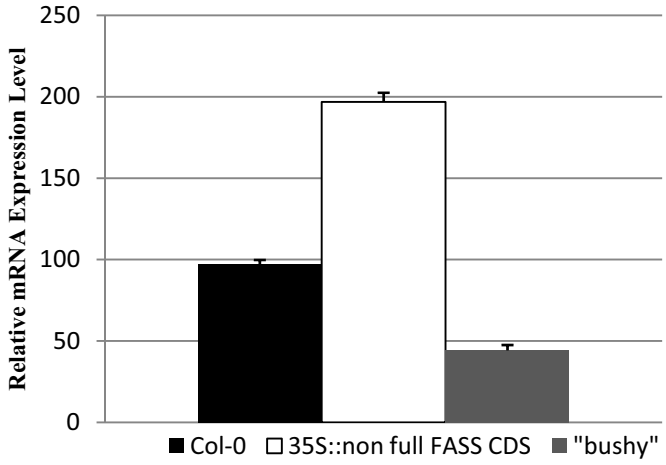

Figure 3-76 Quantitation of semi quantitative RT-PCR analysis related to same expression of *FASS* in 35S::nonfull *FASS* CDS and "*bushy-ff*" plants in compare to expression of *FASS* in Col-0.
RNA expression levels are expressed as relative to actin control and RT-PCRs data at cycle 27 have been shown.

After standardization of actin bands with the described procedure in 3-2-4 and related calculation was revealed that the expression of *FASS* in35S:: Δ*FASS* is ~ 4.28 X more than "*bushy-ff*" and ~ 2 X more than Col-0 (Figure 3-76).

3.2.15 *F-box* At1g77000 and *FASS* are expressed in all plant organs

Since the over-expression of *F-box* At1g77000 and *FASS* genes could complement the phenotype of "*bushy-ff*" plants, I sought to understand the correlation of these two genes. Thus, the organ-specific expression patterns of the *F-box* At1g77000 and *FASS* genes were analyzed. For this purpose, total RNA of Col-0 organs including leaves, roots, flowers, stems and cotyledons was extracted. cDNAs were prepared from extracted RNA and were used as templates in semi quantitative RT-PCR analysis. Results of RT-PCR analysis showed that *F-box* At1g77000 and *FASS* have a similar expression pattern in the various organs (Figure 3-77). *F-box* At1g77000 is mostly expressed in leaves, stems, flowers and cotyledons respectively and very low levels of expression of *F-box* At1g77000 could be detected in roots. *FASS* also follow same expression pattern as *F-box* At1g77000 except that *FASS* has a higher expression in roots as compared to *F-box* At1g77000. However, the general pattern of expression is more or less the same in both loci (Figure 3-77 and Figure 3-78).

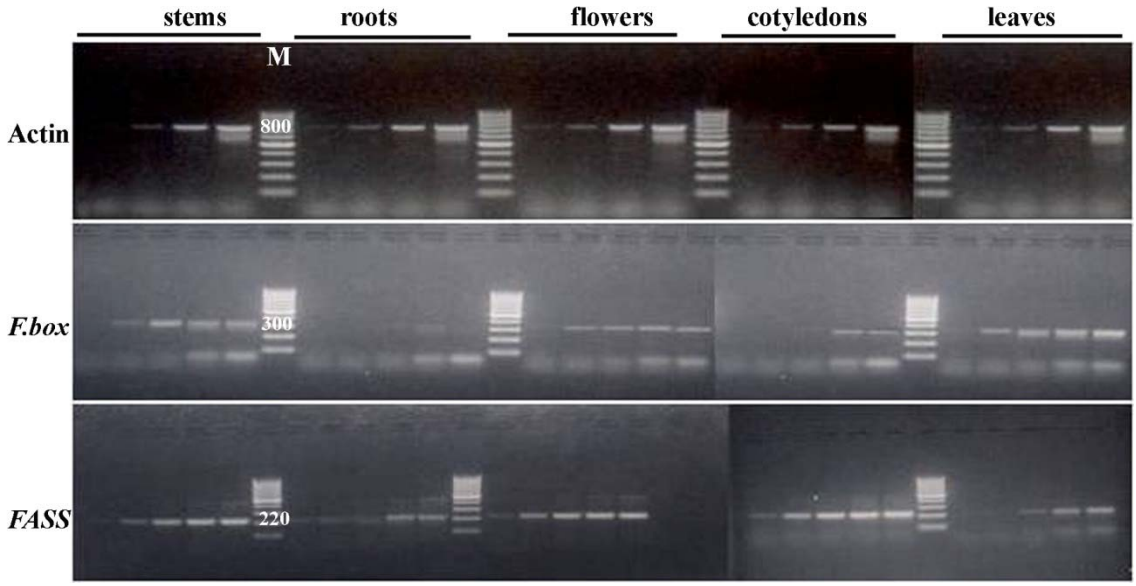

Figure 3-77 Organ-specific expression analysis of F-box and FASS. RNA from the various organs was transcribed into cDNA which served as a template for RT-PCR.
Actin: Semi quantitative RT-PCR with Actin specific (Table 2-3, 58 and 57) oligos; a, Stems; b, roots; c, flowers; d, cotyledons; e, leaves. F-box: Semi quantitative RT-PCR with same cDNA with F-box (Table 2-3, 4 and 3) oligos; a, Stems; b, roots; c, flowers; d, cotyledons; e, leaves. FASS: Semi quantitative RT-PCR with same cDNA with FASS specific (Table 2-3, 33 and 30) oligos. Lanes 1, 2, 3 and 4 correspond to PCR cycle 23, 25, 27 and 30. 100 bp DNA ladder was used.

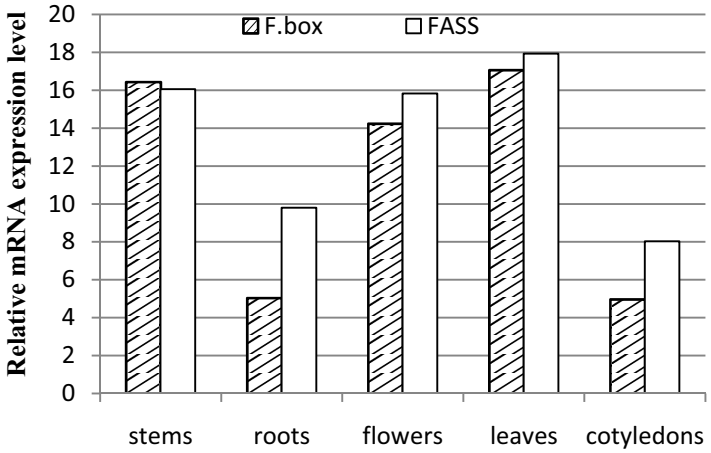

Figure 3-78 Quantitation of semi quantitative RT-PCR analysis of *FASS* and *F-box* At1g77000 gene expression in different organ of plant including stems, roots, flowers, leaves and cotyledons respectively.
RT-PCRs data were shown at cycle 27. RNA expression levels are expressed as relative to actin control.

3.2.16 Tissue-specific expression analysis of *F-box* At1g77000 gene using promoter GUS fusion

To assess the transcriptional activity of the *F-box* At1g77000 gene throughout plant development, a 4. 2kb region upstream from the ATG translational start was amplified by PCR and fused to the *GUS* reporter gene of the binary vector pLH7000 (Figure 2-1). The promoter-reporter gene fusion was transferred into the nuclear genome of Col-0 plants by the floral dip procedure (Clough and Bent, 1998). Ten independent transgenic lines were obtained by Basta-selection and GUS expression was analyzed. In general, GUS activity was detected after over night incubation of the tested tissue in the staining solution. Six of ten lines showed the expression pattern of a gene which was mostly expressed in the veins of leaves, the anthers and the style of flowers and veins and apical ends of cotyledons, respectively and a focalized expression was detectable in certain regions of roots, possibly emerging sites of lateral roots (Figure 3-79). As shown in Figure 3-79 E and F, *F-box* At1g77000 expression in younger leaves and hypocotyls was much higher as compared to older leaves and stems. However, in very young flowers (buds) there was no expression, while in mature flowers expression was easily visible (Figure 3-79, I-L).

Pseudomonas syringe pv. *tomato* (+*AvrRpt2*) is known as a pathogen of *Arabidopsis*. The interaction results in a hypersensitive response on a gene-for-gene resistance basis. Infection with *Pst* (+*AvrRpt2*) also results in massive changes in gene expression (Scheideler *et al*. 2002). We tested the induction of *F-box* At1g77000 expression after exposure to *Pst* (+*AvrRpt2*) and its near-isogenic virulent (*Vir*) strain by staining of *F-box* At1g77000 promoter::*GUS* plants. To this end, the leaves of five independent 6 weeks old transgenic lines were infiltrated with $5x10^6$ cfu ml^{-1} of *Pst* (+*AvrRpt2*) and (*Vir*) strains. Leaves were harvested at t=0, 6, 24 and 36 hours post treatment (hpt) and GUS expression pattern was analysed. The results of analysis indicated that the *F-box* At1g77000 gene was not induced after exposure to any strains of *Pst*. (Figure 3-79, G and H).

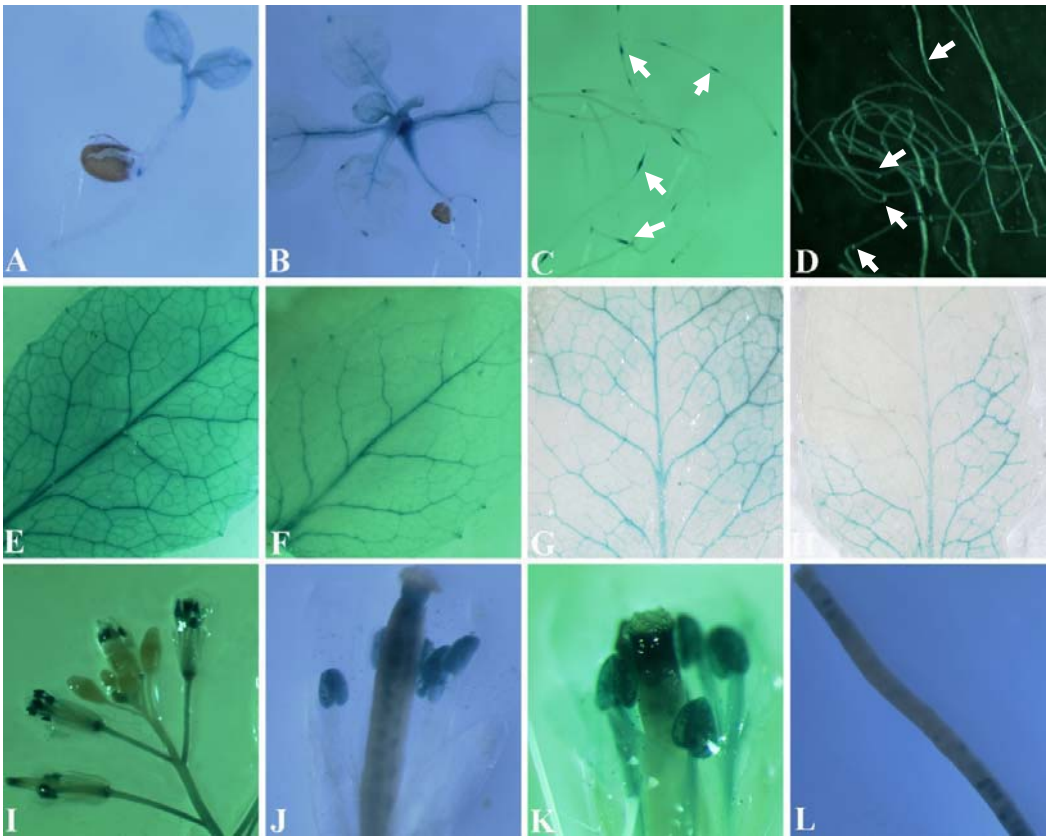

Figure 3-79 Analysis of *F-box* At1g77000 expression pattern by a promoter-reporter (*GUS*) gene fusion.
GUS activity was detected in leaves, flowers and cotyledons of *F-box* At1g77000 promoter::*GUS* plants. A and B: expression of *F-box* At1g77000 in 4 days and 2 weeks old seedling. C and D: expression of *F-box* At1g77000 in roots, arrowheads indicated to stained parts of roots. E and F: expression of *F-box* At1g77000 in young and old leaves. G and H: expression of *F-box* At1g77000 after exposure to *Pst* (+*AvrRpt2*) and (*Vir*), at 48 hours after infiltration. I-L: expression of *F-box* At1g77000 in different flower organs: anthers, ovules, style and siliqua, respectively.

3.2.17 Identification of physical interaction between *F-box* At1g77000 and *FASS* At5g18580 in yeast 190

Since our genetic cross experiments revealed the presence of genetic interaction between *F-box* At1g77000 and *FASS*, therefore we tested the physical interaction between these two proteins as well. To this end, Clontech's matchmaker GAL4 yeast two hybrid system was used for detecting a potential *F-box* At1g77000 and *FASS* At5g18580 physical interaction in yeast strain Y190.

The vectors used in this system were:

pGADT7: carrying the “prey” protein which is fused to AD of GAL4 (GAL4-AD); the plasmid contains the yeast selection marker LEU2 (Figure 2-7 and Figure 2-8).

pGBKT7: carrying the “bait” protein which is fused to DNA–binding domain of GAL4 (GAL4-BD); the plasmid contains the yeast selection marker TRP1 (Figure 2-9 and Figure 2-10).

An interaction between the bait protein from pGBKT7 and the prey protein from pGADT7 creates a novel transcriptional activator with binding affinity for the GAL UAS (Figure 3-81). This factor activates the reporter gene HIS3 allowing growth of the yeast on medium lacking histidine. Moreover, it activates expression of the b-galactosidase turning yeast colonies blue on medium containg X-Gal.

The *F-box* At1g77000 and *FASS* coding sequences were fused in frame to the DNA-BD and the AD of pGBKT7 and pGADT7, respectively. After transformation of the plasmids in yeast strain Y190 and excluding auto-activation (Figure 3-80, A and B), double transformed yeast strains were generated. Thus, one strain carried *FASS* fused to the DNA-BD and *F-box* At1g77000 fused to the AD, while the other strain carried *F-box* At1g77000 fused to the DNA-BD and *FASS* to the AD. As controls served a 14-3-3 gene from *Arabidopsis* also fused to the DNA-BD and the AD (kindly provided by Dr. G. Schmitz, RWTH Aachen University). Double transformants were selected on SD- Ura,- Trp , - Leu (Figure 3-80, C). The transformants were tested for an interaction between *FASS* and *F-box* At1g77000 on SD (-) His (Galactos/Raffinose+ X-Gal) plates. As shown in Figure 3-81, Y190+pGBKT7*FASS+*pGADT7*F-box* At1g77000 could grow properly on SD- His (Galactos/Raffinose+ X-Gal) plates and also produced blue colour because of the presence of X-Gal in the medium (Figure 3-81). The growth on minimal media lacking histidine and blue colour development was indicative for a physical interaction between *FASS* and *F-box* At1g77000. In all other tests double transformants

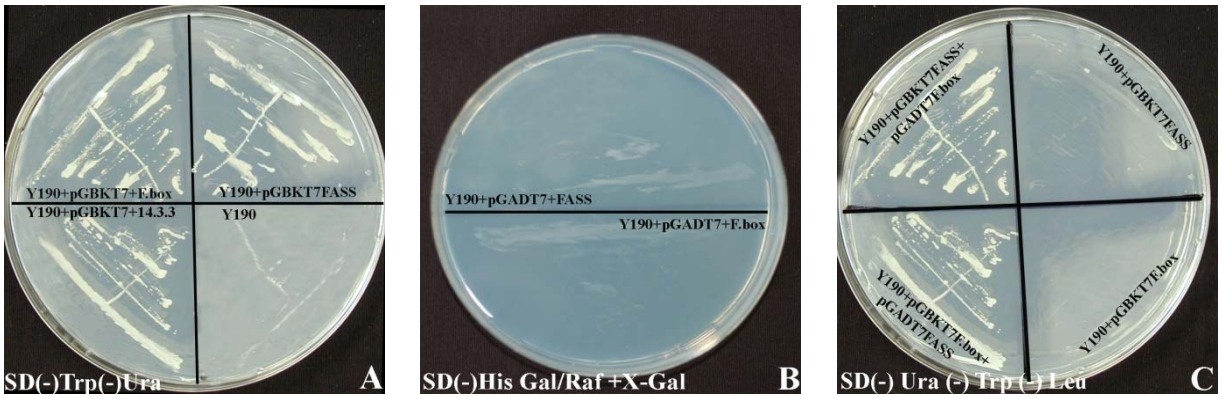

Figure 3-80 Transformation of yeast strain Y190 with plasmids used in the yeast two hybrid assay.
A: Growth of Y190+pGBKT7*F-box* At1g77000, Y190+pGBKT7*FASS* and Y190+pGBKT714.3.3 on SD (-)Trp, (-)Ura plates; Y190 which could not grow on this plate. B: self activation test of Y190+pGADT7*F-box* and Y190+pGADT7*FASS* on SD (-)His Gal/Raf+ X-Gal plate. C: Growth of Y190+pGBKT7*F-box* At1g77000+pGADT7*FASS* and Y190+pGBKT7*FASS+*pGADT7*F-box* At1g77000 on SD (-)Ura, (-)Trp (-) Leu plate.

were unable to grow on SD (-) Trp, (-) Leu, (-) His plates and no colour development was observed (Figure 3-81 and Table 3-2).The western blot analysis imply to expression of *FASS*, *F-box* At1g77000

and 14.3.3 protein down stream of the GAL4-BD under the control of ADH1 promoter in double yeast transformants (Figure 3-82).

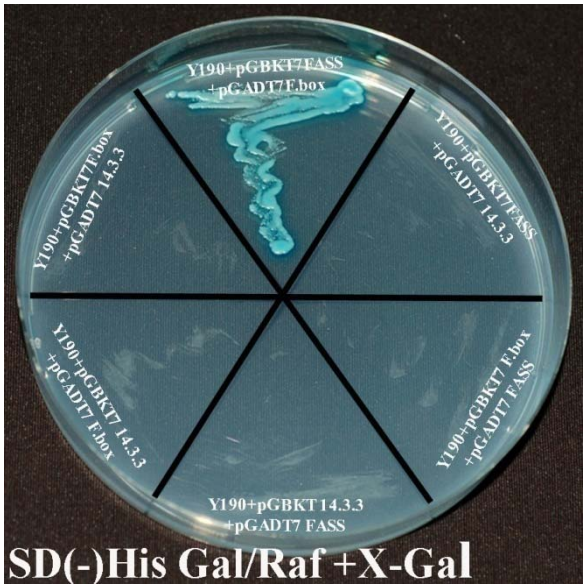

Figure 3-81 Test of physical interaction between F-box At1g77000 and FASS proteins using the yeast two hybrid assay. Y190+pGBKT7*FASS*+pGADT7*F-box* At1g77000 could grow on SD (-) His Gal/Raf+ X-Gal plates and turned blue. Y190+pGBKT7*FASS*+pGADT714.3.3., Y190+pGBKT7*F-box* At1g77000+pGADT7*FASS*, Y190+pGBKT7*F-box* At1g77000+pGADT7*14.3.3*, Y190+pGBKT7*14.3.3*+pGADT7*F-box* At1g77000 and Y190+pGBKT7*14.3.3*+pGADT7*FASS* did not grow on SD (-) His Gal/Raf+ X-Gal plates.

Table 3-2 Different yeast transformants which were created in this study to investigate the physical interaction of F-box At1g77000 and FASS proteins.

Yeast strain	Physical interaction
Y190+pGBKT7 *FASS*+pGADT7 *F-box* At1g77000	Yes
Y190+pGBKT7 *FASS*+pGADT7 14-3-3	No
Y190+pGBKT7 *F-box* At1g77000+pGADT7 *FASS*	No
Y190+pGBKT7 *F-box* At1g77000+pGADT7 14-3-3	No
Y190+pGBKT7 14-3-3+pGADT *F-box* At1g77000	No
Y190+pGBKT7 14-3-3+pGADT *FASS*	No

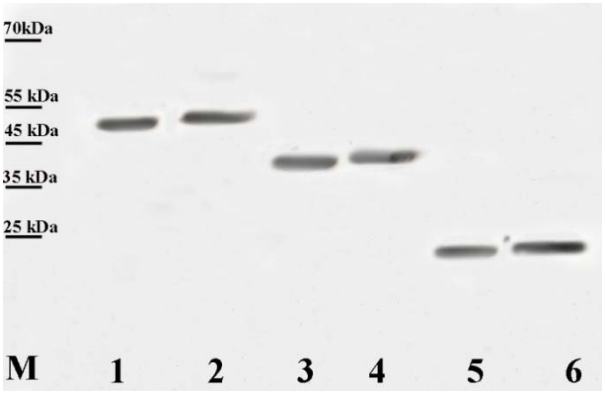

Figure 3-82 Western blot analysis was performed with extracted protein from several yeast strains. 1-Y190+pGBKT7*FASS*+pGADT7*F-box* At1g77000; 2-pGBKT7*FASS*+pGADT714.3.3; 3- pGBKT7*F-box* At1g77000+pGADT714.3.3; 4- pGBKT7*F-box* At1g77000+pGADT7*FASS*; 5- pGBKT714.3.3+pGADT7*FASS*; 6- pGBKT714.3.3+pGADT7*F-box* At1g77000 which expressed FASS, F-box At1g77000 and 14.3.3 protein respectively down stream of the GAL4-BD under the control of ADH1 promoter . Blotted proteins were probed with a primary antibody that reacts specifically with the Myc antigen and a secondary anti-rabbit polyclonal antibody. M, protein ladder.

3.2.18 Localization of *F-box* At1g77000 protein using 35S:: GFP-*F-box* At1g77000 lines

To detect the localization site of the F-box At1g77000 protein inside the living cells of *Arabidopsis*, the coding sequence of *F-box* At1g77000 was amplified, so that Gateway attachment sites (attB1 and attB2) were fused to the end of the PCR band. The PCR band was recombined into pDonor 201 through a BP reaction and the sequence of the plasmid verified. The CDS of the *F-box* At1g77000 gene was recombined into destination vector, pGWB6 (Nakagawa et al., 2007), downstream of the green florescence protein (GFP) CDS and strong 35 CaMV promoter through a LR reaction and again the sequence of the plasmid verified. Finally the recombinant plasmid (Figure 2-6) was transformed into "*bushy-ff*" plants by the floral dip method (Clough and Bent, 1998). All transformed selected T_1 plants were wild-type looking plants (Figure 3-83). The transformed 35S:: GFP-*F-box* At1g77000, phenotypically WT looking plants, were analyzed using fluorescent microscope. GFP was excited at 488 nm and emissions collected at 500 to 515 nm. Confocal microscopy analysis resulted the F-box At1g77000 protein localization inside the cells on the filaments of cytoskeleton microtubules network (Figure 3-84).

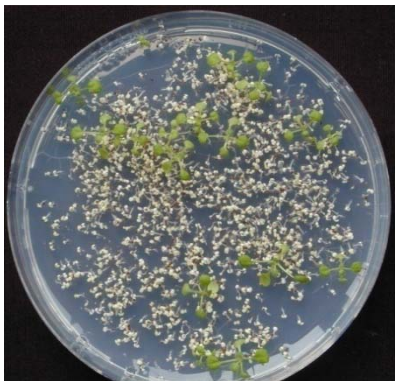

Figure 3-83 Selection of T_1 transformed "*bushy-ff*" plants which were expressing fusion GFP-*F-box* At1g77000 under the control of 35S promoter (35S:: GFP-*F-box* At1g77000) on MS agar plates containing Kan^{50} and Hyg^{50} .

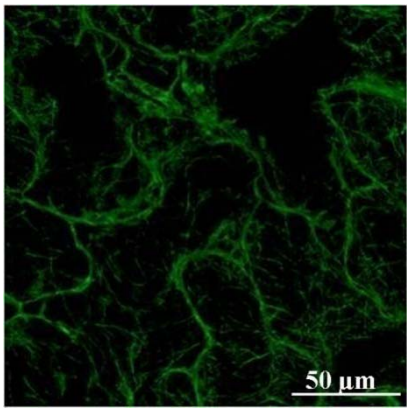

Figure 3-84 F-box At1g77000 protein expression as fusion with GFP in 35S:: GFP-*F-box* At1g77000 T_1 plants leaves.
GFP fusion expression and localization was analyzed using fluorescent microscope. GFP was excited at 488 nm and emissions collected at 500 to 515 nm.

4 DISCUSSION

In this work, I characterized independently two morphology mutants of *Arabidopsis*. Since both mutants share the reduced stature phenotype, I will begin here with a general discussion about reduced plant stature and likely causes of this phenotype before I discuss the individual results on the two mutants separately. The final plant size and form are determined by the cell number and cell size resulting from post embryonic cell division, expansion, and differentiation (Mizukami and Fischer, 2000; Weiss et al., 2005), therefore, reduced stature can be caused by either a lower number of normal-sized cells or by smaller cells or a combination of both. Early studies, which were later substantiated by detailed molecular experiments, suggested that there is an intrinsic mechanism for coordination of cell division and expansion to produce a developmentally predefined 'normal' species size and form.

In general, dwarfism in plants was observed in numerous situations when one of the several mechanisms was disrupted. For instance, mutations in genes that encode enzymes synthesizing plant hormones and/or their signaling, transcription and/or other regulatory factors, cell cycle regulators, cell wall components and/or cytoskeleton organizers caused excessive changes in plant form and stature. For examples, mutation in genes which are involved in the gibberellic acid (GA) biosynthesis or catabolism (Hedden and Phillips, 2000a, b) or GA signaling caused dwarfism (Fridborg et al., 1999; Amador et al., 2001; Olszewski et al., 2002). But also a mutation in genes involved in biosynthesis, degradation or signaling of other hormones, which act as plant growth regulators, like the brassinosteroids (Bishop and Koncz, 2002; Choe et al., 2002) and auxin can cause dwarfism (Cheng et al., 2007). Moreover, mutations in a number of transcriptional regulatory factors and cell cycle controllers also caused different kinds of defects in plant stature and form (Busov et al., 2008; Wang and Li, 2008).

4.1.1 Morphological phenotypes of the *Arabidopsis* "*pgase*" mutant

The isolated *Arabidopsis thaliana* "*pgase*" mutant in the Ta-0 background displayed defects in different plant organs (Figure 3-1). The total size in the "*pgase*" mutant in diameter and height was smaller than that of wild-type plants. Measuring the size of "*pgase*" and Ta-0 root cells showed that the size of the root cells was approximately 15% reduced (Figure 3-2), explaining at least partially, the reduced stature of the mutant plants. However, we did not look at the cell size and the number of the cells in other organs. It might be that the cell size of the other organs or the number of the cells were smaller than in Ta-0, because the size of the "*pgase*" mutant was not just 15% reduced compared to wild-type plants (Figure 3-1).

The leaves of the "*pgase*" mutant were somewhat curved (Figure 3-1). One of the factors which control the leaf curvature and subsequently the surface features is *CINCINATA* (*CIN*) in *Antirrhinum* (=snapdragon) which encodes a TCP domain transcription factor. In *cin* mutants, leaves suffer from a delay in cell division arrest, resulting in an excess of cells, causing curvatures in the leaf surface (Crawford et al., 2004). The *Arabidopsis jaw* mutant is a near phenocopy of the snapdragon *cin* mutant (Figure 1-12), (Palatnik et al., 2003). The *jaw* phenotype is a result of miR159/319-mediated

cleavage of TCP4 mRNA (Palatnik et al., 2003). Thus, there is the possibility that the "*pgase*" mutant might have a defective TCP gene.However, we did not observe the presence of excess cells in the leaves of the *"pgase"* mutants. Despite the fact that, in the *jaw* and "*pgase*" mutants the leaves were somehow curved, the overall appearance of them is quite different. Thus, it is unlikely that in the *"pgase"* mutant a problem in the TCP transcription factor function has occurred.
As mentioned before, plant form and stature is regulated by different factors e.g. genes which are involved in hormone metabolism and signaling. Treatment of the "*pgase*" mutant with gibberellic acid, auxin and brassinolide did not complement the morphology symptoms (Data not shown), suggesting that the phenotype of the "*pgase*" mutant is not caused by malfunction of the biosynthesis of these hormones. However, experiments with exogenous application of hormones do not rule out a defect in hormone perception or signaling in the "*pgase*" mutant.

Cominelli *et al*. in 2008 have shown that overexpression of the *AtMYB41* gene, which encodes an R2R3-MYB transcription factor, results in a dwarf mutant, reduced and wrinkled rosette and cauline leaves with curled-up edges. This phenotype is quite similar to the "*pgase*" mutant. This R2R3-MYB transcription factor controls cell expansion and cuticule deposition in response to abiotic stress (Cominelli et al., 2008). It is possible, that *AtMYB41* might be misexpressed in the "*pgase*" mutant, however, we have not addressed this question experimentally**.**

Arabidopsis *35S::AtMYB41* transgenic lines were inhibited from cell expansion. These plants displayed a similar phenotype to the "*pgase*" mutant. Moreover, *35S::AtMYB41* plants also showed increased transpiration rates, as did the "*pgase*" mutant plants and expression of the *AtMYB41* gene was increased by abiotic stresses to which the "*pgase*" mutant was hypersusceptible. Therefore, the similarity between the phenotypes suggests that "*pgase*" mutant cells could suffer from an inhibition in cell expansion and we consider that the "*pgase*" mutation might have a similar effect on target genes as overexpression of *AtMYB41*.

4.1.2 T-DNA insertion in an *Arabidopsis thaliana* polygalacturonase gene (*PGase*) affects cell wall and morphology/development of plants in the Col-0- and Ta-0 background

The molecular analysis of the "*pgase*" mutant (See 2-5-7), revealed that a T-DNA was integrated in the promoter region of At3g07970 (Figure 3-6). This gene is annotated as encoding for a putative polygalacturonase in *Arabidopsis* which in general plays a role in cell wall carbohydrate metabolism.

The diversity in shape and size of flowering plants results from the different morphologies of the various cell types that make up the vegetative and reproductive organs of the plant body. These cell types may vary in form and often have specialized functions. Changes in tissue and organ morphology that occur during plant growth and development result in large part from controlled cell division together with the structural modification and reorganization of wall components, and the synthesis and insertion of new material into the existing wall (Taiz and Zeiger, 1998).

The primary walls isolated form higher plant tissues are composed predominantly of polysaccharides together with lesser amounts of structural glycoproteins, phenolic esters, ionically and covalently bound minerals, and enzymes. In addition walls contain proteins that are believed to have a role in regulating wall expansion (Taiz and Zeiger, 1998).

Up to three strata may be found in plant cell walls:

- The middle lamella, a layer rich in pectins. This outermost layer forms the interface between adjacent plant cells and glues them together.
- The primary cell wall, generally a thin, flexible and extensible layer formed while the cell is growing.
- The secondary cell wall, a thick layer formed inside the primary cell wall after the cell is fully grown. It is not found in all cell types. In some cells, such as xylem, the secondary wall contains lignin, which strengthens and waterproofs the wall (Taiz and Zeiger, 1998).

Because the middle lamella is the outermost layer in plant cell walls and pectin is the dominant component of this layer therefore, the middle lamella might be the structure most affected by the "*pgase*" mutation. This layer is the first physical barrier in encountering exogenous factors such as biotic and a biotic stresses.

A recent example which explained the role of cell wall structure in plant development, has provided by Brininstool et al., 2008. Their observations are consistent with our results (See 3-1-1 and figure 3-5) and support a role of cell wall structure in plant development, specifically in the shaping of trichomes. They showed that in the *constitutive expressor of pathogenesis-related genes 5* (*cpr*5) mutant, the size and the branch number of the trichomes in leaves was reduced. This mutant displays differences in cell wall structure of leaf and trichome cells in comparison to WT plant cells (Brininstool et al., 2008). As shown in Figure 3-5, there was a change in the trichome numbers of the "*pgase*" mutant. Although in the *cpr*5 mutant no change in the number of trichomes was reported, the findings of them and from us hint to a developmental defect. In view of the fact that, in the *"pgase"* mutant the cells might suffer from changes in their wall structure or composition, these changes could consequently affect trichome development.

The major polysaccharides in the primary wall are cellulose, hemicelluloses and pectin. Pectins are a family of complex polysaccharides that all contain 1,4-linked α-D-galacturonic acid. Pectins account for ~30% of the primary walls of dicotyledenous and non-graminaceous monocotyledenous plants and for between 5 and 10% of the walls of grasses. Pectins are also likely to be present in the walls of ferns, lycopods, and bryophytes. Three classes of pectic polysaccharides have been characterized including homogalacturonans, rhamnogalacturonans I, and rhamnogalacturonans II (Taiz and Zeiger, 1998). Homogalacturonan (HG) may account for up to 60% of the pectin in a primary wall. HG is a linear chain of 1,4-linked α-D-galactosyluronic acid residues in which some of the carboxyl groups are methyl esterified. HG with a high degree of methyl esterification is referred to as "pectin" whereas HG with a low degree of methyl esterification is "pectic acid". Many of the properties and biological

functions of HG are believed to be determined by ionic interactions. Increases in the degree of methyl esterification of HG have been implicated in increased cell separation (Taiz and Zeiger, 1998) .

Polygalcturonases (PGase) and enzyms that fragment HG , are involved in the regulation of the cell wall, and in the process of cell separation, cell loosening and cell expansion (Gonzalez-Carranza et al., 2007). Therefore, according to the suggested roles of PGases, we consider that in the"*pgase*" mutant, somehow changes in the cell wall structure, composition or cell expansion have occurred and consequently, the normal morphology and development of the plant was affected.

A correlation between increasing PGase activity and cell separation was first detected in ripening fruit (Fischer and Bennett, 1983). PGases also play role in abscission, and increases in enzyme activity were reported during the shedding of leaves (Taylor et al., 1993) , flowers (Tucker et al., 1984) and fruit (Bonghi et al., 1992; Henderson et al., 2001). Peterson et al., 1995 and Lashbrook et al., 1998 also showed that the activity of a number of cell wall-degrading enzymes, especially PGases and β-1,4-glucanases, increase during cell separation (Petersen et al., 1995; Lashbrook et al., 1998).

PGases have also been hypothesized to play important roles throughout the life cycle of a plant including germination, pollen grain maturation, anther dehiscence, desiccation, fruit ripening, and pod shatter (Roberts et al., 2002b; Kim et al., 2006). It has been proposed that these hydrolytic enzymes play a contributory role in the breakdown of adhesion between neighbouring cells by bringing about middle lamella degradation (Roberts et al., 2002a).

The *Arabidopsis thaliana* genome contains 69 annotated genes that by amino acid homology and transcript organization could be classified as putative PGases and these can be grouped into multiple clades (Gonzalez-Carranza et al., 2007).

Studies with transgenic plants that over-express a specific endopolygalacturonase (EPG) or have had the levels of endogenous EPG reduced have begun to provide information about the function of HG. For example, neither the supression or over-expression of EPG in tomato fruits affected the fruit ripening process but altered tissue texture and pectin solubility. In contrast, transgenic apples containing additional copies of a fruit-specific EPG as explained below, exhibited several phenotypes in plant appereance (Atkinson et al., 2002).

Three *Arabidobsis* polygalacturonase genes were studied in detail and it was found that At2g41850 (*PGAZAT*) is expressed specifically in abscission zone cells during the shedding of floral organs and At3g57510 (*PGDZAT*) is up-regulated within the dehiscence zone cells of both anthers and pods, and at the site of seed abscission (Jenkins et al., 1996; Jenkins et al., 1999; Roberts et al., 2002a) . The correlation between the cellular site of expression of these two genes and the onset of organ separation supports a role for these PGs in wall breakdown (Gonzalez-Carranza et al., 2007).

By contrast, it has been shown that a T-DNA insertion in At4g20050 (the *QUARTET3* gene) prevents degradation of the pollen mother cell wall, and *QRT3* expressed in yeast exhibited PGase activity

(Rhee et al., 2003). Silencing of an abscission related PGase (At2g41850= *PGAZAT*), delayed the time-course of floral organ loss but did not prevent shedding (Gonzalez-Carranza et al., 2007).

Expression analysis of five PGases, of which At3g07970 was one of them, using reporter fusion constructs and reverse transcription-PCR, revealed that whilst these PGases exhibit high sequence similarity they have distinct patterns of spatial and temporal expression (Gonzalez-Carranza et al., 2007).

The seperate position of At3g07970 in the phylogenetic tree (Figure 4-1) from At2g41850 (*PGAZAT*) and At3g57510 (*PGDZAT*) and the different expression pattern of At3g07970 again suggestd that the role of At3g07970 is quite different from At2g41850 or At3g57510 and thus a role in cell wall loosening and cell expansion is possible.

As mentioned above, Atkinson *et al*., reported constitutive overexpression of a fruit-specific PGase in apple plants resulting in abnormal cell separation within the leaf and in changes in leaf morphology, stomatal function, forming and, ultimately, plant water relations (Atkinson et al., 2002).

In the *"pgase"* mutant we also observed reduced stomata and disturbed plant water relations. This suggests that the *PGase* At3g07970 gene can, also influence somehow the stomata cell development.

However, so far the effect of a polygalacturonase gene family member in regulating the shape and stature of *Arabidopsis* was not reported, and our study is reporting for the first time the role of the *Arabidopsis thaliana* polygalacturonase gene family member, At3g07970, in regulation of plant morphology.

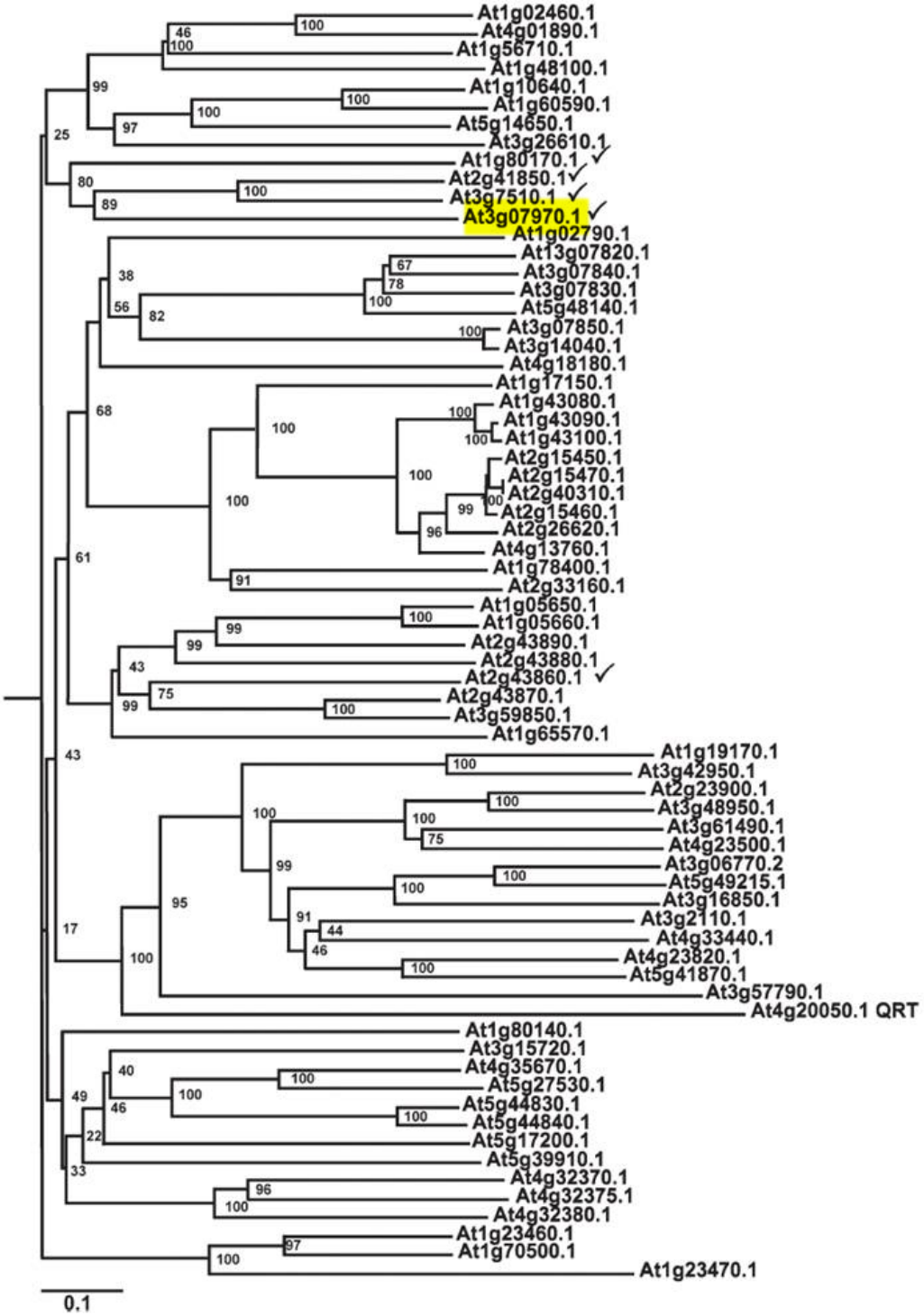

Figure 4-1. Phylogenetic tree generated from amino acid sequences of putative polygalacturonases from *Arabidopsis thaliana.*

The branch lengths are proportional to the amount of inferred evolutionary change and boot strap values are included. Scale indicates 0.1 distance from the root of the tree. A tick indicates genes whose expression has been examined in this study (Gonzalez-Carranza et al., 2007), the highlighted genes is our studied *PGase*: AT3g07970 .

To assess the hypothesis whether the T-DNA insertion in the *PGase* At3g07970 locus caused this phenotype in the "*pgase*" mutant, an independent T-DNA insertion line of At3g07970 from the GABI-Kat collection was analysed. In the T-DNA insertion line 058B07, the T-DNA was inserted in the first exon specifically 5 base pairs (bp) after the predicted ATG start codon of PGase (At3g07970) making it a likely null mutant, *i.e.* that no functional protein will be made (Figure 3-9). This *pgase* knock out line from GABI-Kat collection displayed a morphological phenotype indistinguishable from the initially characterized "*pgase*" mutant (Figure 3-10). Therefore, our proposed hypothesis that the T-DNA insertion in the *PGase* gene is the reason for the phenotype in the "*pgase*" mutant was corroborated.

The results of semi-quantitative RT-PCR analysis indicated that the expression level of *PGase* in the Ta-0 and the Col-0 "*pgase*" mutants was reduced by ~75% relative to wild-type expression levels (Figure 3-11 and Figure 3-12). The fact, that we observe a RT-PCR band in the GABI-Kat mutant is probably due to a transcriptional read-through from the T-DNA. This effect is frequently observed in T-DNA mutants and does not mean that a functional protein can be made from these mRNAs. Complementation of the "*pgase*" mutant phenotype in the Ta-0 background with over expression of *PGase* CDS (Figure 3-14) further confirmed the hypothesis that the T-DNA insertion in the *PGase* gene was responsible for the observed phenotype in the "*pgase*" mutant. While a four- to five-fold reduced expression of the *PGase* At3g07970 gene resulted in curly leaves, overexpression of the gene did not result in a visible alteration of plant morphology, since in the 35S::At3g07970 plants about twice as much mRNA as in wild-type plants was observed, however the morphology of those plants resembled that of wild-type plants. This could be interpreted as a gene with a quite tightly controlled expression. Too little of the mRNA made results in various phenotypes while we were not able to obtain plants with a 10-fold or higher expression level. *NPR1* and *RPS2* are examples of tightly controlled genes. When the CDS of *RPS2* was cloned down stream of the 35S promoter, Kunkel et al. always detected only 2-3 times increased *RPS2* mRNA transcript levels in transgenic plants compared to wild type plants (Kunkel et al., 1993). In the case of 35S::*NPR1* plants, the transcript level, was up to 30 times higher in transgenic plants compared to wild type plants . But the amount of NPR1 protein in over-expression lines was only modestly (2-3 times) increased (Despres et al., 2000; Despres et al., 2003). These results show that plants can not tolerate higher trancript or protein levels of some genes and thus, these genes have tightly controlled expression level. Our data indicate that maybe *PGase* At3g07970 is one of those genes.

4.1.3 Organ specific expression of *PGase*

We analysed PGase expression in various organs. The result of semi quantitative RT-PCR analysis with different *Arabidopsis* organs indicated that *PGase* At3g07970 had generally low mRNA levels and was expressed mostly in roots and stems and in very low amounts expression could be detected in leaves and flowers of Col-0 (Figure 3-17 and Figure 3-18). These data are consistent with the results of Torki *et al*. and Sander *et al*. who demonstrated transcript accumulation of PGase family members in roots, leaves, pollen tubes, flowers, and siliques throughout the development of an *Arabidopsis* plant (Torki et al., 1999; Torki et al., 2000; Sander et al., 2001).

Moreover, Gonzalez-Carranza *et al*. also showed the expression of At3g07970 was very low, since they could not detected any expression of At3g07970 when they fused a 1492bp fragment of the promoter of this gene to the GUS reporter gene (Gonzalez-Carranza et al., 2007). *In silico* analysis of At3g07970 expression using the Genevestigator (Zimmermann et al., 2004) database has confirmed this assertion.

4.1.4 The "*pgase*" mutant was susceptible to infection with *Hyaloperonospora arabidopsidis*

To study the interaction between the "*pgase*" mutants ("*pgase*" mutant in Ta-0 background and GABI-Kat "*pgase*" in Col-0 background) with plant pathogens, the interaction of biotrophic oomycete *Hyaloperonospora arabidopsidis* with the "*pgase*" mutants was studied.The responses of the "*pgase*" mutants were compared with those of the wild type plants, and the hypersusceptible *eds1* genotypes.

The *eds*1 mutant was used to compare the "*pgase*" mutant response results, since Parker *et al*., observed, that the Ws-*eds1* mutant seedlings supported heavy sporulation by *P. arabidopsidis* isolates. Thus the *EDS1* gene which encodes a lipase-like protein, is a necessary component of the resistance response in *Arabidopsis thaliana* (Parker et al., 1996).

Three days after inoculation of leaves of the different genotypes with conidiospores of the isolate NOCO that is virulent on Col-0, hyphal growth within the detached leaves was assessed by trypan blue staining (Figure 3-19). The result of this assay showed that the susceptibility of the "*pgase*" mutant in Col-0 background (Ta-0 was found to be incompatible with NOCO) were indistinguishable to the *eds1* mutant, because the hyphal mass in the "*pgase*" and *eds1* genotypes were same (Figure 3-20).

Hypersusceptibility of *eds1* and similar mutants is manifested by increased mycelial growth, earlier sporulation and more sporangiophores produced as compared to wild-type plants. Since the appearance of the conidiophores on day 5 after inoculation in the "*pgase*" mutant was similar to *eds1* (Figure 3-21), therefore this experiment, corroborate the enhanced susceptibility of the "*pgase*" mutant to *H. arabidopsidis.*

All plant pathogens interact with plant cell walls. At the simplest level, the walls provide a physical barrier between pathogens and the internal contents of plant cells (Vorwerk et al., 2004). The high molecular weight polysaccharides that are the principal components of cell walls are crosslinked by both ionic and covalent bonds into a network that resists physical penetration (Carpita and McCann 2000). In addition, cell walls are dynamic reservoirs of antimicrobial proteins and secondary metabolites that inhibit the growth of many pathogens (Darvill and Albersheim, 1984) and (Thomma et al., 202). Plant cells also have poorly defined mechanisms for sensing and responding to cell wall damage. Many pathogens release enzymes such as polygalacturonases and pectat lyases that degrade cell wall polysaccharides; some of these degradation products elicit defensive responses by plants (Albersheim and Valent, 1974).

If pathogens posses PGases as virulence factors, why was the "*pgase*" mutant hypersusceptible to oomycet infection, rather than more resistant?

Presumably the mutation in the polygalaturonase locus resulted in reorganization of cell wall components, composition, synthesis or insertion of new material into the existing cell walls which facilitated the penetration of the pathogen through the cell walls.

It is also possible that the product of this particular polygalacturonase gene, has signaling-eliciting effect. This would be supported by our data related to non-induction of the *COR78* gene in the "*pgase*" mutant (Figure 3-25). The disrubtion of members of a signaling cascade could easily affect the response of this mutant to different biotic and abiotic stresses (Figure 4-5).

However, little is known about the degree to which the chemical composition of plant cell wall polysaccharides is a factor in the outcome of the plant–pathogen interaction. This situation arises because there are relatively few documented genetic differences in cell wall composition within plant species that could be used to test the role of cell wall polysaccharide composition on disease interactions. Where such differences have been observed in comparisons of natural variation within a species, they are usually accompanied by many other genetic differences that obscure any specific effects of wall composition per se. Similarly, there is at present no way to test whether the substantial differences in cell wall composition between plant species could be a factor in disease resistance (Vorwerk et al., 2004).

Several lines of genetic evidence have implicated cell wall polysaccharide composition in disease. *Arabidopsis* mutants with null mutations in a GPI-anchored putative pectate lyase, encoded by the *PMR6* gene, were found to be highly resistant to powdery mildew (Vogel et al., 2002). The resistance was not dependent on either the salicylic acid or the ethylene or jasmonate signal transduction pathways. Fourier transform infrared (FTIR) spectrophotometry of cell walls from uninfected plants indicated that the mutants had an altered cell wall composition. More recently, novel structural components in the pectic fraction of the *pmr6* walls have been observed by capillary electrophoresis of enzyme digests of cell walls (Vorwerk et al., 2004). Although it is not yet known why the loss of a plant pectate lyase causes resistance, the observation is consistent with the idea that polysaccharide composition is a determinant of disease interactions. The PMR6 enzyme is normally required to modify a pectin molecule during pectin synthesis and deposition in the wall. Perhaps PMR6 processes a precursor to a final form. Loss of this activity results in a novel pectin structure in the wall. Hydrolytic enzymes produced by the mildew fungus release fragments of this novel pectin and these act to elicit a defense response (Vorwerk et al., 2004).

A mutation in the *pmr5* gene rendered *Arabidopsis* resistant to the powdery mildew species *Erysiphe cichoracearum* and *Erysiphe orontii*, but not to the unrelated pathogens *Pseudomonas syringae* or *Hyaloperonospora arabidopsidis PMR5* belongs to a large family of plant-specific genes of unknown function. *pmr5*-mediated resistance did not require signaling through either the salicylic acid or

jasmonic acid/ ethylene defense pathways, suggesting resistance in this mutant may be due either to the loss of a susceptibility factor or to the activation of a novel form of defense. Based on Fourier transform infrared analysis, the *pmr5* cell walls were enriched in pectin and exhibited a reduced degree of pectin modification relative to wild-type cell walls. In addition, the mutant had smaller cells, suggesting a defect in cell expansion. A double mutant with *pmr6*, exhibited a strong increase in total uronic acid content and a more severe reduction in size, relative to the single mutants, suggesting that the two genes affect pectin composition, either directly or indirectly, via different mechanisms. These two mutants highlight the importance of the host cell wall in plant–microbe interactions (Vogel et al., 2004).

Variation in pectin composition has also been associated with stem rust (*Puccinia graminis*) resistance in wheat (Wietholter et al., 2003). Analysis of cell wall composition from a pair of isogenic resistant and susceptible wheat lines revealed a more blockwise distribution of methyl esters in the homogalacturonan of susceptible wheat cultivars compared with a more random distribution in the near-isogenic resistant lines. These authors favor the idea that a successful pathogen must produce a 'suppressor' to counteract the effects of any elicitors produced during the infection process. Presumably a suppressor could be a fungal enzyme that destroys elicitors or, perhaps, an oligosaccharide that competes for the active site of a receptor but does not stimulate the receptor. Thus, the difference in pectin methylation decreases the production or activity of such a suppressor in the resistant isoline (Wietholter et al., 2003).

The pectin structure in the "*pgase*" mutant could be altered in a different way such that it will make it easier for oomycete pathogens to penetrate and form haustoria, explaining the hypersusceptibility phenotype here in a loss-of-function mutant.

These recent results provide evidence that genetic variation in cell wall polysaccharide composition can result in altered disease responses. Many questions remain as to the mechanism underlying the effects and the degree to which naturally occurring variation in cell wall polysaccharide structures might have similar effects.

Additionally, plant cell walls are highly complex in structure and in composition. It is not yet clear why the polysaccharide structures in plant cell walls are so complex. In confronting this question, Albersheim and colleagues originally suggested that some of the structural complexity could represent latent signal molecules involved in defense rather than structures required for the mechanical function of the wall (Albersheim and Valent, 1978).

4.1.5 "*pgase*" mutant was hypersusceptible to abiotic stresses

The response of the "*pgase*" mutants to abiotic stresses e.g. cold, heat, and drought was also studied. The results of these experiments demonstrated that both of the "*pgase*" lines were hypersusceptible for cold and heat stresses (Figure 3-22 and Figure 3-26).

Treating the plants with cold stress, 100% of plants of both *"pgase"* lines were dead 48 hours after cold treatment, while the control genotypes (Col-0 and Ta-0) did not even produce any symptoms in the same condition and the response of complemented "*pgase*" line was similar to Col-0 and Ta-0 plants (Figure 3-22). A cold-response signaling defect was uncovered in the "*pgase*" mutant, since the

cold regulated gene *COR78* was not induced in "*pgase*" lines (Figure 3-25), while it was in the wild-type plants and the complemented "*pgase*" line (Figure 3-23 and Figure 3-24).

Conrath *et al*., showed, that a pretreatment with salicylic acid (SA), β-aminobutyric acid (BABA), dichloroisonicotinic acid (INA) or benzhothiadiazole (BTH) primes plant cells to protect themselves better against abiotic stresses such as wounding high salt, drought and cold stress (Figure 4-2),

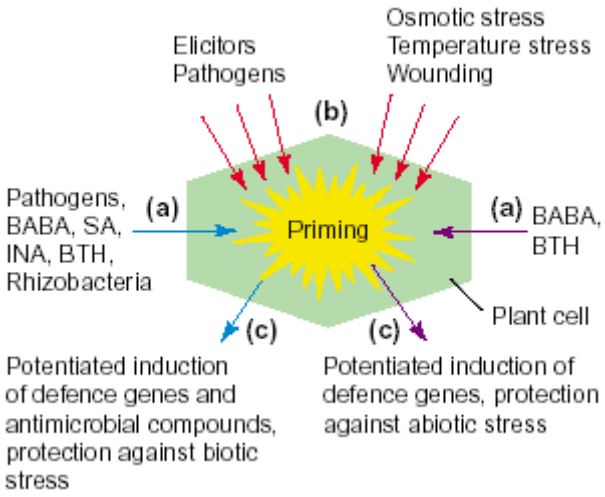

Figure 4-2 The effect of different compouds in priming of the plant cells and the role of priming in response to different biotic and abiotic stresses, a Priming step. b Challenge with biotic or abiotic stress. c Potentiated response. figure taken from Conrath et al., 2002.

(Conrath et al., 2002).

Accordingly, we wanted to discern whether BTH pre-treatment would reduce the observed hypersusceptibility of the "*pgase*" mutant to different abiotic stresses. Spraying the plants three days before cold stress with 100 µm BTH did not recover the hypersusceptibility of the "*pgase*" mutants to cold stress.

Treating wild-type plants with +4°C, the plants did not show any phenotype, while treating the "*pgase*" mutants with +4°C, the plants died (Figure 4-3). In the experiment in which wild-type plants were treated with -15°C, pre treatment of them with BTH, rescued the plants from death (Figure 4-3, data courtesy of Dr. G. Schmitz, RWTH Aachen university). But, the "*pgase*" mutants displayed a dramatic phenotype, since treatment with +4°C killed all plants within 48h (Figure 4-3), and the BTH pre-treatment did not rescue the plants (Figure 4-3). In contrast to wild-type plants in which the *COR78* gene was induced during cold treatment, independent of the presence or absence of BTH, in the "*pgase*" mutants *COR78* was not induced in the presence and absence of BTH (Figure 4-3). The summerized data were simpilified in the integrative model (Figure 4-3).

In the heat shock experiments, both "*pgase*" mutants (in Col-0 and Ta-0 backgrounds) withered 8 hours after incubation at 48°C while control genotypes did not produce any symptom (Figure 3-26). The response of the complemented "*pgase*" mutant was similar to Col-0 and Ta-0 plants. Treating the plants three days before heat shock with 100 µm BTH improved the susceptibility of the "*pgase*" mutants to heat shock (Figure 3-27). Hence BTH treatment had two distinct effects in the "*pgase*" mutant plants in relation to abiotic stress: it could protect from heat stress but could not do so

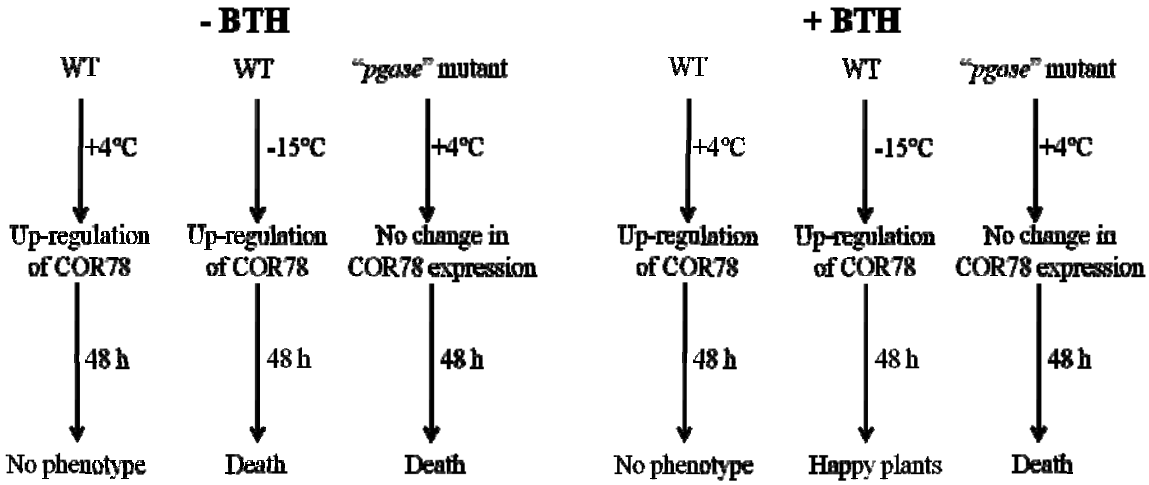

Figure 4-3 Schematic diagram representing the effect of BTH pre treatment on the regulation of cold regulated gene (*COR78*) in wild type plants and "*pgase*" mutant.

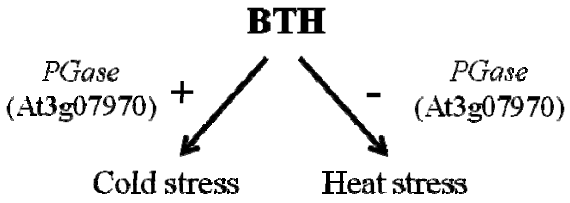

Figure 4-4 Model representing the role of *PGase* At3g07970 gene in response to environmental abiotic stresses including cold and heat stresses.

against cold stress (Figure 4-4).

In the desiccation stress experiment, the complemented "*pgase*" mutant lost almost 80% of their FW of leaves within 3 hours following excision, whereas leaves of the "*pgase*" lines lost only 20% and leaves of Col-0 or Ta-0 plants lost only 30% of their FW in the same period of time (Figure 3-28). These results fit nicely with the morphological defect of the "*pgase*" mutants which contain fewer guard cells on the epidermis in comparison to wild-type plants (Figure 3-5, G- I).

Since a role for *PGase* in desiccation has been shown (Roberts et al., 2002b; Kim and Patterson, 2006), therefore results of our desiccation experiments imply that *PGase* At3g07970 plays a role in regulation of transpiration and water loss in leaves. This role could be direct by affecting cell-cell contacts or indirect by affecting stomata density. Excessive *PGase* At3g07970 might reduce the tight

seal formed between the epidermal cells, thus lowering transpirational resistance. Alternatively, more *PGase* activity could result in more stomata being inserted in the epidermis, thus explaining the data from the transpiration experiment. At least, lowered expression of *PGase* At3g07970 resulted in fewer stomata being inserted into the epidermis.

On the other hand, the *Arabidopsis* transgenic *35S::AtMYB41* lines displayed a similar phenotype as the "*pgase*" mutants, *e g.* stunted growth and curly leaves. In this mutant it was shown that the cells were inhibited from expansion and the leaf surface permeability was altered so that the mutant showed higher water loss and transpiration rate than wild-type plants (Cominelli et al., 2008).

In summary, we conclude that the abnormal appearance of the "*pgase*" mutant is likely the result of defects in cell wall struture or composition (Figure 4-5). Polygalacturonases are the enzymes which catabolise the pectins and polygalacturonans, important components of the cell walls, thus are important for e.g. cell wall loosening and cell expansion and consequently normal form of the plants.

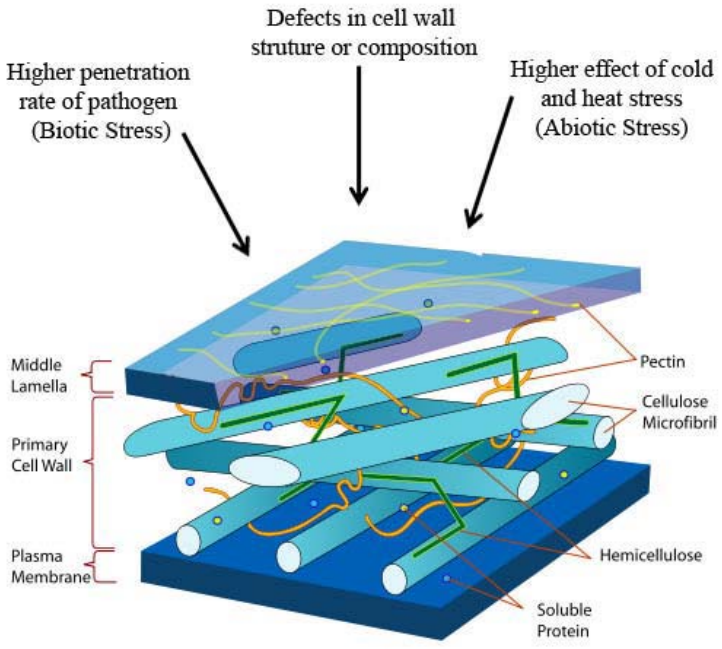

Figure 4-5 The defected cell wall struture in the "*pgase*" mutant which facilitate the penetration of biotic and abiotic stresses and thereby promote their effect.

The increased susceptibilty of the "*pgase*" mutant to biotic and abiotic stresses could be illuminated by different explaination. One explanation could be that the *PGase* gene, in addition to polygalacturonase activity also functions in a signaling cascade that coordinates the responses to various stresses (Figure 4-5).

In view of the fact that pectins are one of the more dominant cell wall components important for the connection between adjacent cells (Figure 4-5), thus any changes in the reorganization or sythesis, might severly affect this role. Therefore, in the "*pgase*" mutant the cells might not be connected suitably and thereby become more susceptible to biotic and abiotic stresses (Figure 4-5). In the case, it has responsibility in signaling, any mutation in this cascade disrupt transfer of the stimulants of plant defence, and thereby the "*pgase*" mutant will be more susceptible against different biotic and abiotic stresses (Figure 4-5).

4.2 "*bushy-ff*" mutant

4.2.1 Morphological phenotypes of the *Arabidopsis* "*bushy-ff*" mutant

The isolated *Arabidopsis thaliana* transgenic "*bushy-ff*" mutant displayed dramatic defects in different plant organs (Figure 3-29). This mutant was compressed in all dimensions and had fewer trichomes which often had fewer arms (Figure 3-29). Analysis of the size of "*bushy-ff*" root cells and Col-0 root cells showed that the number of cells in "*bushy-ff*" mutant appeared normal, however the size was reduced to about 1/3 (Figure 3-31). Thus, the mutant shows hypotrophy rather than hypoplasia and this probably explains the small size of the "*bushy-ff*" mutant.

The many phenotypes observed in the *"bushy-ff*" mutant however, made a scenario different from hormonal and other regulatory factors dysfunction possible: mutations resulting in aberrant cortical microtubule organization and orientation caused strong morphological phenotypes (Figure 1-14, and Figure 3-48), (Mayer et al., 1991; Torres-Ruiz and Jurgens, 1994; Trass et al., 1995; Mc Clinton and Sung, 1997; Whittington et al., 2001; Chu et al., 2007). Also at the cellular level the "*bushy-ff*" mutant displayed alterations as compared to wild- type: the shape of epidermal cells and the spacing of stomata, the differentiation of mesophyll cells into spongy and palisade cells and the branching of the trichomes (Figure 3-35).

Although a differentiation defect in spongy and palisade cells was observed for the "*bushy-ff*" mutant this developmental defect is quite mild and thus not as severe as strong cell differentiation defects observed *e.g.* in classical developmental mutants like *pin* (Blilou et al., 2005), *raspberry* (Yadegari et al., 1994), *shootmeristemless* (*sml*) (Lenhard et al., 2002) or *rootmeristemless* (*rml*) (Cheng et al., 1995) which have dramatic embryo or organ developmental defects.

The different shape of the epidermal cells and spacing of the stomata in "*bushy-ff*" was different from the wild-type stomata spacing. A similar defect was observed after the disorganization of the cortical microtubules in the *fass*=*ton* mutant (Torres-Ruiz and Jurgens, 1994; Camilleri et al., 2002), and thus such a defect may also cause the observed phenotype in "*bushy-ff*".

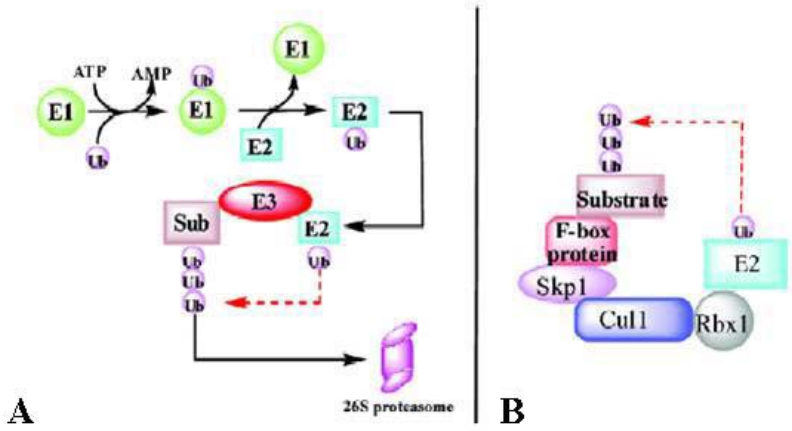

Figure 4-6. A, Ubiquitin (Ub) proteasome pathway and B, structure of Skp1-Cullin-F-box complex (= E3 Ub ligase). Red arrows indicate the process of Ub transfer from E2 Ub-conjugating enzyme to substrate (Sub). E1, Ub-activating enzyme; E3, Ub ligase.

In the "*bushy-ff*" mutant ~30% of the trichomes was one armed (Figure 3-34), a defect known to occur also in the Arabidopsis *zwichel* mutant in which a kinesin-like calmodulin protein was affected (Oppenheimer et al., 1997). This MT motor protein is proposed to provide the MT stability needed for trichome branch initiation (Mathur and Chua, 2000). So, it is possible that also the trichome branching phenotype in the "*bushy-ff*" could relate to microtubules malfunctions.

4.2.2 "*bushy-ff*" carries a T-DNA insertion in an *F-box* At1g77000 locus

The results of molecular analysis with thermal asymmetric interlaced (=adaptor ligation) PCRs revealed that in the "*bushy-ff*" mutant a T-DNA was inserted in the promoter region of the At1g77000 locus encoding an uncharacterized *Arabidopsis* F-box protein. A database search revealed that at least 568 F-box protein-encoding genes are present in the *Arabidopsis thaliana* genome (Kuroda et al., 2002). Members of the F-box protein family contain a conserved F-box domain (35−60 amino acids) in the amino-terminus and different substrate-binding domains such as Trp-Asp repeats or leucine rich repeats in the carboxy-terminus (Figure4-7), (Kuroda et al., 2002). The F-box domain was first described as a sequence motif found in human cyclin F (Bai et al., 1996). Subsequently, it was found that this domain plays a role in mediating protein-protein interactions in a variety of processes, such as polyubiquitination, transcription elongation, centromere binding, and translation repression. In the ubiquitin (Ub) proteasome pathway, the F-box motif links the F-box protein to other components of the SCF (Skp1, Cdc53, *F-box* protein) complex by binding the core SCF component Skp1 or Skp1-like proteins (Haichuan et al., 2007).

The "SCF E3s" are composed of four subunits, cullin1/Cdc53, Rbx1/Roc1/Hrt1, Skp1, and an F-box protein (Figure 4-6). Skp1 in turn binds in its amino terminal domain to the amino terminal domain of cullin1/Cdc53 and cullin1/Cdc53 binds to Rbx1/Roc1/Hrt1 proteins in its C terminal domain thus

forming the tetrameric SCF complex (Gagne et al., 2002). SCF E3 ligases and ubiquitin mediated proteolysis is conserved among eukaryotes (Haichuan et al., 2007).

Most components in the pathway and subunits of the proteasome known from animal and yeast studies have also been identified in plants. Many crucial biological processes in plants, such as hormone response, circadian rhythm, photomorphogenesis, stress response, flower development pathogen defence and senescence are governed by proteolysis (Haichuan et al., 2007). For example, the F-box proteins *TIR1* (*TRANSPORT INHIBITOR RESPONSE 1*), which regulates auxin responses, *SLEEPY1* (*SLY1*) and *SNEEZY* (*SNE*) which regulate the gibberellic acid signaling pathway in *Arabidopsis* (McGinnis et al., 2003; Strader et al., 2004), and gibberellin-insensitive dwarf 2 (GID2) in *Oryza sativa* (Sasaki et al., 2003), ethylene insensitive 3 (EIN3)-binding F-box protein 1 (EBF1) and EBF2, which target the transcriptional activator EIN2 for degradation and regulates ethylene signaling (Guo and Ecker, 2003; Gagne et al., 2004), and finally the F-box protein COI1, a pivotal factor in the JA signal response, that is required for all JA-dependent responses in *Arabidopsis* (Bai et al., 1996) are involved in this pathway and link this pathway to plant hormonal signalling. Many F-box proteins have also been identified in plants that are involved in other cellular and organismal processes. These F-box proteins regulate *e.g.* lateral root formation (Stirnberg et al., 2002; Coates et al., 2006; Dong et al., 2006), light signaling (Harmon and Kay, 2003; Marrocco et al., 2006) or the circadian system (Somers et al., 2004; Imaizumi et al., 2005), influence self incompatibility (Qiao et al., 2004), and control floral development (Ni et al., 2004).

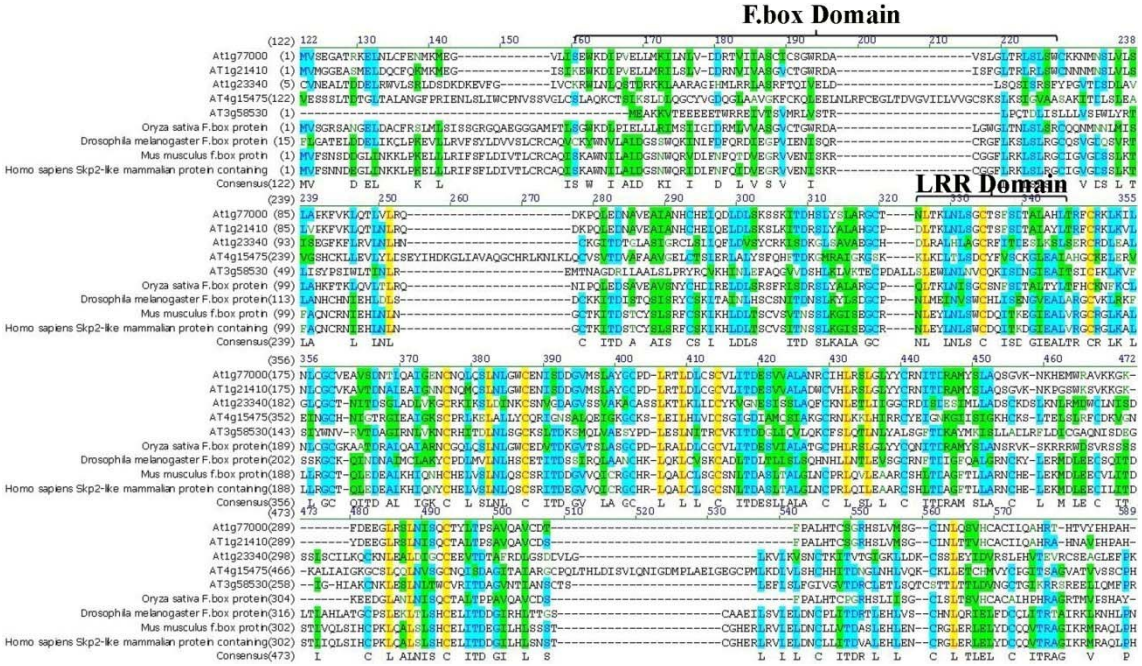

Figure4-7. Multiple sequence alignment of the At1g77000 protein with other *Arabidopsis thaliana* F-box proteins, *Oryza sativa*, *Drosophila melanogaster*, *Mus musculus* and *Homo sapiens SKP* like F-box proteins which displayed significant amino acids similarity to At1g77000.
The domain positions were taken from pfam.

To assess the hypothesis whether the T-DNA insertion in the promoter of the *F-box* At1g77000 locus caused the phenotype of the "*bushy-ff*" mutant, an independent T-DNA insertion line of At1g77000 from the Salk collection was analysed. In the characterized line, the T-DNA was inserted in the promoter region, 243 nucleotides upstream of the predicted start codon (Figure 3-40 and Figure 3-41). In contrast, to "*bushy-ff*" in which the T-DNA was inserted 146 nucleotides upstream of start codon in the promoter of *F-box* At1g77000, the Salk knock out line did not display any morphological phenotype (Figure 3-45). This discrepancy of the phenotype of "*bushy-ff*" and the Salk line could either be related to the different insertion sites in the promoter region of *F-box* At1g77000 locus or the presence of second T-DNA in "*bushy-ff*" line. The results of semi-quantitative RT-PCR analysis indicated that the expression level of *F-box* At1g77000 in "*bushy-ff*" and the Salk line was more or less identical and the expression of the *F-box* At1g77000 gene was ~70% knocked down relative to wild-type levels in both mutants. Also, in the segregation analyses of the "*bushy-ff*" mutant the Gentamycin marker did occur more frequently than expected for a single T-DNA insertion, therefore we concluded that the difference of T-DNA insertion in the promoter was not the main reason for the non-similarity of the phenotypes, rather the presence of a second T-DNA in "*bushy-ff*" was considered.

4.2.3 Presence of a second T-DNA in the "*bushy-ff*" mutant

Our second molecular analysis with thermal asymmetric interlaced (=adaptor ligation) PCRs showed the presence of a second mutation in "*bushy-ff*" (Figure 3-46). The second T-DNA was integrated in an already characterized locus, 123 nucleotides upstream from the ATG in the promoter region of At5g18580 ,named *FASS* (Torres-Ruiz and Jurgens, 1994), (Figure 3-47).

Torres-Ruiz & Jürgens have shown in 1994 that recessive mutations in the *FASS* gene alter the pattern of cell division from the zygote, without interfering with embryonic pattern formation. *fass* mutants can develop into tiny adult plants with all parts, including floral organs, strongly compressed in their longitudinal axis (Figure 1-14 and Figure 3-48). They have shown that *fass* mutations affected cell elongation and orientation of cell walls but do not interfere with cell polarity. Camilleri *et al.* have shown in 2002 that abnormalities of the cortical microtubular cytoskeleton, such as disorganization of the interphase microtubule array and lack of the preprophase band before mitosis, markedly affect cell shape and arrangement as well as overall plant morphology in *ton* (= *fass*) mutants. They mapped the gene and showed that the TON2 protein interacts with an *Arabidopsis* type A subunit of PP2A in the yeast two-hybrid system and thus likely defines a novel subclass of protein phosphatase 2A (PP2A) subunits that are possibly involved in the control of cytoskeletal structures in plants (Camilleri et al., 2002). PP2A, a heterotrimeric protein phosphatase, is a ubiquitous and conserved Serine/Threonine phosphatase with broad substrate specificity and diverse cellular functions. PP2A comprises A and B subunits which are regulatory and a catalytic C subunit. When the PP2A catalytic C subunit associates with the regulatory A and B subunits several species of holoenzymes are produced with distinct functions and characteristics. The A subunit, a founding member of the HEAT repeat protein family (huntington-elongation-A subunit-TOR), is the scaffold required for the formation of the heterotrimeric complex. When the A subunit binds it alters the enzymatic activity of the catalytic subunit, even if the B subunit is absent. While C and A subunit sequences show remarkable sequence conservation throughout eukaryotes, regulatory B subunits are more heterogeneous and are believed to play key roles in controlling the localization and specific activity of different holoenzymes (Camilleri et al., 2002). In addition, accessory proteins and posttranslational modifications (such as methylation) control PP2A subunit associations and activities (Xing et al., 2006; Xu et al., 2006). Comparison of the "*bushy-ff*" mutant with *fass* (=*ton*) mutant showed that although both mutants were severely stunted, there were also clear differences e.g. in the seedling stage they looked morphologically different from each other (Figure 3-51). The molecular analysis to assess the expression level of *FASS* in "*bushy-ff*" and *ton*2-5 revealed that the expression of *FASS* in "*bushy-ff*" was about 50% reduced compared to Col-0 plants while in *ton*2-5 mutant no expression of *FASS* could be detected. Therefore, we found that in the "*bushy-ff*" plants the expression of *FASS* was knocked down, while in the *ton* 2-5 mutant the expression of *FASS* was knocked out (Figure 3-49 and Figure 3-50).

4.2.4 "*bushy-ff*" mutant phenotype is the result of down regulation of *F-box* At1g77000 and *FASS* genes

Our molecular analysis indicated that the "*bushy-ff*" mutant carried two independent mutations and since none of single knock out lines (neither Salk *F-box* At1g77000 knock down nor *ton*2-5) showed really similar morphological phenotypes as "*bushy-ff*", the possibility that a combination of both mutations causes the "*bushy-ff*" phenotype was considered. The results of a genetic cross between Col-0 and "*bushy-ff*" confirmed this claim because in the F_2 generation of this cross 1 out of 16 (1/16) plants looked phenotypically like "*bushy-ff*" and 15 out of 16 (15/16) looked like wild-type (Figure 3-52). The molecular characterization of the F_2 generation of this cross also confirmed the notion that both mutations were contributing in arising of the morphological defects in the "*bushy-ff*" mutant. Molecular characterization of all 6 "*bushy-ff*" looking F_2 plants revealed that all *"bushy-ff*" plants were homozygous for both T-DNA insertions. From the wild-type looking F_2 plants, homozygous lines carrying single T-DNA insertions in either the *FASS* or the *F-box* At1g77000 genes were identified.

To test the correctness of the results from the genetic cross, lines which were constitutively expressing *F-box* At1g77000 or *FASS* were generated in the "*bushy-ff*" background. 100% of the transformed T_1 plants were wild-type looking plants and in the T_2 generation without selection, 1 out of 16 (1/16) plants displayed the "*bushy-ff*" phenotype while 15 out of 16 (15/16) were phenotypically WT looking plants.

These observations implied that restoration of the *F-box* At1g77000 or *FASS* expression in "*bushy-ff*" could complement the "*bushy-ff*" phenotype and is consistent with the results of the "*bushy-ff*" x Col-0 cross which indicated that both mutations were required for the "*bushy-ff*" phenotype.

Molecular analysis with semi quantitative RT-PCRs showed that the *F-box* At1g77000 expression level in the transformed complemented "*bushy-ff*" plants with *F-box* At1g77000 CDS under the control of 35S promoter were 7.4 more than in "*bushy-ff*" and 2.6 times more than in Col-0. With similar semi quantitative RT-PCRs analysis I showed, that the expression of *FASS* in the complemented "*bushy-ff*" plants with *FASS* CDS under the control of 35S promoter were 5.63 times more than in "*bushy-ff*" and 2.25 times more than in Col-0. Chu *et al.,* have shown in 2007 that reduced expression of the *AtCESA2*, a member of the cellulose syntheses enzymes, results in a mild phenotype while a complete knock out of a gene caused a strong phenotype. Their results highlight the differences between the two reverse-genetics approaches, reduction of RNA level (gene silencing) versus gene deletion, as I had observed it for the *FASS* gene.

The truncated (Δ) version of *FASS* CDS which was synthesised from a leaf cDNA library was 40 nucleotides shorter than full-length *FASS* CDS (Figure 3-73) and was also transformed into "*bushy-ff*" plants under the control of 35S promoter. 100% of transformed selected T_1 plants were "*bushy-ff*" looking like plants. Even the molecular analysis indicated that the expression level of the *FASS* in transformed selected "*bushy-ff*" plants with this truncated (Δ) version of *FASS* CDS, was ~4.28 times more than in "*bushy-ff*" and ~2 times more than in Col-0 (Figure 3-76), but the phenotype of the

"*bushy-ff*" could not be complemented (Figure 3-74). This observation indicated that the lost 40 nucleotides are not dispensable for FASS protein function.

4.2.5 *f-box* At1g77000-/- × *fass*-/- cross results confirm the effect of *F-box* At1g77000 and *FASS* mutations in the phenotype of "*bushy-ff*"

As explained in the last section, the results of the Col × "*bushy-ff*" cross indicated that two independent mutations are required for the "*bushy-ff*" phenotype, to reconfirm our finding of the segregation of the "*bushy-ff*" phenotype, another cross between the homozygous single *f-box* At1g77000 knock down line and the single homozygous *fass* knock down mutant was performed. In the F_1 generation 100% of plants were wild-type looking. In F_2 generation ~1 out of 16 (1/16) plants showed "*bushy-ff*" phenotype and ~15 out of 16(15/16) were wild-type looking like plants (Figure 3-60). Therefore, all of our genetic data strongly supported the idea that the severe phenotype in the "*bushy-ff*" mutant was a result of both mutations in *F-box* At1g77000 and *FASS*.

4.2.6 The phenotype of the "*bushy-ff*" was not irrespective of mutant alleles

To address the point whether the "*bushy-ff*" phenotype is due to a combination of a particular set of mutations or the genetic interaction between *F-box* At1g77000 and *FASS* is irrespective of the mutant alleles, three different crosses were performed:

- Salk *f-box* At1g77000 knock down+/- ×*fass* -/- knock down
- *f-box* At1g77000 knock down-/- mutant ×*ton2-5* +/-
- Salk *f-box* At1g77000 knock down+/- mutant× *ton2-5* +/-

The results of first cross revealed that for the "*bushy-ff*" phenotype the nature of the mutation in the *F-box* At1g77000 gene was not limited to the one discovered in the "*bushy-ff*" mutant. Because the Salk *F-box* At1g77000 knock down mutant (line # 070175) which was used in this cross, contained a different insertion site as compared to "*bushy-ff*". In this cross 100% of F_1 plants were wild type-looking plants and in the F_2 generation 1 out of 16 (1/16) plants was "*bushy-ff*" and 15 out of 16 (15/16) were wild type-looking plants (Figure 3-62). Thus, we obtained the same result as for the Col × "*bushy-ff*" cross.

We learned from the results of the second cross that the nature of the mutation in the *fass* gene was specific to generate the "*bushy-ff*" phenotype. Because in this cross 100% of F_1 and F_2 generation plants were wild type-looking plants (Figure 3-64). These results implied that the "*bushy-ff*" phenotype depends on the nature of the *fass* mutation. However, it could also be that the *ton2-5* mutant phenotype which results in a much more pronounced miniature plant size phenotype simply was so strong that the plants carrying the *ton2-5* mutation were not detected among the much larger wild-type plants and thus these plants were not counted in the analysis.

The results of the last cross were quite predictable according to the results of first and second cross results. Since in this cross the *fass* mutation was again the strong *ton2* mutant, in the F_1 and F_2

generation of this cross none of the plants showed the "*bushy-ff*" phenotype and 100% of plants in F_1 and F_2 were normal looking like plants (Figure 3-66) which can be explained as for the second cross.

4.2.7 Expression of *F-box* At1g77000 and *FASS* follow the same pattern in various plant organs

We analysed *F-box* At1g77000 and *FASS* expression throughout *Arabidopsis* development. The result of semi quantitative RT-PCR analysis with different *Arabidopsis* organs indicated that *F-box* At1g77000 is mostly expressed in cotyledons, leaves, stems and flowers and at lower levels in roots (Figure 3-77). The expression of the *FASS* gene followed the same expression pattern except that *FASS* expression in roots was about two-fold higher than that of the *F-box* At1g77000 gene (Figure 3-78). However, since both genes were expressed in all organs tested, the general expression pattern of both genes was quite same. Camilleri *et al*. also have shown the ubiquitous expression pattern of FASS (Camilleri et al., 2002).

Tissue-specific expression analysis of the *F-box* At1g77000 gene using a *F-box* At1g77000-promoter:β-glucuronidase (*GUS*) reporter gene fusion corroborated the results of the organ-specific expression analysis (Figure 3-79).The promoter:β-glucuronidase (*GUS*) reporter gene fusion analysis showed that *F-box* At1g77000 was expressed in almost all organs, specifically in the veins of cotyledons and leaves (Figure 3-79, E and F), the anthers and the style of flowers (Figure 3-79, I-K) and a focalized expression was detectable in certain regions of roots, possibly emerging sites of lateral roots (Figure 3-79, C and D). Thus, the *F-box* At1g77000 gene was expressed mostly in differentiating tissue.

4.2.8 Physical interaction between *F-box* At1g77000 and *FASS*

With different genetic crosses we have found that *F-box* At1g77000 and *FASS* genetically interact with each other. In a number of cases, a genetic interaction was indicative for a physical interaction (Zolman et al., 2005; Chandler et al., 2007; Pérez-Pérez et al., 2008), Therefore, I wanted to answer the question whether the two proteins physically interact with each other using the yeast two hybrid system.

The results of this study revealed that *F-box* At1g77000 and *FASS* physically interacted with each other when the *FASS* CDS was fused to the DNA-binding domain (BD) of GAL4 as a bait protein, and the *F-box* At1g77000 CDS was fused to the activation domain (AD) of GAL4 as a prey protein. The double transformed yeast strain was able to grow on SD - His (Galactose/Raffinose+ X-Gal) plates and also produced the blue colour in the presence of X-Gal in the medium (Figure 3-81). The growth on minimal media lacking histidine and blue colour development was indicative for a physical interaction between FASS and F-box At1g77000. The specificity of this interaction was shown since yeast double transformants which were prepared in different combinations of *FASS* and *F-box* At1g77000 with an *Arabidopsis* 14-3-3 gene (Table 3-2) did not result in growth on medium lacking histidine and also no blue colour developed (Figure 3-81).

Camilleri *et al*. in 2002 have shown that the full length TON2=FASS protein interacts with an *Arabidopsis* type A subunit of protein phosphatase (PP2A).

In summary, Our data suggest that FASS might organize cortical microtubules through the interaction with an F-box protein, thus influencing the stability of signal transduction components like the FASS-interacting protein phosphatase 2A. The complex of *FASS* and *F-box* At1g77000 might cooperate with a third partner which this third partner could be PP2A. When the expression of the *FASS* and *F-box* At1g77000 genes were knocked down less FASS and F-box At1g77000 proteins were made. The lower amounts of protein level possibly destabilizes the trimeric complex thus creating the "*bushy-ff*" phenotype.

4.3 Outlook

According to the finding of Camilleri *et al.* which indicated a physical interaction between *TON2=FASS* and PP2A and contribution of them in the organization of cortical microtubules, and our finding which implied the presence of genetic and physical interaction between TON2=FASS and F-box At1g77000 proteins, performing further studies to determine the relation between PP2A and *F-box* is certainly worthwhile. To this purpose the genetic cross of *f-box* knock down mutant with *pp2a* mutant and testing of the physical interaction between F-box and PP2A could be performed.

Localization of F-box protein inside the cells on cytoskeleton filaments (Figure 3-84), support the idea that *Arabidopsis* F-box At1g77000 protein plays a role in contribution with TON2=FASS and PP2A in the organization of the cortical microtubules during plant development.

5 REFERENCES

Aguilar-Martinez, J.A., Poza-Carrion, C., and Cubas, P. (2007). *Arabidopsis BRANCHED1* acts as an integrator of branching signals within axillary buds. Plant Cell **19,** 458-472.

Albersheim, and Valent, P.S. (1978). Host-pathogen interactions in plants. Plants, when exposed to oligosaccharides of fungal origin, defend themselves by accumulating antibiotics. J Cell Biol. **78,** 627-643.

Albersheim, P., and Valent, B.S. (1974). Host-pathogen interactions: plant pathogens secrete proteins which inhibit enzymes of the host capable of attacking the pathogen. Plant Physiol. **53,** 684-687.

Amador, V., Monte, E., García-Martínez, J.-L., and Prat, S. (2001). Gibberellins signal nuclear import of PHOR1, a photoperiod-responsive protein with homology to *Drosophila armadillo*. Cell **106,** 343-354.

Asami, T., Min, Y.K., Nagata, N., Yamagishi, K., Takatsuto, S., Fujioka, S., Murofushi, N., Yamaguchi, I., and Yoshida, S. (2000). Characterization of brassinazole, a triazole-type brassinosteroid biosynthesis inhibitor. Plant Physiol. **123,** 93-100.

Atkinson, R.G., Schroder, R., Hallett, I.C., Cohen, D., and MacRae, E.A. (2002). Overexpression of polygalacturonase in transgenic apple trees leads to a range of novel phenotypes involving changes in cell adhesion. Plant Physiol. **129,** 122-133.

Ausubel, F.M., Brent, R., and Kingston, R.E. (1994). Current Protocols in Molecular Biology. (New York
Wiley Interscience,).

Bai, C., Sen, P., Hofmann, K., Ma, L., Goebl, M., Harper, J.W., and Elledge, S.J. (1996). SKP1 connects cell cycle regulators to the ubiquitin proteolysis machinery through a novel motif, the F-box. Cell **86,** 263-274.

Bainbridge, K., Sorefan, K., Ward, S., and Leyser, O. (2005). Hormonally controlled expression of the *Arabidopsis MAX4* shoot branching regulatory gene Plant journal **44,** 569-580.

Bangerth, F. (1994). Response of cytokinin concentration in the xylem (*Phaseolus vulgaris* L.) plants to decapitation and relationship to apical dominancebexudate of bean auxin treatment. Planta **194,** 439-442.

Benkova, E., Michniewicz, M., Sauer, M., Teichmann, T., and Seifertova, D. (2003). Local, efflux-dependent aauxin gradients as a common module for plant organ formation. Cell **115,** 591-602.

Bennett, T., Sieberer, Willett, B., Booker, J., Luschnig, C., and Leyser, O. (2006). The *Arabidopsis MAX* pathway controls shoot branching by regulating auxin transport **16,** 553-563.

Bichet, A., Desnos, T., Turner, S., Grandjean, O., and höfte, H. (2001). *BOTERO1* is required for normal orientation of cortical microtubules and anisotropic cell expansion in *Arabidopsis* Plant Journal **25,** 137-148.

Bishop, G.J., and Koncz, C. (2002). Brassinosteroids and plant steroid hormone signaling. Plant Cell **14,** 97-110.

Blilou, I., Xu, J., Wildwater, M., Willemsen, V., Paponov, I., Friml, J., Heidstra, R., Aida, M., Palme, K., and Scheres, B. (2005). The PIN auxin efflux facilitator network controls growth and patterning in *Arabidopsis* roots. Nature **433,** 39-44.

Bonghi, C., Rascio, A., Ramina, A., and Casadoro, G. (1992). Cellulase and polygalacturonase involvement in the abscission of leaf and fruit explants of peach. Plant Molecular Biology **20,** 839-848.

Bradford, M.M. (1976). A rapid and sensitive method for the quantitation of microgram quantities of protein utilizing the principle of protein-dye binding. Anal Biochem **72,** 248-254.

Bradley, D., Ratcliffe, O., Vincent, C., Carpenter, R., and Coen, E. (1997). Inflorescence commitment and architecture in *Arabidopsis*. Science **275,** 80-83.

Brininstool, G., Kasili, R., Simmons, L.A., Kirik, V., Hülskamp, M., and Larkin, J.C. (2008). Constitutive expressor of pathogenesis-related genes5 affects cell wall biogenesis and trichome development. BMC Plant Biol.

Burk, D.H., Liu, B., Zhong, R., Morrison, W.H., and Ye, Z.-H. (2001). A katanin-like protein regulates normal cell wall biosynthesis and cell elongation. Plant Cell **13,** 807-828.

Busov, V.B., Brunner, A.M., and Strauss, S.H. (2008). Genes for control of plant stature and form. New Phytologist **177,** 589- 607.

Busov, V.B., Meilan, R., Pearce, D.W., Ma, C., Rood, S.B., and Strauss, S.H. (2003). Activation tagging of a dominant gibberellin catabolism gene (GA 2-oxidase) from poplar that regulates tree stature. Plant Physiol. **132,** 1283-1291.

Camilleri, C., Azimzadeh, J., Pastuglia, M., Bellini, C., Grandjean, O., and Bouchez, D. (2002). The Arabidopsis *TONNEAU2* gene encodes a putative novel protein phosphatase 2A regulatory subunit essential for the control of the cortical cytoskeleton. Plant Cell **14,** 833-845.

Carrera, E., Bou, J., Garcia-Martinez, J., and Prat, S. (2000). Changes in GA-20 oxidase gene expression stongly affect stem length,tuber induction and tuber yield of potato plants
Plant Journal **22,** 247-256.

Cebolla, A., Vinardell, J., Kiss, E., Olah, B., Roudier, F., Kondorosi, A., and Kondorosi, E. (1999). The mitotic inhibitor *ccs52* is required for endoreduplication and ploidy-dependent cell enlargement in plants. EMBO journal **18,** 4476–4484.

Chandler, J.W., Cole, M., Flier, A., Grewe, B., and Werr, W. (2007). The AP2 transcription factors DORNROSCHEN and DORNROSCHEN-LIKE redundantly control *Arabidopsis* embryo patterning via interaction with PHAVOLUTA. Development **134,** 1653-1662.

Cheng, J.C., Seeley, K.A., and Sung, Z.R. (1995). *RML1* and *RML2*, *Arabidopsis* genes required for cell proliferation at the root tip. Plant Physiol. **107,** 365-376.

Cheng, Y., Dai, X., and Zhao, Y. (2007). Auxin synthesized by the YUCCA flavin monooxygenases is essential for embryogenesis and leaf formation in *Arabidopsis*. Plant Cell **19,** 2430-2439.

Chien, C.T., Bartel, P.L., Sternglanz, R., and Fields, S. (1991). Proc. Natl. Acad. Sci. **88,** 9578-9582.

Choe, S., Schmitz, R.J., Fujioka, S., Takatsuto, S., Lee, M.-O., Yoshida, S., Feldmann, K.A., and Tax, F.E. (2002). *Arabidopsis* brassinosteroid-insensitive *dwarf12* mutants are semidominant and defective in a glycogen synthase kinase 3beta -like kinase. Plant Physiol. **130,** 1506-1515.

Chory, J., Nagpal, P., and Peto, C.A. (1991). Phenotypic and genetic analysis of *det2*, a new mutant that affects light-regulated seedling development in *Arabidopsis*. Plant Cell **3,** 445-459.

Chu, Z., Chen, H., Zhang, Y., Zhang, Z., Zheng, N., Yin, B., Yan, H., Zhu, L., Zhao, X., Yuan, M., Zhang, X., and Xie, Q. (2007). Knockout of the *AtCESA2* gene affects nicrotubule orientation and causes abnormal cell expansion in *Arabidopsis*. Plant Physiol. **143,** 213-224.

Cleary, A.L., and Smith, L.G. (1998). The *tangled1* gene is required for spatial control of cytoskeletal arrays associated with cell division during maize leaf development. Plant Cell **10,** 1875-1888.

Cline, M. (1991). Apical dominance. Bot.Rev **57,** 318-358.

Clough, S.J., and Bent, A.F. (1998). Floral dip: a simplified method for Agrobacterium-mediated transformation of *Arabidopsis thaliana*. . Plant J. **16,** 735-743.

Clouse, S.D., Langford, M., and McMorris, T.C. (1996). A brassinosteroid-insensitive mutant in *Arabidopsis thaliana* exhibits multiple defects in growth and development. Plant Physiol. **111,** 671-678.

Coates, J.C., Laplaze, L., and Haseloff, J. (2006). Armadillo-related proteins promote lateral root development in *Arabidopsis*. Proceedings of the National Academy of Sciences **103,** 1621-1626.

Cockcroft, C.E., den Boer, B.G.W., Healy, J.M.S., and Murray, J.A.H. (2000). Cyclin D control of growth rate in plants. Nature **405,** 575-579.

Cominelli, E., Sala, T., Calvi, D., Gusmaroli, G., and Tonelli, C. (2008). Over-expression of the *Arabidopsis AtMYB41* gene alters cell expansion and leaf surface permeability.

Conrath, U., Pieterse, C.M.J., and Mauch-Mani, B. (2002). Priming in plant-pathogen interactions. Trends in Plant Science **7,** 210-216.

Crawford, B.C.W., Nath, U., Carpenter, R., and Coen, E.S. (2004). *CINCINNATA* controls both cell differentiation and growth in petal lobes and leaves of *Antirrhinum*. Plant Physiol. **135,** 244-253.

Cubas, P., Lauter, N., Doebley, J., and Coen, E. (1999). The TCP domain: a motif found in proteins regulating plant growth and development Plant journal **18,** 215-222.

Darvill, A.G., and Albersheim, P. (1984). Phytoalexins and their elicitiors-a defence against microbial infection in plants. Annual Reviews **35**.

Davies, P.J. (1995). In Plant hormones:physiology, biochemistry and molecular biology (London: UK:Kluwer Academic Publishers), pp. 6-7.

De Veylder, L., Beeckman, T., Beemster, G.T.S., Krols, L., Terras, F., Landrieu, I., Van Der Schueren, E., Maes, S., Naudts, M., and Inze, D. (2001). Functional Analysis of Cyclin-Dependent Kinase Inhibitors of Arabidopsis. Plant Cell **13,** 1653-1668.

Deobley, J., Stec, A., and Hubbard, L. (1997). The evolution of apical dominance in maize. Nature **386,** 485-488.

Despres, C., DeLong, C., Glaze, S., Liu, E., and Fobert, P.R. (2000). The *Arabidopsis* NPR1/NIM1 protein enhances the DNA binding activity of a subgroup of the TGA family of bZIP transcription factors. Plant Cell **12,** 279-290.

Despres, C., Chubak, C., Rochon, A., Clark, R., Bethune, T., Desveaux, D., and Fobert, P.R. (2003). The Arabidopsis NPR1 disease resistance protein is a novel cofactor that confers redox regulation of DNA binding activity to the basic domain/leucine zipper transcription factor TGA1. Plant Cell **15,** 2181-2191.

Dewitte, W., and Murray, J.A. (2003). The plant cell cycle. annual Review of Plant Biology **54,** 235-264.

Doebley, J., Stec, A., and Gustus, C. (1995). Teosinte *branched1* and the origin of maize: evidence for epistasis and the evolution of dominance. Genetics **141,** 333-346.

Doerner, P., Jorgensen, J., You, R., Steppuhn, J., and Lamb, C. (1996). Control of root growth and development by cyclin expression Nature **380,** 520-523.

Dong, L., Wang, L., Zhang, Y.e., Zhang, Y., Deng, X., and Xue, Y. (2006). An auxin-inducible F-box protein *CEGENDUO* negatively regulates auxin-mediated lateral root formation in Arabidopsis. Plant Molecular Biology **60,** 599-615.

Doonan. (2000). Social controls on cell proliferation in plants. Current opinion in plant biology **3,** 482-487.

Elliott, R.C., Betzner, A.S., Huttner, E., Oakes, M.P., Tucker, W.Q.J., Gerentes, D., Perez, P., and Smyth, D.R. (1996). *AINTEGUMENTA*, an APETALA2-like gene of *Arabidopsis* with pleiotropic roles in ovule development and floral organ growth. Plant Cell **8,** 155-168.

Fischer, R.L., and Bennett, A.B. (1983). Role of cell wall hydrolases in fruit ripening. Annual Review of Plant Physiology and Plant Molecular Biology.

Fleming, A.J. (2005). Formation of primordia and phyllotaxy Current Opinion in Plant Biology **8,** 53-58.

Flick, J., and Johnston, M. (1990). Two systems of glucose repression of the GAL1 promoter in *Saccharomyces cerevisiae* Mol. Cell. Biol **10,** 4757-4769.

Fridborg, I., Kuusk, S., Moritz, T., and Sundberg, E. (1999). The *Arabidopsis* dwarf mutant *sh*i exhibits reduced gibberellin responses conferred by overexpression of a new putative zinc finger protein. Plant Cell **11,** 1019-1032.

Friedrichsen, D.M., Nemhauser, J., Muramitsu, T., Maloof, J.N., Alonso, J., Ecker, J.R., Furuya, M., and Chory, J. (2002). Three redundant brassinosteroid early response genes encode outative bHLH transcription factors required for normal growth. Genetics **162,** 1445-1456.

Fukaki, H., Tameda, S., Masuda, H., and Tasaka, M. (2002). Lateral root formation is blocked by a gain-of-function mutation in the *SOLITARY-ROOT*/*IAA14* gene of *Arabidopsis*. Plant Journal **29,** 153-168.

Furutani, I., Watanabe, Y., Prieto, R., Masukawa, M., Suzuki, K., Naoi, K., Thitamadee, S., Shikanai, T., and Hashimoto, T. (2000). The *SPIRAL* genes are required for directional control of cell elongation in *Arabidopsis thaliana*. Development **127,** 4443-4453.

Gabor, L., and Howard, M.G. (2006). MAX1, a regulator of the flavonoid pathway, controls vegetative axillary bud outgrowth in *Arabidopsis*. Proc Natl Acad Sci U S A. **103,** 472-476.

Gagne, J.M., Downes, B.P., Shiu, S.-H., Durski, A.M., and Vierstra, R.D. (2002). The F-box subunit of the SCF E3 complex is encoded by a diverse superfamily of genes in *Arabidopsis*. Proceedings of the National Academy of Sciences **99,** 11519-11524.

Gagne, J.M., Smalle, J., Gingerich, D.J., Walker, J.M., Yoo, S.-D., Yanagisawa, S., and Vierstra, R.D. (2004). Arabidopsis EIN3-binding F-box 1 and 2 form ubiquitin-protein ligases that repress ethylene action and promote growth by directing EIN3 degradation. Proceedings of the National Academy of Sciences **101,** 6803-6808.

Gale, M.D., Law, C.N., Marshall, G.A., and Worland, A.J. (1975). The genetic control of gibberellic acid insensitivity and coleoptile length in a "dwarf" wheat. Heredity **34,** 393-399.

Galweiler, L., Guan, C., Muller, A., Wisman, E., Mendgen, K., Yephremov, A., and Palme, K. (1998). Regulation of polar auxin transport by AtPIN1 in *Arabidopsis* vascular tissue. Science **282,** 2226-2230.

Giulini, A., Wang, J., and Jackson, D. (2004). Control of phyllotaxy by the cytokinin-inducible response regulator homologe *ABPHYL1*. Nature **430,** 1031.

Gonzalez-Carranza, Z.H., Elliott, K.A., and Roberts, J.A. (2007). Expression of polygalacturonases and evidence to support their role during cell separation processes in *Arabidopsis thaliana*. J. Exp. Bot. **58,** 3719-3730.

Greb, T., Clarenz, O., Schafer, E., Muller, D., Herrero, R., Schmitz, G., and Theres, K. (2003). Molecular analysis of the *LATERAL SUPPRESSOR* gene in *Arabidopsis* reveals a conserved control mechanism for axillary meristem formation. Genes Dev. **17,** 1175-1187.

Grebe, M. (2005). PLANT BIOLOGY: enhanced: growth by auxin: when a weed needs acid. Science **310,** 60-61.

Guo, H., and Ecker, J.R. (2003). Plant responses to ethylene gas are mediated by SCFEBF1/EBF2-dependent proteolysis of EIN3 transcription factor. Cell **115,** 667-677.

Haber, A. (1962). Nonessentiality of concurrent cell divisions for degree of polarization of leaf growth.I. Studies withradiation-induced mititic inhibitio. American Journal of Botany **49,** 583-589.

Haichuan, Y., Jiao, W., Nanfei, X., and Ming, P. (2007). Roles of F-box proteins in plant hormone responses. Acta Biochimica et Biophysica Sinica **39,** 915-922.

Harberd, N.P., and Freeling, M. (1989). Genetics of dominant gibberellin-insensitive dwarfism in maize. Genetics **121,** 827-838.

Harmon, F., and Kay, S. (2003). The F box protein AFR is a positive regulator of phytochrome A-mediated light signaling. Cuurent Biology **13,** 2091-2096.

Harper, J.W., Adami, G.R., Wei, N., Keyomarsi, K., and Elledge, S.J. (1993). The p21 Cdk-interacting protein cipl is a potent inhibitor of Gl cyclin-dependent kinases. Cell **75,** 805-816.

Hedden, P., and Phillips, A.L. (2000a). Gibberellin metabolism: new insights revealed by the genes. Trends in Plant Science **5,** 523-530.

Hedden, P., and Phillips, A.L. (2000b). Manipulation of hormone biosynthetic genes in transgenic plants. Current Opinion in Biotechnology **11,** 130-137.

Helliwell, C., Sheldon, C., Olive, M., Walker, A., Zeevaart, J., Peacock, W., and Dennis, E. (1998). Cloning of the *Arabidopsis ent*-kaurene oxidase gene GA3. Proc Natl Acad Sci U S A. **95,** 9019-9024.

Hemerly, A., Engler, J., Bergounioux, C., van, M., Engler, G., Inze, D., and Ferreira, P. (1995). Dominant negative mutants of the Cdc2 kinase uncouple cell division from iterative plant development. EMBO **14,** 3925-3936.

Henderson, J., Davies, H.A., Heyes, S.J., and Osborne, D.J. (2001). The study of a monocotyledon abscission zone using microscopic, chemical, enzymatic and solid state 13C CP/MAS NMR analyses Phytochemistry **56,** 131-139.

Hermanns, M., Slusarenko, A.J., and Schlaich, N.L. (2003). Organ-specificity in a plant disease is determined independently of R gene signaling. MPMI **16,** 752-759.

Hooley, R. (1994). Gibberellin perception at the plasma membrane of *Arena fatua* aleurone protoplasts. Plant Molecular Biology **26,** 1529-1555.

Horiguchi, G., Kim, G., and Tsukaya, H. (2005). The transcription factor AtGRF5 and the transcription coactivator AN3 regulate cell proliferation in leaf primordia of *Arabidopsis thaliana* Plant journal **43**.

Hu, Y., Xie, Q., and Chua, N.-H. (2003). The Arabidopsis auxin-Inducible gene *ARGOS* controls lateral organ size. Plant Cell **15,** 1951-1961.

Hwang, I., and Sheen, J. (2001). Two-component circuitry in *Arabidopsis* cytokinin signal transduction. Nature **413,** 383-389.

Imaizumi, T., Schultz, T.F., Harmon, F.G., Ho, L.A., and Kay, S.A. (2005). FKF1 F-box protein mediates cyclic degradation of a repressor of *CONSTANS* in *Arabidopsis*. Science **309,** 293-297.

Inoue, H., Nojima, H., and Okayama, H. (1990). High efficiency transformation of *Esherichia coli* with plasmids. . Gene **96,** 23-28.

Inze, D., and Veylder, L. (2006). Cell cycle regulation in plant development. Annual review of Genetics **40,** 77-105.

Jenkins, E., Paul, W., Craze, M., Whitelaw, C., Weigand, A., and Roberts, J. (1999). Dehiscence-related expression of an *Arabidopsis thaliana* gene encoding a polygalacturonase in transgenic plants of B*rassica napus*. Plant,Cell,Enviroment **22,** 159-167.

Jenkins, E.S., Paul, W., Coupe, S.A., Bell, S.J., Davies, E.C., and Roberts, J.A. (1996). Characterization of an mRNA encoding a polygalacturonase expressed during pod development in oilseed rape (*Brassica napus* L.). J. Exp. Bot. **47,** 111-115.

Jianming, L., and Chory, J. (1997). A putative leucine-rich repeat receptor kinase involved in brassinosteroid signal transduction. Cell **90,** 929.

Keller, T., Abbott, J., Moritz, T., and Doerner, P. (2006). *Arabidopsis REGULATOR OF AXILLARY MERISTEMS1* controls a leaf axil stem cell niche and modulates vegetative development. Plant Cell **18,** 598-611.

Keogh, R.C., Deverall, B.J., and McLeod, S. (1980). Comparison of histological and physiological responses to *Phakopsora pachyrhizi* in resistant and susceptible soybean. Trans. Br. Mycol. Soc **74,** 329-332.

Kim, J., and Patterson, S.E. (2006). Expression divergence and functional redundancy of polygalacturonases in floral prgan abscission. Plant Signaling and Behavior **1,** 281-283.

Kim, J., Choi, D., and Kende, H. (2003). The AtGRF family of putative transcription factors is involved in leaf and cotyledon growth in *Arabidopsis* Plant Journal **36,** 94-104.

Kim, J., Shiu, S.-H., Thoma, S., Li, W.-H., and Patterson, S. (2006). Patterns of expansion and expression divergence in the plant polygalacturonase gene family. Genome Biology **7**.

Klucher, K.M., Chow, H., Reiser, L., and Fischer, R.L. (1996). The *AINTEGUMENTA* gene of *Arabidopsis* required for ovule and female gametophyte development is related to the floral homeotic gene *APETALA2*. Plant Cell **8,** 137-153.

Koncz, C., and Schell, J. (1986). The promoter of TL-DNA gene 5 controls the tissue-specific expression of chimaeric genes carried by a novel type of *Agrobacterium* binary vector. Mol Gen Genet 204: **204,** 383-396.

Kondorosi, E., Roudier, F., and Gendreau, E. (2000). Plant cell-size control: growing by ploidy? . Current opinion in plant biology **3,** 488-492.

Koornneef, M., and van der Veen, J.H. (1980). Induction and analysis of gibberellin sensitive mutants in *Arabidopsis thaliana* (L.) Heynh. Theor. Appl. Genet **58,** 257-263.

Krizek, B. (1999). Ectopic expression of AINTEGUMENTA in *Arabidopsis* plants results in increased growth of floral organs. Developmental Genetics **25,** 224.

Kunkel, B.N., Bent, A.F., Dahlbeck, D., Innes, R.W., and Staskawicz, B.J. (1993). RPS2, an *Arabidopsis* disease resistance locus specifying recognition of *Pseudomonas syringae* strains expressing the avirulence gene avrRpt2. Plant Cell **5,** 865-875.

Kuroda, H., Takahashi, N., Shimada, H., Seki, M., Shinozaki, K., and Matsui, M. (2002). Classification and expression analysis of *Arabidopsis* F-box-containing protein genes. Plant Cell Physiol. **43,** 1073-1085.

Lashbrook, C.C., Giovannoni, J.J., Hall, B.D., Fischer, R.L., and A.B, B. (1998). Transgenic analysis of tomato endo-beta-1,4-glucanase gene function. role of cel1 in floral abscission Plant journal **13,** 303-310.

Lee, J., Das, A., Yamaguchi, M., Hashimoto, J., Tsutsumi, N., Uchimiya, H., and Umeda, M. (2003). Cell cycle function of a rice B2-type cyclin interacting with a B-type cyclin-dependent kinase Plant journal **34,** 417-425.

Leibfried, A., To2, J.P.C., Busch, W., Stehling, S., Kehle, A., Demar, I., Kieber, J.J., and Lohmann, J.U. (2005). WUSCHEL controls meristem function by direct regulation of cytokinin-inducible response regulators. Nature **438,** 1172-1175.

Lenhard, M., Jurgens, G., and Laux, T. (2002). The WUSCHEL and SHOOTMERISTEMLESS genes fulfil complementary roles in *Arabidopsis* shoot meristem regulation. Development **129,** 3195-3206.

Leyser, H., Pickett, F., Dhamasiri, S., and Estelle, M. (1998). Mutations in the *AXR3* gene of *Arabidopsis* result in altered auxin response including ectopic expression from the *SAUR-AC1* promoter Plant journal **10,** 403-413.

Li, C., Potuschak, T., Colon-Carmona, A., Gutierrez, R.A., and Doerner, P. (2005). *Arabidopsis* TCP20 links regulation of growth and cell division control pathways. Proceedings of the National Academy of Sciences **102,** 12978-12983.

Li, J., and Nam, K.H. (2002). Regulation of brassinosteroid signaling by a *GSK3*/*SHAGGY*-like kinase. Science **295,** 1299-1301.

Li, J., Nam, K.H., Vafeados, D., and Chory, J. (2001). *BIN2,* a new brassinosteroid-insensitive locus in *Arabidopsis*. Plant Physiol. **127,** 14-22.

Li, J., Biswas, M.G., Chao, A., Russell, D.W., and Chory, J. (1997). Conservation of function between mammalian and plant steroid 5alpha -reductases. Proceedings of the National Academy of Sciences **94,** 3554-3559.

Li, X., Qian, Q., Fu, Z., Wang, H., Xiong, G., Zeng, D., Wang, X., Liu, X., Teng, S., Hiroshi, F., Yuan, M., Luok, D., Han, B., and Li, J. (2003). Control of tillering in rice. Nature **422,** 618.

Lloyd, C. (1996). Plant morphogenesis: life on a different plane. Current Biology **5,** 1085.

Louret, O.F., and al, e. (1997). BioTechniques **23,** 816-819.

Marrocco, K., Zhou, Y., Bury, E., Dieterle, M., Funk, M., Genschik, P., Krenz, M., and al, e. (2006). Functional analysis of *EID1,* an F-box protein involved in phytochrome A-dependent light signal transduction. Plant Journal **45,** 423-438.

Mathur, J., and Chua, N.-H. (2000). Microtubule stabilization leads to growth reorientation in *Arabidopsis* trichomes. Plant Cell **12,** 465-478.

Mayer, U., Ruiz, R.A.T., Berleth, T., Miseera, S., and Juurgens, G. (1991). Mutations affecting body organization in the *Arabidopsis* embryo. Nature **353,** 402-407.

Mc Clinton, R.S., and Sung, Z.R. (1997). Organization of cortical microtubules at the plasma membrane in *Arabidopsis*. Planta **201,** 252-260.

McGinnis, K.M., Thomas, S.G., Soule, J.D., Strader, L.C., Zale, J.M., Sun, T.-p., and Steber, C.M. (2003). The Arabidopsis *SLEEPY1* gene encodes a putative F-box subunit of an SCF E3 ubiquitin ligase. Plant Cell **15,** 1120-1130.

Meyerowitz, E.M. (1997). Genetic control of cell division patterns in developing plants. Cell **88,** 299-308.

Mizukami, Y. (2001). A matter of size: developmental control of organ size in plants. Current Opinion in Plant Biology **4,** 533-539.

Mizukami, Y., and Fischer, R.L. (2000). Plant organ size control: *AINTEGUMENTA* regulates growth and cell numbers during organogenesis. Proceedings of the National Academy of Sciences **97,** 942-947.

Monna, L., Kitazawa, N., Yoshino, R., Suzuki, J., Masuda, H., Maehara, Y., Tanji, M., Sato, M., Nasu, S., and Minobe, Y. (2002). Positional cloning of rice semidwarfing gene, *sd-1*: rice "green revolution gene" encodes a mutant enzyme involved in gibberellin synthesis. DNA Res **9,** 11-17.

Muller, D., Schmitz, G., and Theres, K. (2006). *Blind* homologous *R2R3 Myb* genes control the pattern of lateral meristem initiation in *Arabidopsis*. Plant Cell **18,** 586-597.

Nakagawa, T., Kurose, T., Hino, T., Tanaka, K., Kawamukai, M., Niwa, Y., Toyooka, K., Matsuoka, K., Jinbo, T., and Kimura, T. (2007). Development of series of gateway binary vectors, pGWBs, for realizing efficient construction of fusion genes for plant transformation. J Biosci Bioeng. **104,** 34-41.

Nam, K.H., and Li, J. (2004). The Arabidopsis transthyretin-like protein is a potential substrate of BRASSINOSTEROID-INSENSITIVE 1. Plant Cell **16,** 2406-2417.

Ni, W., Xie, D., Hobbie, L., Feng, B., Zhao, D., Akkara, J., and Ma, H. (2004). Regulation of flower development in *Arabidopsis* by SCF complexes. Plant Physiol. **134,** 1574-1585.

Nole-Wilson, S., Tranby, T., and Krizek , B. (2005). *AINTEGUMENTA*-like (*AIL*) genes are expressed in young tissues and may specify meristematic or division-competent states. Plant Molecular Biology **57,** 613-628.

Nordstrom, A., Tarkowski, P., Tarkowska, D., Norbaek, R., Astot, C., Dolezal, K., and Sandberg, G. (2004). Auxin regulation of cytokinin biosynthesis in *Arabidopsis thaliana*: a factor of potential importance for auxin-cytokinin-regulated development. Proceedings of the National Academy of Sciences **101,** 8039-8044.

Okada, K., Ueda, J., Komaki, M.K., Bell, C.J., and Shimura, Y. (1991). Requirement of the auxin polar transport system in early stages of *Arabidopsis* floral bud formation. Plant Cell **3,** 677-684.

Okushima, Y., Overvoorde, P.J., Arima, K., Alonso, J.M., Chan, A., Chang, C., Ecker, J.R., Hughes, B., Lui, A., Nguyen, D., Onodera, C., Quach, H., Smith, A., Yu, G., and Theologis, A. (2005). Functional genomic analysis of the *AUXIN RESPONSE FACTOR* gene family members in *Arabidopsis thaliana*: unique and overlapping functions of *ARF7* and *ARF19*. Plant Cell **17,** 444-463.

Okushima Y, M.I., Quach H, Theologis A. (2005). AUXIN RESPONSE FACTOR 2 (ARF2): a pleiotropic developmental regulator Plant journal **43,** 29-46.

Olszewski, N., Sun, T.-p., and Gubler, F. (2002). Gibberellin signaling: biosynthesis, catabolism, and response pathways. Plant Cell **14,** S61-80.

Oppenheimer, D.G., Pollock, M.A., Vacik, J., Szymanski, D.B., Ericson, B., Feldmann, K., and Marks, M.D. (1997). Essential role of a kinesin-like protein in *Arabidopsis* trichome morphogenesis. Proceedings of the National Academy of Sciences **94,** 6261-6266.

Ori, N., Cohen, Z., Efroni, I., and Pekker, I. (2007). Regulation of *LANCEOLATE* by *miR319* is required for compound-leaf development in tomato. Nature Genetics **39,** 787-791.

Palatnik, J.F., Allen, E., Wu, X., Schommer, C., Schwab, R., Carrington, J.C., and Weigel, D. (2003). Control of leaf morphogenesis by microRNAs. Nature **425,** 257-263.

Palni, L., Burch, L., and Horgan, R. (1993). The effect of auxin concentration on cytokinin stability and metabolism

Planta **5,** 351.

Parker, J.E., Holub, E.B., Frost, L.N., Falk, A., Gunn, N.D., and Daniels, M.J. (1996). Characterization of eds1, a mutation in *Arabidopsis* suppressing resistance to *Peronospora parasitica* specified by several different RPP genes. Plant Cell **8,** 2033-2046.

Peng, J., and Harberd, N.P. (1993). Derivative alleles of the *Arabidopsis* gibberellin-insensitive (gai) mutation confer a wild-type phenotype. Plant Cell **5,** 351-360.

Peng, J., and Harberd, N.P. (1997). Gibberellin deficiency and response mutations suppress the stem elongation phenotype of phytochrome-deficient mutants of *Arabidopsis*. Plant Physiol. **113,** 1051-1058.

Peng, J., Carol, P., Richards, D.E., King, K.E., Cowling, R.J., Murphy, G.P., and Harberd, N.P. (1997). The *Arabidopsis GAI* gene defines a signaling pathway that negatively regulates gibberellin responses Genes Dev. **11,** 3194-3205.

Peng, J.E., Richards, D., Hartley, N., Murphym, G., Devos, K., and al, e. (1999). Green revolution' genes encode mutant gibberellin response modulators. Nature **400,** 456-461.

Pérez-Pérez, J.M., Serralbo, O., Vanstraelen, M., González, C., Criqui, M.-C., Genschik, P., Kondorosi, E., and Scheres, B. (2008). Specialization of CDC27 function in the *Arabidopsis thaliana* anaphase-promoting complex (APC/C). Planu Journal **53,** 78-89.

Petersen, M., Sander, L., Child, R., Onckelen, H.v., Ulvsko.PeterC, and Borkhardt, B. (1995). I s o l a t i o n and characterisation of a pod dehiscence z o n e - s p e c i f i c polygalacturonase from *Brassica napus* **31,** 517-527.

Petrasek, J., Mravec, J., Bouchard, R., Blakeslee, J.J., Abas, M., Seifertova, D., Wisniewska, J., Tadele, Z., Kubes, M., Covanova, M., Dhonukshe, P., Skupa, P., Benkova, E., Perry, L., Krecek, P., Lee, O.R., Fink, G.R., Geisler, M., Murphy, A.S., Luschnig, C., Zazimalova, E., and Friml, J. (2006). PIN proteins perform a rate-limiting function in cellular auxin efflux. Science **312,** 914-918.

Pnueli, L., Carmel-Goren, L., Hareven, D., Gutfinger, T., Alvarez, J., Ganal, M., Zamir, D., and Lifschitz, E. (1998). The *SELF-PRUNING* gene of tomato regulates vegetative to reproductive switching of sympodial meristems and is the ortholog of *CEN* and *TFL1*. Development **125,** 1979-1989.

Qiao, H., Wang, H., Zhao, L., Zhou, J., Huang, J., Zhang, Y., and Xue, Y. (2004). The F-box protein *AhSLF-S2* physically interacts with S-RNases that may be inhibited by the ubiquitin/26S proteasome pathway of protein degradation during compatible pollination in *Antirrhinum*. Plant Cell **16,** 582-595.

Ratcliffe, O.J., Bradley, D.J., and Coen, E.S. (1999). Separation of shoot and floral identity in *Arabidopsis*. Development **126,** 1109-1120.

Reinhardt, D., Mandel, T., and Kuhlemeier, C. (2000). Auxin regulates the initiation and radial position of plant lateral organs. Plant Cell **12,** 507-518.

Reinhardt, D., Pesce, E.-R., Stieger, P., Mandel, T., Baltensperger, K., Bennett, M., Traas, J., Friml, J., and Kuhlemeier, C. (2003). Regulation of phyllotaxis by polar auxin transport. Nature **426,** 255-260.

Reiter, W.-D., Chapple, C., and Somerville, C.R. (1997). Mutants of *Arabidopsis thaliana* with altered cell wall polysaccharide composition. The Plant Journal **12,** 335-345.

Rhee, S.Y., Osborne, E., Poindexter, P.D., and Somerville, C.R. (2003). Microspore separation in the *quartet 3* mutants of *Arabidopsis* is impaired by a defect in a developmentally regulated polygalacturonase required for pollen mother cell wall degradation. Plant Physiol. **133,** 1170-1180.

Riou-Khamlichi, C., Huntley, R., Jacqmard, A., and Murray, J.A.H. (1999). Cytokinin activation of *Arabidopsis* cell division through a D-type cyclin. Science **283,** 1541-1544.

Roberts, J.A., Elliott, K.A., and Gonzalez-Carranza, Z.H. (2002a). Abscission,dehiscence, and other cell separation precesses. Annual Review of Plant Biology **53,** 131-158.

Roberts, J.A., Elliott, K.A., and Gonzalez-Carranza, Z.H. (2002b). Abscission, dehiscence, and other cell separation processes. Annu Rev Plant Biol **53,** 131 - 158.

Rogg, L.E., Lasswell, J., and Bartel, B. (2001). A gain-of-function mutation in *IAA28* suppresses lateral root development. Plant Cell **13,** 465-480.

Rupp, H., Frank , M., Werner, T., Strnad, M., and Schmülling, T. (1999). Increased steady state mRNA levels of the STM and *KNAT1* homeobox genes in cytokinin overproducing *Arabidopsis thaliana* indicate a role for cytokinins in the shoot apical meristem plant journal **18,** 557.

Sakamoto, T. (2006). Phytohormones and rice crop yield: strategies and opportunities for genetic improvement Trangenic Research **15,** 399-404.

Sakamoto, T., Kobayashi, M., Itoh, H., Tagiri, A., Kayano, T., Tanaka, H., Iwahori, S., and Matsuoka, M. (2001). Expression of a gibberellin 2-oxidase gene around the shoot apex is related to phase transition in rice. Plant Physiol. **125,** 1508-1516.

Sakamoto, T., Miura, K., Itoh, H., Tatsumi, T., Ueguchi-Tanaka, M., Ishiyama, K., Kobayashi, M., Agrawal, G.K., Takeda, S., Abe, K., Miyao, A., Hirochika, H., Kitano, H., Ashikari, M., and Matsuoka, M. (2004). An overview of gibberellin metabolism enzyme genes and their related mutants in rice. Plant Physiol. **134,** 1642-1653.

Sambrook, J., and Russel, D.W. (2002). Molecular Cloning - A Laboratory Mannual, ((Cold Spring Habour, New York: Cold Spring Habour Laboratory Press)).

Sander, L., Child, R., Ulvskov, P., Albrechtsen, M., and Borkhardt, B. (2001). Analysis of a dehiscence zone endo-polygalacturonase in oilseed rape (*Brassica napus*) and *Arabidopsis thaliana*: evidence for roles in cell separation in dehiscence and abscission zones, and in stylar tissues during pollen tube growth. Plant Molecular Biology **46,** 469-479.

Sanger, F., Nicklen, S., Coulson, A.R., chain-termination, D.s.w., and inhibitors. (1997). Sequencing with chain-termination inhibitors. Proc. Natl. Acad. Sci. **74,** 5463-5467.

Sasaki, A., Ashikari, M., Ueguchi-Tanaka, M., Itoh, H., Nishimura, A., and al, e. (2002). A mutant gibberellin-synthesis gene in rice. Nature **416,** 701.

Sasaki, A., Itoh, H., Gomi, K., Ueguchi-Tanaka, M., Ishiyama, K., Kobayashi, M., Jeong, D.-H., An, G., Kitano, H., Ashikari, M., and Matsuoka, M. (2003). Accumulation of phosphorylated repressor for gibberellin signaling in an F-box mutant. Science **299,** 1896-1898.

Schmitz, G., Tillmann, E., Carriero, F., Fiore, C., Cellini, F., and Theres, K. (2002). The tomato *Blind* gene encodes a MYB transcription factor that controls the formation of lateral meristems. Proceedings of the National Academy of Sciences **99,** 1064-1069.

Schumacher, K., Schmitt, T., Rossberg, M., Schmitz, G., and Theres, K. (1999). The *Lateral Supreso*r (*Ls*) gene of tomato encodes a new member of the VHID protein family. Proc Natl Acad Sci U S A. **96,** 290-295.

Sekimata, K., Kimura, T., Kaneko, I., Nakano, T., Yoneyama, K., Takeuchi, Y., Yoshida, S., and Asami, T. (2001). A specific brassinosteroid biosynthesis inhibitor, Brz2001: evaluation of its effects on Arabidopsis, cress, tobacco, and rice Planta **312,** 716.

Shannon, S., and Meeks-Wagner, D.R. (1991). A mutation in the *Arabidopsis TFL1* Gene affects inflorescence meristem development. Plant Cell **3,** 877-892.

Shimizu-Sato, S., and Mori, H. (2001). Control of outgrowth and dormancy in axillary buds. Plant Physiol. **127,** 1405-1413.

Sieberer, T., and Leyser, O. (2006). PLANT SCIENCE: auxin transport, but in which direction? Science **312,** 858-860.

Siebert, P.D., Chenchik, A., Kellogg, D.E., Lukyanov , K.A., and Lukyanov, S.A. (1995). An improved PCR method for walking in uncloned genomic DNA. Nucleic Acids Res **23,** 1087-1088.

Smith, L.G., Gerttula, S.M., Han, S., and Levy, J. (2001). TANGLED1: a microtubule binding protein required for the spatial control of cytokinesis in maize. J. Cell Biol. **152,** 231-236.

Somers, D.E., Kim, W.-Y., and Geng, R. (2004). The F-box protein *ZEITLUPE* confers dosage-dependent control on the circadian clock, photomorphogenesis, and flowering time. Plant Cell **16,** 769-782.

Spielmeyer, W., Ellis, M.H., and Chandler, P.M. (2002). Semidwarf (*sd-1*), "green revolution" rice, contains a defective gibberellin 20-oxidase gene. Proceedings of the National Academy of Sciences **99,** 9043-9048.

Stirnberg, P., van de Sande, K., and Leyser, H.M.O. (2002). *MAX1* and *MAX2* control shoot lateral branching in *Arabidopsis*. Development **129,** 1131-1141.

Strader, L.C., Ritchie, S., Soule, J.D., McGinnis, K.M., and Steber, C.M. (2004). Recessive-interfering mutations in the gibberellin signaling gene *SLEEPY1* are rescued by overexpression of its homologue, *SNEEZY*. Proceedings of the National Academy of Sciences **101,** 12771-12776.

Studier, F.W., and Moffatt, B.A. (1986). Use of bacteriophage T7 RNA polymerase to direct selective high-level expression of cloned genes. J. Mol. Biol. **189,** 113.

Sun, T., and Kamiya, Y. (1994). The *Arabidopsis* GA1 locus encodes the cyclase ent-Kaurene synthetase A of gibberellin biosynthesis. Plant Cell **6,** 1509-1518.

Swain, S.M., Tseng, T.-s., and Olszewski, N.E. (2001). Altered expression of *SPINDLY* affects gibberellin response and plant development. Plant Physiol. **126,** 1174-1185.

Szekeres, M., Németh, K., Koncz-Kálmán, Z., Mathur, J., Kauschmann, A., Altmann, T., Rédei, G.P., Nagy, F., Schell, J., & Koncz, C., Bishop, G.J., and Koncz, C. (1996). Brassinosteroids rescue the deficiency of CYP90, a cytochrome P450, controlling cell elongation and de-etiolation in *Arabidopsis*. Cell **85,** 171.

Taiz, L., and Zeiger, E. (1998). Plant physiology. (Singapour association).

Takeda, T., Suwa, Y., Suzuki, M., Kitano, H., Ueguchi-Tanaka, M., Ashikari, M., Matsuoka, M., and Ueguchi, C. (2003). The *OsTB1* gene negatively regulates lateral branching in rice Plant Journal **33,** 513-520.

Talon, M., Koornneef, M., and Zeevaart, J.A.D. (1990a). Endogenous gibberellins in *Arabidopsis thaliana* and possible steps blocked in the biosynthetic Pathways of the semidwarf *ga4* and *ga5* mutants. Proceedings of the National Academy of Sciences **87,** 7983-7987.

Talon, M., Koornneef, M., and Zeevaart, J. (1990b). Accumulation of C19-gibberellins in the gibberellin-insensitive dwarf mutant gai of *Arabidopsis thaliana* (L.) Hehyn. Planta **182,** 501-505.

Tanaka, R., Ikeda, M., Funatsuki, Yukioka, H., Katoh, K., and Konno, H. (2001). Molecular cloning and in situ hybridization of α-l-arabinofuranosidase from carrot cells. PHYSIOL, PLANT **113,** 392-399.

Taylor, J.E., Webb, S.T.J., Coupe, S.A., Tucker, G.A., and Roberts, J.A. (1993). Changes in polygalacturonase activity and solubility of polyuronides during ethylene-stimulated leaf abscission in *sambucus nigra*. J. Exp. Bot. **44,** 93-98.

Thomma, B.P., Cammue, B.P., and Thevissen, K. (202). Plant defensins. Planta **196,** 193-203.

Tian, Q., and Reed, J.W. (1999). Control of auxin-regulated root development by the *Arabidopsis thaliana SHY2*/*IAA3* gene. Development **126,** 711-721.

Tian, Q., Uhlir, N.J., and Reed, J.W. (2002). Arabidopsis *SHY2/IAA3* inhibits auxin-regulated gene expression. Plant Cell **14,** 301-319.

Torki, M., Mandaron, P., Mache, R., and Falconet, D. (2000). Characterization of a ubiquitous expressed gene family encoding polygalacturonase in *Arabidopsis thaliana*. Gene **242,** 427-436.

Torki, M., Mandaron, P., Thomas, F., Quigley, F., Mache, R., and Falconet, D. (1999). Differential expression of a polygalacturonase family in *Arabidopsis thaliana*. Molecular General Genetics **261,** 948-952.

Torres-Ruiz, R.A., and Jurgens, G. (1994). Mutations in the *Fass* gene uncouple pattern formation and morphogenesis in *Arabidopsis* development. Development **120,** 2967-2978.

Trass, J., Bellini, C., Nacry, P., Kroneberger, J., Bouchez, D., and Caboche, M. (1995). Normal differentiation patterns in plants lacking microtubular preprophase bands

Nature **375,** 676-677.

Tucker, G., Schindler, C., and Roberts, J. (1984). Flower abscission in mutant tomato plants. Planta **160,** 164-167.

Ulmasov, T., Hagen, G., and Guilfoyle, T.J. (1997). ARF1, a transcription factor that binds to auxin response elements. Science **276,** 1865-1868.

van der Knaap, E., Kim, J.H., and Kende, H. (2000). A novel gibberellin-induced gene from rice and its potential regulatory role in stem growth. Plant Physiol. **122,** 695-704.

Verkest, A., Weinl, C., Inze, D., De Veylder, L., and Schnittger, A. (2005). Switching the cell cycle. kip-related proteins in plant cell cycle control. Plant Physiol. **139,** 1099-1106.

Vinardell, J.M., Fedorova, E., Cebolla, A., Kevei, Z., Horvath, G., Kelemen, Z., Tarayre, S., Roudier, F., Mergaert, P., Kondorosi, A., and Kondorosi, E. (2003). Endoreduplication mediated by the anaphase-promoting complex activator CCS52A is required for symbiotic cell differentiation in *Medicago truncatula* nodules. Plant Cell **15,** 2093-2105.

Vlieghe, K., Boudolf, V., Bemster, G., Maes, S., Magyar, S., Atanassova, A., de Almedia, E., De, G., Inze, D., and De, V. (2005). The DP-E2F-like gene DEL1 controls the endocycle in *Arabidopsis thaliana*. Current Biology **15,** 59-63.

Vogel, J.P., Raab, T.K., Somerville, C.R., and Somerville, S.C. (2004). Mutations in PMR5 result in powdery mildew resistance and altered cell wall composition. The Plant Journal **40,** 968-978.

Vorwerk, S., Somerville, S., and Somerville, C. (2004). The role of plant cell wall polysaccharide composition in disease resistance. Trends in Plant Science **9,** 203-209.

Wang, H., Zou, Y., Gilmer, S., Whitwil, l.S., and Fowke, L. (2000). Expression of the plant cyclin-dependent kinase inhibitor ICK1 affects cell division, plant growth and morphology. Plant Journal **24,** 613-623.

Wang, H., Jones, B., Li, Z., Frasse, P., Delalande, C., Regad, F., Chaabouni, S., Latche, A., Pech, J.-C., and Bouzayen, M. (2005). The tomato *Aux/IAA* transcription factor I*AA9* is involved in fruit development and leaf morphogenesis. Plant Cell **17,** 2676-2692.

Wang, Y., and Li, J. (2008). Molecular basis of plant architecture. Annual Review of Plant Biology **59,** 253-269.

Ward, S.P., and Leyser, O. (2004). Shoot branching. Current Opinion in Plant Biology **7,** 73-78.

Weiss, J., Delgado-bearoch, L., and Egea-cortines, M. (2005). Genetic control of floral size and proportions **49,** 513-525.

Weller, J., Reid, J., Taylor, S., and Murfet, I. (2007). The genetic control of flowering in pea. Trends in Plant Science **2,** 412-418.

Werner, T., Motyka, V., Strnad, M., and Schmulling, T. (2001). Regulation of plant growth by cytokinin. Proceedings of the National Academy of Sciences**,** 171304098.

Whittington, A.T., Vugrek, O., Wei, K.J., Hasenbein, N.G., Sugimoto, K., Rashbrooke, M.C., and Wasteneys, G.O. (2001). MOR1 is essential for organizing cortical microtubules in plants. Nature **411,** 610-613.

Wietholter, N., Graener, B., Mierau, M., Mort, A.J., and Moerschbacher, B.M. (2003). Differences in the methyl ester distribution of homogalacturonans from near-isogenic wheat lines resistant and susceptible to the wheat stem rust fungus. Molecular Plant-Microbe Interactions **16,** 945-952.

Wilson, R.N., and Somerville, C.R. (1995). Phenotypic suppression of the gibberellin-insensitive mutant (gai) of *Arabidopsis*. Plant Physiol. **108,** 495-502.

Wilson, R.N., Heckman, J.W., and Somerville, C.R. (1992). Gibberellin is required for flowering in *Arabidopsis thaliana* under short days. Plant Physiol. **100,** 403-408.

Winkler, R.G., and Freeling, M. (1994). Analysis of the autonomy of maize *Dwarf1* action in genetic mosaics. J Hered **85,** 377-380.

Wood, W.B. (1996). Host specificity of DNA produced by *Escherichia coli*: bacterial mutations affecting the restriction and modification of DNA. Mol. Biol. **16,** 118-133.

Woodward, A.W., and Bartel, B. (2005). Auxin: regulation, action, and interaction. Ann Bot **95,** 707-735.

Xing, Y., Xu, Y., Chen, Y., and al, e. (2006). Structure of protein phosphatase 2A core enzyme bound to tumor-inducing toxins. Cell **127,** 341-353.

Xu, Y., Xing, Y., Chen, Y., and al, e. (2006). Structure of the protein phosphatase 2A holoenzyme. Cell **127,** 1239-1251.

Yadegari, R., Paiva, G., Laux, T., Koltunow, A.M., Apuya, N., Zimmerman, J.L., Fischer, R.L., Harada, J.J., and Goldberg, R.B. (1994). Cell differentiation and morphogenesis are uncoupled in *Arabidopsis* raspberry embryos. Plant Cell **6,** 1713-1729.

Yamaguchi, S., Sun, T.-p., Kawaide, H., and Kamiya, Y. (1998). The *GA2* locus of *Arabidopsis thaliana* encodes ent-Kaurene synthase of gibberellin biosynthesis. Plant Physiol. **116,** 1271-1278.

Zhong, R., Burk, D., and Ye, Z. (2001). Fibers: a model for studying cell differentiation, cell elongation, and cell wall biosynthesis. Plant Physiol. **126,** 477-479.

Zimmermann, P., Hirsch-Hoffmann, M., Hennig, L., and Gruissem, W. (2004). GENEVESTIGATOR. Arabidopsis microarray database and analysis toolbox. Plant Physiol. **136,** 2621-2632.

Zolman, B.K., Monroe-Augustus, M., Silva, I.D., and Bartel, B. (2005). Identification and functional characterization of *Arabidopsis* PEROXIN4 and the interacting protein PEROXIN22. Plant Cell **17,** 3422-3435.

List of figures

List of figures

List of figures

List of figures

List of tables

List of abbreviations

AD	Activation domain
AM	Apical meristem
Amp	Ampicillin
AN3	ANGUSTIFOLIA3
ANT	*AINTEGUMENTA*
APS	Ammonium persulfate
AS	Antisense
ASK	*Arabidopsis Shaggy-like kinase*
Aux	Auxin
Avr	*Avirulence*
BEE	*BR Enhanced Expression*
bin2	*BR-insensitive 2*
Bl	*BLIND*
BL	Brassinolide
Bla	β-lactamase gene for selection in bacteria (ampicillin/carbenicillin resistance)
Bp	Base pair
BRs	Brassinosteroid(s)
BSA	Bovine serum albumin
°C	degree Celsius
CaMV	Cauliflower mosaic virus
Carb	Carbenicillin
CCS52	Cell cycle switch 52
CDKs	Cyclin-dependent kinase(s)
cDNA	Complementary DNA
cfu	Colony forming units
CIN	*CINCINNATA*
CK(s)	Cytokinin(s)
Col-0	Columbia
CSM	Complement supplement mixture
Cv	Cultivar
det2	*Deetiolated 2*
DMSO	Dimethyl sulfoxide
DNA	Deoxyribonucleic acid
DNA-BD	DNA-binding domain
dNTP	Deoxyribonucleoside triphosphate
dwf	*Dwarfed*
E. coli	*Escherichia coli*
EDS1	*Enhanced disease susceptibility 1*
EDTA	Ethylen diamine tetraacetic acid
Eppi	Eppendorf tube
EtOH	Ethanol
Fig	Figure
G	Glycine

GA(s)	Gibberellin(s)
GAox	Gibberellic acid oxydase
GRF	*GROWTH REGULATOR FACTOR*
hpt	Hour past treatment
IAA(s)	Indole acetic acid
Kb	Kilobase pair
kDa	Kilodalton
km	Kanamycin
L	Liter
LA	LANCEOLATA
LAS	LATERAL SUPPRESSOR
LB	Left border
LB	Luria Bertani medium
LEU2	Leucin selection marker
M	Molarity
mg	Milligram
min	Minute
miRNA	micro RNA
ml	Milliliter
MOPS	3-(N-morpholino) propane sulfonic acid
MPBS	Non-fat skim milk powder in PBS
mRNA	Messenger RNA
MS	Murashige and Skoog Basal medium
MTs	Microtubules
MW	Molecular weight
Nm	Nanometer
NPR1	*Non-expressor of PR1*
OD	Optical density
PAT	Polar auxin transport
PBS	Phosphate buffered saline
PBST	0.1% Tween-20 in PBS
PCR	Polymerase chain reaction
PEG	Poly ethylene glycol
PEL	Pellet
PGase	Polygalacturonse
Pst	*Pseudomonas syringae pv. Tomato*
QTL	Quantitative trait loci
RB	Right border
RE	Restriction enzyme
Rif	Rifampicin
RNA	Ribonucleic acid
RNase	Ribonuclease
rpm	Rounds per minute
RPS2	*Resistance gene to P. syringae pv. Tomato*
RT	Room temperature
RT-PCR	Reverse transcriptase-polymerase chain reaction

s	Second
SAM(s)	Shoot apical mristem(s)
SDS-PAGE	Sodium dodecyl sulphate-polyacrylamide gel electrophoresis
SP	*SELF-PRUNING*
STM	Shootmeristem
SUP	Supernatant
T	Thymin
TAIL	Thermal asymmetric interlaced
Taq	*Thermus aquaticus*
T-DNA	Transfer DNA
TEMED	N, N, N´, N´-tetramethyl ethylene diamine
TFL1	TERMINAL FLOWER1
*ton*2-5	*Tonneau*2-5
Tris	Trishydroxymethylaminomethane
TRP	Tryptophan
TTL	Transthyretin-like
TUA6	Tubulin 6
U	Unit
UCU1	Ultracurvata 1
URA	Uracil
UTR	Untranslated region
UV	Ultraviolet
v/v	Volume per volume
vir	*Virulence*
w/v	Weight per volume
WS	Wassilewskija-0
WT	Wild type
X-gal	5-bromo-4-chloro-3-indolyl- ß- D -galactoside
X-Gluc	X-Glucuronide
YNB	Yeast nitrogene base

Aknowledgement

I would like to thank Prof. Dr. Alan. J. Slusarenko for giving me the chance to work in this institute. I am also very thankful for his supervision, his friendship and his hospitality.

My special thanks go to Dr. Nikolaus Sclaich for providing me with this interesting project and allowing me to pursue the Ph.D project in his group. I appreciate him very much for his critical reading, discussion and correction of this manuscript which made it possible for me to present it in present form.

I would like to thank Prof. Dr. Christoph Peterhänsel for agreeing to act as co-examiner and for their guidance during my Ph.D work.

I also take this opportunity to thank Clarissa Masur, Monika Herman, Gerold Becker, Dr. Nicoletta Schlaich, Dr. Gudrun Schmitz, Reza Sharifi Sirchi, Hedwig Nüssgens, Renate Schulbert, Mohammad Reza Safanejad, Sven Friehe, Rashad Kebeish, Daniela Protz, Nina Zellerhof, Marcus Deissen, Rene Fuchs for their help and interesting discussion. It was my pleasure to work with so many people, from whom I learned a lot.

My special thanks to Aachener Iranian friends who made my stay in Aachen memorable.

Of course, I wish to express my endless thanks to my husband, Javad, for his very kindly support, help and patience.

Last but never the least, I would like to thank all the members of my family especially my parents who always provided me with a wonderful educational opportunities and continue to be a guiding force.

Declaration / Erklärung

Herewith I declare that I have written this PhD thesis myself, using only the referenced literature.

Hiermit versichere ich, dass ich die vorliegende Doktorarbeit selbstständig verfasst und keine anderen als die angebenen Hilfsmittel und Quellen verwendet habe.

Aachen, 2008

Curriculum Vitae

Personal data:

Surname:	Pooraiiouby
First name:	Rana
Date of birth:	23.09.1979
Place of birth:	Marand, Iran
Nationality:	Iranian
Religion:	Muslem
Marital status:	Married
Address in Iran:	549, Rajaii street, Maran, Iran
Address in Germany:	Vaalser str. 1, 52074-Aachen, Germany

Education data:

1985-1990:	Primary school, Marand, Iran
1990-1993:	Graduate school, Marand, Iran
1993-1997:	High school, Marand, Iran
1997-2001:	Bachelor of Science, Urmia University, Iran
2001-2004:	Master of Science, Urmia University, Iran
2005-2008:	PhD student, Institute of Plant Physiology (Bio III), Aachen, Germany